$\mathbb{Z}_N$ lattice gauge theories in a ladder geometry

Jens Havgaard Nyhegn

Niels Bohr Institute
University of Copenhagen
Lyngbyvej 2, DK-2100, Copenhagen, Denmark

Master's thesis in Physics
Advisor: Michele Burrello

Dated: September 6, 2020
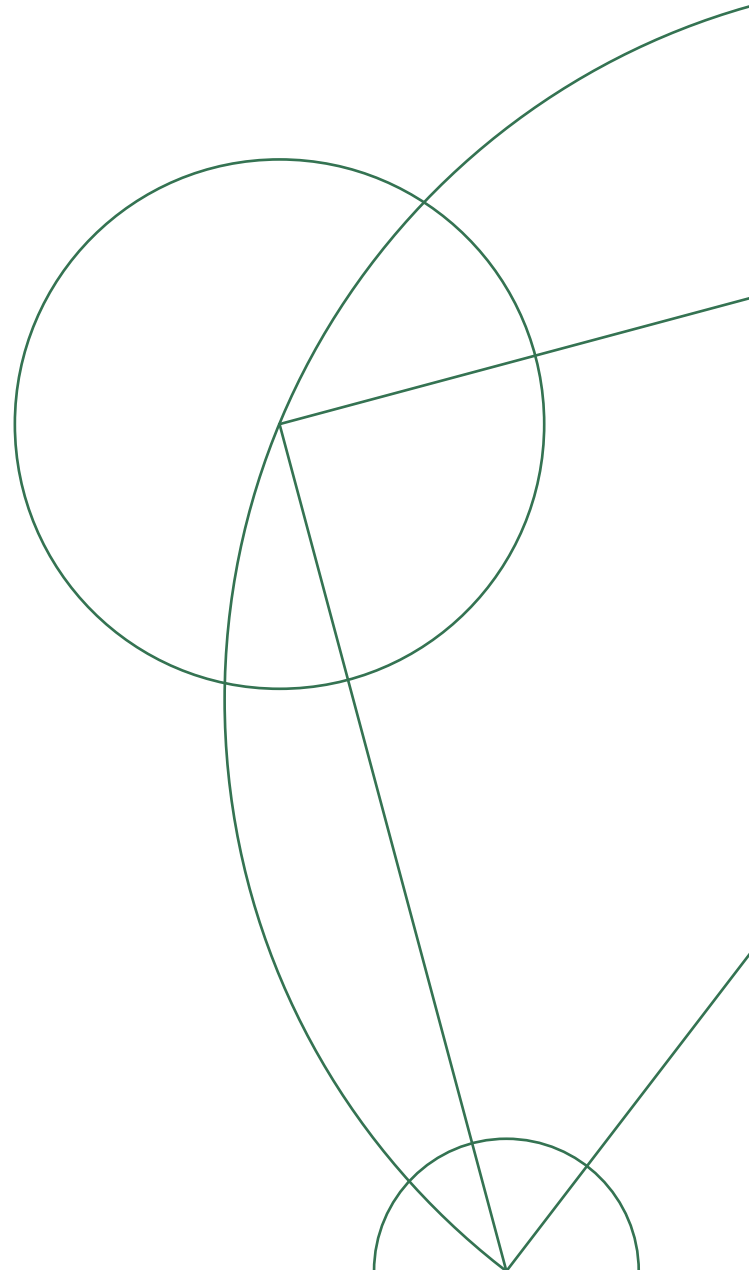
Abstract

Since lattice gauge theories (LGT) were first introduced by *Kenneth G. Wilson* to study the quark confinement problem in 1974, it has proven itself in many areas of high energy physics. Must prominently it has obtained nonperturbative results in the theory of the strong interactions, Quantum Chromodynamics. In the last years a great effort has been put into approaching LGTs with techniques developed in the field of quantum many-body physics. In deploying these techniques less complex toy models have been constructed, in order for the analytical and numerical work to be comprehensive before approaching more complicated systems. In this thesis the full Kogut-Susskind Hamiltonian with a generic $\mathbb{Z}_N$ gauge symmetry is investigated. This is done in a ladder geometry, which is a geometry allowing for the tough plaquette interactions to be incorporated. First the pure $\mathbb{Z}_N$ lattice gauge theory (PLGT) is investigated perturbatively. Thereafter Higgs matter is introduced and by using techniques inspired by bosonization techniques, a phase diagram is predicted. This is further investigated in the case of $N = 5$, were the system is predicted to support a gapless phase, which is in good agreement with predictions obtained using density matrix renormalization group techniques.

Acknowledgements

Contents

Chapter 1

Introduction

As physicists we concern ourselves with the workings of nature, and at the root of all workings lie the fundamental particles and their interactions. The current theory describing this clockwork is the gauge field theory called the *Standard Model*. A gauge field theory is a quantum field theory where forces are mediated by the exchange of vector bosons and particles are described by excitations of matter fields. This theory has shown successful in describing all forces of nature except for gravity and it was truly cemented by the discovery of the predicted Higgs boson at CERN [1].

The *Standard Model* is referred to as the theory of everything and one should in theory be able to extract the occurrence of rainbows from it. It is not an easy model to handle though, and physicist most often attack the model perturbatively by the use of Feynman diagrams. In describing the weak and electromagnetic (QED) interactions, this perturbative approach has helped in understanding countless of phenomena. In describing the Strong interactions (QCD) this method works well for high energies but fades for low, and it does so due to the well-know asymptotic freedom [2, 3]. This leads to quarks being free particles and weakly interacting at high energies while in our low energy world they are subject to quark-confinement hence confined into hadrons and are strongly interacting [4]. Strongly interacting particles are not easy to handle perturbatively and other methods are needed.

One way this problem is being dealt with, is by considering a descritized description in the form of lattice gauge theories (LGT) instead of the continuous description [5–7]. LGT has established itself by both making analytical and numerical predictions where one of the landmarks is the spectra obtained for both hadrons and light mesons through Monte Carlo techniques [8]. The studies of LGT by Monte Carlo techniques is though limited by the sign problem [9] which becomes problematic when considering fermionic matter with a finite chemical potential [10].

In the last years novel techniques have been proposed to overcome this obstacle, and a great effort has been put into deploying the techniques developed in the field of quantum many-body physics [11]. In this effort the quantum many-body physics community has sought out experimental realization of quantum simulators by trapped ions [12] and in ultra cold atom systems [13–17]. Obtaining such simulators would allow for the experimental study of these perturbatively inaccessible regimes. Numerically LGTs have been approached by tensor network (TN) calculations [18] based on the Kogut and Susskind Hamiltonian formulation [19].

Behind any scientific technique lies many cumulative steps where complexity is added in a comprehensive manner. The same is true for this approach. Here people have successfully developed toy models to capture essential parts of the physics [20], and before considering the non-Abelian nature of QCD, the Abelian case of QED is approached, where again the simpler case of low dimensionality is preferred. Lower dimensionality simplifies the analytical work and leaves space for the techniques of TN to mature and later be able to attack higher dimensional problems. Having the analytical development running parallel with the development of TN techniques simultaneously yield a basis for comparing results and thereby leaving more established results.

In wanting to be able to compare the analytical work with the results obtained using TN techniques

a modification of the continuous Lie groups describing the local gauge symmetries of the *Standard Model* is needed. If taking the example of QED one can interpret its $U(1)$ symmetric nature as the electric flux being able to take an infinite possibility of values. In the language of Hilbert space, this means that one has infinite many states to simulate. This is not computationally possible to handle and one needs to somehow modify the continuous symmetry. Here two possible ways have been put forward. One approach is to truncate the $U(1)$ symmetry, thereby only considering the electric flux to be able to take integer values up to some maximum value [21–23]. This effectively also leads to the system only being able to have a limited number of charges present. Another approach is to consider a discrete and cyclic Z_N symmetry [18, 24–26]. This limits the electric flux to take N discrete values which in the large N is to approximate the $U(1)$ symmetry. In 1D it is shown to rapidly converge to represent the true $U(1)$ symmetry of QED for large N [27]. Z_N symmetry models are also of interest in themselves, and have been considered as models describing 2D topological ordered systems [28].

The vision with this approach to High energy physics (HEP) is to be able to both make analytical predictions and simulate theories using TN techniques in $(3 + 1)$ dimension. At the moment the community has mainly focused on (1+1) dimensional LGTs but recently moved on to investigations of (2+1) dimensional problems with truncated $U(1)$ or discrete Z_N symmetries [18, 23, 29, 30].

This thesis will neither investigate a $(1+1)$ or a $(2+1)$ dimensional problem but instead the quasi $(1+1)$ dimensional ladder geometry with a discrete Z_N symmetry. Compared to the $(1 + 1)$ problem this geometry can include plaquette interactions, and is the simplest geometry capable of doing so. These interactions have shown hard to handle and this geometry therefore stands as a stepping stone from where methods can be developed to attack higher dimensional problems which includes these interactions. This geometry also allows for the full Kogut and Susskind Hamiltonian to be deployed, and it will be so by also incorporating Higgs matter [24, 31].

The aim of this thesis is to investigate LGTs on a ladder geometry with a generic local $\mathbb{Z}_N$ gauge symmetry and it is structured as follows: In Chapter 2 one finds an analysis of the $\mathbb{Z}_2$ pure lattice gauge theory (PLGT) where no matter is introduced. This chapter is meant to work as a technical introduction into the study of LGTs. In chapter 3 this analysis will be extended to a generic N and continued in chapter 4 where perturbative calculations are performed in order to investigate the confining or deconfining behavior of the system. This will in particular be investigated by inserting static charges into the system. Chapter 5 will move away from the PLGT by adding Higgs matter to the system. This allows for a richer phase diagram where in certain limits similar analysis as performed for the PLGT will be done. In chapter 6 one finds the low energy technique of bosonization to be introduced. This technique will then be applied in a simplified limit before the full Hamiltonian is approached in chapter 9. From the bosonized description the model will be investigated using renormalization group (RG) techniques. In chapter 6 this is done to first order. Chapter 7 offers second order RG derivation, where by the use of the real space RG approach the RG flow equations are found. These equations are solved numerically and the result is stated. In chapter 8 the bosonization of the full model is attacked and a first order RG analysis is performed. In Chapter 9 the real space RG technique is left behind in favor of the momentum space approach. The momentum space approach is used to derive the flow equations which are solved numerically and held up against results obtained using TN techniques.

Chapter 2

$\mathbb{Z}_2$ pure lattice gauge theory

This chapter presents a technical introduction to how lattice gauge theories (LGT) are constructed and investigated. In this thesis the geometry investigated is the ladder geometry shown in Fig. 2.1. This geometry is a quasi 1D structure meaning it has a mix of features from both the 1D and truly 2D system. It is as well the simplest geometry where plaquette interactions can be incorporated. In the system one can have both matter particles and gauge bosons, where the matter can be of different kinds. The matter particles live on the sites of the ladder while the gauge bosons live on the links. As a technical introduction to the subject it makes sense to consider the simplest case. This is the pure lattice gauge theory (PLGT) which contains solely gauge bosons.
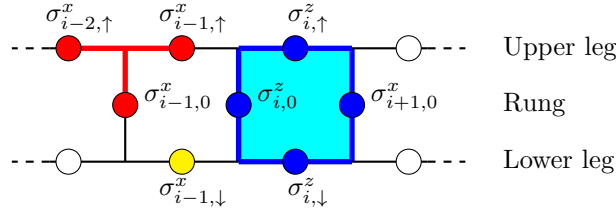
Figure 2.1 | Schematic representation of the PLGT. This figure illustrates the geometry along with the interactions of the system. The yellow color represents the electrical field term, red the gauge constrain and blue the plaquette interactions. This figure as well shows how the different links are labeled in the superscripts, where $(r, 0)$ denotes links on the rung, $(r, \uparrow)$ on the upper leg and $(r, \downarrow)$ on the lower leg

2.1 The Hamiltonian and gauge generators

To describe the gauge bosons d.o.f. two unitary operators τ and σ are introduced. These operators are each others conjugated operators, and related by a discrete Fourier transform [32, 33][1], similar to operators describing space and momentum. If taking the generic case of having a local $\mathbb{Z}_N$ gauge symmetry then these operators fulfills

$$\sigma^N = \mathbb{1} = \tau^N. \tag{2.1.1}$$

---

[1]This operator is know as the Schur matrix.

This leaves us with a unique cyclic behavior of the operators, and for a generic state in the σ-basis one has [2]

$$\sigma \left|s\right\rangle_\sigma = \omega^s \left|s\right\rangle_\sigma \ , \quad \tau \left|s\right\rangle_\sigma = \left|s+1 \ mod \ N\right\rangle_\sigma \ \text{and} \quad \omega \equiv e^{i\frac{2\pi}{N}}. \tag{2.1.2}$$

leaving us with the fundamental algebraic equation

$$\sigma\tau = \omega\tau\sigma. \tag{2.1.3}$$

Having specified the algebraic rules, it is now possible to give an intuitive picture of how the operators work. If imagining a continuous clock in the complex plane which is separated into N discrete times equally separated, then in the σ-basis one finds the σ-operator to indicate the time while the τ-operator rotates the hand in clockwise direction. In the τ-basis the τ-operator will tell the time while the σ-operator will rotate the hand in counter-clockwise direction. This intuition is the reason for the operators being denoted quantum clock-operators.

If now taking the simplest case of having a $\mathbb{Z}_2$ symmetry one finds $\omega = -1$ and only the discrete states $\left|s = \pm 1\right\rangle$ are possible. From the above relations one finds the algebra to be fulfilled by the usual Pauli matrices, which is also why the $\mathbb{Z}_2$ theory is denoted the Ising gauge theory. In 2D this theory has been extensively investigated in [24, 34, 35], and the Hamiltonian describing this theory is the Kogut-Susskind Hamiltonian introduced in [35] and is given by

$$H = -\frac{1}{g}\sum_{i=1}^{L-1}\sigma^z_{i,\uparrow}\sigma^z_{i,\downarrow}\sigma^z_{i,0}\sigma^z_{i+1,0} - \sum_{s=0,\downarrow,\uparrow}\sum_{i=1}^{L}\sigma^x_{i,s} \ , \quad g \geq 0. \tag{2.1.4}$$

Where the following mapping has been used

$$\sigma \to \sigma^z \ , \quad \tau \to \sigma^x, \tag{2.1.5}$$

and later, when the different terms are given a physical meaning, it will make sense why $g \geq 0$ is necessary. Had matter also been present, one would need a new set of operators describing those d.o.f.

In comparison to the Ising Hamiltonian, the Kogut-Susskind Hamiltonian shows both a global $\mathbb{Z}_2$ symmetry and a local $\mathbb{Z}_2$ gauge symmetry. The global $\mathbb{Z}_2$ symmetry is generated by

$$\mathcal{G} = \prod_{\bar{r}}\sigma^x_{\bar{r}} \tag{2.1.6}$$

where $\bar{r}$ indicates that the products run over all links. This is a symmetry of the system meaning that $[H, \mathcal{G}] = 0$, such that these two operators can be simultaneously minimized and the ground state can be chosen to be an eigenstate of $\mathcal{G}$ as well. This is physical symmetry which in the case of the quantum Ising model is responsible for the spontaneous symmetry breaking related to the phase transition. This means that by understanding how $\mathcal{G}$ acts on the ground state one can distinguish the two thermodynamic phases appearing at zero temperature. In the ferromagnetic or ordered phase the symmetry is spontaneously broken in the thermodynamic limit and $\mathcal{G}$ maps one degenerate ground state into the other. Instead in the paramagnetic or disordered phase the ground state is an eigenstate of this operator. A gauge symmetry is much different to this, and cannot be assigned any direct physical meaning, and should instead be seen as a constrain on the system. If a configuration does not fulfill the gauge constrains, then it is not a configuration which can be physical realized. In the next part this will be made more concrete.

An important aspect of LGT and just in general gauge theories is that the Hilbert space over-represents the physical states. This means that multiple vectors in the Hilbert space or states can represent the same physical state. To understand how this works it is intuitive to look at a single junction shown in Fig. 2.2. In a LGT one finds a gauge generator accompanying each junction or

---

[2]With the σ-basis being the basis where the σ-operator is diagonal.
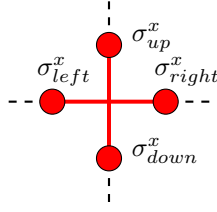
Figure 2.2 | 2D Junction. This figure illustrates the gauge constrain for vertex which is present in a 2D LGT and not the ladder geometry. It also illustrates how the local gauge constrain is generated by an operator which acts on all the neighboring links of the vertex.

vertex. For this vertex we define the gauge generator by G_r. This gauge generator is an operator acting on all d.o.f. of the neighboring links illustrated in red in Fig. 2.2, and it generates the local gauge symmetry present at each vertex. This operator, as in the ferromagnetic case for $\mathcal{G}$, maps one state in the Hilbert space onto another, but while the two degenerate ground states in the ferromagnetic case display a physical difference by the magnetization pointing in different directions, no such difference is found between the two states in the gauge theory. If writing the state of the vertex as $|\psi_v\rangle$ then this can explicitly be stated as

$$G_r |\psi_v\rangle = |\psi'_v\rangle \ , \quad \langle\psi_v|\psi'_v\rangle = 1. \tag{2.1.7}$$

An important feature of the system is now that using either $|\psi_v\rangle$ or $|\psi'_v\rangle$ to represent the physical state must yield the same result when measuring any physical quantity. This means that all observables need to invariant under G_r, which one states as the observable being gauge invariant. For the energy this translates to

$$[H, G_r] = 0 \ , \quad \forall \ r \tag{2.1.8}$$

Where one should take notice of the subscript, which states that this symmetry is a local symmetry. It might seem odd to choose a theory which over-represents the physical states, which, in some sense, artificially attributes a non-physical symmetry to the system. The technical reason is, that in Quantum field theory this is a way of creating a consistent theory where forces are mediated by vector bosons [36], but the important feature of it is that Eq. (2.1.8) restricts the possible interactions allowed in the Hamiltonian, thereby restricting the dynamics of the system. The reason why this restriction is needed can be found by rewriting the operators in terms of more familiar fields. From [10, 37] one has

$$\sigma_{r,s} \sim e^{iA_{r,s}} \ , \quad \tau_{r,s} \sim e^{i\frac{2\pi}{N}E_{r,s}} \tag{2.1.9}$$

Where one concretely sees how the $\mathbb{Z}_N$ theory only considers the electric flux to be able to take N possible values, since the electric field is defined modulus N. Since τ describes the electric field one denotes a link with the properties $\tau_{link} |\psi_{link}\rangle = \omega^n |\psi_{link}\rangle$ for $n \neq 0$ as a link with an electric flux line going through it.

Now Gauss' law states

$$\nabla \cdot \vec{E}(\vec{r}) = \rho(\vec{r}), \tag{2.1.10}$$

In Chapter 6 Higgs mater will be introduced for the now we are considering the PLGT where no matter is present, which effectively mean $\rho = 0$. This means that the electric flux at each point must be zero. If this is not true then the configuration cannot be realized in our physical world. Gauss' law therefor sets a constrain on the configurations the system can be in. This ultimately limits the Hilbert space such that only states fulfilling Gauss' law, physical states, should be considered. With Eq. (2.1.9) it is possible to define this sub space of the Hilbert space denoted the physical Hilbert space, where all

configurations fulfills Gauss' law. If writing $\sigma_x = \tau$ then for the vertex in Fig. 2.2 Gauss' law can be written as

$$\tau^{up}(\tau^{down})^\dagger(\tau^{left})^\dagger\tau^{right} \sim e^{i\pi((E_{right}-E_{left})+(E_{up}-E_{down}))} \approx e^{i\pi a\nabla\cdot\vec{E}} = e^{i\pi a\rho} \tag{2.1.11}$$

where the discretized definition of the divergence is used and a is the lattice spacing. Taking the Hermitian conjugates is unnecessary since τ represent the Pauli matrices, but it will be instructive when considering a generic $\mathbb{Z}_N$ symmetry. For this vertex the above operator therefore represents the net electric flux going out of a vertex, and since no charges are present it must be demanded for any physical state that this net flux is zero modulus $N = 2$ [3]. For the junction this translates into

$$G_r \equiv \sigma^x_{up}(\sigma^x_{down})^\dagger(\sigma^x_{left})^\dagger\sigma^x_{right} \quad , \text{ and} \tag{2.1.12}$$

$$G_r \ket{\psi_{phys}} = \ket{\psi_{phys}} \ , \quad \forall\, r \tag{2.1.13}$$

As seen in Eq. (2.1.9) σ or σ_z represents the vector potential which is a gauge dependent field. This implies that measuring A will depend in which state is used to represent the given physical state. Taking the example above and representing the state in the σ_z-basis, this means that $\sigma_z \ket{\psi_v}_\sigma$ and $\sigma_z \ket{\psi'_v}_\sigma$ will yield different results even though both states represents the same physical configuration. The gauge generator when acting on a physical state represented in the σ_x basis will yield the same state, while in the σ_z-basis it will translate the state into another state which represents the same physical configuration.

Translating this analysis into the ladder geometry one finds that instead the vertices to only have three connecting links instead of four in the 2D case shown in Fig. 2.2. Comparing to Eq. (2.1.11) this means that there exists no E_{up} or E_{down} depending on weather a top or bottom vertex is considered. The gauge generators therefore becomes

$$\boldsymbol{G}_{i,s} \equiv \sigma^x_{i,s}\sigma^x_{i+1,s}\sigma^x_{i+1,0} \quad , \text{ and} \tag{2.1.14}$$

$$\boldsymbol{G}_{i,s} \ket{\Psi_{phys}} = \ket{\Psi_{phys}} \quad \forall\, i\ , \quad s = \uparrow,\downarrow \tag{2.1.15}$$

which in Fig. 2.1 is represented in red and $\boldsymbol{G}_{i,s}$ should be understood as being defined at the vertex of the connecting links it acts on. The local $\mathbb{Z}_2$ gauge symmetry also constitute itself by the gauge generators fulfilling $\boldsymbol{G}_r^2 = \mathbb{1}$, and the last line not only defines the physical sector of the Hilbert space but also in combination with Eq. (2.1.8) says that the Hamiltonian cannot project a physical state out of the physical sector.

The expression shown in Eq. (2.1.9) can also help to understand the physics behind the different terms in the Hamiltonian. Since the electric field is gauge invariant and appears explicitly in the σ_x-operator, this operator is present in the Hamiltonian and represents the energy density of the electric field[4]. Instead the gauge field A is gauge dependent and one needs to find a combination of σ_z operators which constitute a gauge invariant quantity. The lowest order combination is the plaquette term, which is also a term present in the two dimensional Toric Code [38]. To get a physical understanding of this term lets again utilize the definitions in (2.1.9) to get

$$\sigma^z_{i,0}\sigma^z_{i,\uparrow}\sigma^z_{i+1,0}\sigma^z_{i,\downarrow} \sim e^{i(A_{i,0}+A_{i,\uparrow}+A_{i+1,0}+A_{i,\downarrow})} = e^{i\oint_{p_i}\mathbf{A}\cdot d\mathbf{l}} = e^{i\Phi_{B_i}} \tag{2.1.16}$$

where the closed path integral is taken over the i'th plaquette. The lowest order combination of σ_z operators being gauge invariant is therefore a term which measures the magnetic flux in a given plaquette[5]. Going back to the Hamiltonian one can now give the condition $g \geq 0$ some physical meaning. If g were able to take negative values, one would have a system which could minimize its energy by spontaneously creating either magnetic or electric fluxes, which would be a theory that could not be reconciled with the theory of electromagnetism.

---

[3]For a true $U(1)$ symmetry the net flux should be zero, but since this theory theory only defined the electric field modulus N this will be reflected in Gauss' law.

[4]In the continuum and $U(1)$ limit $(\tau + \tau^\dagger)$ will be proportional to E^2 and describe the true energy density of the electric field.

[5]This will as well in the continuum and $U(1)$ limit become proportional to B^2 and describe the true energy density of the magnetic field.

2.2 Choosing a gauge

Having a redundant Hilbert space can be difficult to work with, and it therefore makes sense to chose a single state to represent the physical configuration. Again taking the example of the junction in Fig. 2.2. Understanding what it means to choose a gauge is different in the two bases. In the σ_z-basis all states are represented twice in the Hilbert space leading to

$$|\psi_v\rangle = |\text{up, down, left, right}\rangle_z = |\pm 1, \pm 1, \pm 1, \pm 1\rangle_z \tag{2.2.1}$$

where

$$G_r |\psi_v\rangle = |\psi'_v\rangle = |\mp 1, \mp 1, \mp 1, \mp 1\rangle_z \tag{2.2.2}$$

By choosing a gauge one chooses a subspace of the Hilbert space where all physical configurations are represented only once. For the junction one can do this by demanding $\sigma_{up}^z |\psi\rangle = |\psi\rangle$. Thereby one chooses to work in a subspace where $\sigma_{up}^z = \mathbb{1}$. If instead representing the state in σ_x-basis one finds G_r to be unity. This means that there is a relation between the four sites, such that by specifying three of the sites the last will ultimately be specified. Since the gauge was chosen such that $\sigma_{up}^z = \mathbb{1}$ it makes sense to eliminate σ_{up}^x by using this relation. Using that we are working in the subspace where $G_r = \mathbb{1}$ one finds $\sigma_{up}^x = \sigma_{down}^x \sigma_{left}^x \sigma_{right}^x$. By having this local gauge symmetry it is possible to eliminate a single d.o.f., and describe it in terms of the other d.o.f. of the vertex.

The redundancy therefore leaves a freedom in describing the dynamics of the system. One can choose a specific set of states to represent all the actual physical states, thereby getting rid of the redundancy. However, by doing so, one needs to make sure, that the Hamiltonian is rewritten such that it only works in this new subspace of the physical Hilbert space and cannot map any state out of it. This is done by using that $G_r = \mathbb{1}$ holds true for the whole physical Hilbert space. The procedure is called gauge fixing and is equivalent to choosing a specific gauge.

A gauge which gets rid of the redundancy is called the axial gauge. In electrodynamics this gauge corresponds to choosing $\hat{\mathbf{n}} \cdot \vec{\mathbf{A}} = 0$. Now the direction $\hat{\mathbf{n}}$ can be chosen as one pleases, but in the ladder geometry one will not get rid of all the redundancy by choosing it to be vertical. A simple way of realizing this, is by thinking of the gauge generator at each vertex as a constrain which makes the d.o.f of the surrounding links dependent on one another. This means that by using this constrain, one can at each vertex eliminate one of the surrounding links d.o.f. With this in mind one realizes that choosing $\hat{\mathbf{n}}$ to be vertically for the ladder geometry, will not eliminate all the redundancy. This is because one for example can choose the constrains on the lower leg to eliminate the rung d.o.f., which leaves the constrains of the upper leg unused. The d.o.f. of the upper leg will therefore still be dependent on one another.

Instead the horizontal direction is chosen, and the d.o.f. of the legs are eliminate or gauge out by demanding

$$\sigma_{i,s}^z |\Psi_{phys}\rangle = |\Psi_{phys}\rangle \quad \forall \, i \, , \, s \in \uparrow, \downarrow. \tag{2.2.3}$$

as done in [24, 34]. The next step is to rewrite the Hamiltonian such that it only operates in the subspace of the physical Hilbert space where Eq. (2.2.3) holds, effectively making the dynamics of the whole system described by rung d.o.f. By using the gauge requirement the plaquette terms trivially simplifies to

$$\underline{\mathrm{H}} = \ldots - \frac{1}{g} \sum_i \sigma_{i,0}^z \sigma_{i+1,0}^z, \tag{2.2.4}$$

where the bar beneath indicates that the Hamiltonian is written in the axial gauge. The electric field terms are less trivial to project into this subspace but as the junction example showed one needs to use the constrains set by the gauge generators. Before doing so, a short intermezzo on the boundaries of this system is needed.
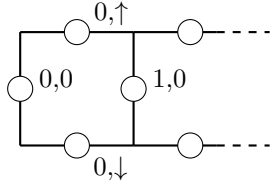
Figure 2.3 | Illustration of a smooth boundary. This figure shows how the boundary of the strip containing site 1 is constructed.
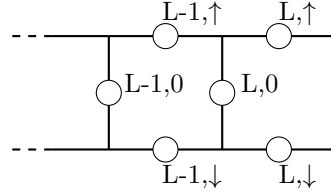
Figure 2.4 | Boundary conditions. This figure shows how the boundary of the strip containing site L is constructed.

The gauge generators at the boundaries take different forms depending on how the boundary is terminated, in this thesis I will adopt two convenient ways of terminating the boundaries which will be used when system length, L, is considered finite. It can either be smooth, which is depicted in Fig. 2.3, or it can be rough which is depicted in Fig. 2.4. To illustrate both boundaries, we choose for this part smooth-rough boundaries, meaning that to the leftmost boundary is smooth and the rightmost is rough. With this termination the gauge generators at the boundaries becomes

$$\boldsymbol{G}_{0,s} = \sigma^x_{0,s}\sigma^x_{0,0}$$
$$\boldsymbol{G}_{L,s} = \sigma^x_{L-1,s}\sigma^x_{L,s}\sigma^x_{L,0} \tag{2.2.5}$$

Had one chosen rough-rough boundaries it would not be possible to eliminate all the d.o.f of legs since there would be more links than vertices in the legs. In Table 2.1 one sees the different possibilities and what they entail. With the smooth-rough boundary one could have added the unfinished plaque-

Left \ Right	Rough	Smooth
Rough	Compared to Eq. (2.2.5) one finds $\boldsymbol{G}_{0,s} = \sigma^x_{0,s}\sigma^x_{0,0}\sigma^x_{1,s}$. With this construction the axial gauge is not possible.	This is equivalent to the boundary configuration investigated below.
Smooth	What is used in the analysis below.	Compared to Eq. (2.2.5) one finds $\boldsymbol{G}_{L,s} = \sigma^x_{L-1,s}\sigma^x_{L,0}$. With this construction the axial gauge is also possible.

Table 2.1| Different boundary constructions. In this table one can read how different constructions of the boundaries resolve in different features.

tte operator $\sigma^z_{L,0}\sigma^z_{L,\uparrow},\sigma^z_{L,\downarrow}$, which is gauge invariant. This term would though break the global $\mathbb{Z}_N$ symmetry generated by $\mathcal{G}$, and is not considered.

Back to the gauge fixing. Eq. (2.1.14) demands $G_{i,s} = \mathbb{1}$ to hold for any state in the physical subspace of the Hilbert space. This mean that by only working in the physical subspace one finds $\sigma^x_{i+1,j} = \sigma^x_{i,s}\sigma^x_{i,0}$, except at the left boundary where $\sigma^x_{0,s} = \sigma^x_{0,0}$. Utilizing these relations yields

$$\sigma^x_{i,s} = \sigma^x_{i-1,s}\sigma^x_{i,0} = \sigma^x_{i-2,s}\sigma^x_{i-1,0}\sigma^x_{i,0} = ... = \prod_{j=0}^{i}\sigma^x_{j,0}, \tag{2.2.6}$$

where $\boldsymbol{G}_{i,s}$ has been utilized i-number of times. Had the system been constructed with a rough-rough boundary, one could not simply exchange $\sigma^x_{0,s}$ with $\sigma^x_{0,0}$, instead the σ_x-operator of the extra link would be attached to this string operator that introduces a domain-wall (or kink) in the rung states [34]. Physically one can understand this rewriting by seeing $\sigma^x_{i,s}$ as an operator which introduces a

magnetic flux into the ith plaquette from the outside. The string operator above instead introduces a magnetic flux from the outside at the 0th plaquette and moves it down the ladder and into the ith plaquette. The operators on each side of the equal sign in Eq. (2.2.6) therefore result in the same physical configuration.

With this rewriting the Hamiltonian in the axial gauge takes the form

$$\underline{H} = \sum_{i=0}^{L-1} -\frac{1}{g}\sigma_i^z\sigma_{i+1}^z - \sum_{i=0}^{L}\sigma_i^x - 2\sum_{i=0}^{L}\prod_{j=0}^{i}\sigma_j^x, \tag{2.2.7}$$

The second index is neglected since all the operators act on the rung sites, and the factor of 2 comes from doing the rewriting described in Eq. (2.2.6) for both legs. The global symmetry represented by $\mathcal{G}$ is mapped into

$$\underline{S}_G = \prod_{i=0}^{L}\sigma_i^x \tag{2.2.8}$$

Which again would not be a symmetry of the system if the unfinished plaquette operator was present in the Hamiltonian.

Before moving on to mapping this into a more familiar Hamiltonian, a few features becomes instructive to point out. In the ferromagnetic limit of $g \to 0$ one finds two degenerate ground states which can be written as

$$\{||s\rangle\rangle_z \equiv |s\rangle_{1,z}|s\rangle_{2,z}...|s\rangle_{L,z} = (\underline{S}_G)^s ||0\rangle\rangle_z \ , \ s = 0,1 \ \}. \tag{2.2.9}$$

where the states for the sake of convenience are labeled as $|0\rangle$ and $|1\rangle$ instead of the respective $|1\rangle$ and $|-1\rangle$. One sees that $\underline{S}_G$ maps $||0\rangle\rangle_z$ into $||1\rangle\rangle_z$. Looking at the Hamiltonian in Eq. (2.2.7) one finds this operator to be present in the Hamiltonian. This means that even in the thermodynamic limit the degenerate ground states will mix for any finite g, which ultimately results in a splitting of the degeneracy to first order in g. This yields a special point at $g = 0$ where the degeneracy is present but for $g > 0$ no degeneracy will show.

2.3 Dual transformation

In [32, 34, 39] the authors present a bond-algebraic duality which maps the non-local Hamiltonian in Eq. (2.2.7) into the quantum Ising model in both a transverse and longitudinal field. The duality mapping is in essence a transformation to a new representation of the algebra of Pauli matrices. The relation between the two representations is given by

$$\sigma_i^z\sigma_{i+1}^z \to \tau_{\tilde{i}}^x \quad \text{for } i < L, \text{ and } \sigma_L^z \to \tau_{\tilde{L}}^x$$
$$\prod_{l\leq i}\sigma_l^x \to \tau_{\tilde{i}}^z \ , \quad \sigma_i^x \to \tau_{\tilde{i}-1}^z\tau_{\tilde{i}}^z \ , \ i \neq 0$$
$$\sigma_0^x \to \tau_{\tilde{0}}^z \tag{2.3.1}$$

The tilde refers to fact that the new coordinates are defined on the dual lattice, where $\tilde{i}$ is defined to be between site i and i+1. Looking at Eq. (2.3.1) one sees how the electric field term takes the form of the magnetic flux term in the new representation and vice versa. The physical intuition of this mapping is therefore that the electric and magnetic field are mapped into one another.

Utilizing this new representation the Hamiltonian takes the form

$$\underline{\tilde{H}} = \sum_{i=0}^{L-1}\left(-\frac{1}{g}\tau_i^x - \tau_i^z\tau_{i+1}^z\right) - 2\sum_{i=0}^{L}\tau_i^z - \tau_0^z. \tag{2.3.2}$$

where the tilde indicates that this Hamiltonian is written in the dual representation. One also sees the same number of operators being present, which relates to the fact that the mapping preserves the number of d.o.f. and thereby the dimension of the Hilbert space. Comparing this to the textbook Ising model in both a transverse and longitudinal field one finds τ_L^x to be missing. To investigate this it makes sense to consider the mapping of the symmetry generator $\mathcal{G}$. This operator is mapped into $\tilde{\mathcal{G}} = \tau_L^z$, and in the dual representation the ground state presented in the τ_x basis in the $g \to 0$ limit instead becomes

$$\{||\tilde{s}\rangle\rangle_x \equiv |0\rangle_{1,x} |0\rangle_{2,x} ... |0\rangle_{L-1,x} |\tilde{s}\rangle_{L,x} = (\tilde{\mathcal{G}})^{\tilde{s}} ||0\rangle\rangle_x \ , \ \tilde{s} = 0, 1 \ \}. \tag{2.3.3}$$

What this reflects is a holographic symmetry [40], where under the dual mapping the global $\mathbb{Z}_2$ symmetry is projected onto the boundary. Again it is observed that the degeneracy generated by this symmetry will be lifted to first order in g by having $\tilde{\mathcal{G}}$ appearing in the dual Hamiltonian.

By taking the thermodynamic limit and focusing on the bulk properties for any $g > 0$ one can forget about τ_L not appearing in the Hamiltonian. Doing so, this Hamiltonian describes the Ising model with both a transverse and a longitudinal field, which is a model containing no spontaneous symmetry breaking for a finite g [41, 42], and therefore showing no phase transitions. Had one applied the same bond-algebraic duality to a truly 2D system, one would instead have found the 2D Ising model in only a transverse field [34] which contains a phase transition [43] between the ferro and para magnetic phase. The PLGT is therefore able to distinguish the dynamics of the the ladder geometry and the 2D system.

Chapter 3

$\mathbb{Z}_N$ pure lattice gauge theory

In this section the attention is still on the PLGT but for the system showing a generic $\mathbb{Z}_N$ gauge symmetry. In doing so the dimensions of the Hilbert space will be extended and the clock operators represented by larger matrices. In the case of $\mathbb{Z}_2$ symmetry one found the Pauli matrices to describe the d.o.f of the gauge bosons. For a generic N we need to generalize these operators to a $N \times N$ dimensional space.

3.1 Pauli matrices in N-dimensional space

In Eq. (2.1.2) and (2.1.3) the fundamental equations describing the gauge d.o.f are presented. The operators satisfying this algebra, which is known as the Weyl group algebra [32], is denoted the clock operators due to the interpretation earlier explained. To rephrase, the operators behave as

$$\sigma^N = \mathbb{1} = \tau^N \ , \quad \sigma^\dagger = \sigma^{N-1} \ , \quad \tau^\dagger = \tau^{N-1} \ , \quad [\tau, \tau^\dagger] = [\sigma, \sigma^\dagger] = 0 \tag{3.1.1}$$

$$\sigma\tau = \omega\tau\sigma. \tag{3.1.2}$$

Where Eq. (3.1.2) is the most common choice used in the literature [44–46]. This choice leads to defining τ as turning the clock hand clockwise since

$$\sigma\tau \left| m \right\rangle_\sigma = \omega\tau\sigma \left| m \right\rangle_\sigma = e^{i\frac{2\pi}{N}(m+1)}\tau \left| m \right\rangle_\sigma . \tag{3.1.3}$$

such that σ is an eigenstate of $(\tau \left| m \right\rangle)$ with eigenvalue $e^{i\frac{2\pi}{N}(1+m)}$. Instead $\tau^\dagger$ turns the hand counter clock wise. Doing the same analysis for a state represented in the τ-basis would show σ to turn the hand counter clockwise. In matrix form the operators take the following form in the σ-basis

$$\sigma = \begin{pmatrix} 1 & 0 & 0 & 0 & \ldots & 0 \\ 0 & \omega & 0 & 0 & \ldots & 0 \\ 0 & 0 & \omega^2 & 0 & \ldots & 0 \\ 0 & 0 & 0 & \ddots & & \vdots \\ \vdots & \vdots & \vdots & & & 0 \\ 0 & 0 & 0 & \ldots & 0 & \omega^{N-1} \end{pmatrix} , \quad \tau = \begin{pmatrix} 0 & 0 & 0 & \ldots & 0 & 1 \\ 1 & 0 & 0 & \ldots & 0 & 0 \\ 0 & 1 & 0 & \ldots & 0 & 0 \\ 0 & 0 & \ddots & & 0 & 0 \\ \vdots & \vdots & & & & \vdots \\ 0 & 0 & 0 & \ldots & 1 & 0 \end{pmatrix} , \tag{3.1.4}$$

which reduces to the Pauli matrices σ_z and σ_x in the case of $N = 2$.

A feature of the Pauli matrices is that raised to the power two they yield the identity. This effectively means that one cannot distinguish which way around the clock the hand turns. For $N > 2$ τ and σ are not self-adjoint, and one can distinguish this. Physically this means that it is now possible to distinguish between which direction the electric and gauge field points. Which way being the positive

direction is therefore needed to be specified. In Fig. 3.1 it is seen how this is defined. Horizontally the direction is chosen to be positive towards the right, while vertically upwards is defined as the positive direction. With this definition, the operator exciting an electric flux going clockwise around the i'th
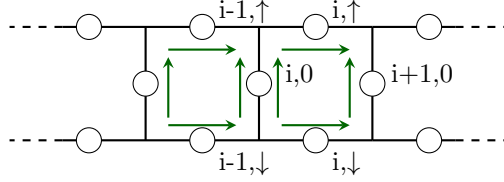
Figure 3.1 | Schematic representation of the positive direction. This figure shows a schematic representation of the Z_N strip, with the green arrow indicating the orientation defined to be positive for the electric field.

plaquette is

$$\sigma_{i,0}^{\dagger}\sigma_{i,\uparrow}^{\dagger}\sigma_{i+1,0}\sigma_{i,\downarrow}. \tag{3.1.5}$$

Such that $|N-1\rangle_{\tau}^{i,0}$ presents an electric flux line going downwards and $|1\rangle_{\tau}^{i+1,0}$ a flux line going upwards [1]. It also instructive to go back to the physical quantity described by the plaquette operator showed in Eq. (2.1.16). Wanting the plaquette terms to measure the magnetic flux through the plaquette, it needs to be of the form

$$B_i \sim e^{e^{i \oint_{p_i} \mathbf{A} \cdot d\mathbf{l}}} \tag{3.1.6}$$

where B_i is defined as the plaquette operator. By dividing the contour into the four discrete segments of the plaquette and defining counter-clock wise as the positive direction, one sees that on the left and top this will point in the negative direction while to the right and at the bottom it will point in the positive direction. This means that this can be divided into

$$B_i \sim e^{i \oint_{p_i} \mathbf{A} \cdot d\mathbf{l}} \approx e^{i(-A_{i,0}-A_{i,\uparrow}+A_{i+1,0}+A_{i,\downarrow})} \sim \sigma_{i,0}\sigma_{i,\uparrow}\sigma_{i+1,0}^{\dagger}\sigma_{i,\downarrow}^{\dagger} \tag{3.1.7}$$

where the relation in Eq. (2.1.9) is used. Wanting the gauge constrains to demand Gauss law fulfilled at each vertex, they also need modification. Again utilizing Eq. (2.1.9) the gauge generators need to yield

$$G_{i,\uparrow} \sim e^{ia\frac{2\pi}{N}\boldsymbol{\nabla}\cdot\mathbf{E}_{i,\uparrow}} = e^{i\frac{2\pi}{N}[-(E_{i,\uparrow}-E_{i-1,\uparrow})+E_{i,0}]} \tag{3.1.8}$$

$$G_{i,\downarrow} \sim e^{ia\frac{2\pi}{N}\boldsymbol{\nabla}\cdot\mathbf{E}_{i,\downarrow}} = e^{i\frac{2\pi}{N}[-(E_{i,\downarrow}-E_{i-1,\downarrow})-E_{i,0}]}. \tag{3.1.9}$$

For this to hold one finds

$$G_{i,\uparrow} = \tau_{i-1,\uparrow}\tau_{i,\uparrow}^{\dagger}\tau_{i,0} \tag{3.1.10}$$

$$G_{i,\downarrow} = \tau_{i-1,\downarrow}\tau_{i,\downarrow}^{\dagger}\tau_{i,0}^{\dagger} \tag{3.1.11}$$

Here one should notice the difference between the gauge generators of each leg, which comes from the fact that for the upper leg the electric flux of the rung should be positive if it is to point toward the vertex, while for the lower leg a positive electric flux in the rung means it is pointing away.

---

[1] Looking at the Hamiltonian, one sees that the electric field term will attribute both these states the same energy cost. This is consistent with the fact that the energy cost of having an electric field is proportional to $|E|^2$ and is not directional dependent. The same holds for the energy cost of exciting a magnetic flux in a plaquette.

3.2 The Hamiltonian

Using Eq. (3.2.5) it is now possible to state the Kogut-Susskind Hamiltonian for a generic N

$$H = -\frac{1}{g} \sum_{i=0}^{L-1} (\sigma_{i,0}^{\dagger} \sigma_{i,\uparrow}^{\dagger} \sigma_{i+1,0} \sigma_{i,\downarrow} + \text{H.c.}) - \sum_{i=0}^{L} \sum_{s=0,\uparrow,\downarrow} (\tau_{i,s} + \tau_{i,s}^{\dagger}). \tag{3.2.1}$$

where the smooth-rough boundary has been chosen[2] [3]. The gauge generators are given by

$$G_{i,\uparrow} = \tau_{i-1,\uparrow} \tau_{i,\uparrow}^{\dagger} \tau_{i,0} , \quad G_{i,\downarrow} = \tau_{i-1,\downarrow} \tau_{i,\downarrow}^{\dagger} \tau_{i,0}^{\dagger} \quad \text{for} \quad i \neq 0 \tag{3.2.2}$$

$$G_{0,\uparrow} = \tau_{i,\uparrow}^{\dagger} \tau_{i,0} , \quad G_{0,\downarrow} = \tau_{0,\downarrow}^{\dagger} \tau_{i,0}^{\dagger} \tag{3.2.3}$$

3.2.1 Axial gauge

As for the $\mathbb{Z}_2$ case it is impractical to work in the whole physical Hilbert, and it is convenient to work in some specific gauge or subspace of the physical Hilbert space where physical configurations are uniquely presented. To fix the gauge, the axial gauge is chosen which demands the following of the subspace

$$\sigma_{i,s} |\psi_{axial}\rangle = |\psi_{axial}\rangle , \quad \forall \, i \, , \, s \in \{\uparrow, \downarrow\}. \tag{3.2.4}$$

Again the plaquette term trivially becomes

$$\underline{\mathrm{H}} = \ldots - \frac{1}{g} \sum_{i}^{L-1} \sigma_{i+1}^{\dagger} \sigma_i + \text{h.c.}. \tag{3.2.5}$$

To make sure that the Hamiltonian only works in this subspace and does not project any state out of it, we need to rewrite the electric field terms of the legs. This is again done by using the gauge generators to rewrite the electric field terms of the legs in terms of the ones in the rung. With $\boldsymbol{G} = \mathbb{1}$ being true in the physical Hilbert space, the electric field terms of the legs can be rewritten in the same fashion as before

$$\tau_{i,\uparrow} = \tau_{i-1,\uparrow} \tau_{i,0} = \tau_{i-2,\uparrow} \tau_{i-1,0} \tau_{i,0} = \ldots = \prod_{j=0}^{i} \tau_{j,0}$$

$$\tau_{i,\downarrow} = \tau_{i-1,\downarrow} \tau_{i,0}^{\dagger} = \tau_{i-2,\downarrow} \tau_{i-1,0}^{\dagger} \tau_{i,0}^{\dagger} = \ldots = \prod_{j=0}^{i} \tau_{j,0}^{\dagger}. \tag{3.2.6}$$

Where one should imagine that the first equal sign comes from using $G_{i,s}$, the next would come by using $G_{i-1,s}$ and so on until $G_{0,s}$ is used to reach the result. As previously explained, the physical intuition behind this rewriting comes from the operators on each side of the equal sign creating the physical configuration change. Both introduce a magnetic flux in the ith plaquette, and these two operators will change any physical state in the same manner. This comes from the fact that the commutation relation, with respect to any gauge invariant operator, is the same for the two operators. This can be seen by realizing that in the PLGT all gauge invariant operators containing σ-operators will be built from products of the plaquette operators. If the operators on each side of the equal sign in Eq. (3.2.6) commute in the same way with all plaquette operators then they will change all observables of the

---

[2]This can be seen by there being as many links on each legs as there are in the rung.

[3]This Hamiltonian corresponds to the one in Eq. (2.1.4) up to a factor of 2.

system in the same way.

$$B_j \tau_{i,\uparrow} = \begin{cases} \omega \tau_{i,\uparrow} B_j & \text{if } j = i \\ \tau_{i,\uparrow} B_j & \text{otherwise} \end{cases} \tag{3.2.7}$$

$$B_j \prod_{m=1}^{i} \tau_{m,0}^{\dagger} = \begin{cases} \omega \prod_{m=0}^{i} \tau_{m,0}^{\dagger} B_j & \text{if } j = 1 \\ \prod_{m=0}^{i} \tau_{m,0}^{\dagger} B_j & \text{otherwise,} \end{cases} \tag{3.2.8}$$

where both operators trivially commute with all possible combinations of τ-operators and the same holds for $s = \downarrow$.

The Hamiltonian represented in the axial gauge becomes

$$\underline{H} = -\frac{1}{g} \sum_{i=0}^{L-1} (\sigma_{i+1}^{\dagger} \sigma_i + \text{H.c.}) - \sum_{i=0}^{L} (\tau_i + \tau_i^{\dagger}) - 2 \sum_{i=0}^{L} (\prod_{j \leq i} \tau_j + \prod_{j \leq i} \tau_j^{\dagger}). \tag{3.2.9}$$

In the ferromagnetic limit of $g \to 0$ and the thermodynamic limit of $L \to \infty$ the global symmetry generated by $\mathcal{G}$ is spontaneously broken

$$\mathcal{G} \equiv \prod_{i=0}^{L} \tau_j. \tag{3.2.10}$$

and the ground states are

$$\{ ||s\rangle\rangle_{\sigma} \equiv |s\rangle_{1,\sigma} |s\rangle_{2,\sigma} \dots |s\rangle_{L,\sigma} = (\mathcal{G})^s ||0\rangle\rangle \;,\; s = 0, 1, \dots N - 1 \}, \tag{3.2.11}$$

Again $\mathcal{G}$ appears in the Hamiltonian such that for $g > 0$ the degenerate ground state manifold will be split to first order in g, thereby destroying the ordered phase and restoring the symmetry of the GS, which is not degenerate any longer.

3.2.2   Dual transformation

To get this Hamiltonian in a more familiar form the bond-algebraic duality is again used. In the generic N case the mapping states

$$\sigma_i^{\dagger} \sigma_{i+1} \to \tilde{\tau}_i^{\dagger} \quad \text{for } i \neq L, \quad \sigma_L \to \tilde{\tau}_L \tag{3.2.12}$$

$$\prod_{j=0}^{i} \tau_j \to \tilde{\sigma}_i \;,\quad \tau_i \to \tilde{\sigma}_{i-1}^{\dagger} \tilde{\sigma}_i \quad \text{for } i \neq 0, \quad \tau_0 = \tilde{\sigma}_0 \tag{3.2.13}$$

From where the Hamiltonian represented in the dual basis becomes

$$\underline{\tilde{H}} = -\frac{1}{g} \sum_{i=0}^{L-1} (\tau_i^{\dagger} + \tau_i) - \sum_{i=1}^{L} (\sigma_{i-1}^{\dagger} \sigma_i + \sigma_i^{\dagger} \sigma_{i-1}) - 2 \sum_{i=0}^{L} (\sigma_i + \sigma_i^{\dagger}) - (\sigma_0 + \sigma_0^{\dagger}), \tag{3.2.14}$$

where the tildes have been neglected. This looks much like the p-clock model with both a transverse and longitudinal field [46, 47] with the exception of τ_L missing. The reason for this is most easily understood in the limit of $g \to 0$, where we know $\mathcal{G}$ is spontaneously broken. Through this dual mapping on finds $\tilde{\mathcal{G}} = \sigma_L$, such that the ground states can be written as

$$\{ ||\tilde{s}\rangle\rangle_{\tau} = |0\rangle_{1,\tau} |0\rangle_{2,\tau} \dots |0\rangle_{L-1,\tau} |\tilde{s}\rangle_{L,\tau} = (\tilde{\mathcal{G}})^{\tilde{s}} ||0\rangle\rangle_{\tau} \;,\; \tilde{s} = 0, 1, \dots N - 1 \}. \tag{3.2.15}$$

The missing τ_L operator therefore represent how the global $\mathbb{Z}_N$ symmetry is projected onto the boundary. Again one finds that for $g > 0$ the degeneracy is split due to $\tilde{\mathcal{G}}$ being present in the Hamiltonian.

If only caring about the bulk properties in the thermodynamic limit for $g > 0$ one can forget that τ_L is not appearing in Hamiltonian. By doing so one is left with the 1D quantum p-clock model in both a transverse and longitudinal field.

The 1D quantum p-clock model in solely a transverse field has been extensively studied in the literature (see, for example, [47]). It is known that for $N < 5$ this model shows a disordered and ordered phase [48], while for $N \geq 5$ an intermediate gapless phase is found with transitions of the Berezinskii–Kosterlitz–Thouless (BKT) type. The model with an added longitudinal field has not been studied to the same degree, but in the next section different features will be investigated.

3.3 Confined and deconfined phases

A supporting pillar in the research field of lattice gauge theories is the prediction of the confined phase in QCD where quarks are confined into composite particles [5, 6]. The confined phase describes a phase where the energy increases linearly with the separation distance of two opposite static charges[4]. If defining $\Delta E(R)$ as the difference in energy between having introduced two static charges at a distance R apart and having no charges, the confined phase will yield

$$\Delta E(R) = TR \tag{3.3.1}$$

for a large R compared to the lattice spacing [34]. T denotes the "string tension", and has the unites of energy per unit length.

To see whether this system supports such phase, one can introduce such two static charges, where by investigating the new ground state and the energy cost of separating the charges one can determine if the phase shows confining of deconfining behavior. This is investigated perturbatively in the following two sections.

3.3.1 $g \gg 1$

Instead of taking a finite but large g, it is instructive to first look at the case of $g \to \infty$ where the energy of introducing an electric flux dominates and the system is described by

$$H^{(0)} = -\sum_{i=0}^{L} \sum_{s=0,\uparrow,\downarrow} (\tau_{i,s}^\dagger + \tau_{i,s}). \tag{3.3.2}$$

with the ground state given by

$$||0\rangle\rangle_\tau \equiv \bigotimes_r |0\rangle_{\tau,r}. \tag{3.3.3}$$

Hence a product state where no electric flux is present. Having the ground state being an eigenstate of the τ operators, which directly describes a measurable quantity, it becomes instructive to not choose a specific gauge in the following part. This leads to the physical configuration of the system showing more clearly.

Wanting to introduce two opposite charges with infinite mass into the system, the gauge generators must define a different physical Hilbert space where this holds. For the sake of simplicity, both charges are inserted in the upper leg, which will insure that the shortest path between them is unique[5]. At position $\bar{x} = (x, \uparrow)$ a positive charge is introduced, and at position $\bar{y} = (y, \uparrow)$ a negative where $y > x$. This leads to two new constraints on the physical Hilbert space

$$\begin{aligned} \boldsymbol{G}_{\bar{x}} |\psi_{phys}\rangle &= \bar{\omega} |\psi_{phys}\rangle \\ \boldsymbol{G}_{\bar{y}} |\psi_{phys}\rangle &= \omega |\psi_{phys}\rangle \end{aligned} \tag{3.3.4}$$

---

[4]Static essentially means the charges have infinite mass and cannot propagate anywhere
[5]Had one chosen the charges to be on two different legs, one would find the ground state to be a super position of the shortest paths.

such that Gauss law now states the presence of two opposite charges at $\bar{x}$ and $\bar{y}$.

In order to construct the ground state, one should keep in mind that everywhere but $\bar{x}$ and $\bar{y}$ the ground state $|GS\rangle$ needs to fulfill $\boldsymbol{G}_{i,s}|GS\rangle = |GS\rangle$. As presented above the limit of $g \to \infty$ will favor having no electric flux line present. Due to Eq. (3.3.4) one must have some electric flux line present, and the system will try to minimize the number of these. To get an idea of what the ground state looks like, it can help look at the vertex at $\bar{x}$ shown in Fig. 3.2. Here one sees how the constraint at
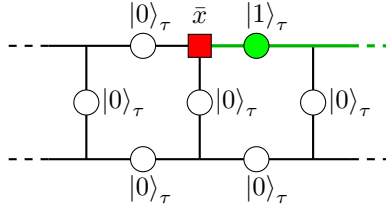
Figure 3.2 | **Schematic representation of a physical state**. This figure shows a possible physical state when a static charge as been introduced at position $\bar{x}$. Acting on this state with $\boldsymbol{G}_{\bar{x}}$ will fulfill what is required by Eq. (3.3.4). From Eq. (3.2.3) one gets that the state to the right of the vertex with charge, $(x + 1, \uparrow)$, needs to be in the state $|1\rangle_\tau$, while if the electric flux had leaved along one of the other two links they should be in $|-1\rangle_\tau$. These three possibilities all ensure Eq. (3.3.4) to hold, but other of higher excitations of the τ-states are also possible.

position $\bar{x}$ in Eq. (3.3.4) demands, that at least one electric flux line must leave the site. Next the gauge generator at the position right of the vertex at $\bar{x}$, $(x + 1, \uparrow)$ has the constraint $\boldsymbol{G}_{i,s}|GS\rangle = |GS\rangle$. This means that since one electric flux is entering another one must leave, and this is what is depicted by the continuing green line in Fig. 3.2. It would also be possible to abide the constraint by deexciting the rung link, so that it would be in state $|N - 1\rangle_\tau$.

From Eq. (3.3.2) the energy cost of changing a link from state $|0\rangle_\tau$ to $|k\rangle_\tau$ is $2(1 - \cos\left(\frac{2\pi}{N}k\right))$. The Hamiltonian therefore energetically favours states with no electric flux excited at each link. In this way one can construct the ground state by making sure that the minimum amount of links have been excited and the different gauge constraints to be fulfilled. Proceeding in this way yields a ground state where the shortest path between $\bar{x}$ and $\bar{y}$ denoted $\gamma(\bar{x}, \bar{y})$, defines the path along which the links are excited. This is shown in Fig. 3.3, where the green lines describe links being in the excited $|1\rangle_\tau$ state and the black lines a links in $|0\rangle_\tau$. The ground state is written as
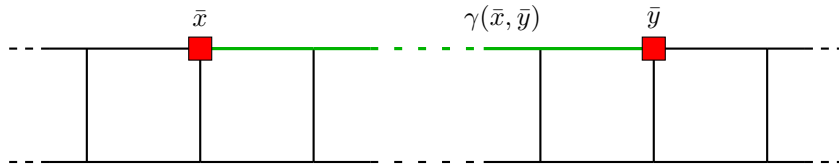
Figure 3.3 | **Schematic representation of the ground state**. This figure shows the ground state of a system having two opposite charges. The green lines represent links in state $|1\rangle_\tau$ whereas the black lines represent links in the state $|0\rangle_\tau$. $\gamma(\bar{x}, \bar{y})$ is the shortest path between $\bar{x}$ and $\bar{y}$.

$$||0; \gamma(\bar{x}, \bar{y})\rangle\rangle_\tau \equiv \bigotimes_{i \notin \gamma} |0\rangle_{\tau,i} \bigotimes_{j \in \gamma} |1\rangle_{\tau,j} \tag{3.3.5}$$

Had the charges been switched around one would find the excited states to be in $|N - 1\rangle_\tau$ instead, from where an analogy is found to electromagnetism, where the field lines change direction depending on it being a positive or negative charge.

In order to tell weather or not this regime supports confinement of charges, the energy as function of the distance between the charges, $R = |\bar{x} - \bar{y}|$, needs to be calculated. Using Eq. (3.3.2) the ground state energy with the static charges becomes

$$E_{\bar{x},\bar{y}} = 2R - 2R\cos\left(\frac{2\pi}{N}\right) - 3 \cdot 2L = 2R(1 - \cos\left(\frac{2\pi}{N}\right)) + E_0 \tag{3.3.6}$$

$$\Delta E(\bar{x}, \bar{y}) = 2(1 - \cos\left(\frac{2\pi}{N}\right))R = TR \tag{3.3.7}$$

Where E_0 is the ground state energy with no charges. Comparing this to Eq. (3.3.1), this limit is shown to support a confined phase with the string tension given by $T = 2(1 - \cos(2\pi/N))$. It is observed that the local gauge symmetry determines the strength of the string tension and that it decreases for increasing N. This result is also in agreement with the result presented in [34] for a 2D system with $N = 2^6$.

If turning on a large but finite g, one introduces perturbations to the system which is now investigated to see whether they support the confined phase or destroy it. The perturbation to the Hamiltonian takes the form

$$\mathrm{H}^{(1)} = -\frac{1}{g}\sum_{i=0}^{L-1}(\sigma_{i,0}^\dagger\sigma_{i,\uparrow}^\dagger\sigma_{i+1,0}\sigma_{i,\downarrow} + h.c.), \tag{3.3.8}$$

In non-degenerate perturbation theory one finds the first non-zero contribution coming from the second order term. This term yields

$$\mathrm{E}_{\bar{x},\bar{y}}^{(2)} = \frac{-1}{g^2}\left(\left(\frac{1}{4(1 - \cos(2\pi/N))} + \frac{1}{2(3 - 2\cos(2\pi/N) - \cos(4\pi/N))}\right)R \right.$$
$$\left. + \frac{2}{8(1 - \cos(2\pi/N))}(L - R)\right) \tag{3.3.9}$$

Where the first term comes from exciting a plaquette between the two charges, where exciting a plaquette refers to operation $B_i|\psi\rangle$ and deexciting refers to $B_i^\dagger|\psi\rangle$. The second term comes from deexciting a plaquette between the two charges, and the last term comes from doing any of two outside of the charges, so in the other $(L - R)$ plaquette. If doing perturbation theory for the system without charges one finds

$$\mathrm{E}_0^{(2)} = \frac{-1}{g^2}\frac{2}{8(1 - \cos(2\pi/N))}(L). \tag{3.3.10}$$

Such that the difference in energy between the ground state with no charges and the one with is

$$\Delta\mathrm{E} = \left(2(1 - \cos(2\pi/N)) - \frac{1}{g^2}\left(\frac{1}{2(3 - 2\cos(2\pi/N) - \cos(4\pi/N))}\right)\right)R + \mathcal{O}(1/g^4)$$
$$= TR + \mathcal{O}((1/g^4). \tag{3.3.11}$$

Which still shows linearity up to fourth order in $1/g$ but with a diminished string tension. It is therefore possible to imagine, that by decreasing the value of g one would find $T \to 0$, but this analysis tells that the confining phase is stable when turning on weak plaquette interactions. It also suggest that the stability of this phase diminishes with increasing N, since the string tension goes down as a result. Another remark is that to fourth order, there will appear terms proportional to R^2, since the fourth order contribution has the possibility of exciting and de-exciting two plaquettes between the charges. The onset of a quadratic term, however, would not change the confined nature of this phase.

---

[6]To get the same Hamiltonian as in [34] one though has to scale the Hamiltonian by $1/2$. This scaling also ensure that the Hamiltonian in Eq. (3.2.1) becomes equivalent to the $\mathbb{Z}_2$ Hamiltonian shown in Eq. (2.1.4).

The above analysis was performed in no specific gauge, which showed no added complexity in comparison with doing it in specific gauge. This was due to the τ-basis being a basis where there occurs no physical redundancy in the Hilbert space. Performing these calculations in no specific gauge gives the possibility of observing the physical configuration of the ground state with two static charges present. This would have been obscured by choosing a specific gauge. In appendix B one finds the calculations performed in the axial gauge, which show the same result.

3.3.2 $g \to 0$

In this limit it is instructive to see how the same calculations as done in the limit of $g \to \infty$ are performed without choosing a gauge, but also tedious. The tediousness comes from the fact that multiple states in the σ-basis corresponds to the same physical state, so one has to be cautious in performing different calculations such that no state is accounted for multiple times. The instructive part comes in how different terms in the perturbative calculations can be represented diagramatically and how one can get an understanding of the physical configuration of the ground state. In appendix B such calculations are found, but in the following part the axial gauge is chosen.

Calculations in the Axial gauge

The Hamiltonian in the axial gauge is found in Eq. (3.2.9). By taking the limit of $g \to 0$ the ground state becomes the N-times degenerate state $||s\rangle\rangle$ described in Eq. (3.2.11), but before deploying the tools given to us by perturbation theory, the boundary can be changed which eases the calculations.

In the section on the $\mathbb{Z}_2$ strip different boundaries were discussed, where we in the part above chose the smooth-rough boundaries (SR). If instead choosing smooth-smooth by adding a rung link at the rightmost end, it is possible to get rid of the redundancy found in the ground state manifold. Choosing SS leaves us with two new gauge generators, such that in addition to ones found in Eq. (3.2.3) there is

$$G_{L+1,\uparrow} = \tau_{L,\uparrow}\tau_{L+1,0} , \quad G_{L+1,\downarrow} = \tau_{L,\downarrow}\tau_{L+1,0}^{\dagger}. \tag{3.3.12}$$

With this new boundary construction new terms needs to be added to the Hamilton, and it becomes

$$H = -\frac{1}{g}\sum_{i=0}^{L}(\sigma_{i,0}^{\dagger}\sigma_{i,\uparrow}^{\dagger}\sigma_{i+1,0}\sigma_{i,\downarrow} + \text{H.c.}) - \sum_{i=0}^{L}\sum_{s=\uparrow,\downarrow}(\tau_{i,s} + \tau_{i,s}^{\dagger}) - \sum_{i=0}^{L+1}(\tau_{i,0} + \tau_{i,0}^{\dagger}). \tag{3.3.13}$$

An important feature to notice for this new construction is that two new gauge generators were added while only one new d.o.f was. One could therefore quickly believe that this leads to the possibility of eliminating two extra d.o.f when choosing a gauge, but this is not possible due to the relation

$$\prod_{i=0}^{L+1} G_{i,\uparrow}G_{i,\downarrow} = \mathbb{1} \tag{3.3.14}$$

which ultimately means that by fixing the gauge for all vertices except one, this vertex will be in a specific gauge[7]. Changing the boundaries to SS thereby only leaving us with the possibility of eliminating one extra d.o.f. Let us take the example of the axial gauge. If imagining the system being in some generic product state represented in the σ-basis, one can use a given gauge generator to ensure Eq. (3.2.4) for the site the right of just that vertex. To ensure this one does not need the extra gauge generators of Eq. (3.3.12). One can though use one of these generators to ensure the extra constraint

$$\sigma_{L+1,0}|\psi_{axial}\rangle = |\psi_{axial}\rangle . \tag{3.3.15}$$

---

[7]Another way of saying this, is that gauge generators are not all independent. Instead one can move one of the gauge constraint to the other side, such that acting on a state with that specific generator corresponds to acting with all the other gauge constraints on the state.

Thereby one uses all the gauge generators except for one of the extra constraints, but the gauge is now fully fixed[8].

In comparison to the previous part where the gauge was fixed, one now needs to keep the static charges in mind, and more specifically one should be conscious about the relation found in Eq. (3.3.4). Having these new constraints leads to Eq. (3.2.6) becoming

$$\tau_{i,\uparrow} = \tau_{i-1,\uparrow}\tau_{i,0} = \tau_{i-2,\uparrow}\tau_{i-1,0}\tau_{i,0} = ... = \prod_{j=0}^{i} \tau_{j,0} \quad \text{for } i \notin \gamma(\bar{x}, \bar{y})$$

$$\tau_{i,\uparrow} = \tau_{i-1,\uparrow}\tau_{i,0} = \tau_{i-2,\uparrow}\tau_{i-1,0}\tau_{i,0} = ... = \omega \prod_{j=0}^{i} \tau_{j,0} \quad \text{for } i \in \gamma(\bar{x}, \bar{y})$$

$$\tau_{i,\downarrow} = \tau_{i-1,\downarrow}\tau_{i,0}^{\dagger} = \tau_{i-2,\downarrow}\tau_{i-1,0}^{\dagger}\tau_{i,0}^{\dagger} = \prod_{j=0}^{i} \tau_{j,0}^{\dagger} \tag{3.3.16}$$

Where one sees that for $i \in \gamma$ the kink operator picks up a phase. This comes from Eq. (3.3.4) since one will use the $G_{\bar{x}}$ operator but not $G_{\bar{y}}$ in the rewriting. From $G_{\bar{x}}$ and $G_{\bar{y}}$ one respectively gets

$$\tau_{x,\uparrow} = \omega\tau_{x-1,\uparrow}\tau_{x,0} \tag{3.3.17}$$

$$\tau_{y,\uparrow} = \omega^{*}\tau_{y-1,\uparrow}\tau_{x,0} \tag{3.3.18}$$

such that for $i \geq y$ the two phases will cancel one another while for $i \in \gamma$ the phase from $G_{\bar{x}}$ will remain.

Using Eq. (3.3.16) and the extra constraint found in Eq. (3.3.15) the Hamiltonian in the axial gauge takes the form

$$\underline{H}_{SS} = -\frac{1}{g}\sum_{i=0}^{L-1}(\sigma_i^{\dagger}\sigma_{i+1} + \text{H.c.}) - \frac{1}{g}(\sigma_L + \sigma_L^{\dagger}) - \sum_{i=0}^{L}(\tau_i + \tau_i^{\dagger})$$

$$-2\sum_{i\notin\gamma(\bar{x},\bar{y})}\left(\prod_{i\geq j}\tau_j^{\dagger} + \text{H.c.}\right) - \sum_{i\in\gamma(\bar{x},\bar{y})}\left((\omega+1)\prod_{i\geq j}\tau_j + \text{H.c.}\right) - \left(\prod_{i=0}^{L}\tau_i + \prod_{i=0}^{L}\tau_i^{\dagger}\right) \tag{3.3.19}$$

The second term comes from the extra constraint, which ultimately breaks the global $\mathbb{Z}_N$ symmetry in the ferromagnetic limit. The second term in the second line comes from the electric field term from both legs in between the charges, where the upper leg picks up a phase while the lower does not. By setting this phase to 1, one finds the Hamiltonian describing the system with no static charges present. The last term in the second line comes from the electric field term of the last rung site at $(L+1, 0)$. Having specified the gauge this Hamiltonian now operates in Hilbert space where no physical configuration is represented more than once. This shows how inserting static charges into the system directly changes the dynamics of the system. Before when no gauge was chosen, one had to be care full with choosing a ground state where all the gauge constraints were fulfilled, but doing the calculations this way eliminates that worry.

Going back to case of $g \to 0$ the system now ends up in a non-degenerate ground state given by $||0\rangle\rangle_{\sigma}$, such that by turning on a small but finite g it is possible to use non-degenerate perturbation

---

[8]One could also choose $\sigma_{0,0}|\psi_{axial}\rangle = |\psi_{axial}\rangle$.

theory. With the Hamiltonian and the perturbation given by

$$\underline{\mathrm{H}}^0 = -\frac{1}{g} \sum_{i=0}^{L-1} (\sigma_i^\dagger \sigma_{i+1} + \mathrm{H.c.}) - \frac{1}{g}(\sigma_L + \sigma_L^\dagger) \qquad (3.3.20)$$

$$\underline{\mathrm{H}}^1 = -\sum_{i=0}^{L}(\tau_i + \tau_i^\dagger) - 2\sum_{i\notin\gamma(\bar{x},\bar{y})}\left(\prod_{i\geq j}\tau_j^\dagger + \mathrm{H.c.}\right) - \sum_{i\in\gamma(\bar{x},\bar{y})}\left((\omega+1)\prod_{i\geq j}\tau_j + \mathrm{H.c.}\right)$$

$$-\left(\prod_{i=0}^{L}\tau_i + \prod_{i=0}^{L}\tau_i^\dagger\right) \qquad (3.3.21)$$

In the limit of $g = 0$ one finds that the terms changed by the presence of the static charges are not present, and one finds

$$E^0_{\bar{x},\bar{y}}(g \to 0) = -\frac{2L}{g} = E^0(g \to 0) \qquad (3.3.22)$$

Where $E^0(g \to 0)$ represents the ground state energy with no static charges. This leads to $\Delta E(g \to 0) = 0$ and thereby supporting a deconfined phase where charges with a finite mass would be able to move freely around.

Next we turn on a small but finite g, which from non-degenerate perturbation theory gives us the lowest order correction to the energy

$$E_{SS}(1 >> g) = -\frac{2L}{g} - g\frac{9L + 34 - 4R\left(1 - \cos\left(2\pi/N\right)\right)}{2(1 - \cos\left(2\pi/N\right))} + \mathcal{O}(g^5) \qquad (3.3.23)$$

From where one finds by taking $R \to 0$

$$\Delta E(1 >> g) = 2gR = TR. \qquad (3.3.24)$$

One therefore observes the deconfined phase to be unstable under this perturbation, since to the lowest order in yields a linear increase in energy between the two charges with separation distance. This is again a different result from having a truly 2D system which is shown in Appendix D, where the energy decreases exponentially as a function of the separation distance thereby still support a deconfining phase.

Chapter 4

Higgs matter

In this chapter we want to expand the model to incorporate dynamical matter, and more precisely Higgs matter [24]. In introducing matter one needs to specify the algebra of the operators describing the matter d.o.f., and how they transform under the local gauge transformation. This defines which interactions are possible to incorporate in the Hamiltonian and therefore ultimately defines the dynamics of the system.

4.1 The Hamiltonian

If defining the Hermitian creation operator of the Higgs boson as ζ, then it transforms in the following way

$$\zeta_r \quad \rightarrow \quad \zeta_r' \equiv \boldsymbol{G}_r^\dagger \zeta_r \boldsymbol{G}_r = \omega \zeta_r. \tag{4.1.1}$$

[24, 31, 34]. Since the gauge generators and ζ does not commute one must have that the Higgs matter and the gauge bosons interact, which ultimately means that the Higgs bosons carry charge. This is not trivially seen and will be easier understood when the gauge generators are defined. This relation also shows the cyclic behavior of the charge. If one were to perform this gauge transformation N-times, then ζ would be transformed back into it self and no phase would show. The charge is therefore, as the electric field, only defined modulus N which leads to the fact, that if one were to excite N Higgs bosons at the same site, ζ^N, no charge would be excited.

Next we define the Hermitian operator η. This operator is conjugated to ζ and it, instead of exciting the Higgs field, measures if any Higgs matter or charge is present at the given site. These two operators fully describe the d.o.f. of the Higgs matter, and they obey the following onsite algebraic relations

$$\zeta^N = \mathbb{1} = \eta^N \ , \quad \zeta^\dagger = \zeta^{N-1} \ , \quad \eta^\dagger = \eta^{N-1} \ , \quad [\eta, \eta^\dagger] = 0 = [\zeta, \zeta^\dagger] \tag{4.1.2}$$

$$\zeta\eta = \omega\eta\zeta. \tag{4.1.3}$$

The operators both commute with σ and τ. This is again the familiar quantum clock operators, which also describe the gauge bosons. From Eq. (4.1.3) one finds η and ζ to behave as the following in the η-basis

$$\eta \left|s\right\rangle_\eta = \omega^s \left|s\right\rangle_\eta \ , \quad \zeta \left|s\right\rangle_\eta = \left|s - 1 \text{ mod N} \right\rangle_\eta \tag{4.1.4}$$

such that ζ in the same manner as σ turns the clock handle counter-clockwise, while in the basis where ζ is diagonal one will find η to turn it clock wise. In the τ basis one should interpret s as the charge modulus N present at the site, and one can represent the operator as

$$\eta \sim e^{i\frac{2\pi}{N}\rho} \tag{4.1.5}$$

With this relation it is again possible to define the physical Hilbert space by demanding Guass' law to be fulfilled at each vertex. Since dynamical matter is present the gauge generators need modification, such that instead of the net flux of the electric field being zero, it instead describes the charge density present at the site. This leads to gauge generators being defined as

$$\begin{aligned} \boldsymbol{G}_{i,\uparrow} &= \tau_{i-1,\uparrow}\tau_{i,0}\tau_{i,\uparrow}^{\dagger}\eta_{i,\uparrow} \sim e^{i\frac{2\pi}{N}(\nabla\mathbf{E}-\rho)} \\ \boldsymbol{G}_{i,\downarrow} &= \tau_{i-1,\downarrow}\tau_{i,0}^{\dagger}\tau_{i,\downarrow}^{\dagger}\eta_{i,\downarrow} \sim e^{i\frac{2\pi}{N}(\nabla\mathbf{E}-\rho)}, \end{aligned} \tag{4.1.6}$$

For any state in the physical Hilbert space one therefore demands

$$\boldsymbol{G}_r \left|\psi_{phys}\right\rangle = \left|\psi_{phys}\right\rangle \tag{4.1.7}$$

Form Eq. (4.1.1) one therefore realizes that ζ will map any physical state out of the physical Hilbert space and into the non-physical Hilbert space since

$$\zeta_r' \left|\psi_{phys}\right\rangle = \boldsymbol{G}_r^{\dagger}\zeta_r \left|\psi_{phys}\right\rangle = \omega\zeta_r \left|\psi_{phys}\right\rangle \tag{4.1.8}$$

such that the state $\zeta_r \left|\psi_{phys}\right\rangle$ does not obey Gauss' law due to the ω appearing. Having ζ_r appearing on its own in the Hamiltonian is therefore not possible, since it would break the gauge invariance of the Hamiltonian. Knowing the gauge generators and the how ζ and η transform, it is possible to derive the Hamiltonian from the condition $[G_r, H] = 0$ for all r.

As explained, one cannot have terms which excites a single Higgs boson. Looking at the gauge generators one sees that exciting a Higgs boson in a vertex must be accompanied by exiting an electric flux line in one of the neighboring links. If taking the example of $\zeta_{i,\uparrow}$, the lowest order term which commutes with $\boldsymbol{G}_{i,\uparrow}$ is one of the following combinations

$$\zeta_{i,\uparrow}\sigma_{i,\uparrow}\,,\quad \zeta_{i,\uparrow}\sigma_{i,0}^{\dagger}\,,\quad \zeta_{i,\uparrow}\sigma_{i-1,\uparrow}^{\dagger}. \tag{4.1.9}$$

These terms will though not commute with the gauge operator at the other end of the excited links. For it to do so these three operators must be either accompanying by another σ operator, which excites an electric flux leaving the connected vertex or a $\zeta^{\dagger}$ which excites a negative charge at the vertex. If taking the first case, one would as well not find this operator to be gauge invariant [1], so to lowest order the gauge invariant operator exciting the Higgs field will be given by

$$\zeta_{i,\uparrow}\sigma_{i,\uparrow}\zeta_{i+1,\uparrow}^{\dagger}\,,\quad \zeta_{i,\uparrow}\sigma_{i,0}^{\dagger}\zeta_{i,\downarrow}^{\dagger}\,,\quad \zeta_{i,\uparrow}\sigma_{i-1,\uparrow}^{\dagger}\zeta_{i-1,\uparrow}^{\dagger}. \tag{4.1.10}$$

Next we would like to incorporate a single site mass term. This term should ascribe excitations of the Higgs field an energy cost, and should therefore not commute with ζ. The lowest order of such is simply the η_r operator, which is trivially seen to be gauge invariant. Higher order gauge invariant terms can be incorporated, but these would be higher order terms, so products of the gauge invariant terms presented. The Hamilton describing the dynamics of the Higgs mater is therefore given by

$$\begin{aligned} \mathrm{H} = ... &- \lambda \left(\sum_{s=\uparrow,\downarrow}\sum_{i=0}^{L-1}\left(\zeta_{i,\uparrow}\sigma_{i,\uparrow}\zeta_{i+1,\uparrow}^{\dagger} + \mathrm{H.c}\right) + \sum_{i=0}^{L}\left(\zeta_{i,\uparrow}\sigma_{i,0}^{\dagger}\zeta_{i,\downarrow}^{\dagger} + \mathrm{H.c}\right) \right) \\ &- \frac{1}{\lambda}\sum_{s=\uparrow,\downarrow}\sum_{i=0}^{L}\left(\eta_{i,s} + \eta_{i,s}^{\dagger}\right) \end{aligned} \tag{4.1.11}$$

Here the physical meaning behind the presented scaling of the terms, λ and $1/\lambda$, is found by realizing, that if $\lambda \to 0$ the cost of exciting the Higgs field is infinite, and so it should not be possible to excite it. This means that the proportional constant in front of the ζ-term should be zero in this limit. In the other extreme similar arguments are present, and this is too consistent with [34].

---

[1] In the case of having a SR boundary there are two exceptions to this, which will be elaborated on later.

This analysis clearly shows how a gauge theory differs from any other, since by demanding this local gauge symmetry one finds specific terms simply not being allowed in the Hamiltonian, which would not have been the case otherwise.

In combination with the interactions of the gauge bosons the complete Hamiltonian with SS boundaries states

$$H = -\frac{1}{g} \sum_{i=0}^{L-1} (\sigma_{i,0}^\dagger \sigma_{i,\uparrow}^\dagger \sigma_{i+1,0} \sigma_{i,\downarrow} + \text{H.c.}) - g \left(\sum_{i=0}^{L-1} \sum_{s=\uparrow,\downarrow} (\tau_{i,s} + \tau_{i,s}^\dagger) + \right.$$

$$\left. \sum_{i=0}^{L} (\tau_{i,0} + \tau_{i,0}^\dagger) \right) - \frac{1}{\lambda} \sum_{i=1}^{L} \sum_{j=\uparrow,\downarrow} (\eta_{i,s} + \eta_{i,s}^\dagger) -$$

$$\lambda \left(\sum_{i=0}^{L-1} \sum_{s=\uparrow,\downarrow} (\zeta_{i,s}^\dagger \sigma_{i,s}^\dagger \zeta_{i+1,s} + \text{h.c}) + \sum_{i=0}^{L} (\zeta_{i,\uparrow}^\dagger \sigma_{i,0} \zeta_{i,\downarrow} + \text{H.c}) \right) \qquad (4.1.12)$$

The Hamiltonian is schematically represented in Fig. 4.1. In the figure the red color represents the gauge generator of the upper leg, blue the plaquette interactions, yellow the electric field term, green the tunneling term and orange the mass term of the Higgs field.
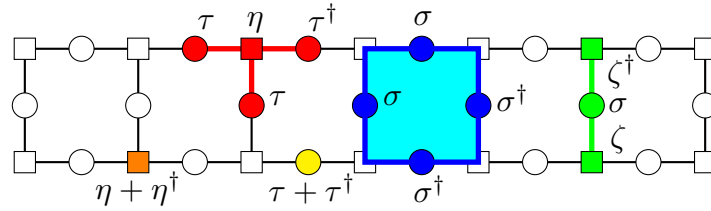
Figure 4.1 | Schematic representation of the interactions. The blue part represents the plaquette interactions, red the gauge generators, green the tunneling term, orange the mass term of the higgs field and yellow the electric field term.

4.2   Gauge fixing

Having introduced the Higgs matter one finds $2(L+1)$ new d.o.f. entering the system, and they enter without new gauge constraints accompanying them. This complicates the system substantially, but since the Higgs matter couples to the gauge bosons there also occurs new ways of fixing the gauge, which might show useful. The first gauge in our arsenal is the axial gauge.

4.2.1   Axial gauge

Since the boundaries are chosen to be smooth-smooth, the conditions for the axial gauge are given in Eq. (3.2.4) and (3.3.15). This means that the, as in Eq. (3.2.6), the electric field terms of the legs need to be described in terms of now both the Higgs matter and the gauge bosons on the rung. Utilizing the gauge generators in Eq. (4.1.6) and the fact that the Hamiltonian operates in Hilbert space where $G_r |\psi\rangle = |\psi\rangle$ the rewriting yields

$$\tau_{i,\uparrow} = \tau_{i-1,\uparrow} \tau_{i,0} \eta_{i,\uparrow} = ... = \prod_{j \leq i} \tau_{j,0} \eta_{j,\uparrow}$$

$$\tau_{i,\downarrow} = \tau_{i-1,\downarrow} \tau_{i,0}^\dagger \eta_{i,\downarrow} = ... = \prod_{j \leq i} \tau_{j,0}^\dagger \eta_{j,\downarrow} \qquad (4.2.1)$$

If instead one were to choose $\sigma_{0,0}\,|\psi_{axial}\rangle = |\psi_{axial}\rangle$ instead of $\sigma_{L,0}\,|\psi_{axial}\rangle = |\psi_{axial}\rangle$, which is an arbitrary choice, then one would find the above modified kink operators being terminated at the right must boundary instead of left.

Inserting this into the Hamiltonian along with the axial gauge constraints leads to

$$\underline{\text{H}} = -\frac{1}{g}\left(\sum_{i=0}^{L-2}(\sigma_i^\dagger \sigma_{i+1} + \text{H.c.}) + \underline{(\sigma_{L-1} + \sigma_{L-1}^\dagger)}\right) - g\left(\sum_{i=0}^{L-1}\left(\prod_{j\leq i}\tau_j \eta_{j,\uparrow}\right.\right.$$

$$\left.\left. + \prod_{j\leq i}\tau_j^\dagger \eta_{j,\downarrow} + \text{H.c.}\right) + \sum_{i=0}^{L-1}(\tau_i + \tau_i^\dagger) + \underline{\left(\eta_{L,\uparrow}\prod_{i=0}^{L-1}\eta_{i,\uparrow}\tau_i + \text{H.c}\right)}\right) - \frac{1}{\lambda}\sum_{i=0}^{L}\sum_{s=\uparrow,\downarrow}(\eta_{i,s} + \eta_{i,s}^\dagger)$$

$$-\lambda\left(\sum_{i=0}^{L-1}\sum_{s=\uparrow,\downarrow}\left(\zeta_{i,s}^\dagger \zeta_{i+1,s} + \text{H.c}\right) + \sum_{i=0}^{L-1}(\zeta_{i,\uparrow}^\dagger \sigma_i \zeta_{i,\downarrow} + \text{H.c}) + \underline{(\zeta_{L,\uparrow}^\dagger \zeta_{L,\downarrow} + \text{H.c})}\right) \quad (4.2.2)$$

Where the three underlined terms are boundary terms appearing from the condition $\sigma_{L,0}\,|\psi_{axial}\rangle = |\psi_{axial}\rangle$. If one where to choose smooth-rough boundaries these three terms would not show[2]. Having incorporated the Higgs matter means that a rough boundary can be either terminated with a link or a vertex. In Appendix A this is though shown to yield the same Hamiltonian in the axial gauge, due to the terminating vertex being accompanied by an extra gauge constraint.

4.2.2 Unitary gauge

As explained the unitary gauge gauges out the Higgs matter by demanding

$$\zeta_r\,|\psi_{uni}\rangle = |\psi_{uni}\rangle \quad (4.2.3)$$

A physical intuition is again presented in the language of electromagnetism. In electromagnetism one can choose to uniquely describe the system in terms of the charges and their positions, but it also possible to uniquely describe the system in terms of the electric and magnetic field. In the unitary gauge one chooses to describe the system in terms of the gauge bosons and thereby the electric and magnetic field. To gauge out the Higgs matter we again tend to the gauge generators and find

$$\eta_{i,\uparrow}^\dagger = \tau_{i,\uparrow}^\dagger \tau_{i-1,\uparrow}\tau_{i,0} \equiv \boldsymbol{V}_{i,\uparrow}\,, \quad \eta_{i,\downarrow}^\dagger = \tau_{i,\downarrow}^\dagger \tau_{i-1,\downarrow}\tau_{i,0}^\dagger \equiv \boldsymbol{V}_{i,\downarrow}\ \text{ for }\ i\neq 0,L$$

$$\eta_{0,\uparrow}^\dagger = \tau_{0,\uparrow}^\dagger \tau_{0,0} \equiv \boldsymbol{V}_{0,\uparrow}\,, \quad \eta_{L,\uparrow}^\dagger = \tau_{L-1,\uparrow}\tau_{L,0} \equiv \boldsymbol{V}_{L,\uparrow}\,,$$

$$\eta_{0,\downarrow}^\dagger = \tau_{0,\downarrow}^\dagger \tau_{0,0}^\dagger \equiv \boldsymbol{V}_{0,\downarrow}\,, \quad \eta_{L,\downarrow}^\dagger = \tau_{L-1,\downarrow}\tau_{L,0}^\dagger \equiv \boldsymbol{V}_{L,\downarrow} \quad (4.2.4)$$

With the last line being a result of SS boundaries. Had one instead chosen RR boundaries the top line would be true for all sites. $\boldsymbol{V}_{i,s}$ will forwardly be denoted the vertex operator and correspond to the gauge constraints of the PLGT. With these relations the Hamiltonian in the unitary gauge becomes

$$\bar{H} = -g\sum_{i,s=0,\uparrow,\downarrow}(\tau_{i,s} + \tau_{i,s}^\dagger) - \frac{1}{g}\sum_{i=0}^{L-1}(\sigma_{i,0}^\dagger \sigma_{i,\uparrow}^\dagger \sigma_{i+1,0}\sigma_{i,\downarrow} + \text{H.c.})$$

$$-\lambda\sum_{i,s=0,\uparrow,\downarrow}(\sigma_{i,s} + \sigma_{i,s}^\dagger) - \frac{1}{\lambda}\sum_{i=1}^{L}(\tau_{i,\uparrow}^\dagger \tau_{i-1,\uparrow}\tau_{i,0} + \tau_{i,\downarrow}^\dagger \tau_{i-1,\downarrow}\tau_{i,0}^\dagger + \text{H.c.})$$

$$-\frac{1}{\lambda}(\tau_{1,\uparrow}^\dagger \tau_{1,0} + \tau_{L,\uparrow}\tau_{L+1,0} + \tau_{1,\downarrow}^\dagger \tau_{1,0}^\dagger + \tau_{L,\downarrow}\tau_{L+1,0}^\dagger + \text{H.c.}) \quad (4.2.5)$$

Where the bar over H represents, that the Hamiltonian is written in the Unitary gauge. This Hamiltonian is far from simple, but as done previously one can search for a dual transformation which will

---

[2]Had one incorporated the unfinished plaquette term for the SR boundaries, then the $\sigma_{L-1} + \sigma_{L-1}^\dagger$ would still appear.
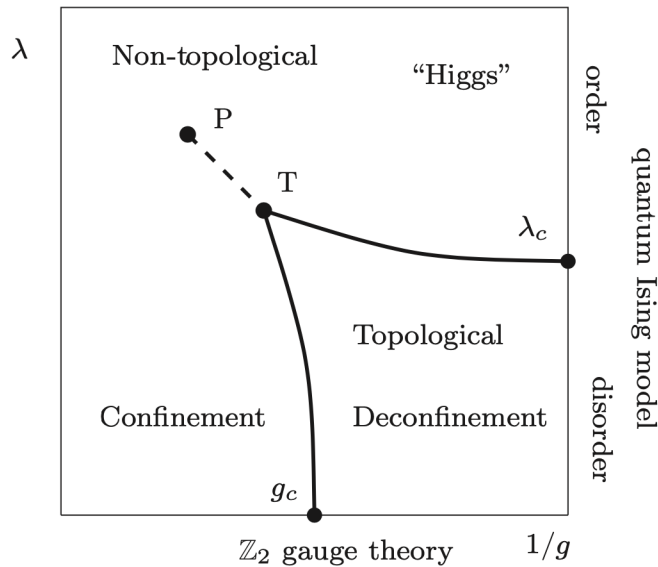
Figure 4.2 | Phase diagram for 2D system . This figure present the phase diagram found in [24, 34], where λ and g are same parameters as shown in Eq. (4.1.12). Here one should note that the 2D system supports both a confined and deconfined phase. Source: [34].

.

help simplifying things. In Appendix C one finds a dual mapping transforming the electric field into the magnetic. In the PLGT this offered a neat mapping to the 1D N-clock model in both a transverse and longitudinal field, but having incorporated the Higgs matter complicates things and no simple picture is offered by this mapping.

4.3   Confined and deconfined phases

Having introduced the Higgs matter it again becomes valid to ask weather or not the system supports both a confined and a deconfined phase. In [24, 34] a truly 2D quantum system with Higgs matter and a local Z_2 gauge symmetry was investigated, and the phase diagram is presented in Fig. 4.2. In the phase diagram one observes the system to both support a deconfined and a confined phase. A rather peculiar feature of the phase diagram in 2D, is that it is symmetric around the off-diagonal. This is due to the Hamiltonian in the unitary gauge being self-dual up to a constant when mapping $\sigma_x, \sigma_z \to \sigma_z, \sigma_x$. This does not hold for the ladder geometry, and one therefore needs to investigate both the bottom line, $\lambda \to 0$ and the line to the right at $g \to 0$ separately. Let us start with $\lambda \to 0$.

Looking at the Hamiltonian in Eq. (4.1.12), one notices that sending $\lambda \to 0$ makes the Higgs matter decouple from the gauge bosons. It does so by simultaneously making the mass term of Higgs field diverge, such that no dynamical matter is present. The physical Hilbert space is therefore, in this limit, mapped into the subspace where $\eta_r = \mathbb{1}$. One is therefore left with the PLGT investigated in Chapter 3 [3]. In that chapter it was shown how only one gapped phase supporting confinement is expected except at the special point $g = 0$, where the system was deconfining.

At the special point of $g, \lambda \to 0$ the system will be in a deconfined phase, and all along the line of $g \to 0$ in the phase diagram one will have $\Delta E = 0$. The intuition behind this is that by looking at the Hamiltoninan in Eq. (4.1.12), one finds that by taking $g \to 0$ the cost of exciting an electric flux line

---

[3]This could also be realized by looking at the Hamiltonian in the unitary gauge, Eq. (E.1), where in the limit of $\lambda \to 0$ it becomes the same as the PLGT Hamiltonian, with the gauge constrains being obeyed by having the vertex terms diverging.

in any of the links is zero. In the procedure of inserting two static charges, it will not cost any energy to insert the charges. Instead it can be, that there will be an energy cost associated with the electric flux line going between the two charges. In the limit of $g \to 0$ this though comes for free. One will therefore have $\Delta E = 0$ independently of the value of λ . This is further investigated and explained in Appendix F.

In the limit of $g \to 0$ there is though expected to be at least one phase transition. This is expected due to the form of the Hamiltonian in axial gauge for $g \to 0$. In this limit one finds the quantum N-clock model given by

$$\underline{H} = -\frac{1}{\lambda} \sum_{i=0}^{L} \sum_{s=\uparrow,\downarrow} (\eta_{i,s} + \eta_{i,s}^\dagger)$$

$$-\lambda \left(\sum_{i=0}^{L-1} \sum_{s=\uparrow,\downarrow} \left(\zeta_{i,s}^\dagger \zeta_{i+1,s} + \text{H.c} \right) + \sum_{i=0}^{L} (\zeta_{i,\uparrow}^\dagger \zeta_{i,\downarrow} + \text{H.c}) \right) \tag{4.3.1}$$

with all the gauge bosons being in the state $|0\rangle_\sigma$. In the case of $N = 2$, this become the Ising model in a transverse field which both shows a ordered-disordered phase transition in (1+1) and (2+1) dimensions. One therefore expects the quasi (1+1) dimensional ladder structure to also show a ordered-disordered phase transition. In (1+1) dimensions for a generic N it is shown in [46, 47, 49, 50], that for $N \leq 4$ one finds a disordered-ordered phase transition, while for $N > 4$ and intermediate gapless phase presents itself. The way we should interpret having $\Delta E = 0$ for $g \to 0$ is therefore, that the expected phases cannot be distinguished by inserting two static charges and investigating their behavior as a function of the separation length.

A strong indicator of a phase transition is found by observing how the degeneracy of the ground state manifold behave, as in the Ising case, where the ordered phase shows a degeneracy and the disordered does not. This is investigated in Appendix E. In the analysis it is shown how by constructing the system with rough-rough boundaries, it is possible to have a degenerate ground state for $\lambda \ll 1$, while for $\lambda \gg 1$ there will be no degeneracy, which indicates a phase transition. If instead, one where to construct the system with SS or SR boundaries the degeneracy of the ground state would be present for $\lambda = 0$ but split for $\lambda > 0$. The degeneracy approach is therefore deemed inconclusive, since it depends too much on the boundary conditions chosen.

The next approach in trying to distinguish the expected phases, is looking at the expectation value of the gauge operator associated with the creation of a meson-like states.

4.4 Bound states of matter for $g \to 0$

In the confined phase, the Higgs particles will be closely bound in pairs of opposite charges, such that, in the more classical sense, one can think of these bound states as particles on their own. Instead in the deconfined phase, the Higgs particles will not be bound to other particles and are free to move. To capture the differences between these two phases one can look at the operator associated with the creation of the meson-like particle

$$\bar{\boldsymbol{M}}_{\gamma(\bar{x},\bar{y})} \equiv \zeta_{\bar{x}}^\dagger \prod_{r \in \gamma} \sigma_r^{(\dagger)} \zeta_{\bar{y}} \tag{4.4.1}$$

and the superscript (†) is not a mistake, and it will now be described what it means. $\prod_{r \in \gamma} \sigma_r^{(\dagger)}$ describes the excitation of some open string of electric flux going from vertex $\bar{x}$ to $\bar{y}$ where $\bar{x} \neq \bar{y}$. This open string will only create a net flux different from zero in the starting and ending vertex, so at $\bar{x}$ and $\bar{y}$. This means that for all other vertices, this operator will create one flux line going in and another going out, and this is what the superscript (†) is to defined to describe. This means that $\prod_{r \in \gamma} \sigma_r^{(\dagger)}$ will commute with all $\boldsymbol{V}_r$ except for $r = \bar{x}$ or $r = \bar{y}$. In Fig. 4.3 one sees a schematic representation

of a meson excitation. The open string is associated with the green lines, where one sees how the superscript (†) is defined such to ensure, that the flux line goes from $\bar{x}$ to $\bar{y}$. In the unitary gauge, this
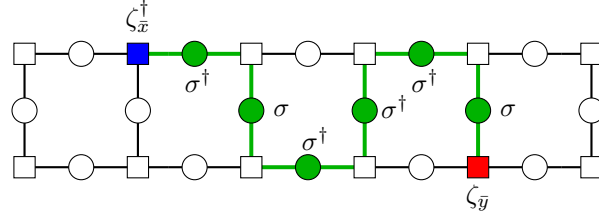
Figure 4.3 | Meson excitation. In this figure one sees a meson excitation associated with the $M_{\gamma(\bar{x},\bar{y})}$. The green lines represent how the open string is constructed, such that it describes an electric flux line going from $\bar{x}$ to $\bar{y}$. σ excites and electric flux line goes against the defined positive direction while $\sigma^\dagger$ follows it.

becomes just the open string.

Calculating the expectation value of this operator can help us understand the behavior of the dynamical Higgs matter in the two phases at $g \to 0$. To do so, we choose the unitary gauge leaving the system described by Eq. (E.1) and

$$\bar{M}_{\gamma(\bar{x},\bar{y})} = \prod_{r \in \gamma} \sigma_r^{(\dagger)} \tag{4.4.2}$$

Using the axial gauge one can express the ground state for the two extremes, $\lambda \to 0, \infty$, as

$$|GS\rangle = ||0\rangle\rangle_\sigma \ , \quad \text{for } \lambda \to \infty \tag{4.4.3}$$

$$|GS\rangle = \Pi_p ||0\rangle\rangle_\tau \ , \quad \text{for } \lambda \to 0 \quad \text{where,} \tag{4.4.4}$$

$$\Pi_p \equiv \prod_{i=0}^{L-1} \sum_{n=0}^{N-1} \frac{(\boldsymbol{B}_i)^n}{\sqrt{N}} \ , \quad \boldsymbol{B}_i \equiv \sigma_{i,0}^\dagger \sigma_{i,\uparrow}^\dagger \sigma_{i+1,0} \sigma_{i,\downarrow}. \tag{4.4.5}$$

and by using these, one finds

$$\left\langle \bar{\boldsymbol{M}}_{\gamma(\bar{x},\bar{y})} \right\rangle = 0 \quad \text{for } \lambda \to 0$$

$$\left\langle \bar{\boldsymbol{M}}_{\gamma(\bar{x},\bar{y})} \right\rangle = 1 \quad \text{for } \lambda \to \infty \tag{4.4.6}$$

This shows, that in the limit of $\lambda \to \infty$ the two Higgs excitations will be correlated even when infinitely far apart while for $\lambda \to 0$ they will not be correlated at all. This therefore indicates, that in the limit of $\lambda \to 0$ the Higgs particle will not notice one another and can be seen as individual particles while for $\lambda \to \infty$, they will be correlated at all length scales. Looking at the mass term of the Higgs matter one notice, how these two extremes correspond to having no mass and infinite. For $\lambda \to \infty$ one will therefore have Higgs particles everywhere, which is what $\left\langle \bar{\boldsymbol{M}}_{\gamma(\bar{x},\bar{y})} \right\rangle = 1$ indicates, and for small λ the Higgs field will not be excited. To understand the behavior better in the two limits, a perturbative analysis is now presented.

The limit of $\lambda \gg 1$

If turning on a large but finite λ this can be approached perturbatively, with the perturbation given by

$$\bar{H}_1 = \frac{-1}{\lambda} \sum_r \left(\boldsymbol{V}_r + \boldsymbol{V}_r^\dagger \right) \tag{4.4.7}$$

In calculating the corrections to the ground state, one will find that the maximum number of vertices being excited to some order is given by that order [51]. The n'th order correction to the ground state will be proportional to $(1/\lambda^2)^n$ and have at maximum of n different vertices excited. An example of a nth order correction is given by

$$|GS\rangle = \frac{1}{\mathcal{N}} \left(1 + ... + A\frac{1}{\lambda^{2n}} \prod_{i=l+1}^{l+n} \boldsymbol{V}_{i,\uparrow} + ... \right) ||0\rangle\rangle_\sigma \, , \qquad (4.4.8)$$

where $A = \mathcal{O}(1)$ and $\mathcal{N}$ describes the normalization factor.

With this in mind we now turn to the expectation value of the meson operator

$$\langle\langle GS||_\sigma \bar{\boldsymbol{M}}_{\gamma(\bar{x},\bar{y})} ||GS\rangle\rangle_\sigma \qquad (4.4.9)$$

where γ instead of Γ should be interpreted as the shortest string of σ operators between $\bar{x}$ and $\bar{y}$. This calculation will not be performed, but the behavior as a function of $|\bar{x}-\bar{y}| = R$ can still be deduced. In this calculation it will be important how the product of $\boldsymbol{V}_r$ operators commute with $\bar{\boldsymbol{M}}_{\gamma(\bar{x},\bar{y})}$, which is due to $\bar{\boldsymbol{M}}_{\gamma(\bar{x},\bar{y})} ||0\rangle\rangle_\sigma = ||0\rangle\rangle_\sigma$. If considering a connected product of n vertex operators, where $n < R+1$ and the first vertex operator in the product is the vertex operator at $\bar{x}$ or $\bar{y}$, then it will not be possible to construct a product which commutes with $\bar{\boldsymbol{M}}_{\gamma(\bar{x},\bar{y})}$. If instead considering $n = R+1$ then it becomes possible to construct the a product of all vertex operators between $\bar{x}$ and $\bar{y}$, which commutes with the string of σ-operators in $\bar{\boldsymbol{M}}_{\gamma(\bar{x},\bar{y})}$. This leads to

$$[\prod_{r\in\gamma(\bar{x},\bar{y})} \boldsymbol{V}_r \, , \, \bar{\boldsymbol{M}}_{\gamma(\bar{x},\bar{y})}] = 0 \qquad (4.4.10)$$

The reason for this is must easily illustrated if taking $\bar{x} = (x,\uparrow)$ and $\bar{y} = (y,\uparrow)$. In this case one finds

$$[\prod_{r\in\gamma(\bar{x},\bar{y})} \boldsymbol{V}_r \, , \, \bar{\boldsymbol{M}}_{\gamma(\bar{x},\bar{y})}] = [\tau_{x-1,\uparrow} \prod_{y\geq i\geq x} \tau_{i,0}\tau_{y,\uparrow}^\dagger \, , \, \prod_{y>i\geq x} \sigma_{i,\uparrow}] = 0 \qquad (4.4.11)$$

If now taking the limit of $R \to \infty$ we define

$$\left\langle \bar{\boldsymbol{M}}_{\gamma(\bar{x},\bar{y})} \right\rangle \equiv \left\langle \bar{\boldsymbol{M}}_\infty(1/\lambda) \right\rangle . \qquad (4.4.12)$$

If again considering a string of vertex operators with the first vertex operator being at the boundary where a charge is sited, then no finite string will commute with $\bar{\boldsymbol{M}}_\infty$. This differs when choosing the separation distance R to be finite. This means that to the $(R+1)^{th}$ order, one has a correction to the expectation values which differs from the correction in the case of $R \to \infty$, since one to this order can create a string of excited vertices which commutes with $\bar{\boldsymbol{M}}_{\gamma(\bar{x},\bar{y})}$. Looking at Eq. (4.4.8) this means that for $n = R+1$ one will find a different contribution when calculating $\left\langle \bar{\boldsymbol{M}}_\gamma \right\rangle$ compared to $\left\langle \bar{\boldsymbol{M}}_\infty \right\rangle$. One can therefore write

$$\left\langle \bar{\boldsymbol{M}}_{\gamma(\bar{x},\bar{y})} \right\rangle = \left\langle \bar{\boldsymbol{M}}_\infty(1/\lambda) \right\rangle + A_1(1/\lambda)\lambda^{-2R}$$
$$= \left\langle \bar{\boldsymbol{M}}_\infty(1/\lambda) \right\rangle + A_1(1/\lambda)e^{-R/\xi_1(1/\lambda)} \qquad (4.4.13)$$

For $\lambda \to \infty$ one finds $\xi_1(1/\lambda) \to 0$ and $\left\langle \bar{\boldsymbol{M}}_\infty(1/\lambda) \right\rangle \to 1$. For a finite but large λ one instead finds $\left\langle \bar{\boldsymbol{M}}_\infty(1/\lambda) \right\rangle < 1$ and $\xi_1(1/\lambda) > 0$.

In the limit of $\lambda \gg 1$ one finds the mass of the Higgs matter being small, such that the energy cost associated with exciting the field is small. This means, that in this limit one will find an extensive number of Higgs particles excited. With this in mind, one can now get an intuitive picture of the result. If exciting the Higgs field at $\bar{x}$ and $\bar{y}$, then these will be interacting for $R < \xi_1$ and thereby be correlated differently from when R is increased beyond ξ_1. When R is increased the exponential part will vanish, and there will no longer be a R dependence. This can be interpreted as the particle at $\bar{x}$ instead of seeing the other particle at $\bar{y}$, now just sees a cloud of charge, where the specific position of $\bar{y}$ no longer matters. In this limit, screening is there expected to be present.

The limit of $\lambda \ll 1$

In the limit of $\lambda \to 0$ the ground state can be expressed as shown in Eq. (4.4.4), and the perturbation to the Hamiltonian takes the form

$$\bar{H}_1 - \lambda \sum_{i,s=0,\uparrow,\downarrow} (\sigma_{i,s} + \sigma_{i,s}^{\dagger}). \tag{4.4.14}$$

Having $[\Pi_p, \bar{H}_1] = 0$ means, that in the perturbative calculations one can neglect Π_p, by making sure that no considered excited state takes the form $\prod_i \boldsymbol{B}_i |GS\rangle$, since this will be equivalent to $|GS\rangle$ due to $\prod_i \boldsymbol{B}_i \prod_p = \prod_p$.

If now perturbatively finding the corrections to the ground state, one have that to a given order the maximum number of excited links will be the same as that given order. Wanting to calculate $\langle \bar{\boldsymbol{M}}_{\gamma(\bar{x},\bar{y})} \rangle$, one realizes that $\bar{\boldsymbol{M}}_{\gamma(\bar{x},\bar{y})}$ corresponds to a perturbation to the ground state occurring to the Rth order. This means, that the Rth order correction to the ground state will yield a state of the kind

$$\propto \lambda^{2R} \bar{\boldsymbol{M}}_{\gamma(\bar{x},\bar{y})} ||0\rangle\rangle_\tau \tag{4.4.15}$$

All orders of λ below λ^{2R} will yield a zero contribution, since the perturbation to $||0\rangle\rangle_\tau$ in some way needs to eliminate $\bar{\boldsymbol{M}}_{\gamma(\bar{x},\bar{y})}$. From the state above one therefore finds the contribution

$$\langle \bar{\boldsymbol{M}}_{\gamma(\bar{x},\bar{y})} \rangle = ... + A\lambda^{2R} \langle\langle 0||_\tau \bar{\boldsymbol{M}}_{\gamma(\bar{x},\bar{y})}^{\dagger} \bar{\boldsymbol{M}}_{\gamma(\bar{x},\bar{y})} ||0\rangle\rangle_\tau \tag{4.4.16}$$

where $A = \mathcal{O}(1)$. This analysis therefore leads to the following behavior

$$\langle \bar{\boldsymbol{M}}_{\gamma(\bar{x},\bar{y})} \rangle = A_2(\lambda) e^{-R/\xi_2(\lambda)} , \quad \xi_2(\lambda) \propto \frac{1}{\ln(1/\lambda)} \tag{4.4.17}$$

The two results expressed in Eq. (4.4.13) and (4.4.17) are similar to the results found in [24] for a truly 2D system. In [24] the behavior in Eq. (4.4.17) was found the in the deconfined phase, while the behavior shown in Eq. (4.4.13) was found in the Higgs phase, where screening was shown to be present.

Chapter 5

Bosonization for $g \to 0$

Bosonization is a technique widely studied and used to obtain low-energy descriptions of 1D quantum models. It can be used to transform either continuous or discretized models of either fermionic or bosonic matter into continuous models described by bosonic fields [34, 52–54]. The idea behind this technique is, that in the low energy limit one can describe the system on terms the charge density and current density operators which satisfy bosonic-like commutation relations [34]. This suggests a connection between these operators and a bosonic field θ. One can then define a mapping between the charge density and current density operators and a bosonic θ-field, where the mapping must preserve the commutation and the algebraic properties.

The considered model in this thesis neither contains true bosonic or fermionic d.o.f., and a low-energy bosonized mapping will not be performed. Instead I present a mapping between the clock-operators and the bosonic fields, which is heavily inspired by the bosonization techniques. A similar strategy has recently been applied to $\mathbb{Z}_2$ LTGs in [55].

The bosonization technique is often used as a stepping stone to the application of Renormalization group (RG) techniques (see, for example [53–56]). This technique offers tools which can help in determining the phases of the system where perturbative methods fail. An RG analysis will therefore later be performed, but first the mapping is presented.

5.1 Bosonization

In the above perturbative analysis the unitary gauge was used, but in wanting to use the techniques provided by bosonization it shows useful to utilize the axial gauge where the plaquette interactions is not present. This Hamiltonian in the axial gauge is stated in Eq. (4.3.1), and as shown in the previous chapter one in the limit of $g \to 0$ retrieves the N-clock model with a transverse field

$$\underline{\mathrm{H}} = -\frac{1}{\lambda} \sum_{s=\uparrow,\downarrow} \sum_{i=0}^{L} (\eta_{i,s} + \eta_{i,s}^{\dagger}) - \lambda \left(\sum_{s=\uparrow,\downarrow} \sum_{i=0}^{L-1} (\zeta_{i,s}^{\dagger}\zeta_{i+1,s} + \mathrm{H.c.}) + \sum_{i=0}^{L} (\zeta_{i,\uparrow}^{\dagger}\zeta_{i,\downarrow} + \mathrm{H.c.}) \right) \qquad (5.1.1)$$

For a 1D chain, this is shown to have two gapped phases for $N < 5$, while for $N \geq 5$ a critical phase appears at intermediate values of λ [46, 47, 49, 50]. It now becomes interesting to see, if these features are present in the ladder geometry as well.

In order to capture the universal features of the LGT model in the bosonized description, we need to ensure that the mapping preserves the symmetries of the Hamiltonian along with the commutation relations. Having two legs in our system, we choose to introduce two pairs of bosonic field operators, namely $(\theta_{\uparrow}(x), \theta_{\downarrow}(x))$ and their dual field operators $(\phi_{\uparrow}(x), \phi_{\downarrow}(x))$. Both fields are defined modulo 2π.

These fields are related by the duality relations

$$\partial_t \theta_s = v_s K_s \partial_x \phi_s \ , \quad \partial_t \phi_s = \frac{v_s}{K_s} \partial_x \theta_s \ , \tag{5.1.2}$$

With v being the propagation velocity of the fields and K_s the Luttinger parameter, which later will be specified[1]. When transforming the model into a model with the d.o.f. represented by the bosonic fields, it must be ensured that the commutation relations of the respective terms are the same. From this demand and following [53], the commutation relations are chosen to be

$$[\phi_s(x), \theta_{s'}(y)] = i\frac{2\pi}{N}\Theta(y-x)\delta_{s,s'} \ ^2 \tag{5.1.3}$$

$\Theta(x)$ is the Heaviside step function with the convention $\Theta(x \geq 0) = 1$ and $\Theta(x < 0) = 0$. Here one should notice the non-locality of the commutation relations, which is also a feature showing itself later when considering the mapping of the clock-operators. With this in place, it now becomes possible to define η and ζ in terms of the fields. A convention which can be shown to satisfy the same commutation relations is given by

$$\eta_{j,s} \to e^{-i(\phi_s(j\cdot a) - \phi_s((j+1)\cdot a))} \ , \quad j \neq L$$
$$\eta_{L,s} \to e^{-i\phi_s(L\cdot a)}$$
$$\zeta_{j,s} \to e^{-i\theta_s(j\cdot a)} \tag{5.1.4}$$

with a being the lattice constant. From Eq. (5.1.3) one finds

$$\eta_{j,s}\zeta_{i,s} \to e^{-i(\phi_s(j\cdot a) - \phi_s((j+1)\cdot a))}e^{-i\theta_s(j\cdot a)} =$$
$$e^{-i(\phi_s(j\cdot a) - \phi_s((j+1)\cdot a)) - i\theta_s(j\cdot a) - \frac{1}{2}[(\phi_s(j\cdot a) - \phi_s((j+1)\cdot a)), \theta_s(j\cdot a)]} =$$
$$e^{-i(\phi_s(j\cdot a) - \phi_s((j+1)\cdot a)) - i\theta_s(j\cdot a) - \frac{1}{2}[(\phi_s(j\cdot a) - \phi_s((j+1)\cdot a)), \theta_s(j\cdot a)]} =$$
$$\sqrt{\omega^*}e^{-i(\phi_s(j\cdot a) - \phi_s((j+1)\cdot a)) - i\theta_s(j\cdot a)} =$$
$$\sqrt{\omega^*}e^{\frac{1}{2}[\theta_s(j\cdot a)], (\phi_s(j\cdot a) - \phi_s((j+1)\cdot a))}e^{-i\theta_s(j\cdot a), (\phi_s(j\cdot a) - \phi_s((j+1)\cdot a))}e^{-i(\phi_s(j\cdot a) - \phi_s((j+1)\cdot a))} \to$$
$$\omega^*\zeta_{i,s}\eta_{j,s} \tag{5.1.5}$$

where the Baker–Campbell–Hausdorff (BCH) formula has been used once between the first and second line and then again, but in an opposite manner, between the forth and fifth line. This is, as needed, consistent with the commutation relation shown in Eq. (4.1.3). A problem one should notice is that by the fields taking continuous values the relation $\eta_{j,i}^N = 1 = \zeta_{j,i}^N$ no longer holds on both sides of the arrow. This will be fixed later.

As earlier explained, one also needs to keep track of the symmetries of the Hamiltonian, by which making sure that the Hamiltonian in the new representation upholds the same symmetries. The global $\mathbb{Z}_N$ symmetry of the N-clock model is the one generated by $\boldsymbol{F} \equiv \prod_{i,s} \eta_{i,s}$. In the bosonized description the Hamiltonian should now be invariant under the transformation generated by $\boldsymbol{F} = e^{-i(\phi_\uparrow(0) + \phi_\downarrow(0))}$. Baring this mind, we now tend to the Hamiltonian. In terms of the bosonic fields one finds

$$\zeta_{j,s}^\dagger \zeta_{j+1,s} + \text{H.c} \to 2\cos(\theta_s(j \cdot a) - \theta_s((j+1) \cdot a)) \tag{5.1.6}$$

$$\zeta_{j,s}^\dagger \zeta_{j,\bar{s}} + \text{H.c} \to 2\cos(\theta_s(j \cdot a) - \theta_{\bar{s}}(j \cdot a)) \tag{5.1.7}$$

$$\eta_{j,s} + \eta_{j,s}^\dagger \to 2\cos(\phi_s(j \cdot a) - \phi_s((j+1) \cdot a)) \tag{5.1.8}$$

Before taking the continuous limit of $a \to 0$, it is important to ensure the invariance of the Hamiltonian under $\boldsymbol{F}$. From the commutation relations stated in Eq. (5.1.3), one sees that Eq. (5.1.6) and (5.1.7)

---

[1]When bosonizing fermions this velocity will correspond to the Fermi velocity

[2]The choice has some arbitrariness to it, and one can find the restrictions in [34].

have the possibility of not commuting with $\boldsymbol{F}$, and this needs to be ensured

$$\boldsymbol{F}\zeta_{i,s}^\dagger \zeta_{i+1,s} = \zeta_{i,s}^\dagger \boldsymbol{F} e^{[\phi_s(0),\theta_s(i\cdot a)]}\zeta_{i+1,s} =$$
$$\zeta_{i,s}^\dagger \zeta_{i+1,s}\boldsymbol{F} e^{([\phi_j(0),\theta_s(i\cdot a)]-[\phi_s(0),\theta_s((i+1)\cdot a)])} = \zeta_{i,s}^\dagger \zeta_{i+1,s}\boldsymbol{F} \tag{5.1.9}$$

and for the rung tunneling term

$$\boldsymbol{F}\zeta_{i,\uparrow}^\dagger \zeta_{i,\bar{\downarrow}} = \zeta_{i,\uparrow}^\dagger \boldsymbol{F} e^{[\phi_\uparrow(0),\theta_\uparrow(i\cdot a)]}\zeta_{i,\downarrow} =$$
$$\zeta_{i,\uparrow}^\dagger \zeta_{i,\downarrow}\boldsymbol{F} e^{([\phi_\uparrow(0),\theta_\uparrow(i\cdot a)]-[\phi_\downarrow(0),\theta_\downarrow((i)\cdot a)])} = \zeta_{i,\uparrow}^\dagger \zeta_{i,\downarrow}\boldsymbol{F} \tag{5.1.10}$$

which indeed verifies $\boldsymbol{F}$ to still be a symmetry in the bosonized language. The terms in the bosonized description therefore contain the same symmetry. In taking the continuous limit of $a \to 0$ the following Taylor expansions is performed

$$\theta_s(x) - \theta_s(x+a) \approx a\partial_x \theta_s(x) \quad \phi_s(x) - \phi_s(x+a) \approx a\partial_x \phi_s(x) \tag{5.1.11}$$

Such that the cosines terms takes the form

$$2\cos\left(a\partial_x \theta_s(x)\right), \quad 2\cos\left(a\partial_x \phi_s(x)\right) \tag{5.1.12}$$

if taking the limit of $a \to 0$, then these terms can be approximated by

$$-2\cos\left(a\partial_x \theta_s(x)\right) + -2\cos\left(a\partial_x \phi_s(x)\right) \approx (a^2\partial_x \theta_s)^2 + a^2(\partial_x \phi_s)^2 + \text{Const.} \tag{5.1.13}$$

where the constant is neglected. Now using the Rectangular Approximation Method to turn the summation into an integral by

$$\sum_{i=0}^{L} \to \int_0^L \frac{\mathrm{d}x}{a} \tag{5.1.14}$$

one retrieves the following Hamiltonian

$$\underline{\mathrm{H}} = \int_0^L \frac{\mathrm{d}x}{a} \left[a^2 \sum_{s=\uparrow,\downarrow} \left(\lambda(\partial_x \theta_s)^2 + \frac{1}{\lambda}(\partial_x \phi_s)^2 \right) - 2\lambda \cos\left(\theta_\uparrow - \theta_\downarrow\right) \right] \tag{5.1.15}$$

Comparing this to the interacting Luttinger model [34], one sees that $1/\lambda$ takes the place of the Luttinger parameter K.

As earlier explained this mapping did not preserve the discrete cyclic Z_N behavior $(\eta_i)^N = 1 = (\zeta_i)^N$. In the Hamiltonian above one has instead upgraded the cyclic Z_N behavior to a continuous $U(1)$ behavior. A way of fixing this is by adding the two additional interactions as done in [49, 57]

$$-M_\theta \cos\left(N\theta\right) \quad, \quad -M_\phi \cos\left(N\phi\right) \tag{5.1.16}$$

These terms will be referred to as the background interaction (BGI) terms and both terms commute with $\boldsymbol{F}$. M_i is positive and, as a first approximations, considered to be larger than all other energy scales of the system. Later an estimate of these parameters will be derived. These terms ensures θ and ϕ to take the discrete values $n\frac{2\pi}{N}$ for $n = 0, 1, ..., N-1$.

One can interpret the BGI terms is by going back to the discrete Hamiltonian. From Eq. (5.1.4) the background interaction terms correspond to the terms

$$-M_\phi \sum_{s=\uparrow,\downarrow} \sum_{i=0}^{L} \left(\prod_{m=i}^{L} (\eta_{m,s})^N + \text{h.c.} \right) - M_\theta \sum_{s=\uparrow,\downarrow} \sum_{i=0}^{L} ((\zeta_{k,s})^N + (\zeta_{i,s}^\dagger)^N). \tag{5.1.17}$$

So the way one can think about the above procedure is that first we upgrade the global Z_N symmetry to a $U(1)$. Then by incorporating the background interaction terms we break the $U(1)$ back down to a Z_N symmetry.

All this results in the following description

$$\underline{\mathrm{H}} = \int \frac{dx}{a} \left[\sum_{s=\uparrow,\downarrow} \left(a^2 \left(\frac{1}{K} (\partial_x \theta_s)^2 + K (\partial_x \phi_s)^2 \right) - M_\theta \cos (N\theta_s) - M_\phi \cos (N\phi_s) \right) \right.$$
$$\left. -2\lambda \cos (\theta_\uparrow - \theta_\downarrow) \right] , \quad K \equiv \frac{1}{\lambda} \qquad (5.1.18)$$

Here the jumping term between the two legs, Eq. (5.1.7), has the profound effect on the system of breaking the self-duality of the model. Where self-dual means that the system is invariant up to some constant when mapping $\phi \to \theta$ and $\theta \to \phi$. This would be true in 1D [47]. Next one notices that the BGI terms for θ contains a Z_N symmetry, such that without the term connecting the legs the system would have a $Z_N \otimes Z_N$ symmetry. Instead the rung tunneling term breaks this down to a Z_N which is generated by simultaneously sending $\theta_{\uparrow/\downarrow} \to \theta_{\uparrow/\downarrow} + 2\pi/N$.

Now one realizes that the Hamiltonian is also invariant when sending $\phi_s \to \phi_s + 2\pi/N$. One could therefore think that the system contains a $Z_N \otimes Z_N \otimes Z_N$ symmetry, but here one should be careful. ϕ and θ are not each others conjugated fields but instead each others dual fields[3]. If denoting the conjugated field to θ by $\Pi(x)$, which can be interpreted as a canonical momentum field, then one has $\Pi(x) \propto \partial_x \theta$, which from Eq. (5.1.2) leads to the symmetry of the ϕ-fields not being as easily translated into something physical. Later this symmetry and its consequences will be investigated, but one should not take note of this symmetry for the moment. Another important thing to mention is that this "symmetry" does not persist for any finite system, since the finite length would introduce a term proportional to $\cos (\phi_s(L))$ in the Hamiltonian, which comes from Eq. (5.1.4). These two terms will break this symmetry.

The coupling between the two legs also introduces another concern. Later when the RG procedure is introduced it becomes important to calculated correlation functions. These correlation functions are calculated perturbatively with respect to the quadractic part of the Hamiltonian. In doing so one wishes to have two uncorrelated fields meaning $\langle \theta_s(x)\theta_{\bar{s}}(x) \rangle = 0$. This is though not true for these pairs of bosonic fields due to the rung tunneling term. This can be seen by expanding the two θ-fields in the rung tunneling term around some minima. This would lead to a term of the kind $(a^2/2)(\partial_x \theta_1)(\partial_x \theta_2)$, which ultimately leaves $\langle \theta_s(x)\theta_{\bar{s}}(x) \rangle \neq 0$. To get rid of this coupling, one can make the following unitary transformation into the charge and spin sector. This is a standard diagonalization procedure [34, 53, 54, 58], with the names of the sectors being an artefact of the use when considering fermionic systems with spin[4][5]. The unitary transformation is as follow

$$\theta_\rho \equiv \frac{\theta_\uparrow + \theta_\downarrow}{\sqrt{2}} , \quad \theta_\sigma \equiv \frac{\theta_\uparrow - \theta_\downarrow}{\sqrt{2}}$$
$$\phi_\rho \equiv \frac{\phi_\uparrow + \phi_\downarrow}{\sqrt{2}} , \quad \phi_\sigma \equiv \frac{\phi_\uparrow - \phi_\downarrow}{\sqrt{2}} \qquad (5.1.19)$$

This transformation preserves the commutation relation making it both a unitary and canonical transformation. A feature of the new fields not easily realized is the periodicity. This is most easily understood by an illustration as in fig. 5.1. In this figure one sees how the periodicity of one of fields depends on the other. For example one observes how if $\theta_\sigma = 0$ then θ_ρ is defined in the interval $[0, \sqrt{2}2\pi[$.

---

[3]An example of two conjugated fields are the momentum and position fields.

[4]When saying "diagonalization" it refers to a having a Hamiltonian which does not mix the different sectors, such that the quadratic part does not have mixing terms.

[5]In some literature these sectors are also denoted the symmetric and anti-symmetric sectors.
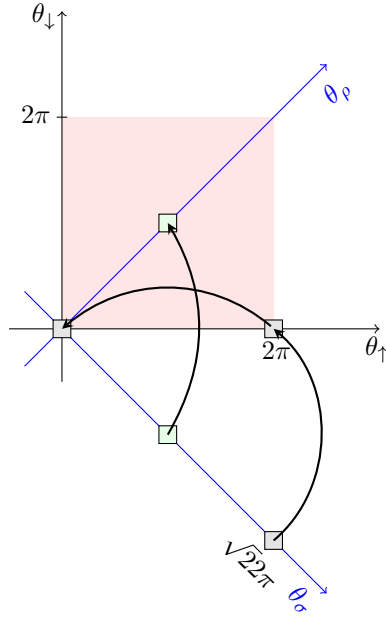
Figure 5.1 | Graphically representation of the periodicity of the fields. This figure illustrates the periodicity of the different θ-fields, which is similar for the ϕ-fields. The red-shaded area illustrates where the fields are defined, and where all other values are mapped into. This mapping is given by $\theta_{\uparrow,\downarrow} \mod 2\pi = \theta_{\uparrow,\downarrow}$. For the fields $\theta_\uparrow$ and $\theta_\downarrow$ this mapping is trivial, but for θ_ρ and θ_σ the mapping becomes less trivial. The green and grey squares illustrates two mappings, with the arrow indicating where they are mapped to. For the grey one sees how $\theta_\sigma = \sqrt{2}2\pi$ is mapped in to $\theta_\sigma = 0$. Another important feature to notice is that for $\theta_\sigma = 0$, one finds $\theta_\rho \in [0, 2\sqrt{2}\pi[$.

After this unitary and canonical transformation the Hamiltonian takes the diagonal form

$$\underline{H} = \int \frac{dx}{a} \left[a^2 \sum_{s=\sigma,\rho} \left(\lambda(\partial_x \theta_s)^2 + \frac{1}{\lambda}(\partial_x \phi_s)^2 \right) - 2M_\theta \cos\left(\frac{N}{\sqrt{2}}\theta_\rho\right) \cos\left(\frac{N}{\sqrt{2}}\theta_\sigma\right) \right.$$

$$\left. -2M_\phi \cos\left(\frac{N}{\sqrt{2}}\phi_\rho\right) \cos\left(\frac{N}{\sqrt{2}}\phi_\sigma\right) - 2\lambda \cos\left(\sqrt{2}\theta_\sigma\right) \right] =$$

$$\int dx \left[a \sum_{s=\sigma,\rho} \left(\frac{1}{K}(\partial_x \theta_s)^2 + K(\partial_x \phi_s)^2 \right) - 2m_\theta \cos\left(\frac{N}{\sqrt{2}}\theta_\rho\right) \cos\left(\frac{N}{\sqrt{2}}\theta_\sigma\right) \right.$$

$$\left. -2m_\phi \cos\left(\frac{N}{\sqrt{2}}\phi_\rho\right) \cos\left(\frac{N}{\sqrt{2}}\phi_\sigma\right) - \frac{2\lambda}{a} \cos\left(\sqrt{2}\theta_\sigma\right) \right] \qquad (5.1.20)$$

where $m_s \equiv M_s/a$.

5.2 Correlation Function

In wanting to be able to distinguish different phases a useful tool is calculating the two-point correlation functions. These functions tell us how different regions of the system are correlated. In one region of the phase diagram one could for example have an exponential decay for some operator, meaning that the correlation between two points of the system is exponentially suppressed with the separation distance. If in another region of the phase diagram the same correlation function shows a power law behavior, then this is strong indicator of these two regions being distinct phases.

Calculating the correlation function with the respect to complete Hamiltonian in Eq. (5.1.20) shows great difficulties, and one therefore needs to do it perturbatively with the zeroth order provided by the quadratic part of the Hamiltonian. The point of this section is therefore to be able to calculate the two correlation functions $\langle \theta(x)\theta(0) \rangle_0$ and $\langle \phi(x)\phi(0) \rangle_0$, where the subscript 0 represents the correlation function to be taken with respect to the quadratic part. In the actual correlation function will not be calculated here, instead the Hamiltonian will be rewritten into a form where results from [34, 52, 53] can be used.

Following the derivations of [53] the following Hamiltonian is considered

$$H_0 = \frac{v_s}{2\pi} \int d^2x \left[(\partial_x \theta_s')^2 + (\partial_x \phi_s')^2 \right] \tag{5.2.1}$$

where θ_s' and ϕ_s', as the above fields, are each others dual fields and are related by Eq. (5.1.2) as well. The velocity v_s describes the propagation speed of the fields, and is most easily realized be rewriting this as the massless Klein-Gordon equations with two fields propagating in opposite directions [53]. These fields have commutation relations given by

$$\left[\frac{\phi_s'(x)}{\pi}, \theta_s'(x') \right] = i\Theta(x' - x). \tag{5.2.2}$$

by considering the Lagrangian description, it is in [53] shown that

$$\langle \theta_s'(x)\theta_s'(0) \rangle_0 \approx \frac{-1}{2} \ln |x| + \frac{1}{2} \ln \Lambda_{min}^{-1} , \quad \langle \theta_s'^2 \rangle_0 \approx \frac{1}{2} \ln \left(\frac{\Lambda_{max}}{\Lambda_{min}} \right) \tag{5.2.3}$$

$$\langle \phi_s'(x)\phi_s'(0) \rangle_0 = \frac{-1}{2} \ln |x| + \frac{1}{2} \ln \Lambda_{min}^{-1} , \quad \langle \phi_s'^2 \rangle_0 = \frac{1}{2} \ln \left(\frac{\Lambda_{max}}{\Lambda_{min}} \right) \tag{5.2.4}$$

where Λ_{min} represents the infrared (IR) momentum cut-off given by $2\pi/L$ and Λ_{max} the ultraviolet (UV) cut-off given by $2\pi/a$. An intuitive understanding of the equations to the right is offered by thinking of the limit $x \to 0$. In going from the discretized description we introduced the lattice spacing as the UV cut-off and hence the smallest length scale. In our continuous model it therefore does not make sense to ask questions about what happens at length scales smaller than this. Our expression in Eq. (5.2.14) will therefore not be true for $x < a$, and as explained in [53] these expressions for the correlation functions will only be valid in the regime of $a \ll r \ll L$. So while this description treats x as continuous variable all operators do not exhibit variations on scales of the order a, meaning that by taking the limit of $x \to 0$ one should approximately get the same result as for $x = a$ [6].

The commutation relations of the charge and spin fields are given in Eq. (5.1.3). Comparing this to one in Eq. (5.2.2), one sees that the fields needs to be scaled by $\sqrt{N/2}$ to fulfil the same relations. By comparing the Hamiltonian in Eq. (5.2.1) with the Gaussian part of the one in Eq. (5.1.20), one finds that that another rescaling is needed to take care of the Luttinger parameter. If considering this, one finds the relations between the primed and unprimed fields

$$\sqrt{\frac{2}{NK}} \phi' = \phi , \quad \sqrt{\frac{K2}{N}} \theta' = \theta \tag{5.2.5}$$

Using this relation one can map Eq. (5.2.1) into the quadratic part of Eq. (5.1.20). Inserting this yields

$$H_0 = \frac{2a}{N} \int d^2x \left[\frac{1}{K} (\partial_x \theta_s)^2 + K(\partial_x \phi_s)^2 \right] = \frac{v_s}{2\pi} \int d^2x \left[\frac{1}{K} (\partial_x \theta_s)^2 + K(\partial_x \phi_s)^2 \right] , \quad v_s = \frac{4\pi a}{N} \tag{5.2.6}$$

from where the propagation velocity of both fields becomes $v_s = 4\pi a/N$ [7].

---

[6] In momentum space this correspond to not considering oscillations greater than Λ_{max}

[7] The factor of K does change the velocity of the fields since one can define new fields with the same commutation relations without it being present. If rewriting this into the Klein-Gordon equation, K will as well just be some parameter scaling the propagating fields and eventually not change the velocity.

With this mapping of the fields one can use the previous stated result in Eq. (5.2.4), to find

$$\langle \theta'_s(x)\theta'_s(0)\rangle_0 = \frac{N}{2K} \langle \theta_s(x)\theta_s(0)\rangle_0 \tag{5.2.7}$$

$$\langle \phi'_s(x)\phi'_s(0)\rangle_0 = \frac{NK}{2} \langle \phi_s(x)\phi_s(0)\rangle_0 \tag{5.2.8}$$

The correlation functions with regards to the quadratic part of Eq. (5.1.20) therefore becomes

$$\langle \theta(x)\theta(0)\rangle_0 = \frac{-K}{N} \ln |x| + \frac{K}{N} \ln \Lambda_{min}^{-1} \ , \quad \langle \theta_s^2 \rangle_0 = \frac{K}{N} \ln \left(\frac{\Lambda_{max}}{\Lambda_{min}}\right)$$

$$\langle \phi(x)\phi(0)\rangle_0 = \frac{-1}{KN} \ln |x| + \frac{1}{NK} \ln \Lambda_{min}^{-1} \ , \quad \langle \phi_s^2 \rangle_0 = \frac{1}{KN} \ln \left(\frac{\Lambda_{max}}{\Lambda_{min}}\right) \tag{5.2.9}$$

5.2.1 Scaling dimensions

These correlation functions are the building blocks for finding the scaling dimension of the different cosine terms. The scaling dimension defines how a term behaves to first order under the RG procedure. It defines if a term grows and becomes relevant or if it decreases and becomes irrelevant. To have better intuition of this procedure, it makes sense to present the conceptual approach of the RG technique.

The RG analysis is based on the fact that close to a phase transition the microscopic length scales of the system are unimportant and the only important length scale is the correlation length ξ. This parameter describes how different regions are correlated and at a phase transition this parameter diverges. By ξ diverging one finds the fluctuations of the system to be statistically self-similar, which effectively means that on all length scales the system will look the same[8]. Close to this transition point one instead of having a diverging ξ has a large but finite ξ, and instead of the system being self-similar on all length scales, it will instead be self-similar on length scales much smaller than ξ. This self-similarity is what the RG procedure takes advantage of. It does so by integrating out d.o.f. on length scales $x \ll \xi$, which due to self-similarity means that configurations after this procedure are statistically similar to the configurations before. The assumption is then that the Hamiltonian after the procedure stays similar to the original one. This is then used iteratively until one is left with a simpler uncorrelated d.o.f. of the length scale ξ. As done in [59] one can divide the RG procedure into three parts:

1. ***Coarse − Grain***: The procedure is started of by integrating out the d.o.f. of the smallest length scales. If considering the smallest length scale to be the lattice spacing a and some parameter $b > 1$, then this step corresponds averaging out fluctuations occurring at length scales $ab > |\boldsymbol{x}| \geq a$. If considering the field $\phi(\boldsymbol{x})$ then the coarse-grained field will essentially correspond to

$$\bar{\phi}(\boldsymbol{x}) = \frac{1}{(ba)^d} \int_{cell} \mathrm{d}^d\boldsymbol{y} \ \phi(\boldsymbol{y}) \tag{5.2.10}$$

   Which describes how the fluctuations within the cell of length ab has been averaged out. If imagining a picture, then this can be seen as a worsening of the resolution.

2. ***Rescale***: Now due to this change of resolution the picture will look different to the original, which is not what we wanted. We wanted self-similarity, and the reason for this not being the case yet, is that the length scale has not be changed according to this coarse-graining. Still being in the picture analogy, one will need to "zoom out", such that the resolution given by a is restored. This is done by the scaling

$$\boldsymbol{x}' = \frac{\boldsymbol{x}}{b} \tag{5.2.11}$$

---

[8]One can find beautiful videos illustrating this feature for the Ising model at `https://www.youtube.com/watch?v=MxRddFrEnPc`

After this step we are left with not only $\bar{\phi}(\boldsymbol{x'})$ but also a rescaled correlation length $\xi' = \xi/b$, which indicates how the system is to be described by less correlated fields if not at the transition point.

3 **Renormalise**: The last problem to be taken care of is the contrast of the picture. If considering the picture to be made out of black and white pixels, then the two previous steps would result in a picture where pixels due to the averaging could become grey. Wanting the system to be self-similar after this rescaling therefore leads to defining a renormalised field

$$\phi'(\boldsymbol{x'}) = \frac{1}{\zeta}\bar{\phi}_{\boldsymbol{x'}} \tag{5.2.12}$$

where the parameter ζ is to take care of this contrast distortion.

Having $\xi' = \xi/b$ also indicates that the RG procedure will, if not at the transition point, take one further away from the transition point. If for the 2D Ising model one were on the ferromagnetic side of the transition point, then this procedure would take one deeper into the ferromagnetic phase. The renormalized fields obtained from this procedure will therefore describe fields that are deep inside the given phase.

If just considering the BGI term of the ϕ-fields presented in Eq. (5.1.16), then the RG procedure will, as being shown explicitly later, lead to the following mapping of the Hamiltonian

$$H[\phi, \theta] = \int_a^L \mathrm{d}x... - 2m_\phi \cos\left(\frac{N}{\sqrt{2}}\phi_\rho\right)\cos\left(\frac{N}{\sqrt{2}}\phi_\sigma\right) \ \to$$
$$H'[\phi', \theta'] = \int_a^L \mathrm{d}x'... - 2m_\phi' \cos\left(\frac{N}{\sqrt{2}}\phi_\rho'\right)\cos\left(\frac{N}{\sqrt{2}}\phi_\sigma'\right). \tag{5.2.13}$$

Where all the different scaling constants is put into the renormlised parameter m_ϕ' such that the Hamiltonian describing the new renormalized system is self-similar to the original one. As will be shown later, one finds $m_{\phi'}' = b^{y_\phi}m_\phi$ such that if $y_\phi > 0$ the term will grow and be relevant in the RG-sense, while if $y_\phi < 0$ it will diminish and be irrelevant. If the term grows, then one is at the side of the transition point where this term dominates. If instead $y_\phi = 0$ one is at the transitions point where the Hamiltonian is self-similar on all length scales, which is realized by having $H[\phi, \theta] = H'[\phi', \theta']$ due to $m_{\phi'}' = m_\phi$.

The parameter y_ϕ is given by $y_\phi = (d - \Delta)$ where Δ is the scaling dimension of the term and d is the space-time dimension, which in this case is 2. This will later be explicitly shown, but first one can get around this rather complicated procedure and find the scaling dimensions of the terms as follows. If considering a term of the kind $\cos(\alpha\mathcal{O}(x))$, one can by splitting up the cosine terms into the respective exponential functions, find the scaling dimension by computing the two point correlation function

$$\left\langle e^{-i\alpha\mathcal{O}(x)}e^{i\alpha\mathcal{O}(0)}\right\rangle_0 \propto \frac{1}{|x|^{2\Delta}} \tag{5.2.14}$$

where Δ will be the scaling dimension of the operator $e^{\pm i\alpha\mathcal{O}(x)}$ (see, chapter 8 in [60]). By using the fact that the cumulant expansion for a Gaussian theory states

$$\langle e^{\alpha x}\rangle = e^{\langle x^2\rangle\alpha^2/2} \quad , \text{ for } \langle x\rangle = 0 \tag{5.2.15}$$

and the BCH formula, one express the two point correlation function as

$$\left\langle e^{-i\alpha\mathcal{O}(x)}e^{i\alpha\mathcal{O}(0)}\right\rangle_0 = \left\langle e^{-i\alpha(\mathcal{O}(x)-\mathcal{O}(0))}\right\rangle_0 = e^{\frac{(-i\alpha)^2}{2}\left\langle(\mathcal{O}(x)-\mathcal{O}(0))^2\right\rangle_0} = e^{-\alpha^2\langle\mathcal{O}^2\rangle_0}e^{\alpha^2\langle\mathcal{O}(x)\mathcal{O}(0)\rangle_0} \tag{5.2.16}$$

where it has been used that all the operators considered here will commute with operators at different locations.

Having Eq. (5.2.15) to be true can be related to the fact, that the Gaussian part is invariant under the translations $\theta/\phi \to \theta/\phi + \alpha$, such that all correlators not invariant under this translation must yield zero. An example of this is

$$\left\langle e^{i\phi(x)} \right\rangle_0 = e^{i\alpha} \left\langle e^{i\phi(x)} \right\rangle_0 \tag{5.2.17}$$

such that one must have $\left\langle e^{i\phi(x)} \right\rangle_0 = 0$. If Considering ϕ and θ one finds by using Eq. (5.2.19)

$$e^{-\alpha^2 \left\langle \phi^2 \right\rangle} \approx e^{\frac{\alpha^2}{KN} \ln \frac{\Lambda_{max}}{\Lambda_{min}}} = \left(\frac{\Lambda_{max}}{\Lambda_{min}} \right)^{\frac{\alpha^2}{KN}}$$

$$e^{-\alpha^2 \left\langle \theta^2 \right\rangle} \approx e^{\frac{\alpha^2 K}{N} \ln \frac{\Lambda_{max}}{\Lambda_{min}}} = \left(\frac{\Lambda_{max}}{\Lambda_{min}} \right)^{\frac{\alpha^2 K}{N}} \tag{5.2.18}$$

Where one should notice that this correlation function will yield zero in the thermodynamic limit of $L \to \infty$. In the correlation function considered in Eq. (5.2.16) one though finds a finite result even in the thermodynamic limit. Considering the θ and ϕ fields one finds

$$\left\langle e^{-i\alpha\theta(x)} e^{i\alpha\theta(0)} \right\rangle_0 = \frac{A_\theta}{|x|^{\frac{\alpha^2 K}{N}}}$$

$$\left\langle e^{-i\alpha\phi(x)} e^{i\alpha\phi(0)} \right\rangle_0 = \frac{A_\phi}{|x|^{\frac{\alpha^2}{KN}}} \tag{5.2.19}$$

By using these relations one can calculate the scaling dimensions of the cosine terms in Eq. (5.1.20). By only considering first order RG flow the Luttinger parameters will not flow, but to second order this will not be true. The Luttinger parameters of the different sectors will therefore be given a subscript, but are to first order in the RG analysis equal. The scaling dimensions are stated in Table 5.1. Where $D_{\phi,\theta}$ corresponds to the scaling dimension of the background interaction terms and D_σ

Δ	Relevant for
$D_\theta = \frac{N}{4} \left(K_\sigma + K_\rho \right)$	$K < \frac{4}{N}$
$D_\phi = \frac{N}{4} \left(1/K_\sigma + 1/K_\rho \right)$	$K > \frac{N}{4}$
$D_\sigma = \frac{K_\sigma}{N}$	$K < 2N$

Table 5.1| Scaling dimensions. In this table one can read how the different terms in Eq. (5.1.18) scale under the RG procedure. To the right one finds for which values of K the different terms are relevant where it has been used that $K_\sigma = K_\rho = K$ for the first order analysis.

the rung tunneling term. In performing the RG procedure one will find the terms to be relevant if D_s is smaller than the space-time dimension. In the column to the right one sees for which values of K this holds. This trivial way of finding the scaling dimension is convenient, but to truly understand this procedure one needs to perform the three steps above, which will be done now.

As previously explained the self-similarity means that the configurations look statistically alike before and after the RG procedure. To describe this statistically we need to get a hold of the partition function, where the path integral formulation is used (for derivation see Chap. 3 in [34]). The first thing needed is to translate the Hamiltonian into the Lagrangian language which will lead to the action. This is done by

$$H = \int \mathrm{d}x \Pi(x)(\partial_t \theta) - \mathcal{L} \tag{5.2.20}$$

where $\mathcal{L}$ describes the Langrangian density, which needs to be integrated over time. In the equation one finds Π. This operator describes the canonical momentum field of θ and fulfills the usual commutation

relations $[\Pi(x), \theta(x')] = -i\delta(x - x')$. Now the dual field is defined in terms of Π as $\Pi \propto \partial_x \phi$ [34], and in order for this commutation relation and Eq. (5.1.3) to hold one finds $\Pi = (N/2\pi)\partial_x \phi$. This means $\Pi = (N/2\pi Kv)\partial_t \theta = (2a/kv^2)\partial_t \theta$ such that Eq. (5.2.20) states

$$
\begin{aligned}
\mathcal{L} = \int \mathrm{d}x \Pi(x)(\partial_t \theta) - H &= \int \mathrm{d}x \left[a \sum_{s=\sigma,\rho} \left(\frac{2}{Kv^2}(\partial_t \theta_s)^2 \right) - \left(a \sum_{s=\sigma,\rho} \left(\frac{1}{K}(\partial_x \theta_s)^2 + \frac{1}{Kv^2}(\partial_t \theta_s)^2 \right) \right. \right. \\
&\quad \left. \left. -2m_\theta \cos\left(\frac{N}{\sqrt{2}}\theta_\rho\right)\cos\left(\frac{N}{\sqrt{2}}\theta_\sigma\right) - 2m_\phi \cos\left(\frac{N}{\sqrt{2}}\phi_\rho\right)\cos\left(\frac{N}{\sqrt{2}}\phi_\sigma\right) - \frac{2\lambda}{a}\cos\left(\sqrt{2}\theta_\sigma\right) \right) \right] \\
&= -\int \mathrm{d}x \left[\frac{a}{v} \sum_{s=\sigma,\rho} \left(\frac{v}{K}(\partial_x \theta_s)^2 + \frac{1}{Kv}(\partial_\tau \theta_s)^2 \right) \right. \\
&\quad \left. -2m_\theta \cos\left(\frac{N}{\sqrt{2}}\theta_\rho\right)\cos\left(\frac{N}{\sqrt{2}}\theta_\sigma\right) - 2m_\phi \cos\left(\frac{N}{\sqrt{2}}\phi_\rho\right)\cos\left(\frac{N}{\sqrt{2}}\phi_\sigma\right) - \frac{2\lambda}{a}\cos\left(\sqrt{2}\theta_\sigma\right) \right]
\end{aligned}
\tag{5.2.21}
$$

where one should notice that the imaginary time, τ, has been used. Using this Lagrangian density one can now define the partition function in form of a path integral as

$$
Z = \int D\phi D\theta e^{\int \mathrm{d}\tau \mathcal{L}[\phi,\theta]} = \int D\phi D\theta e^{-S[\phi,\theta]}
\tag{5.2.22}
$$

With this in place one can now tend to the RG analysis. By following the momentum space approach in [53], one makes the definitions

$$
\theta = \theta_> + \theta_< , \quad \phi = \phi_> + \phi_<
\tag{5.2.23}
$$

where $\theta_>$ describes the fast oscillating modes for $\Lambda'_{min} < k < \Lambda_{mi}$ with $\lambda'_{min} = 2\pi/ab$ and $b > 1$. b is the parameter describing hoe coarse-grained we want our system. In momentum space one can show, that this leads to $(\partial_x \phi)^2 = (\partial_x \phi_<)^2 + (\partial_x \phi_<)^2$, which also holds for θ. This means that the quadratic part of the action does not mix the fast oscillating and slow oscillating modes. This is though not true for S_1. This leads to the following rewriting of the partition function

$$
\mathcal{Z} = \int D\phi D\theta e^{-S[\phi,\theta]} =
$$

$$
\mathcal{Z}_0^> \int D\phi_< D\theta_< e^{-S_0[\phi_<,\theta_<]} \frac{1}{\mathcal{Z}_0^>} \int D\phi_> D\theta_> e^{-S_1[\phi_>,\phi_<,\theta_>,\theta_<]} e^{-S_0[\phi_>,\theta_>]} =
$$

$$
\mathcal{Z}_0^> \int D\phi_< D\theta_< e^{-S_0[\phi_<,\theta_<]+\ln\left\langle e^{-S_1[\phi_>,\phi_<,\theta_>,\theta_<]} \right\rangle_>}
\tag{5.2.24}
$$

Where $\langle ... \rangle_>$ is the expectation value with respect to the fast oscillating modes and $D_{\phi/\theta}$ means the integration of all possible functions of $\phi_s(x,\tau)$ and $\theta_s(x,\tau)$.

Next b is defined as $b = 1 + dl$, with dl being an infinitesimal quantity, such that we coarse-grain the system infinitesimally. Doing it like this, means that one can predict the infinitesimal change of the renormalized parameters which can be used to derive how the parameters "flow" when performing this procedure continuously.

Using this one can define $\langle ... \rangle_>$ as an operation which in momentum space integrates out $k \in [2\pi/a, 2\pi/(ab)]$ and in real space $x \in [a, ab]$. By doing this one should then define a new smallest length scale, $a' = ab$ and $\Lambda'_{min} = 2\pi/(ab)$. If looking at Eq. (5.2.18) one finds

$$
e^{-\alpha^2 \left\langle (\phi^>)^2 \right\rangle_>} \approx e^{\frac{\alpha^2}{KN} \ln \frac{\Lambda'_{min}}{\Lambda_{min}}} = \left(\frac{\Lambda'_{min}}{\Lambda_{min}} \right)^{\frac{\alpha^2}{KN}}
$$

$$
e^{-\alpha^2 \left\langle (\theta^>)^2 \right\rangle_>} \approx e^{\frac{\alpha^2 K}{N} \ln \frac{\Lambda'_{min}}{\Lambda_{min}}} = \left(\frac{\Lambda'_{min}}{\Lambda_{min}} \right)^{\frac{\alpha^2 K}{N}}
\tag{5.2.25}
$$

which comes from the fact that the maximum momentum considered in $\langle ... \rangle_>$ will be Λ'_{min}, such that in the above analysis one finds this result by taking $\Lambda_{max} \to \Lambda'_{min}$.

In Eq. (5.2.24) $\mathcal{Z}_0^>$ is the partition function for fast oscillating quadratic part of the Hamiltonian, where the $\mathcal{Z}_0^>$ in front is an irrelevant constant for this analysis and is neglected. Next we utilize the cumulant expansion

$$\ln \left\langle e^{-S_1[\phi_>,\phi_<,\theta_>,\theta_<]} \right\rangle_> = -\langle S_1 \rangle_> + \frac{1}{2}\left(\langle S_1^2 \rangle_> - \langle S_1 \rangle_>^2 \right) + ... + \frac{(-1)^l}{l!} \langle S_1^l \rangle_>^c + ... \qquad (5.2.26)$$

where the superscript c stands for the connected pieces. From this one can write the effective action after having integrated out the fast oscillating d.o.f. to second order as

$$S_{eff} = S_0 - \ln \left\langle e^{-S_1[\phi_>,\phi_<,\theta_>,\theta_<]} \right\rangle_> \approx S_0 + \langle S_1 \rangle_> - \frac{1}{2}\left(\langle S_1^2 \rangle_> - \langle S_1 \rangle_>^2 \right) + O(S_1^3) \qquad (5.2.27)$$

By considering this approximation only to first order, then the rung tunneling term yields

$$\langle S_{rung} \rangle_> = \int_{ab}^L dx^2 \frac{\lambda}{a} \left[\left\langle e^{i\sqrt{2}\theta_\sigma^>} \right\rangle_> e^{i\sqrt{2}\theta_\sigma^<} + \left\langle e^{-i\sqrt{2}\theta_\sigma^>} \right\rangle_> e^{-i\sqrt{2}\theta_\sigma^<} \right] =$$
$$\int_{ab}^L dx^2 \frac{\lambda}{a} \left[e^{i\sqrt{2}\theta_\sigma^<} + e^{-i\sqrt{2}\theta_\sigma^<} \right] e^{\frac{(i\sqrt{2})^2}{2}\langle (\theta_\sigma^>)^2 \rangle_>} \qquad (5.2.28)$$

where the new boundaries on the integral comes from path integral in Eq. (5.2.24) only considering the slow oscillating part. Which also means that the superscript, $<$, for the slow oscillating modes could be neglected, but it is intuitive explicit show them.

By using Eq. (5.2.25) one finds

$$\langle S_{rung} \rangle_> = \int_{ab}^L dx^2 \frac{\lambda}{a} \left[e^{i\sqrt{2}\theta_\sigma^<} + e^{-i\sqrt{2}\theta_\sigma^<} \right] \left(\frac{\Lambda'_{min}}{\Lambda_{min}} \right)^{\frac{K}{N}} \qquad (5.2.29)$$

Expanding to first order in dl and neglecting the superscript yields

$$\langle S_{rung} \rangle_> = \int_{ab}^L dx^2 \frac{2\lambda}{a} \cos(\sqrt{2}\theta_\sigma(x))(1 - \frac{K}{N}dl) \qquad (5.2.30)$$

Wanting to be able to relate this new effective low energy description to the description before the fast oscillating modes were integrated out, we need to rescale x such that it again is define as $x' \in [a, L]$. This is done by defining $x' = x/b$ which yields $d^n x = d^n x'(1 + ndl)$ were n represents the space-time dimension, which in this case is 2. This all leads to

$$\langle S_{rung} \rangle_> = \int_a^L dx^2 \frac{2\lambda}{a} \cos(\sqrt{2}\theta_\sigma(x)) \left[1 + \left(2 - \frac{K}{N} \right) dl \right] = \int_a^L dx^2 \frac{2\lambda'}{a} \cos(\sqrt{2}\theta_\sigma(x)) \qquad (5.2.31)$$

$$\lambda' = \lambda + d\lambda \qquad (5.2.32)$$

Where the prime represent the new renormalized parameter and $d\lambda$ is the change of this parameter due to the infinitesimal flow, and L is to be considered infinite such that $L/b \to L$. This yields the RG equation for λ to be

$$\frac{d\lambda}{dl} = \left(2 - \frac{K}{N} \right) \lambda = (2 - D_\sigma) \lambda \qquad (5.2.33)$$

where one sees that for $D_\sigma < 2$ the term will grow, thereby making it relevant. Comparing this to the mapping shown in Eq. (5.2.13) one could as well have written $\lambda' = b^{(2-K/N)}\lambda$, in order to show where the expression $y_\phi = (d - \Delta)$ came from.

5.2.2 Relevant or irrelevant

When a term is deemed relevant it means that in RG procedure that given term will become increasingly important. If looking at the rung tunneling term which is scaled by λ and considering $K < 2N$, then this term is deemed relevant. This effectively means that after coarse graining and rescaling the renormalized parameter will increase immensely thereby resulting in a renormalized Hamiltonian with the renormalized term

$$H' = \int \mathrm{d}x... - \lambda' \cos\left(\sqrt{2}\theta_\sigma\right) , \quad \lambda' >> \lambda \tag{5.2.34}$$

here the prime indicates it to be renormalized. This renormalization therefore predicts, that for $K < 2N$ the system wants to pin θ_σ to the minimum zero, in order to minimize the energy. Setting θ_σ to be exactly zero is a semiclassical approximation, since the quantum nature of the system means there will be fluctuations around the minimum, but the renormalized system will highly suppress these. Bearing this in mind, let us look at two examples of this

By Taking the limit of $\lambda \to \infty$ one can from Table 5.1 extract that both the rung tunneling term and the BGI term for θ are relevant. These terms commute and can be simultaneously minimized. The renormalized Hamiltonian therefore wishes to pin both θ_σ and θ_ρ. The rung tunneling term is minimized by demanding $\theta_\sigma = 0$. In Fig. 5.1 one sees how $\theta_\sigma = \sqrt{2}2\pi$ is mapped in to $\theta_\sigma = 0$, such that only one minimum is present. The background interaction term will pin θ_ρ to a multiple of $\sqrt{2}2\pi/N$, and in order to know the number of minima we again tend to Fig. 5.1. There one finds that $\theta_\sigma = 0$ leads to $\theta_\rho \in [0, 2\sqrt{2}\pi[$. This means that θ_ρ will have N minima. What this means is most clearly seen, by going back to the original fields.

From Eq. (5.1.19) one sees that $\theta_\sigma = 0$ results in $\theta_\uparrow = \theta_\downarrow$, such that one finds

$$\theta_\rho = n\frac{\sqrt{2}2\pi}{N} = \sqrt{2}\theta$$

$$\theta_\downarrow = \theta_\uparrow = n\frac{2\pi}{N} \quad , \text{ for } \quad n = 0, 1, ..., N-1 \tag{5.2.35}$$

Then by using Eq. (5.1.4) and the fact that this term commutes with $\partial_x\theta_s$, this is translated to the ground state of the renormalized system being

$$\{|GS\rangle = ||k\rangle\rangle_\zeta \equiv |k, k, ..., k\rangle_\zeta \ , \ k = 0, 1, 2, ..., N-1\} \tag{5.2.36}$$

The degeneracy of the θ-fields should therefore be interpreted as a degeneracy of the predicted ground state. This ground state is also consistent with the ferromagnetic ground state of the clock description, Eq. (5.1.1), in the large λ limit.

Having a sector being pinned entails that the spectrum of that sector is gapped [53, 54, 56]. This means that by predicting both sectors to be pinned the system will be in a gapped phase. A way of understanding this in this limit is, that since the discrete cyclic behavior of the fields withstands the renormalization procedure, it will cost a finite amount of energy to make a local excitation of the fields to any of the other discrete values. Had this symmetry not survived the procedure, one could turn the fields an infinitesimal amount and thereby create an excitation costing an infinitesimal amount of energy. If having a sector unpinned is therefore interpreted, as the system being in a gapless phase.

Now let us draw our attention to D_ϕ. If taking the limit of $\lambda \to 0$ one finds this term to be the only one relevant. This means that the two fields ϕ_ρ and ϕ_σ are pinned and fulfills

$$\phi_\rho = \frac{\sqrt{2}2\pi}{N}n \ , \ \phi_\sigma = \frac{\sqrt{2}2\pi}{N}m \tag{5.2.37}$$

where one again needs to consider the dependent periodicity of the two fields. If considering this, then one finds $2N$ minima. In terms of the original fields one finds

$$\phi_\uparrow = \frac{2\pi}{N}(n+m) \ , \ \phi_\downarrow = \frac{2\pi}{N}(n-m) \tag{5.2.38}$$

41

Translating this back to the discretized description by Eq. (5.1.4), one sees that for all values of n and m it will correspond to having a ground state where $\eta_{i,s} |GS\rangle = |GS\rangle$ leading to

$$|GS\rangle = ||0\rangle\rangle_\eta \tag{5.2.39}$$

which is consistent with the discretized description in this limit. Had one solely looked at the fields, one would, as in the case for the θ-fields above, expect a N-times degenerate of the ground state. This is though not the case, and as previously explained, this is due to the symmetry of the ϕ-fields not being as easily translated into physical features of the system. In this limit the theory therefore predicts a non-degenerate and gapped ground state.

5.3 Phase diagram

In this section the predictions of the first order RG analysis will be investigated further. In Fig. 5.2 one sees a graphically representation of where the different terms are relevant. In figure the brightest
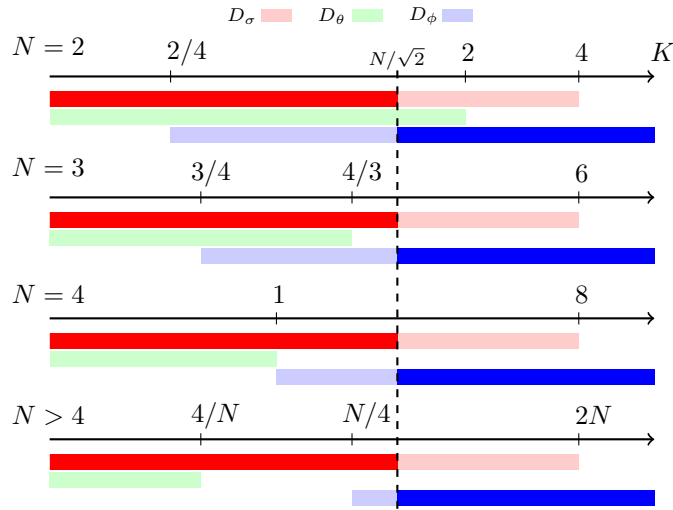
Figure 5.2 | Graphically representation the relevance of the terms. This figure illustrates for the different values of N where the different terms will be relevant as a function of K. The different terms will be relevant for the specific value of K if there color code shows below. Here one notices that for $N > 4$ one finds a finite region where none of the background interactions will be relevant. The dotted line represent where $D_\phi = D_\sigma$ [9].

color represents the most relevant term, while the faded color means that the term is relevant but not the most relevant. In the region $K \in [N/4, 2N]$ one finds the rung tunneling term and the BGI term for the ϕ-fields to be relevant[10]. These two terms do not commute, such that they cannot be minimized simultaneously and are therefore denoted competing terms. The dotted line represents where $D_\sigma = D_\phi$, meaning that the two terms are equally relevant. Taking the case of $N = 2$, one finds that each side of the dotted line the system will like to pin either both θ- or both ϕ-fields. The analysis therefore predicts a phase transition between the ordered and disordered phase of the Ising model at this point.

Next to this transition in the figure one finds regions where competing terms are both relevant, and the most crucial region is for $N \geq 3$ where for $K \in [N/4, N/\sqrt{2}]$ one finds the background interactions

---

[9]If erasing the D_σ-color code, then this figure would represent the 1D N-clock model instead of the ladder geometry.
[10]For $N < 4$ one finds the region $K \in [N/4, 4/N]$ where also the background interaction term for the θ-fields is relevant, but since the rung tunneling term is more relevant and commutes with this term we can for now neglect this term.

for the θ fields to be irrelevant. In this region the rung tunneling term is the most relevant, and since $[\phi_\sigma(x), \theta_\sigma(y)] \neq 0$ this entails that by pinning θ_σ one finds ϕ_σ to fluctuate wildly[11]. Having ϕ_σ to fluctuate wildly means that any operator of the kind $e^{i\alpha\phi_\sigma}$ will have exponentially decaying correlations [54]. To see what this results in, one should consider the correlation function of some operator and expand it perturbatively in the non-quadratic part. From the Hamiltonian one can define the action as

$$S_0 = \int_0^L \mathrm{d}^2x \left[\frac{1}{2\pi K_\sigma} \left(\frac{(\partial_\tau \theta_\sigma)^2}{v} + v(\partial_x \theta_\sigma)^2 \right) + \frac{1}{2\pi K_\rho} \left(\frac{(\partial_t \theta_\rho)^2}{v} + v(\partial_x \theta_\rho)^2 \right) \right] \tag{5.3.1}$$

$$S_\theta = \int_0^L \mathrm{d}^2x \left(2m_\theta \cos\left(\frac{N}{\sqrt{2}}\theta_\rho\right) \cos\left(\frac{N}{\sqrt{2}}\theta_\sigma\right) + \frac{2\lambda}{a} \cos\left(\sqrt{2}\theta_\sigma\right) \right) \tag{5.3.2}$$

$$S_\phi = \int_0^L \mathrm{d}^2x \left(2m_\phi \cos\left(\frac{N}{\sqrt{2}}\phi_\rho\right) \cos\left(\frac{N}{\sqrt{2}}\phi_\sigma\right) \right) \tag{5.3.3}$$

If seeing $S_1 \equiv S_\theta + S_\phi$ as a perturbation to the quadratic part, then one can as in [61] write the expectation value of the operator $\mathcal{A}$ as

$$\langle \mathcal{A} \rangle = \frac{\int \mathcal{D}_\theta \mathcal{D}_\phi \mathcal{A} e^{-S[\phi,\theta]}}{\int \mathcal{D}_\theta \mathcal{D}_\phi e^{-S[\phi,\theta]}} = \frac{\int \mathcal{D}_\theta \mathcal{D}_\phi \mathcal{A} e^{-S_1} e^{-S_0}}{\int \mathcal{D}_\theta \mathcal{D}_\phi e^{-S_1} e^{-S_0}} = \frac{\mathcal{Z}_0 \left(\langle \mathcal{A} \rangle_0 - \langle \mathcal{A} S_1 \rangle_0 + \langle \mathcal{A} S_1^2/2 \rangle_0 + ... \right)}{\mathcal{Z}_0 \left(1 - \langle S_1 \rangle_0 + \langle S_1^2/2 \rangle_0 + ... \right)} =$$
$$\sum_{n=0}^{\infty} \frac{(-1)^n}{n!} \langle \mathcal{A} S_1^n \rangle_0^c \approx \langle \mathcal{A} \rangle_0 - (\langle \mathcal{A} S_1 \rangle_0 - \langle S_1 \rangle_0) + \mathcal{O}(S_1^2) \tag{5.3.4}$$

where the superscript c refers to the connected average.

If considering the region where θ_σ is pinned, such that all correlation functions of the kind $e^{i\alpha\phi_\sigma}$ are exponentially suppressed, one finds Eq. (5.3.4) becoming

$$\langle \mathcal{A} \rangle \approx \langle \mathcal{A} \rangle_0 - (\langle \mathcal{A} S_\theta \rangle_0 - \langle S_\theta \rangle_0) + \mathcal{O}(S_1^2) \tag{5.3.5}$$

since S_ϕ consist of solely operators of the $e^{i\alpha\phi_\sigma}$ kind. If now reexponentiating this, then it corresponds to simply neglecting the BGI term for ϕ. In Fig. 5.2 this corresponds to neglecting the faded blue to left of the dotted line, and to the right one should neglect the red and also the green for $N = 2$. For $N > 2$ this results in the charge sector not being pinned in the region $K \in [4/N, N/\sqrt{2}]$ thereby predicting the charge sector to be gapless and the charge sector gapped. Simply neglecting this term is though not the whole story, since to second order it can still contribute.

5.3.1 Two-step-RG

In the analysis above one simply considered the coupling constants to flow towards infinity, and after this it was determined which field the RG procedure would pin. The bosonized description is though a low-energy description, meaning we have finite energy scales to consider, over which the bosonization fails. In the conceptual description of the RG procedure this should be understood as, when the fast oscillating modes are continuously integrated out, then for example in the region where the rung tunneling term is the most relevant, the rung tunneling term will grow rapidly and after a while it will strongly couple the different spin sector regions of the renormalized system. When these regions become to strongly coupled, the bosonized description is expected to fail, and the RG flow should be terminated. These energy scales over which the bosonization fails sets a threshold for the coupling constants, such that the RG flow should be terminated after this has been reached. This for example means, that in the region where the rung tunneling term is the most relevant, one should initiate the flow until the coupling constant reaches this finite threshold, where after the θ_σ-field is approximated

---

[11]Again one can find an analogy in the momentum and position fields, even though these are conjugated operators and not dual. If one pins down the position then the uncertainty of the momentum is large.

to be pinned. Using this approximation, one can thereby write an effective Hamiltonian for charge sector, which is not pinned yet, and initiate the flow once more.

The two-step-RG procedure is a procedure dividing the flow into different steps and can be expressed as follows: First one initiate the initial flow. Then one let the parameters or coupling constants flow until a parameter reaches the threshold or all of the parameters flow below some minimum for which a gapless phase is expected. In the first case, one can have two cases. Either the initial flow pins all fields, which in our case will happen for $K > N/\sqrt{2}$, or it can happen that the initial flow does not pin all the fields, which happens for $K < N/\sqrt{2}$. In this region one finds the rung tunneling term to be the most relevant, meaning it will reach the threshold first and thereby pin θ_σ to zero. The next step is then to insert $\theta_\sigma = 0$, and then write an effective Hamiltonian for charge sector for which the flow can continue. If again taking the conceptual description of the RG procedure, one can also see this as the two sectors being self-similar on different length scales, such that the RG flow should be terminated differently for the two sectors.

In finding the effective Hamiltonian to first order one has, that by θ_σ being pinned the BGI term for the ϕ fields can be neglected. Inserting $\theta_\sigma = 0$ therefore yields

$$\underline{\mathrm{H}}_{eff} = \int \mathrm{d}x \left(a \left[K (\partial_x \phi_\rho)^2 + \frac{1}{K} (\partial_x \theta_\rho)^2 \right] - 2m'_\theta \cos\left(\frac{N}{\sqrt{2}} \theta_\rho \right) \right) \tag{5.3.6}$$

where the bar above the parameters indicates them to be renormalized. From this effective Hamiltonian one can again calculate the scaling dimension of the background interaction term. Now it states $D_{\theta'} = NK/4$ making it relevant for $K < 8/N$. This means that as the system pins θ_σ, it simultaneously makes the background term more relevant. Focusing on the charge sector one finds in Fig. 5.3 a graphical representation of where the different terms are relevant and pins this sector. From the
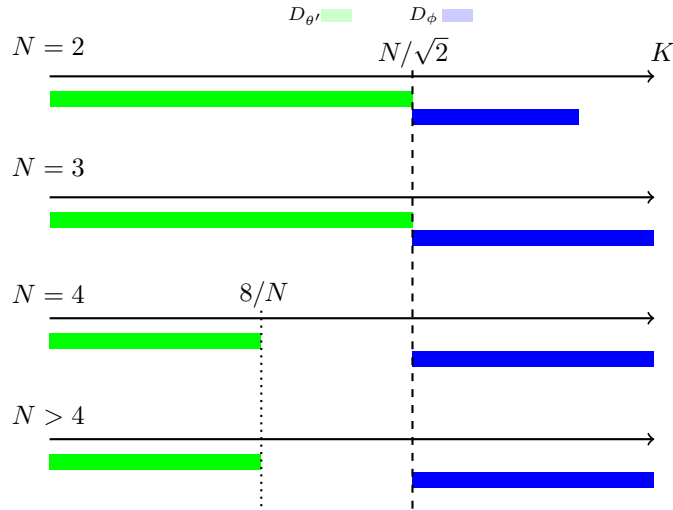
Figure 5.3 | **Graphically representation of the relevance of the effective terms**. This figure illustrates for which value of K the different terms will pin the different field of the charge sector. Here one sees that the first order RG analysis leaves an extended region for $N > 3$ where the charge sector is gapless.

graphical representation one sees that this two-step-RG procedure predicts to first order a gapless phase for for $N > 3$. It as well predicts gapped-gapped transitions for $N < 4$.

Comparing Fig. 5.3 to 5.2 one sees that for $N < 4$ there is predicted a gapped-gapped transition for both sectors at $K = N/\sqrt{2}$. At $K = N/\sqrt{2}$ for $N \geq 4$ there will instead be a gapped-gapped transition for the spin sector, while for the charge sector there will be a gapped-gapless transition. At $K = 8/N$ another gapped-gapless transition is predicted for the charge sector. This result we though know to be

wrong for $N = 4$ from the unitary mapping presented in [47]. With this mapping it is possible to map the $\mathbb{Z}_4$ clock operators into two pairs of $\mathbb{Z}_2$ Ising operators, thereby essentially mapping the global $\mathbb{Z}_4$ symmetry into a $\mathbb{Z}_2 \times \mathbb{Z}_2$ symmetry such that the phase diagram should coincide with that of the $\mathbb{Z}_2$ Ising theory. For $N = 4$ this therefore tell, that only a ordered-disordered phase transition should be present. We therefore move on to consider higher order terms, in the hope that a remedy is found.

5.3.2 Quasi second order RG

In this section a quasi second order RG analysis is presented. This analysis is not consistent in the orders of S_1 considered, and will take second order terms of the Hamiltonian into account while not considering the running of the Luttinger parameters. This analysis is used to shine a light on what can happen to higher orders before deploying the full second order analysis.

In regions where two terms are competing, the first order analysis simply neglects the term which is not the most relevant. For $K \in [N/4, N/\sqrt{2}]$ this presented itself by predicting a gapless phase for $N \geq 4$, since the BGI term for the ϕ-fields was neglected, due to the rung tunneling term being more relevant. Neglecting the ϕ BGI term is though not the whole story, and to second order in S_1 this term will contribute.

As in [54] one can look at the normalized partition function to see how in this region the term to second order will contribute to the effective Hamiltonian.

$$\frac{Z}{Z_0} = \frac{1}{Z_0} \int \mathcal{D}_\theta \mathcal{D}_\phi e^{-S_0} e^{-S_1} = \left\langle e^{-S_1} \right\rangle_0 = 1 - \langle S_1 \rangle_0 + \frac{1}{2} \left\langle S_1^2 \right\rangle_0 + ... \tag{5.3.7}$$

Now the way this procedure works is by first initiating the RG flow. If we take the case of $K < N/\sqrt{2}$, so where the rung tunneling term is most relevant, then one should imagine letting the flow run until θ_σ is pinned. If so one can write

$$S_0' = \int \mathrm{d}^2 x \left[\frac{1}{2\pi K_\sigma} \left(\frac{(\partial_\tau \theta_\sigma)^2}{v} + v(\partial_x \theta_\sigma)^2 \right) + \frac{1}{2\pi K_\rho} \left(\frac{(\partial_t \theta_\rho)^2}{v} + v(\partial_x \theta_\rho)^2 \right) - \frac{2\lambda'}{a} \cos \left(\sqrt{2}\theta_\sigma \right) \right] \tag{5.3.8}$$

$$S_1' = \int \mathrm{d}^2 x \left[2m_\phi' \cos \left(\frac{N}{\sqrt{2}}\phi_\rho \right) \cos \left(\frac{N}{\sqrt{2}}\phi_\sigma \right) + 2m_\theta' \cos \left(\frac{N}{\sqrt{2}}\theta_\rho \right) \cos \left(\frac{N}{\sqrt{2}}\theta_\sigma \right) \right] = S_\phi' + S_\theta' \tag{5.3.9}$$

$$S_\phi \equiv \int \mathrm{d}^2 x \left[2m_\phi \cos \left(\frac{N}{\sqrt{2}}\phi_\rho \right) \cos \left(\frac{N}{\sqrt{2}}\phi_\sigma \right) \right] \;, \quad S_\theta \equiv \int \mathrm{d}^2 x \left[2m_\theta \cos \left(\frac{N}{\sqrt{2}}\theta_\rho \right) \cos \left(\frac{N}{\sqrt{2}}\theta_\sigma \right) \right] \tag{5.3.10}$$

Where the prime denotes the renormalized constants, which is a result of the initial flow. In this region one finds $\lambda' \gg m_\phi', m_\theta'$, which is why S_1 is seen as perturbation. Due to this relation one can insert $\theta_\sigma = 0$ and have all correlation functions of the kind $e^{-i\alpha\phi_\sigma}$ be exponentially decaying. This means that S_θ becomes just $2m_\theta' \cos \left(\frac{N}{\sqrt{2}}\theta_\rho \right)$. The normalized partition function becomes

$$\frac{Z}{Z_0} = \frac{1}{Z_0} \int \mathcal{D}_\theta \mathcal{D}_\phi e^{-S_0} e^{-S_1} = \left\langle e^{-S_1} \right\rangle_0 = 1 - \langle S_\theta \rangle_0 + \frac{1}{2} \left(\left\langle S_\theta^2 + S_\phi^2 + 2S_\theta S_\phi \right\rangle_0 \right) + ... = \tag{5.3.11}$$

Where due to the exponential decay the "$S_\theta S_\phi$" term is eliminated, and if only keeping the lowest order of each term we can neglect S_θ^2 [12]. This leaves us with S_ϕ^2. Since the Hamiltonian does not have

---

[12]This can be done because all orders promotes the same behavior, while the lowest order term has the smallest scaling dimension making it the most relevant term.

any mixing between the two sectors one can write

$$\frac{1}{2}\left\langle S_\phi^2 \right\rangle_0 = 2m_\phi'^2 \int \mathrm{d}^2x_1 \mathrm{d}^2x_2 \left\langle \cos\left(\frac{N}{\sqrt{2}}\phi_\rho(x_1)\right)\cos\left(\frac{N}{\sqrt{2}}\phi_\sigma(x_1)\right)\cos\left(\frac{N}{\sqrt{2}}\phi_\rho(x_2)\right)\cos\left(\frac{N}{\sqrt{2}}\phi_\sigma(x_2)\right) \right\rangle_0 =$$

$$2m_\phi'^2 \int \mathrm{d}^2x_1 \mathrm{d}^2x_2 \left\langle \cos\left(\frac{N}{\sqrt{2}}\phi_\rho(x_1)\right)\cos\left(\frac{N}{\sqrt{2}}\phi_\rho(x_2)\right) \right\rangle_0 \left\langle \cos\left(\frac{N}{\sqrt{2}}\phi_\sigma(x_1)\right)\cos\left(\frac{N}{\sqrt{2}}\phi_\sigma(x_2)\right) \right\rangle_0 =$$

$$2m_\phi'^2 \int \mathrm{d}^2x_1 \mathrm{d}^2x_2 \left\langle \cos\left(\frac{N}{\sqrt{2}}\phi_\rho(x_1)\right)\cos\left(\frac{N}{\sqrt{2}}\phi_\rho(x_2)\right) \right\rangle_0 \frac{1}{4}\sum_{\mu,\nu=\pm1}\left\langle e^{\frac{N}{\sqrt{2}}(\mu\phi_\sigma(x_1)+\nu\phi_\sigma(x_2))} \right\rangle_0$$

$$(5.3.12)$$

Due the exponential suppression of $e^{-i\alpha\phi_\sigma}$ correlations, one sees that the only possible contribution comes from $\nu = -\mu$ while having $x_1 = x_2$. One can therefore as in [54] make the approximation

$$\left\langle \cos\left(N/\sqrt{2}\phi_\sigma(x_1)\right)\cos\left(N/\sqrt{2}\phi_\sigma(x_2)\right) \right\rangle_0 \approx D\delta(x_1 - x_2) \quad {}^{13} \qquad (5.3.13)$$

where D is an $\mathcal{O}(1)$ constant. This leads to

$$\frac{1}{2}\left\langle S_\phi^2 \right\rangle_0 \approx 2Dm_\phi'^2 \int \mathrm{d}^2x \left\langle \cos^2\left(\frac{N}{\sqrt{2}}\phi_\rho\right) \right\rangle_0 = m' \int \mathrm{d}^2x \left\langle \cos\left(2\frac{N}{\sqrt{2}}\phi_\rho\right) \right\rangle_0 + \mathrm{Const.} =$$

$$\left\langle \tilde{S}_\phi \right\rangle_0 + \mathrm{Const.} \qquad (5.3.14)$$

where $m' \equiv Dm_\phi'^2$. By neglecting the constant and reexponentiating one finds

$$\frac{Z}{Z_0} = \left\langle e^{-(S_\theta - \tilde{S}_\phi)} \right\rangle_0 \qquad (5.3.15)$$

The effective Hamiltonian for the charge sector therefore becomes

$$\underline{\mathrm{H}}_{eff}^\rho = \frac{v}{2\pi}\int \mathrm{d}x \left(K_\rho(\partial_x\phi_\rho)^2 + \frac{1}{K_\rho}(\partial_x\theta_\rho)^2 + m'\cos\left(\sqrt{2}N\phi_\rho\right) - 2m_\theta'\cos\left(\frac{N}{\sqrt{2}}\theta_\rho\right) \right) \qquad (5.3.16)$$

where the scaling dimensions are given by

$$D_{\bar{\phi}} = \frac{N}{K_\rho} \ , \quad K_\rho > \frac{N}{2}$$

$$D_{\bar{\theta}} = \frac{K_\rho N}{4} \ , \quad K_\rho < 8/N \qquad (5.3.17)$$

If translating this term back into the discretized language one finds

$$H = ... + \frac{m'}{2}\sum_i \left(\prod_{m=i}^{L}(\eta_{m,\uparrow}\eta_{m,\downarrow})^N + \mathrm{h.c.} \right), \qquad (5.3.18)$$

and one can therefore see it as another BGI term, which is proportional to the identity when reinserting the discrete $\mathbb{Z}_N$ symmetry. There will also appear other higher order terms, but for now this will be the important one, since it has the possibility of pinning the charge sector. Later other higher order terms will be considered.

In Fig. 5.4 one finds a graphical representation of the scaling dimensions for the different terms present in Eq. (5.3.16). Comparing this to the first order analysis in Fig. 5.3 one finds, that the gapless phase has shrunk and is completely removed for $N = 4$. This analysis also predicts the phase diagram

---

[13] This approximation can be interpreted as if having θ_σ being constant, then since ϕ_σ is related to the Fourier transform of θ_σ, due to them not commuting, then one finds ϕ_σ becoming a Dirac delta function.
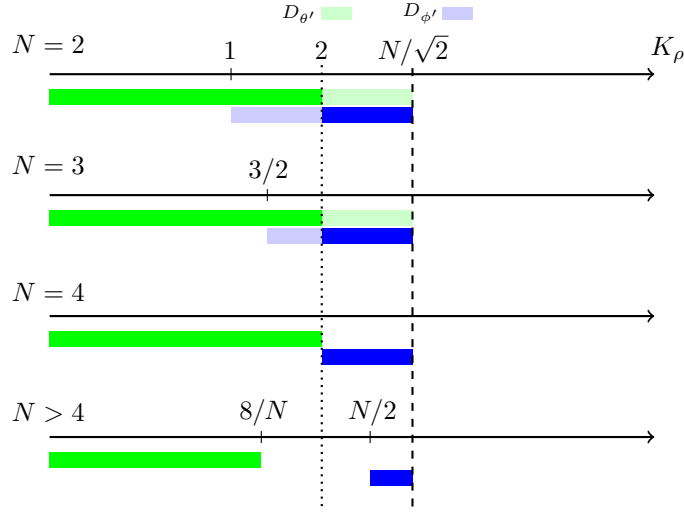
Figure 5.4 | Graphically representation of quasi second order prediction. This figure illustrates for which value of K_ρ the different terms in Eq. (5.3.16) are relevant. The dashed line at $K_\rho = 2$ represents where the terms are equally relevant so $D_{\theta'} = D_{\phi'}$, which is where the analysis predicts a phase transition. The dashed line at $K_\rho = N/\sqrt{2}$ represents where the rung tunneling term will pin θ_σ, by being more relevant than the BGI term of the ϕ-fields. There higher order BGI term is therefore only necessary to consider after this point. At last, this analysis predicts a gapless phase only for $N > 4$.

for $N = 4$ to coincide with that of $N = 2$, which is what the mapping presented in [47] predicted. It also predicts a new phase for $K \in [N/2, N/\sqrt{2}]$ where ϕ_ρ and θ_σ are pinned, which is a phase not possible to predict from the first order analysis. Later this phase will show to be highly relevant.

With this two-step-RG procedure one should connect Fig. 5.4 and Fig. 5.2, by thinking of two discrete flows. Under the initial flow one should look at Fig. 5.2, where one sees that for $K > N/\sqrt{2}$ the initial flow will simultaneously pin both ϕ-field and no effective Hamiltonian is needed. For $K > N/\sqrt{2}$ one instead sees that the initial flow first will pin θ_σ, due to the rung tunneling term being the most relevant. One should therefore see this as the first discrete flow in the two-step-RG procedure. After this one writes an effective Hamiltonian for the unpinned sector, where the quasi second order analysis yields a second order term, which then yields the scaling analysis shown in Fig. 5.4. This approach therefore predicts a clear distinction between $N \leq 4$ and $N > 4$, which the observables of the system should be able to show.

5.4 Observables and order parameter

In wanting to differentiate phases a useful tool is to measure the behavior of correlation functions. These functions tell how separated regions of the system are correlated, and how far away different perturbations are felt. For a gauge theory one finds, due to Elitzur's theorem, that expectation values which are gauge-dependent will average to zero. A simple way to see this is by considering the fact that the Hamiltonian in Eq. (5.1.20) is invariant under

$$\phi_\rho, \theta_\rho, \phi_\sigma \to \phi_\rho, \theta_\rho, \phi_\sigma + \frac{\sqrt{2}2\pi}{N} \tag{5.4.1}$$

while no translational symmetry is found for θ_σ. This means that if any observable is not also invariant under this translation, then it must average to zero [52]. If the operator $\mathcal{O}$ is not invariant under any

of these translations then

$$\left\langle e^{i\mathcal{O}} \right\rangle = \left\langle e^{i(\mathcal{O} + \frac{\sqrt{2}2\pi}{N})} \right\rangle = e^{i\frac{\sqrt{2}2\pi}{N}} \left\langle e^{i\mathcal{O}} \right\rangle = 0 \tag{5.4.2}$$

Where it has been used that all lattice operators for the system in terms of the bosonic fields are written in the form $e^{i\mathcal{A}}$. The reason θ_σ represents operators which always are gauge invariant in this limit, is because this field represents the rung tunneling term which is gauge invariant [14]. This limits the number of correlation functions, but the literature still offers plenty to choose from. In the case where the system is diagonalized by going to the spin and charge sector, these operators though need modification in order to probe each of these individually.

One of these operators is the meson string, which is the same as the one previously defined in Eq. (4.4.1), except it is now only defined to live in one of the legs as

$$M_s(x,y) = \zeta_{x,s} \left(\prod_{j=x}^{y-1} \sigma_{j,s} \right) \zeta_{y,s}^\dagger , \quad s = \uparrow, \downarrow \tag{5.4.3}$$

Which, as previously explained, excites an electric field line between the two excited Higgs bosons at position (x,s) and (y,s). In the axial gauge this operator becomes

$$\underline{M}_s(x,y) = \zeta_{x,s} \zeta_{y,s}^\dagger \tag{5.4.4}$$

In terms of the bosonic fields one finds that this operator probes θ_s, and is described by

$$\underline{M}_s(x,y) \to e^{i(\theta_s(x) - \theta_s(y))} \tag{5.4.5}$$

If neglecting boundary conditions and focusing on the bulk properties then three types of behavior are predicted by bosonization. If a phase pins θ_s then it predicts $\langle \underline{M}_s(x,y) \rangle = 1$, so a constant behavior independent on $R = |x - y|$. If instead pinning ϕ_s, then one finds an exponential decaying behavior $\langle \underline{M}_s(x,y) \rangle \propto e^{-R/\xi}$, since θ_s will fluctuate wildly. In the following section ξ always represents some unspecified correlation length. At last if both θ_s and ϕ_s are not pinned, yielding a gapless phase, then one can neglect the none-quadratic part of the Hamiltonian leaving

$$\left\langle e^{i(\theta_s(x) - \theta_s(y))} \right\rangle = \left\langle e^{i(\theta_s(x) - \theta_s(y))} \right\rangle_0 = e^{-\frac{1}{2}\left\langle (\theta_s(x) - \theta_s(y))^2 \right\rangle_0} = \frac{A_\theta}{|x|^{\frac{K}{N}}}, \tag{5.4.6}$$

where the result in Eq. (5.2.19) has been used. This is a power law behavior, and it states that a gapless system will show similar behavior on all length scales.

In the above analysis one finds a gapless phase, where the charge sector is unpinned. Since $\underline{M}_s$ probes both the charge and spin sector due to Eq. (5.1.19), the analysis only predicts this operator to show a constant or an exponential decaying behavior. In order to solely probe the charge and spins sector, one can from $\underline{M}_s(x,y)$ construct to new operators

$$\underline{M}_\rho(x,y) = \underline{M}_\uparrow(x,y) \underline{M}_\downarrow(x,y) \tag{5.4.7}$$

$$\underline{M}_\sigma(x,y) = \underline{M}_\uparrow(x,y) \underline{M}_\downarrow(x,y)^\dagger \tag{5.4.8}$$

Using these operators and the quasi second order predictions, it is now possible to make some predictions. From the above analysis one finds for $N \leq 4$

$$\langle M_\rho(x,y) \rangle = \begin{cases} \text{Const.} & , K < 2 \\ \propto e^{-R/\xi} & , K > 2 \end{cases} \tag{5.4.9}$$

$$\langle M_\sigma(x,y) \rangle = \begin{cases} \text{Const.} & , K < \frac{N}{\sqrt{2}} \\ \propto e^{-R/\xi} & , K > \frac{N}{\sqrt{2}} \end{cases} \tag{5.4.10}$$

$$\tag{5.4.11}$$

---

[14] In the limit of $g \to 0$ one finds $\overline{\zeta_{\uparrow,r} \sigma 0, r \zeta_{\downarrow,r}^\dagger} \to \zeta_{\uparrow,r} \zeta_{\downarrow,r}^\dagger$ which translates to $e^{i\sqrt{2}\theta_\sigma}$, such that $e^{i\alpha\theta_\sigma}$ represents the gauge invariant rung tunneling operator to some power.

While for $N > 4$ a different behavior for $\underline{M}_\rho$ is predicted

$$\langle M_\rho(x,y) \rangle = \begin{cases} \text{Const.} & , K < \frac{8}{N} \\ \frac{A_\theta}{|x|^{K/N}} & , \frac{8}{N} < K < \frac{N}{2} \\ \propto e^{-R/\xi} & , \frac{N}{2} < K \end{cases} \tag{5.4.12}$$

$$\tag{5.4.13}$$

By measuring the behavior of M_ρ one can thereby distinguish the different phases [15].

A similar operator is the two-point correlation function associated with

$$R(x,y) \equiv \zeta_{x,\uparrow}^\dagger \sigma_{x,0} \zeta_{x,\downarrow} \zeta_{y,\uparrow} \sigma_{y,0}^\dagger \zeta_{y,\downarrow}^\dagger . \tag{5.4.14}$$

which in the limit of $g \to 0$ is the same as M_σ in the axial gauge and will only probe the spin sector. For this operator one also finds $R(x,y) = \underline{R}(x,y)$. Next we have the Wilson loop defined by

$$W(x,y) \equiv \sigma_{x,0} \prod_{j=x}^{y-1} \left(\sigma_{j,\uparrow} \sigma_{j,\downarrow}^\dagger \right) \sigma_{y,0}^\dagger \tag{5.4.15}$$

which simply corresponds to a string of plaquette operators. This operator measures the total magnetic flux between x and y. In the limit of $g \to 0$ this operator equals 1 for all λ, and in the axial gauge it simply becomes

$$\underline{W}(x,y) = \sigma_{x,0} \sigma_{y,0}^\dagger \tag{5.4.16}$$

In similar fashion to the 't Hooft loop operator defined in [34], one can define

$$G_\uparrow(r) = \tau_{r,\uparrow} \prod_{j>r} \tau_{j,0} , \quad G_\downarrow(r) = \tau_{r,\downarrow}^\dagger \prod_{j>r} \tau_{j,0} . \tag{5.4.17}$$

In this geometry this operator is not a loop but as the 't Hooft loop operator, it commutes with all plaquette operators thereby not introducing any magnetic flux into the system. Instead it introduces a magnetic flux at the end and then moves it down the ladder until the flux exits the system at the rth plaquette. In the axial gauge these operator becomes

$$\underline{G}_\uparrow(r) = \prod_{j>r} \eta_{j,\uparrow}^\dagger , \quad \underline{G}_\downarrow(r) = \prod_{j>r} \eta_{j,\downarrow} . \tag{5.4.18}$$

Such that these two operator respectively probes the $\phi_\uparrow$ and $\phi_\downarrow$ fields. From these one can construct

$$G_\rho(r) = G_\uparrow(r) G_\downarrow^\dagger(r) = \tau_{r,\uparrow} \tau_{r,\downarrow} , \quad \underline{G}_\rho(r) = \prod_{j>r} \eta_{j,\uparrow}^\dagger \eta_{j,\downarrow}^\dagger \tag{5.4.19}$$

$$G_\sigma(r) = G_\uparrow(r) G_\downarrow(r) = \tau_{r,\uparrow} \tau_{r,\downarrow}^\dagger \prod_{j>r} \tau_{j,0}^2 , \quad \underline{G}_\sigma(r) = \prod_{j>r} \eta_{j,\uparrow}^\dagger \eta_{j,\downarrow} . \tag{5.4.20}$$

Which, as seen by the representation in the axial gauge, probes the charge and spin sector respectively.

In similar a fashion to when studying the quantum Ising chain, one would like to define an order parameter, which could separate the ferromagnetic and para-magnetic phase. For this system this would correspond to ζ_r. This is though not a gauge invariant operator, which is because, as earlier explained, that for a system with smooth-smooth boundaries a global Z_N symmetry representing charge conservation is present, and the operator ζ_r does not preserve this. In order to get around this, one could though open up the boundary to the right resulting in a rough-smooth boundary. Doing

---

[15]When an operator is inside $\langle ... \rangle$ the bar is omitted since the correlation is gauge invariant.

this one finds the gauge invariant boundary term $\sigma_{0,s}\zeta^{\dagger}_{0,s}$ which breaks the charge conservation and one can thereby construct the gauge invariant operator

$$O_{r,s} = \zeta_{r,s} \prod_{j=0}^{r-1} \sigma^{\dagger}_{j,s} \qquad (5.4.21)$$

This operator is similar to the meson operator, and it brings a charge into the system from the rough boundary and simultaneously creates a flux line going from the rough boundary to the charge. In the axial gauge this operator states

$$\underline{O}_{r,s} = \zeta_{r,s} \qquad (5.4.22)$$

thereby taking the place of an order parameter, which describes the magnetization of the system. This order parameter would locally be able to distinguish between the phase where both ϕ-fields are pinned and the phase where both θ-fields are pinned. It would not locally be able to distinguish the gapless phase. One should though remember that order parameters looks quite different in the different gauges. One could for example take the example of

$$G_{\rho}(r) = \tau_{\uparrow,r}\tau_{\downarrow,r} \qquad (5.4.23)$$

which in the axial gauge becomes

$$\underline{G}_{\rho}(r) = \prod_{j>r} \eta^{\dagger}_{\uparrow,j}\eta^{\dagger}_{\downarrow,j} \sim e^{-i\sqrt{2}\phi_{\rho}} \qquad (5.4.24)$$

but in the unitary gauge this stays local, such that if simulating the system in the unitary gauge description this local operator can be used to distinguish different phases.

If forgetting the above order parameters one finds in Fig. 5.5 a schematic representation of the predicted behavior of the observables. In this figure one sees that no single observable can distinguish
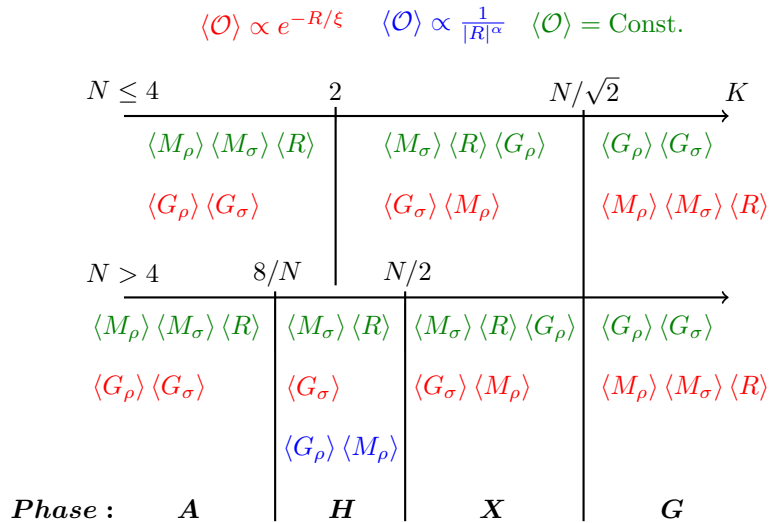
Figure 5.5 | Predictions of quasi second order analysis. In this figure one finds the predicted behavior of the quasi second order analysis. In top one finds the color code, where all the correlation functions in red represent them to show exponentially decaying behavior, blue represents power law behavior and green constant behavior. Here one sees that no single operator can distinguish all phases.

all the phases predicted. For $N > 4$ one can for example use M_{ρ} to distinguish the three phases to the left, while one would also need to look at M_{σ}, R or G_{σ}, so operators probing the spin sector,

to distinguish the two rightmost phases. The rightmost phase, phase $\boldsymbol{G}$, is the previously predicted deconfined phase, where due to $\langle M_{\sigma,\rho} \rangle$ showing exponential decay, the Higgs matter will not interact unless close by one another. In this phase the mass term of the Higgs matter will be large, such that not many Higgs particles will be present. This also indicated by $\langle G_{\sigma,\rho} \rangle$ being constants, which means that excitations of the Higgs field will be highly suppressed. In the section on bound states of matter, one finds perturbative calculations performed for $\langle M_{\downarrow/\uparrow} \rangle$ which showed these to have exponentially decaying behavior, which is consistent with these predictions.

Instead in phase $\boldsymbol{X}$ one finds $\langle M_\sigma \rangle$ to show constant behavior while $\langle M_\rho \rangle$ will be exponentially decaying. This still means that $\langle M_{\downarrow/\uparrow} \rangle$ will show exponentially decaying behavior, since they probe both the charge and spin sector, but it is not the whole story. Having $\langle M_\sigma \rangle$ being constant means, that excitations of the kind associated with the operator $\zeta_{i,\uparrow}\zeta_{i,\downarrow}^\dagger$ will be present in the system. These bound states of matter can be thought of as dipole particles, since one finds opposite charges excited in the legs. This was not predicted by the perturbative calculations.

In the gapless phase $\boldsymbol{H}$ one will find the gapless excitation to be associated with $\zeta_{i,\uparrow}\zeta_{i,\downarrow}$, so an excitation of the same charge in both legs. Instead the dipole excitation will still be gapped. Had one considered operators which solely probed either the $\uparrow$- or $\downarrow$-sector, one would not find any power law behavior but only exponential decay or constant behavior. This therefore illustrates the importance describing the system in terms of the charge and spin sectors. The last phase, $\boldsymbol{A}$, is what we denote the Higgs phase. Here all excitations of the Higgs field will be gapped but, and the renormalized system be a condensate of meson particles. This is most easily seen by translating the system back into the discretized language, where since the BGI term for the θ-fields and the rung tunneling term are the relevant terms one is left with

$$\underline{H}' = -\lambda \sum_{s=\uparrow,\downarrow} \sum_{i=0}^{L-1} \left(\zeta_{i,s}\zeta_{i+1,s}^\dagger + \text{H.c.} \right) - \lambda' \sum_{i=0}^{L} \left(\zeta_{i,\uparrow}\zeta_{i,\downarrow}^\dagger + \text{H.c.} \right) \tag{5.4.25}$$

where it has been used that in the first order analysis the Luttinger parameter does not change. With this, the ground state of the renormalized system can be expressed as

$$|GS\rangle = \prod_{i=0}^{L} \sum_{n=0}^{N-1} \frac{\left(\zeta_{i,\uparrow}^\dagger \zeta_{i,\downarrow} \right)^n}{\sqrt{N}} \prod_{j=0}^{L-1} \sum_{n=0}^{N-1} \frac{\left(\zeta_{j,\uparrow}^\dagger \zeta_{j+1,\uparrow} \right)^n}{\sqrt{N}} \sum_{n=0}^{N-1} \frac{\left(\zeta_{j,\downarrow}^\dagger \zeta_{j+1,\downarrow} \right)^n}{\sqrt{N}} \, ||0\rangle\rangle_\eta \tag{5.4.26}$$

which is consistent with the ground state found in the limit of $\lambda \to \infty$. Now the $\zeta\zeta^\dagger$ operators are associated with the creation of a meson, such that this ground state corresponds to a meson condensate, where an unspecified number of mesons are present.

To conclude this section, one sees that by considering higher order terms, new phases can appear and the new terms considered can strongly influence the predicted phase diagram. In order to be more certain of the predictions offered by the bosonized description, one should therefore tend to a true second order RG analysis.

5.5   Second order RG for $g = 0$ in real space

In this section the second order RG calculations are performed in real space following the calculations performed in [52]. If comparing this approach with the momentum space approach one does not care about the renormalized action $S'[\phi', \theta']$, but instead one looks at how different correlation functions behave under the RG procedure. The starting point is the action

$$S_0 = \int \mathrm{d}^2x \left[\frac{1}{2_\sigma} \left(\frac{(\partial_\tau \theta_\sigma)^2}{v} + v(\partial_x \theta_\sigma)^2 \right) + \frac{1}{2\pi K_\rho} \left(\frac{(\partial_\tau \theta_\rho)^2}{v} + v(\partial_x \theta_\rho)^2 \right) \right] \tag{5.5.1}$$

$$S_1 = \int \mathrm{d}^2 x \left[2m_\theta \cos\left(\frac{N}{\sqrt{2}}\theta_\rho\right) \cos\left(\frac{N}{\sqrt{2}}\theta_\sigma\right) \right.$$
$$\left. + 2m_\phi \cos\left(\frac{N}{\sqrt{2}}\phi_\rho\right) \cos\left(\frac{N}{\sqrt{2}}\phi_\sigma\right) + \frac{2\lambda}{a} \cos\left(\sqrt{2}\theta_\sigma\right) \right] \tag{5.5.2}$$

Where the different Luttinger parameters have been given subscripts to indicate which sector they belong to. This approach cares about the behavior of the correlation functions when the fluctuations at the smallest length scales are integrated out. To capture the behavior of terms which probes both sectors as the BGI terms, one needs to consider correlation functions probing both sectors. In the this analysis the following correlation function is considered

$$\left\langle \prod_{s=\sigma,\rho} e^{-i\phi_s(x_1)} e^{i\phi_s(x_2)} \right\rangle \tag{5.5.3}$$

This correlation function is taken with respect to the whole action and it is therefore not feasible to calculate. Instead one tends to a perturbative expansion in S_1, which from Eq. (5.3.4) leads to

$$\left\langle \prod_{s=\sigma,\rho} e^{-i\phi_s(x_1)} e^{i\phi_s(x_2)} \right\rangle = \left\langle \prod_{s=\sigma,\rho} e^{-i\phi_s(x_1)} e^{i\phi_s(x_2)} e^{-S_1} \right\rangle_0 = \left\langle \prod_{s=\sigma,\rho} e^{-i\phi_s(x_1)} e^{i\phi_s(x_2)} \right\rangle_0$$
$$- \left(\left\langle \prod_{s=\sigma,\rho} e^{-i\phi_s(x_1)} e^{i\phi_s(x_2)} S_1 \right\rangle_0 - \left\langle \prod_{s=\sigma,\rho} e^{-i\phi_s(x_1)} e^{i\phi_s(x_2)} \right\rangle_0 \langle S_1 \rangle_0 \right)$$
$$+ \frac{1}{2} \left(\left\langle \prod_{s=\sigma,\rho} e^{-i\phi_s(x_1)} e^{i\phi_s(x_2)} S_1^2 \right\rangle_0 - \left\langle \prod_{s=\sigma,\rho} e^{-i\phi_s(x_1)} e^{i\phi_s(x_2)} \right\rangle_0 \langle S_1^2 \rangle_0 \right.$$
$$\left. + 2 \left\langle \prod_{s=\sigma,\rho} e^{-i\phi_s(x_1)} e^{i\phi_s(x_2)} \right\rangle_0 (\langle S_1 \rangle_0)^2 - 2 \left\langle \prod_{s=\sigma,\rho} e^{-i\phi_s(x_1)} e^{i\phi_s(x_2)} S_1 \right\rangle_0 \langle S_1 \rangle_0 \right) + ... \tag{5.5.4}$$

5.6 Second order calculations for the background interactions

In this section the expansion in Eq. (5.5.4) will be calculated to second order. In order to spare the reader for too many calculations this sections will focus on the BGI term for the ϕ-fields, and the contribution from the others is easily realized from these.

5.6.1 First order contribution

The zeroth order is trivially calculated using the previously shown correlation functions, instead the first order term shows more difficulties. The first quantity we look at is $\langle S_1 \rangle_0$. Using the cumulant expansion and separating the exponentials all the terms take the form

$$\langle S_1 \rangle_0 \propto \left\langle e^{\pm i \frac{N}{\sqrt{2}}\phi_\sigma} e^{\pm i \frac{N}{\sqrt{2}}\phi_\rho} \right\rangle_0 = e^{-\frac{N^2}{4}\langle \phi_\sigma^2 \rangle_0} e^{-\frac{N^2}{4}\langle \phi_\rho^2 \rangle_0} = \left(\frac{a}{L}\right)^{\frac{N}{K2}} \tag{5.6.1}$$

Where the last step comes from Eq. (5.2.18). In the thermodynamic limit of $L \to \infty$ these correlation functions can safely be neglected. That this correlation function equals zero could also have been realized from the Hamiltonian being invariant under $\phi_s \to \phi_s + \alpha$, which means

$$\left\langle e^{i\beta\phi_s} \right\rangle_0 = \left\langle e^{i\beta(\phi_s+\alpha)} \right\rangle_0 = e^{i\beta\alpha} \left\langle e^{i\beta\phi_s} \right\rangle_0 \tag{5.6.2}$$

which evidently must lead to $\left\langle e^{i\beta\phi_s} \right\rangle_0$ being zero [52]. This argument can also be used to neglect the second first order term since all terms can be written on the form

$$\frac{m_\theta}{2} \int_{L>|\mathbf{x}_3|>a} \mathrm{d}^2 x_3 \prod_{s=\sigma,\rho} \left\langle e^{-i\phi_s(x_1)} e^{i\phi_s(x_2)} e^{\pm i\frac{N}{\sqrt{2}}\phi_\rho(x_3)} e^{\pm i\frac{N}{\sqrt{2}}\phi_\sigma(x_3)} \right\rangle_0 \qquad (5.6.3)$$

which is not invariant under taking either $\phi_\sigma \to \phi_\sigma + \alpha$ or $\phi_\rho \to \phi_\rho + \alpha$ separately. Doing the calculations would therefore show this term be proportional to some power of $1/L$, which in the thermodynamic limit yields zero. Having all first order contribution yielding zero is consistent with [52–54]. Had one not taken the thermodynamic limit this term would instead break the translational invariance of the system, but by considering only the bulk properties of the system, this could still be safely neglected in the large L limit.

5.6.2 Second order contribution

For the second order contribution the first thing to notice is that the two last terms proportional to $\langle S_1 \rangle_0$ will yield zero in the thermodynamic limit due to Eq. (5.6.1), and we are therefore left with

$$\frac{1}{2} \left(\left\langle \prod_{s=\sigma,\rho} e^{-i\phi_s(x_1)} e^{i\phi_s(x_2)} S_1^2 \right\rangle_0 - \left\langle \prod_{s=\sigma,\rho} e^{-i\phi_s(x_1)} e^{i\phi_s(x_2)} \right\rangle_0 \left\langle S_1^2 \right\rangle_0 \right) =$$

$$\frac{1}{2}(2m_\phi)^2 \frac{1}{2^4} \int \mathrm{d}^2 x_3 \mathrm{d}^2 x_4 \left(\prod_{s=\sigma,\rho} \sum_{\mu=\pm 1} \left\langle e^{-i\phi_s(x_1)} e^{i\phi_s(x_2)} e^{-i\frac{\mu N}{\sqrt{2}}\phi_s(x_3)} e^{i\frac{\mu N}{\sqrt{2}}\phi_s(x_4)} \right\rangle_0 \right.$$

$$\left. - \prod_{s=\sigma,\rho} \sum_{\mu=\pm 1} \left\langle e^{-i\phi_s(x_1)} e^{i\phi_s(x_2)} \right\rangle_0 \left\langle e^{-i\frac{\mu N}{\sqrt{2}}\phi_s(x_3)} e^{i\frac{\mu N}{\sqrt{2}}\phi_s(x_4)} \right\rangle_0 \right) \qquad (5.6.4)$$

Where it has been used that if considering terms of the kind $e^{-i\phi_i(x_3)} e^{-i\phi_i(x_4)}$ or $e^{i\phi_i(x_3)} e^{i\phi_i(x_4)}$ it will not be invariant under a translation of the ϕ-fields and therefore yield zero [16]. In order to have the time component and the space component to behave the same, meaning that later they will be localized in the same neighborhood, one makes the scaling $x_1 = (x, y = v\tau)$. This brings out a factor of $1/v^2$.

If considering the first term in the parentheses one finds

$$\frac{m_\phi^2}{v^2 2^3} \int \mathrm{d}^2 x_3 \mathrm{d}^2 x_4 \prod_{s=\sigma,\rho} \sum_{\mu=\pm 1} e^{\frac{-1}{2}\left\langle \left[(-\phi_s(x_1)+\phi_s(x_2)) - \frac{\mu N}{\sqrt{2}}\phi_\rho(x_3) + \frac{\mu N}{\sqrt{2}}\phi_\rho(x_4) \right]^2 \right\rangle_0}$$

$$= \frac{m_\phi^2}{v^2 2^3} \int \mathrm{d}^2 x_3 \mathrm{d}^2 x_4 \prod_{s=\sigma,\rho} \sum_{\mu=\pm 1} \left\langle e^{-i\phi_s(x_1)} e^{i\phi_s(x_2)} \right\rangle_0 \left\langle e^{-i\frac{\mu N}{\sqrt{2}}\phi_s(x_3)} e^{i\frac{\mu N}{\sqrt{2}}\phi_s(x_4)} \right\rangle_0$$

$$e^{\frac{\mu N}{\sqrt{2}}\left(\langle \phi_s(x_1)\phi_s(x_3) \rangle_0 - \langle \phi_s(x_1)\phi_s(x_4) \rangle_0 - \langle \phi_s(x_2)\phi_s(x_3) \rangle_0 + \langle \phi_s(x_2)\phi_s(x_4) \rangle_0 \right)} \qquad (5.6.5)$$

The correlation functions presented in the above terms are all given by the relations found in Eq. (5.2.19), where for simplicity we define

$$F_{\phi,s}(x - x') \equiv \left\langle (\phi_s(x) - \phi_s(x'))^2 \right\rangle_0 = \frac{2}{K_s N} \ln\left(\frac{|x - x'|}{a} \right) \qquad (5.6.6)$$

---

[16] Had one not taken the limit of $L \to \infty$ then the otherwise eliminated terms would again yield a contribution which was not translational invariant and proportional to $1/L$.

With this, the second order contribution takes the form

$$\frac{m_\phi^2}{v^2 2^3} \prod_{s'=\sigma,\rho} e^{-\frac{1}{2} F_{\phi,s'}(x_1-x_2)} \int d^2x_3 d^2x_4 e^{-\frac{N^2}{4} F_{\phi,\rho}(x_3-x_4)} e^{-\frac{N^2}{4} F_{\phi,\sigma}(x_3-x_4)}$$

$$\left(\prod_{s=\sigma,\rho} \sum_{\mu=\pm 1} e^{\frac{\mu N}{\sqrt{2}} (F_{\phi,s}(x_1-x_3) - F_{\phi,s}(x_1-x_4) + F_{\phi,s}(x_2-x_4) - F_{\phi,s}(x_2-x_3))} - 1 \right) \qquad (5.6.7)$$

Since a describes the lattice spacing and therefore the smallest length scale of the system one can, as in [52], take this to be $a \ll 1$. Looking at the definition of $F_{\phi,s}$ in Eq. (5.6.6) one finds that in this limit, the integral will be dominated by $|x_3 - x_4| \ll 1$. This lead to the introduction of center of mass and relative coordinates

$$r = x_3 - x_4 \ , \quad R = \frac{x_3 + x_4}{2} \qquad (5.6.8)$$

leading to

$$\frac{m_\phi^2}{v^2 2^3} \prod_{s'=\sigma,\rho} e^{-\frac{1}{2} F_{\phi,s'}(x_1-x_2)} \int d^2r d^2R \ e^{-\frac{N^2}{4} F_{\phi,\rho}(r)} e^{-\frac{N^2}{4} F_{\phi,\sigma}(r)}$$

$$\left(\prod_{s=\sigma,\rho} \sum_{\mu=\pm 1} e^{\frac{\mu N}{\sqrt{2}} [F_{\phi,s}(x_1-[R+r/2]) - F_{\phi,s}(x_1-[R-r/2]) + F_{\phi,s}(x_2-[R-r/2]) - F_{\phi,s}(x_2-[R+r/2])]} - 1 \right) \qquad (5.6.9)$$

Due the intragral being dominated by $|r| << 1$ one can expand this to first order in r which yields

$$\frac{m_\phi^2}{v^2 2^3} \prod_{s'=\sigma,\rho} e^{-\frac{1}{2} F_{\phi,s'}(x_1-x_2)} \int d^2r d^2R \ e^{-\frac{N^2}{4} F_{\phi,\rho}(r)} e^{-\frac{N^2}{4} F_{\phi,\sigma}(r)}$$

$$\left(\prod_{s=\sigma,\rho} \sum_{\mu=\pm 1} e^{\frac{\mu N}{\sqrt{2}} r [\nabla_R F_{\phi,s}(x_2-R) - \nabla_R F_{\phi,s}(x_1-R)]} - 1 \right)$$

$$\approx \frac{m_\phi^2}{v^2 2^3} \prod_{s'=\sigma,\rho} e^{-\frac{1}{2} F_{\phi,s'}(x_1-x_2)} \int d^2r d^2R e^{-\frac{N^2}{4} F_{\phi,\rho}(r)} e^{-\frac{N^2}{4} F_{\phi,\sigma}(r)}$$

$$|r|^2 N^2 \sum_{s=\sigma,\rho} [\nabla_R F_{\phi,s}(x_2-R) - \nabla_R F_{\phi,s}(x_1-R)]^2 \qquad (5.6.10)$$

where the sum over μ eliminates the first order term in the expansion of the exponential. If now using integration by parts and neglecting the boundary term this translates into

$$-\frac{m_\phi^2}{v^2 2^3} \prod_{s'=\sigma,\rho} e^{-\frac{1}{2} F_{\phi,s'}(x_1-x_2)} \int d^2r d^2R \ e^{-\frac{N^2}{4} F_{\phi,\rho}(r)} e^{-\frac{N^2}{4} F_{\phi,\sigma}(r)}$$

$$|r|^2 N^2 \sum_{s=\sigma,\rho} [F_{\phi,s}(x_2-R) - F_{\phi,s}(x_1-R)] \nabla_R^2 [F_{\phi,s}(x_2-R) - F_{\phi,s}(x_1-R)] \qquad (5.6.11)$$

If focusing on the R-integral one realizes by the use of

$$\nabla_{\mathbf{R}}^2 \ln \left(\frac{|\mathbf{R} - \mathbf{r}|}{a} \right) = 2\pi \delta^2(\mathbf{R} - \mathbf{r}) \qquad (5.6.12)$$

that it can be translated into

$$\int d^2R \sum_{s=\sigma,\rho} [F_{\phi,s}(x_2-R) - F_{\phi,s}(x_1-R)] \nabla_R^2 [F_{\phi,s}(x_2-R) - F_{\phi,s}(x_1-R)] = -\frac{2^4\pi}{N^2} \sum_{s=\sigma,\rho} \frac{1}{K_s^2} \ln \left(\frac{|x_1 - x_2|}{a} \right)$$

$$(5.6.13)$$

if inserting this along with the definition of $F_{\phi,s}$ one is left with

$$
\underbrace{\left[\left(\frac{a}{|x_1 - x_2|}\right)^{\frac{1}{K_\sigma N} + \frac{1}{K_\rho N}}\right]}_{\left\langle \prod_{s=\sigma,\rho} e^{-i\phi_s(x_1)} e^{i\phi_s(x_2)} \right\rangle_0} \frac{2\pi m_\phi^2}{v^2} \left(\frac{1}{K_\rho^2} + \frac{1}{K_\sigma^2}\right) \ln\left(\frac{x_1 - x_2}{a}\right) \int \mathrm{d}^2 r \left(\frac{a}{r}\right)^{\frac{N}{2K_\rho} + \frac{N}{2K_\sigma}} r^2 \tag{5.6.14}
$$

Where it is indicated how the first part corresponds to the zeroth order contribution. By performing the r-integral in polar coordinates one finds

$$
\left[\left(\frac{a}{|x_1 - x_2|}\right)^{\frac{1}{K_\sigma N} + \frac{1}{K_\rho N}}\right] \frac{4\pi^2 m_\phi^2}{v^2} \left(\frac{1}{K_\rho^2} + \frac{1}{K_\sigma^2}\right) \ln\left(\frac{|x_1 - x_2|}{a}\right) \int \mathrm{d}r \left(\frac{a}{r}\right)^{\frac{N}{2K_\rho} + \frac{N}{2K_\sigma}} r^3 \tag{5.6.15}
$$

Here it becomes instructive to take a small break and state what the goal is. Due to the self-similarity close to the transition point, one finds that by integrating out the d.o.f of the smallest length scales the correlation function should look the same. This means that if writing the new expression such that it takes the form of the zeroth order, one can see how the parameters develops under the procedure. The wanted result therefore looks like

$$
\left\langle \prod_{s=\sigma,\rho} e^{-i\phi_s(x_1)} e^{i\phi_s(x_2)} e^{-S_1} \right\rangle_0 = \left(\frac{a}{|\mathbf{z}_{1,2}|}\right)^{\frac{1}{NK_\rho^{eff}} + \frac{1}{NK_\sigma^{eff}}} \tag{5.6.16}
$$

This means that one should massage the expression above a bit. By doing so, one finds

$$
\left\langle \prod_{s=\sigma,\rho} e^{-i\phi_s(x_1)} e^{i\phi_s(x_2)} e^{-S_1} \right\rangle_0 \approx
$$

$$
\left(\frac{a}{|x_1 - x_2|}\right)^{\frac{1}{K_\rho N} + \frac{1}{K_\sigma N}} - \left(\frac{a}{|x_1 - x_2|}\right)^{\frac{1}{K_\rho N} + \frac{1}{K_\sigma N}} \frac{4\pi^2 m_\phi^2}{v^2} \left(\frac{1}{K_\rho^2} + \frac{1}{K_\sigma^2}\right) \ln\left(\frac{a}{|x_1 - x_2|}\right)
$$

$$
\int \mathrm{d}r \left(\frac{a}{r}\right)^{\frac{N}{2K_\rho} + \frac{N}{2K_\sigma}} r^3 = \left(\frac{a}{|x_1 - x_2|}\right)^{\frac{1}{K_\rho N} + \frac{1}{K_\sigma N}} \left(1 - \ln\left(\frac{a}{|x_1 - x_2|}\right)^A\right) \approx
$$

$$
\left(\frac{a}{|x_1 - x_2|}\right)^{\frac{1}{K_\rho N} + \frac{1}{K_\sigma N} - A} = \left(\frac{a}{|x_1 - x_2|}\right)^{\frac{1}{NK_\rho^{eff}} + \frac{1}{NK_\sigma^{eff}}} \tag{5.6.17}
$$

Between the two last lines it is assumed that the quantity inside the parentheses is small such that it can be exponentiated. From this one can now study how K_ρ and K_σ behave under the RG procedure. If focusing on the exponent one finds

$$
\frac{1}{NK_\rho^{eff}} + \frac{1}{NK_\sigma^{eff}} = \frac{1}{NK_\rho} + \frac{1}{NK_\sigma} - A =
$$

$$
\frac{1}{NK_\rho} + \frac{1}{NK_\sigma} - \frac{4\pi^2 m_\phi^2}{v^2} \left(\frac{1}{K_\rho^2} + \frac{1}{K_\sigma^2}\right) \int_a^\infty \mathrm{d}r \left(\frac{a}{r}\right)^{\frac{N}{2K_\rho} + \frac{N}{2K_\sigma}} r^3 \tag{5.6.18}
$$

The next step is to integrate out the d.o.f of the smallest length scales. To do this the parameter b is again introduced where $b = 1 + dl$ with dl being infinitesimal. By integrating out fluctuations between

$[a, ab]$ one finds

$$\frac{4\pi^2 m_\phi^2}{v^2} \left(\frac{1}{K_\rho^2} + \frac{1}{K_\sigma^2} \right) \int_a^\infty dr \left(\frac{a}{r} \right)^{\frac{N}{2K_\rho} + \frac{N}{2K_\sigma}} r^3 =$$

$$\frac{4\pi^2 m_\phi^2}{v^2} \left(\frac{1}{K_\rho^2} + \frac{1}{K_\sigma^2} \right) a^4 \int_a^\infty \frac{dr}{a} \left(\frac{a}{r} \right)^{\frac{N}{2K_\rho} + \frac{N}{2K_\sigma} - 3} =$$

$$\frac{4\pi^2 m_\phi^2}{v^2} \left(\frac{1}{K_\rho^2} + \frac{1}{K_\sigma^2} \right) a^4 \left(\int_a^{ab} \frac{dr}{a} \left(\frac{a}{r} \right)^{\frac{N}{2K_\rho} + \frac{N}{2K_\sigma} - 3} + \int_{ab}^\infty \frac{dr}{a} \left(\frac{a}{r} \right)^{\frac{N}{2K_\rho} + \frac{N}{2K_\sigma} - 3} \right) =$$

$$\frac{4\pi^2 m_\phi^2}{v^2} \left(\frac{1}{K_\rho^2} + \frac{1}{K_\sigma^2} \right) a^4 \left((b-1) + b^{4 - \left(\frac{N}{2K_\rho} + \frac{N}{2K_\sigma} \right)} \underbrace{\int_a^\infty \frac{dr'}{a} \left(\frac{a}{r'} \right)^{\frac{N}{2K_\rho} + \frac{N}{2K_\sigma} - 3}}_{r' = r/b} \right) =$$

$$\frac{4\pi^2 m_\phi^2}{v^2} \left(\frac{1}{K_\rho^2} + \frac{1}{K_\sigma^2} \right) a^4 ln(b) + \frac{2\pi^2 N \tilde{m}_\phi^2}{v^2} \left(\frac{1}{K_\rho^2} + \frac{1}{K_\sigma^2} \right) a^4 \int_a^\infty \frac{dr'}{a} \left(\frac{a}{r'} \right)^{\frac{N}{2K_\rho} + \frac{N}{2K_\sigma} - 3} \tag{5.6.19}$$

Where the tilde represent the renormalized constants.

This leads to the first RG equation for m_ϕ given by

$$\tilde{m}_\phi = m_\phi b^{2 - \left(\frac{N}{4K_\rho} + \frac{N}{4K_\sigma} \right)} \tag{5.6.20}$$

where by using the infinitesimal nature of dl one has $b^n = 1 + ndl$, such that $\tilde{m}_\phi$ can be expressed as

$$\tilde{m}_\phi = m_\phi + \frac{dm_\phi}{dl} \cdot dl \tag{5.6.21}$$

Form where RG flow equation can be read off as

$$\frac{dm_\phi}{dl} = m_\phi \left(2 - \left(\frac{N}{4K_\rho} + \frac{N}{4K_\sigma} \right) \right) \tag{5.6.22}$$

Which agrees with the first order scaling dimension previously found.

Moving on the focus is now put on the Luttinger parameters K_ρ. As previously explained one wants to make the correlation function self-similar, and before integrating out the smallest length scales we had

$$\left\langle \prod_{s=\sigma,\rho} e^{-i\phi_s(x_1)} e^{i\phi_s(x_2)} e^{-S_1} \right\rangle_0 \approx \left(\frac{a}{|\mathbf{z}_{1,2}|} \right)^{\frac{1}{NK_\rho} + \frac{1}{NK_\sigma} - \frac{4\pi^2 m_\phi^2}{v^2} \left(\frac{1}{K_\rho^2} + \frac{1}{K_\sigma^2} \right) \int_a^\infty dr \left(\frac{a}{r} \right)^{\frac{N}{2K_\rho} + \frac{N}{2K_\sigma}} r^3} \tag{5.6.23}$$

After integrating out the d.o.f. it should instead take the self-similar form

$$\left(\frac{a}{|\mathbf{z}_{1,2}|} \right)^{\frac{1}{N\tilde{K}_\rho} + \frac{1}{N\tilde{K}_\sigma} - \frac{2\pi^2 N \tilde{m}_\phi^2}{v^2} \left(\frac{1}{\tilde{K}_\rho} + \frac{1}{\tilde{K}_\sigma} \right) \int_a^\infty dr \left(\frac{a}{r} \right)^{\frac{N}{2K_\rho} + \frac{N}{2K_\sigma}} r^3} \tag{5.6.24}$$

where the tilde represents the renormalized parameters. Using $\ln b = dl$ one can deduces

$$\frac{1}{N\tilde{K}_\rho} + \frac{1}{N\tilde{K}_\sigma} = \frac{1}{NK_\rho} + \frac{1}{NK_\sigma} - \underbrace{\frac{4\pi^2 m_\phi^2}{v^2} \left(\frac{1}{K_\rho^2} + \frac{1}{K_\sigma^2} \right) a^4 \, dl}_{= \frac{d}{dl} \left(\frac{1}{K_\sigma N} + \frac{1}{K_\sigma N} \right)} \tag{5.6.25}$$

Since the BGI terms act in the exact same way for both the charge and spins sector, the contribution to the flow equations of the two Luttinger parameters must be equivalent. Using this yields

$$\frac{\mathrm{d}}{\mathrm{d}l} \left(\frac{1}{K_s N} \right) = -\frac{1}{2} \frac{4\pi^2 m_\phi^2}{v^2} \left(\frac{1}{K_\rho^2} + \frac{1}{K_\sigma^2} \right) a^4 \tag{5.6.26}$$

such that the contribution from this term to the RG equations becomes

$$\frac{dK_s}{dl} = ... + K_s^2 \frac{2\pi^2 N m_\phi^2}{v^2} \left(\frac{1}{K_\rho^2} + \frac{1}{K_\sigma^2} \right) a^4 = ... + K_s^2 \frac{M_\phi^2 N^3}{8} \left(\frac{1}{K_\rho^2} + \frac{1}{K_\sigma^2} \right) \tag{5.6.27}$$

Where it has been inserted that $v = 4\pi a/N$ and ... indicates how this is only the contribution from the BGI term of the ϕ-fields.

Had one instead looked at

$$\left\langle \prod_{s=\sigma,\rho} e^{-i\theta_s(x_1)} e^{i\theta_s(x_2)} e^{-S_1} \right\rangle_0 \tag{5.6.28}$$

One would find the contribution from the BGI term of the θ-fields. Instead of going through this rather tedious calculation one more time, one can instead use how the quadratic action is invariant under dual transformation of $\theta_s \to \phi_s$ and $K_s \to K_s^{-1}$. Since the BGI term of the θ-fields are the dual of the BGI term of the ϕ-fields, one can simply in Eq. (5.6.27) take $K_s \to K_s^{-1}$ in order to find the contribution from the BGI term of the θ-fields. This leads to

$$\frac{\mathrm{d}K_s}{\mathrm{d}l} = ... - \frac{2\pi^2 N m_\phi^2}{v^2} \left(K_\rho^2 + K_\sigma^2 \right) a^4 = ... - \frac{M_\theta^2 N^3}{8} \left(K_\rho^2 + K_\sigma^2 \right), \tag{5.6.29}$$

and is a trick also used in [53].

For the rung tunneling term one can choose to only look at

$$\left\langle e^{-i\theta_\sigma(x_1)} e^{i\theta_\sigma(x_2)} e^{-S_1} \right\rangle_0 \tag{5.6.30}$$

since the term only probes the spin sector. Doing the same calculations as above yields the following contributions

$$\frac{\mathrm{d}K_\sigma}{\mathrm{d}l} = ... - K_\sigma^2 \frac{8\pi^2 \lambda^2}{N v^2} a^2 = ... - K_\sigma^2 \frac{N\lambda^2}{2} \tag{5.6.31}$$

$$\frac{\mathrm{d}\lambda}{\mathrm{d}l} = \lambda(2 - \frac{K_\sigma}{N}) \tag{5.6.32}$$

For $g = 0$ the real space second order RG calculations therefore leads to flow equations

$$\frac{\mathrm{d}K_\sigma}{\mathrm{d}l} = K_\sigma^2 \frac{M_\phi^2 N^3}{8} \left(\frac{1}{K_\rho^2} + \frac{1}{K_\sigma^2} \right) - \frac{M_\theta^2 N^3}{8} \left(K_\rho^2 + K_\sigma^2 \right) - K_\sigma^2 \frac{N\lambda^2}{2} \tag{5.6.33}$$

$$\frac{\mathrm{d}K_\rho}{\mathrm{d}l} = K_\rho^2 \frac{M_\phi^2 N^3}{8} \left(\frac{1}{K_\rho^2} + \frac{1}{K_\sigma^2} \right) - \frac{M_\theta^2 N^3}{8} \left(K_\rho^2 + K_\sigma^2 \right) \tag{5.6.34}$$

$$\frac{\mathrm{d}\lambda}{\mathrm{d}l} = \lambda(2 - \frac{K_\sigma}{N}) \tag{5.6.35}$$

$$\frac{dM_\phi}{dl} = M_\phi \left(2 - \frac{N}{4} \left(\frac{1}{K_\rho} + \frac{1}{K_\sigma} \right) \right) \tag{5.6.36}$$

$$\frac{dM_\theta}{dl} = M_\theta \left(2 - \frac{N}{4} \left(K_\rho + K_\sigma \right) \right) \tag{5.6.37}$$

These coupled differential equations can now be solved numerically, from where one can obtain the predicted phase diagram. Now a different derivation of the second order flow equations which primarily follows [54] is presented in Appendix J.

5.7 Solving the flow equations numerically

In solving these equations numerically one needs to do two things. First an upper and lower limit has to be found. The upper limit describes the largest energy scale of the system and a term is deemed relevant when the coupling constant reaches this limit. The lower limit instead describes when a term is deemed irrelevant. These limits therefore determine when the flow can be terminate. If considering the effective action in Eq. (6.3.31), one could have the case of all parameters being below the upper limit except for GE',G' and E'. These three terms pin all the fields and the flow can thereafter be terminated, since the system is expected to then pin all the ϕ-fields corresponding to the $\boldsymbol{E}$ phase in Fig. 6.4. Secondly one needs to determine parameters in front of the BGI terms so M_s. This is also needed in order to estimate the upper and lower energy scale, and will therefore be the first assignment.

5.7.1 Classical Sine-Gordon model

In order to estimate the M_s parameters one can look at the classical Sine-Gordon model given by

$$H = \int \mathrm{d}x \left(a \left[K(\partial_x \phi_s)^2 + \frac{1}{K}(\partial_x \theta_s)^2 \right] - m_s \cos\left(N\theta_s\right) \right) \tag{5.7.1}$$

If for the quantum system one would take $\lambda \to \infty$, then this Hamiltonian would correspond to the effective dual Hamiltonian of the $\uparrow$ and $\downarrow$ sectors. In this limit the elementary excitations will be domain walls, such that to the left of the domain wall all sites will be in $|n\rangle_\zeta$ while to the right they will be in $|n \pm 1\rangle$. Using Eq. (5.1.1) the energy cost of such excitations in this limit become $\Delta E = 2\lambda(1 - \cos 2\pi/N)$. Now the trick is that by considering the classical Sine-Gordon model one can relate the cost of such excitations to the the parameter m_s. Following Chap. 16 in [60], the first step is to rewrite the Hamiltonian in terms of the θ-field by using the relations

$$\partial_\tau \theta_s = iv_s K_s \partial_x \phi_s , \quad \partial_\tau \phi_s = i\frac{v_s}{K_s}\partial_x \theta s ^{17}, \tag{5.7.2}$$

this yields

$$H = \int \mathrm{d}x \left(\frac{a}{K_s v} \left[\frac{1}{v}(\partial_t \theta_s)^2 + v(\partial_x \theta_s)^2 \right] + m_s \left(1 - \cos\left(N\theta_s\right)\right) \right) \tag{5.7.3}$$

Where in order to find the equation of motion one should tend to the Lagrangian description, where in order to follow [60] the following scaling is performed

$$\phi' = \phi\sqrt{\frac{N}{2}} , \quad \theta' = \theta\sqrt{\frac{N}{2}} \tag{5.7.4}$$

Form where one finds the Lagrangian density to be

$$\mathcal{L} = \int \mathrm{d}x \left[\frac{1}{2\pi K_s} \left(\frac{1}{v}\left(\partial_t \theta_s\right)^2 - v\left(\partial_x \theta_s\right)^2 \right) + \underbrace{m_s \left(1 - \cos\left(\sqrt{2N}\theta_s\right)\right)}_{V(\theta_s)} \right] \tag{5.7.5}$$

For this field to minimize the energy it must obey the Euler-Lagrange equations which results in

$$\frac{1}{\pi K_s} \left[\frac{1}{v}\partial_t^2 \theta_s + v\partial_x^2 \theta_s \right] + \partial_{\theta_s} V(\theta_s) = 0 \tag{5.7.6}$$

---

[17]These relations are stated in [34, 53] and comes from how the dual field is defined in relation to the canonical momentum field.

As explained in the [60] one can investigate the kink perturbation by solely looking at the static solution, which can be associated with a transformation taking one into the rest frame of the kink. One therefore sets $\partial_t \theta_s = 0$ leading to

$$\frac{v}{\pi K} \partial_x^2 \theta_s = m_s \sqrt{2N} \sin\left(\sqrt{2N} \theta_s\right) \tag{5.7.7}$$

If rewriting the expression as $\partial_x^2 \theta_s = -\partial_{\theta_s} \bar{V}(\theta_s)$ where $\bar{V}$ represent the rescaled potential, and exchanging the letter x with t then one has

$$\partial_t^2 \theta_s = -\partial_{\theta_s} \bar{V}(\theta_s) \to m_s \ddot{\theta}_s = -\frac{\partial \bar{V}}{\partial \theta_s} \ , \quad m_s = 1. \tag{5.7.8}$$

From this one realizes that this equations is equivalent to an equation describing the dynamics of a particle subject to the potential given by $-\bar{V}$, where the function θ_s describes the position of the particle. This is most easily realized by inserting $\partial_{\theta_s} \bar{V} = -\sin\left(\sqrt{2N} \theta_s\right) m_s \pi K_s / v$ from where one can draw an analogy to the classical pendulum. For a particle moving in a conservative force field one has a conserved quantity, namely the mechanical energy W. This is, in a similar fashion as to the classical pendulum, given by

$$W = \frac{1}{2}(\partial_x \theta_s)^2 - \bar{V}(\theta_s) = \frac{1}{2}(\partial_x \theta_s)^2 + \frac{m_s \pi K}{v}\left(\cos\left(\sqrt{2N} \theta_s\right) - 1\right) \tag{5.7.9}$$

In order to determine W one should draw on the physical intuition saying that the solution of this field must show a finite energy. If looking at the Hamiltonian this leads to $V(\theta_s(x \to \pm\infty)) \to 0$ and $\partial_x \theta_s(x \to \pm\infty)) \to 0$, meaning that if H is to be finite the energy density must die out at $x \to \pm\infty$. If interpreting this result in terms of the fictitious particle, then this means that if letting the system develop for an infinitely amount of time, $x \to \infty$, the kinetic energy along with the potential energy of the field must converge to zero[18]. This means that $W(t \to \pm\infty) = 0$, but since the mechanical energy is conserved at any time one finds $W = 0$. With this new relation shows

$$0 = \frac{1}{2}(\partial_x \theta_s)^2 + \frac{m_s \pi K}{v}\left(\cos\left(\sqrt{2N} \theta_s\right) - 1\right) \to \partial_x \theta_s = \sqrt{2\frac{m_s \pi K}{v}\left(1 - \cos\left(\sqrt{2N} \theta_s\right)\right)} \tag{5.7.10}$$

$$\frac{d\theta}{\sqrt{2}\sin\left(\sqrt{\frac{N}{2}}\theta_s\right)} = \sqrt{\frac{2\pi K_s m_s}{v}}dx \tag{5.7.11}$$

Integrating the last expression from x_0 to x on both side yields

$$\theta_s(x) = \frac{4}{\sqrt{2N}} \arctan\left(e^{\sqrt{\frac{2\pi K_s N m_s}{v}}(x - x_0)}\right) \tag{5.7.12}$$

The solution sees plotted in Fig. 5.6, where one clearly sees how at x_0 the field jumps from 0 to the next minima $2\pi/\sqrt{2N}$ [19].

Having found the $\theta_s(x)$ as a function of x it is now possible to calculate the energy of this configuration. Since this describes the static solution one finds

$$H = -\mathcal{L} = \int \mathrm{d}x \frac{v}{2\pi K_s}(\partial_x \theta_s)^2 - V(\theta_s) = \int \mathrm{d}x \frac{v}{\pi K_s}(\partial_x \theta_s)^2 \tag{5.7.13}$$

---

[18]Essentially this means the kinetic energy will be that $\partial_x \theta_s = 0$ and then one will find the particle locked in one of the potentials maximum $\theta_s = n2\pi/\sqrt{2N}$.

[19]To be exact Eq. (5.7.11) yields both a positive and negative solution, where only the positive is considered. If considering the negative solution then the field jumps from 0 to $-2\pi/\sqrt{2N}$ instead, so a kink associated with jumping to the other nearest minimum.
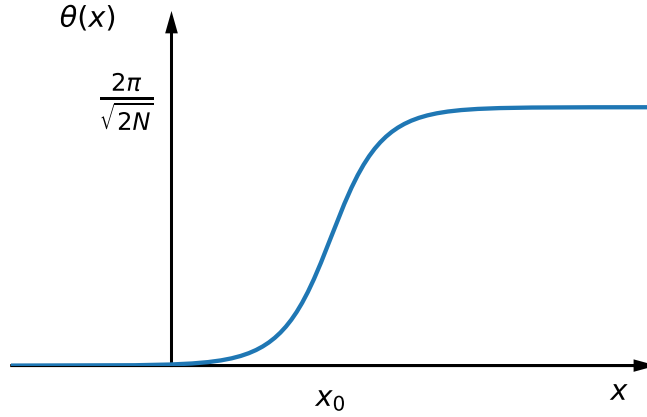
Figure 5.6 | Plot of kink solution. This figure shows the predicted θ solution from the classical analysis of the kink perturbation. Here one clearly sees the characteristic of the kink, where to the left of x_0 the field is zero and after it jumps to the next minima of the potential $2\pi/\sqrt{2N}$.

where the relation from Eq. (5.7.10) has been used. Inserting Eq. (5.7.12) and taking $x_0 = 0$ yields

$$H = \int_{-\infty}^{\infty} \mathrm{d}x \frac{v}{\pi K_s} \left(\frac{4}{\sqrt{2N}} \right)^2 \frac{2\pi K_s N m_s}{v} \frac{e^{2\sqrt{\frac{2\pi K_s N m_s}{v}}x}}{\left(1 + e^{2\sqrt{\frac{2\pi K_s N m_s}{v}}x}\right)^2} =$$

$$\int_{-\infty}^{\infty} \mathrm{d}x 16 m_s \frac{e^{2\sqrt{\frac{2\pi K_s N m_s}{v}}x}}{\left(1 + e^{2\sqrt{\frac{2\pi K_s N m_s}{v}}x}\right)^2} = \int_{-\infty}^{\infty} \mathrm{d}x' 16 m_s \sqrt{\frac{v}{2\pi K_s N m_s}} \frac{e^{2x'}}{(1 + e^{2x'})^2} =$$

$$\int_{-\infty}^{\infty} \mathrm{d}x' \sqrt{\frac{8 m_s v}{\pi K_s N}} \frac{1}{\cosh(x')^2} = 4\sqrt{\frac{2 m_s v}{\pi K_s N}} \tag{5.7.14}$$

which means that this analysis predicts the energy difference between having θ_s being pinned to the same minimum everywhere and having a kink perturbation is given by $\Delta E = 4\sqrt{\frac{2 m_s v}{\pi K_s N}}$. If now looking at the cost of such perturbation for the discretized Hamiltonian in the limit of $g \to 0$ one finds the previously stated $\Delta E = 2\lambda(1 - \cos(2\pi/N))$. Setting these two energy costs equal to one another yields

$$m_s = \frac{\pi N K_s \lambda^2}{8v}(1 - \cos(2\pi/N))^2 = \frac{\pi N K_s \lambda^2}{8v}(1 - \cos(2\pi/N))^2 = \frac{N^2 \lambda}{32a}(1 - \cos(2\pi/N))^2 \tag{5.7.15}$$

From where one finds $M_s = m_s a$ to be independent of the lattice spacing. Had one instead considered $\lambda \to 0$ and made the dual transformation of $\theta_s \to \phi_s$ and $\lambda \to \frac{1}{\lambda}$ one would find the parameters in front of the BGI for the ϕ-fields. This all leads to the following estimates

$$M_{\theta,\uparrow} = M_{\theta,\downarrow} = M_\theta = \frac{N^2 \lambda}{32}(1 - \cos(2\pi/N))^2$$

$$M_{\phi,\uparrow} = M_{\phi,\downarrow} = M_\phi = \frac{N^2}{32\lambda}(1 - \cos(2\pi/N))^2 \tag{5.7.16}$$

which are estimates that will be the most correct deep inside the ordered and disordered phases, in the flow equations they are though approximated to hold true for all values of λ.

5.7.2   Numerical solutions

With the estimates given in Eq. (5.7.16) all energy scales of the system are known, and one can now set an upper and lower limit for the flow. These limits should reflect energy scales larger than the bare
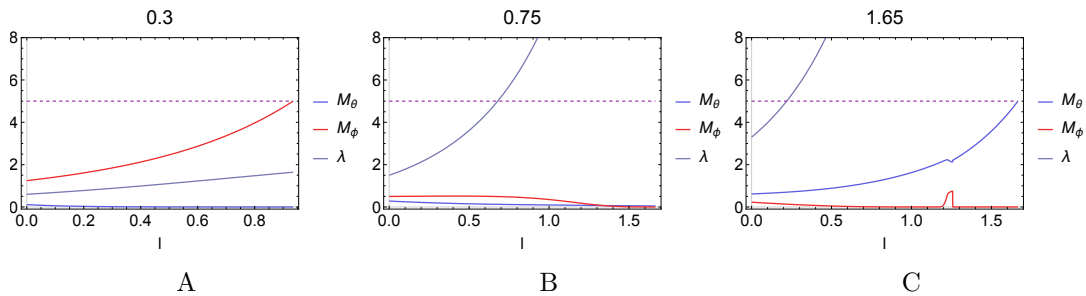
Figure 5.7 | Plots of RG flow. These three figure show the RG flow for the different terms in Eq. (5.1.20) with the initial values from the left being $\lambda = 0.3, 0.75, 1.65$. The upper cutoff is indicated by the dashed purple line and the lower is 0.1. In figure **A** one finds BGI term for the ϕ-fields to be the must relevant thereby pinning the both ϕ-fields. In figure **B** one finds the rung tunneling term to be relevant and the others not to be. This therefore corresponds to the gapless phase where only θ_σ is pinned. At last figure **C** shows the case of both the rung tunneling and the BGI term for the θ-fields to be relevant. This corresponds to the ordered phase where both the θ-fields are pinned.

energy scales of the system. In the two extremes of λ, the largest energy scales are given by λ and $1/\lambda$, while for intermediate values these will be of the order 1. This means that different limits should be set in different regimes.

Thanks to the provided Mathematica file created by *Apollonas S. Matsoukas-Roubeas* and modified by *Michele Burrello* the RG flow equations were solved. The solutions obtained using the equations shown in Eq. (5.6.33-5.6.37) were highly unstable, and could therefore not be used to determine the different phase. Instead the equations derived in Appendix J showed to be stable and where therefore used. The equations were solved for $N = 5$ in the region $\lambda \in [0.1, 2]$ with the lower limit set by $LC = 0.2$ and the upper set by the maximum value of $UC = \{3\lambda, 5, 2/\lambda\}$. In Fig. 5.7 one sees three different plots of the RG flow. From this numerical solution the gapless-gapped transitions show in the vicinity of $\lambda = 0.4$ and $\lambda = 1$. Compared to the first order predictions the phase is shifted to larger values of λ, but as previously explained this procedure does not take higher order terms into account, and as seen from both the two-step RG and the quasi-second order analysis these terms can drastically shrink the gapless phase. This result is therefore not to be trusted and instead we move on to the bosonization of the full model where the flow equations are derived using the momentum space approach.

Chapter 6

Bosonization of the full model

Having only considered different limits of the model, this chapter will try to attack the full model with the techniques offered by the bosonization techniques. As in the case of $g = 0$ the model is most easily bosonized in the axial gauge, where the plaquette interactions simplifies. The Hamiltonian in the axial gauge with SS boundaries is given in Eq. (4.3.1), but to get rid of the boundary terms the To get rid of the boundary terms underlined in blue the SR boundaries are chosen which yields

$$\underline{H} = -\frac{1}{g}\sum_{i=1}^{L}(\sigma_i^\dagger \sigma_{i+1} + \text{H.c.}) - g\left(\sum_{i=1}^{L}\left(\prod_{j>i}^{L+1}\tau_j^\dagger \eta_{j,}^\dagger +\right.\right.$$

$$\left.\prod_{j>i}^{L+1}\tau_j \eta_{j,\downarrow}^\dagger + \text{h.c.}\right) + \sum_{i=1}^{L+1}(\tau_i + \tau_i^\dagger)\right) - \frac{1}{\lambda}\sum_{i=1}^{L+1}\sum_{j=1}^{2}(\eta_{i,s} + \eta_{i,s}^\dagger) -$$

$$\lambda\left(\sum_{i=1}^{L}\sum_{s=,\downarrow}\left(\zeta_{i,s}^\dagger \zeta_{i+1,s} + \text{h.c}\right) + \sum_{i=1}^{L+1}(\zeta_{i,}\sigma_i^\dagger \zeta_{i,\downarrow}^\dagger + \text{H.c})\right) \tag{6.0.1}$$

In bosonizing the full model one needs to introduce an additional field to describe d.o.f. of the gauge bosons. Similar to the mapping presented in Eq. (5.1.4) one finds

$$\tau_j \to e^{-i(\phi_0(j\cdot a) - \phi_i((j+1)\cdot a))} \quad, \quad j \neq L$$

$$\tau_{L,i} \to e^{-i\phi_0(L\cdot a)}$$

$$\sigma_j \to e^{-i(\theta_0(j\cdot a))} \tag{6.0.2}$$

Which, in the same way as in Eq. (5.1.6-5.1.8), leads to

$$\sigma_j^\dagger \sigma_{j+1} + \text{H.c} \to 2\cos(\theta_0(j\cdot a) - \theta_0(ja + a))) \tag{6.0.3}$$

$$\tau_j + \tau_j^\dagger \to 2\cos(\phi_i(j\cdot a) - \phi_i(ja + a))) \tag{6.0.4}$$

Going to the continuous description of $a \to 0$ one makes the same approximation as in Eq. (5.1.11) turning the above terms into the quadratic part of the Hamiltonian. The rest of the terms are mapped as

$$-\lambda(\zeta_{i,}^\dagger \sigma_i \zeta_{i,\downarrow} + \text{H.c}) \to -2\lambda\cos(\theta - \theta_\downarrow - \theta_0) \tag{6.0.5}$$

$$-g\sum_{i=1}^{L}\left(\prod_{j>i}^{L+1}\tau_j^\dagger \eta_{j,}^\dagger + \prod_{j>i}^{L+1}\tau_j \eta_{j,\downarrow}^\dagger + \text{h.c.}\right) \to -2g\left(\cos(\phi_1 + \phi_0) + \cos(\phi_2 - \phi_0)\right) \tag{6.0.6}$$

Where the term in the first line is denoted the rung tunneling term, while the other is denoted the electric field term of the legs. To ensure the discrete $\mathbb{Z}_N$ behavior of the gauge bosons a BGI term is also incorporated

$$H = \int \mathrm{d}x... - M_{\phi,0} \cos\left(N\phi_0\right) - M_{\theta,0} \cos\left(N\theta_0\right) \tag{6.0.7}$$

Combining all the above one is left with the complete bosonized Hamiltonian

$$\underline{\mathrm{H}} = \int \frac{dx}{a} \left[\sum_{s=,\downarrow,0} \left(a^2 \left(\frac{1}{K_s}(\partial_x\theta_s)^2 + K_s(\partial_x\phi_s)^2 \right) - M_{\theta,s} \cos\left(N\theta_s\right) - M_{\phi,s} \cos\left(N\phi_s\right) \right) - \right.$$

$$\left. -2\lambda \cos\left(\theta_1 - \theta_2 - \theta_0\right) - 2g\left(\cos\left(\phi_1 + \phi_0\right) + \cos\left(\phi_2 - \phi_0\right)\right) \right]$$

$$K = K_\downarrow \equiv K = \frac{1}{\lambda} \;,\quad K_0 = g \;,\quad M_{s,} = M_{s,\downarrow} \equiv M_s \tag{6.0.8}$$

In order to be able to compare this analysis with one presented in Chapter 5, one transforms the ↑- and ↓-fields into the charge and spin sector leaving

$$\underline{\mathrm{H}} = \int \frac{dx}{a} \left[\sum_{s=\sigma,\rho,0} a^2 \left(\frac{1}{K_s}(\partial_x\theta_s)^2 + K_s(\partial_x\phi_s)^2 \right) - \underline{M_{\theta,0} \cos\left(N\theta_0\right)} - \underline{M_{\phi,0} \cos\left(N\phi_0\right)} \right.$$

$$-\underline{2M_\theta \cos\left(\tfrac{N}{\sqrt{2}}\theta_\rho\right)\cos\left(\tfrac{N}{\sqrt{2}}\theta_\sigma\right)} - \underline{2M_\phi \cos\left(\tfrac{N}{\sqrt{2}}\phi_\rho\right)\cos\left(\tfrac{N}{\sqrt{2}}\phi_\sigma\right)} - \underline{2\lambda \cos\left(\sqrt{2}\theta_\sigma - \theta_0\right)}$$

$$\left. -\underline{4g \cos\left(\tfrac{\phi_\rho}{\sqrt{2}}\right)\cos\left(\tfrac{\phi_\sigma}{\sqrt{2}} + \phi_0\right)} \right] \;,\quad K_\sigma = K_\rho = K \tag{6.0.9}$$

where the underlined colors are for later use. Comparing this to Eq. (5.1.20) one sees a clear distinction between the two. Changing to this new basis does not diagonalize the Hamiltonian, since for example the rung tunneling term mixes the spin and gauge boson sector. The different sectors are therefore not independent and no unitary transformation can diagonolize the system for arbitrary values of g and λ. For the first order RG analysis this does not propose a major problem, but in the second order analysis there will show unwanted terms which need to be dealt with.

6.1 First order analysis for $N = 5$

The first order analysis predicts no flow of the Luttinger parameters, such that the phase diagram can be predicted by solely looking at the scaling dimensions. The scaling dimensions are found using the trick shown in Eq. (5.2.14), and the results are stated in Tab. 6.1. With these scaling dimensions it is now possible to start the machinery and determine the predicted phases. The following analysis will be performed for $N = 5$, since the interesting gapless phase is expected to appear in this case.

Using Tab. 6.1 one can determined for which values of λ and g the different terms become relevant, and in Fig. 6.1 one finds a plot showing just that. In the figure the color codes of the different terms matches the underlining color in Eq. (6.0.9). In the figure the arrows indicate in which direction the different terms are relevant. Taking the case of the BGI term for the $\theta_{\sigma,\rho}$ fields, the green line, one sees that the arrow points to the left, meaning that this term will be relevant to the left of the green line. This figure does not tell the whole story, since some of the terms will be competing. All the BGI terms will commute with the background terms of the other sectors. This is not trivially seen but going back to the discretized language this is easily realized. The BGI terms for the gauge bosons takes the form

$$H = ... - \frac{M_{\phi,0}}{2} \sum_{i=0}^{L} \left(\prod_{j\leq i}(\tau_j)^N + \mathrm{H.c} \right) - \frac{M_{\theta,0}}{2} \sum_{i=0}^{L} \left((\sigma_j)^N + \mathrm{H.c} \right) \tag{6.1.1}$$

Δ	Relevant for
$D_{\theta,0} = \dfrac{NK_0}{2}$	$K_0 < \frac{4}{N}$
$D_{\phi,0} = \dfrac{N}{2K_0}$	$K_0 > \frac{N}{4}$
$D_{\theta} = \dfrac{N}{4}(K_\sigma + K_\rho)$	$K < \frac{4}{N}$
$D_{\phi} = \dfrac{N}{4}\left(\dfrac{1}{K_\sigma} + \dfrac{1}{K_\rho}\right)$	$K > \frac{N}{4}$
$D_{\sigma} = \dfrac{1}{2N}(2K_\sigma + K_0)$	$2K + K_0 < 4N$
$D_{g} = \dfrac{1}{2N}\left(\dfrac{1}{2K_\sigma} + \dfrac{1}{2K_\rho} + \dfrac{1}{K_0}\right)$	$\dfrac{1}{K} + \dfrac{1}{K_0} < 4N$

Table 6.1| Scaling dimensions. In this table one can read how to first order the different terms in Eq. (6.0.9) scales under the RG flow. To the right one finds for which values of K and K_0 the different terms are relevant.

Which along with the discretized BGI terms shown in Eq. (5.1.17) are seen to all commute. The BGI terms for all θ-fields will commute with the rung tunneling term but not any other. The opposite holds for the ϕ background terms. These will commute with all other terms than the rung tunneling term. At last we find the electric field term of the legs and the rung tunneling term to commute. To
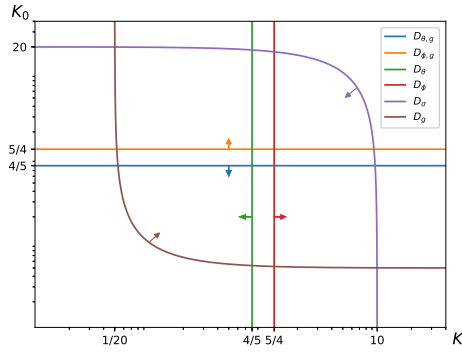
Figure 6.1 | Relevant terms for N=5 . In this figure one finds a plot showing in which regions the different terms will be relevant. The lines indicate when $D_s = 2$, so when the term is marginal relevant, and the arrows indicate to which side of the line the term is relevant.
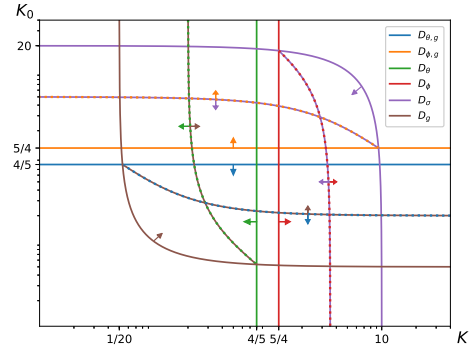
Figure 6.2 | Relevant and competing terms for N=5 . In this figure one finds a plot showing in which regions the different terms will be relevant along with dashed multicolored lines showing where two competing terms are equally relevant. For example the brown and blue colored line indicates where the blue and brown scaling dimensions are equal. This therefore corresponds to $D_{\theta,0} = D_g$. Now along this line one finds two arrows, indicating in which direction the given colored term will win.

illustrate what this means, one can look at Fig. 6.1. If taking the green line, one sees that this will be competing with the brown line in the region, where they are both relevant. The same holds for the blue and brown line, the red and purple along with the orange and purple.

In Fig. 6.2 one sees on top of the plot from Fig. 6.1, lines showing which terms are competing, and where the different terms are winning. If taking the example of the green and brown line, one finds a line with colors alternating between brown and green. This line indicates where the terms are equally relevant. The brown arrow then indicates to which side the brown term is most relevant, and the green arrow to the side where the green term is most relevant.

If looking at the blue/brown line, indicating $D_{\theta,0} = D_g$, then below this line one can to first order simply erase the brown line and above erase the blue line. Looking at the green/brown line one can to the left of this erase the brown line and to the right erase the green line. Following this procedure one is left with the figure shown in Fig. 6.3.
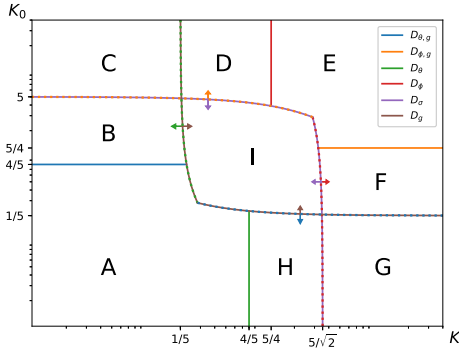
Figure 6.3 | Winning terms for N=5 . In this figure one finds a plot showing in which regions the different terms are relevant and winning along with a labeling of the predicted phase.
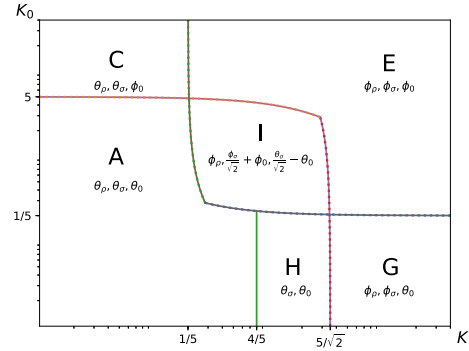
Figure 6.4 | First order phase diagram for N=5. In this figure one finds the phase diagram predicted by the first order RG analysis. Beneath each label the fields pinned in that region is stated.

This figure shows regions where all the winning terms are commuting. In Tab. 6.2 one finds a table showing the terms, that are relevant in the different regions. From this table one sees that the phase

Region	Pinned terms
A	$\cos\left(N\theta_0\right),\ \cos\left(\sqrt{2}\theta_\sigma - \theta_0\right)$ and $\cos\left(\theta_\rho \frac{N}{\sqrt{2}}\right)\cos\left(\theta_\sigma \frac{N}{\sqrt{2}}\right)$
B	$\cos\left(\theta_\rho \frac{N}{\sqrt{2}}\right)\cos\left(\theta_\sigma \frac{N}{\sqrt{2}}\right),\ \cos\left(\sqrt{2}\theta_\sigma - \theta_0\right)$
C	$\cos\left(\theta_\rho \frac{N}{\sqrt{2}}\right)\cos\left(\theta_\sigma \frac{N}{\sqrt{2}}\right)$ and $\cos\left(N\phi_0\right)$
D	$\cos\left(N\phi_0\right),\ \cos\left(\frac{\phi_\rho}{\sqrt{2}}\right)\cos\left(\frac{\phi_\sigma}{\sqrt{2}} - \phi_0\right)$
E	$\cos\left(N\phi_0\right),\ \cos\left(\frac{\phi_\rho}{\sqrt{2}}\right)\cos\left(\frac{\phi_\sigma}{\sqrt{2}} + \phi_0\right)$ and $\cos\left(\phi_\rho \frac{N}{\sqrt{2}}\right)\cos\left(\phi_\sigma \frac{N}{\sqrt{2}}\right)$
F	$\cos\left(\frac{\phi_\rho}{\sqrt{2}}\right)\cos\left(\frac{\phi_\sigma}{\sqrt{2}} + \phi_0\right)$ and $\cos\left(\phi_\rho \frac{N}{\sqrt{2}}\right)\cos\left(\phi_\sigma \frac{N}{\sqrt{2}}\right)$
G	$\cos\left(N\theta_0\right)$ and $\cos\left(\phi_\rho \frac{N}{\sqrt{2}}\right)\cos\left(\phi_\sigma \frac{N}{\sqrt{2}}\right)$
H	$\cos\left(N\theta_0\right)$ and $\cos\left(\sqrt{2}\theta_\sigma - \theta_0\right)$
I	$\cos\left(\frac{\phi_\rho}{\sqrt{2}}\right)\cos\left(\frac{\phi_\sigma}{\sqrt{2}} + \phi_0\right)$ and $\cos\left(\sqrt{2}\theta_\sigma - \theta_0\right)$

Table 6.2| Relevant terms. In this table one finds the relevant and winning terms of the different regions shown in Fig. 6.3.

diagram can be simplified even further. If taking the example of Region **F**. In this region one finds the rung tunneling term along with the $\phi_{\sigma/\rho}$ BGI term to be relevant. In region **E**, one finds on top of these two relevant terms the ϕ_0 BGI term to be relevant. This though predicts the exact same ground state, and the two regions therefore belong to the same phase. The same analysis could be done for

region D and E, leading to these three regions all belonging to the same phase. In region A and B one as well have the same fields pinned. This leads to predicted phase diagram being the one shown in Fig. 6.4. The behavior of the different phases is described below.

A. In this region the system will be completely gapped, and all the θ-fields will be pinned. This correspond to the Higgs phase, with the renormalized system being a meson condensate state as described in Chapter 5.

C. This phase is fully gapped with θ_σ, θ_ρ and ϕ_0 being pinned. Due to ϕ_0 being pinned there will be no electric flux line going between the legs. Having θ_σ and θ_ρ pinned though means, that there will be a condensate of mesons. These mesons will though be confined to the individual legs, such that no electric flux line between the legs is excited.

E. This phase is fully gapped and has all the ϕ-fields pinned. This is what is denoted the confined phase, and for $\lambda = 0$ this corresponds to the para magnetic phase in the Potts model. Having all the ϕ-fields pinned essentially means that no electric flux line or Higgs particles are excited.

G. This phase is fully gapped and will have θ_0, ϕ_σ and ϕ_ρ pinned. For $\lambda, g = 0$ this phase will turn into the ordered ferromagnetic phase in the Potts description of the PLGT. This phase could look deconfining, but as explained in Appendix H, this is not expected to happen for $g > 0$. At $g = 0$ exciting an electric flux line is for free, and one has a deconfining phase with $\Delta E = 0$.

H. This region will not be fully gapped, since one only finds θ_0 and θ_σ to be pinned, while the charge sector is unpinned. This analysis therefore predicts the gapless phase found in the $g \to 0$ analysis to be extend for finite g.

I. This is again a fully gapped phase where ϕ_ρ, $\phi_\sigma/\sqrt{2} - \phi_0$ and $\sqrt{2}\theta_\sigma - \theta_0$ will be pinned.

and the behavior of the observables are stated in Table 6.3.

Phase	Exponential decaying	Constant	Algebraic decay
A	$\langle G_s \rangle$	$\langle M_s \rangle$, $\langle W \rangle$, $\langle R \rangle$	
C	$\langle G_s \rangle$, $\langle W \rangle$, $\langle R \rangle$	$\langle M_s \rangle$	
E	$\langle M_s \rangle$, $\langle W \rangle$, $\langle R \rangle$	$\langle G_s \rangle$	
G	$\langle M_s \rangle$, $\langle R \rangle$	$\langle G_s \rangle$, $\langle W \rangle$	
H	$\langle G_\sigma \rangle$	$\langle W \rangle$, $\langle R \rangle$, $\langle M_\sigma \rangle$	$\langle M_\rho \rangle$, $\langle G_\rho \rangle$
I	$\langle W \rangle$, $\langle M_\rho \rangle$, $\langle M_\sigma \rangle$, $\langle G_\rho \rangle$	$\langle G_\rho \rangle$, $\langle R \rangle$	

Table 6.3| Behavior of observables. This table shows how the different observables would behave in the predicted regions, which ultimately could be used to distinguish the different phases. Here one should observe the usefulness of the two point correlation function R, which solely probes the mixed sector proportional to $\sqrt{2}\theta_\sigma - \theta_0$.

These different phase boundaries should though not be trusted completely. One still has the possibility of the regions being adiabatically connected as in the case of $\lambda = 0$, the PLGT, where only one phase is expected, but the bosonized model predicts two. In appendix G one finds this elaborated, and it is shown how the two phases predicted by the bosonized description actually are adiabatically connected and corresponds to the same phase. A region which cannot be adiabatically connected to the surrounding regions is the gapless phase H, which is now further investigated.

6.1.1 $g \ll 1$

To further investigate the gapless phase we can try to write an effective Hamiltonian in the limit of $g \ll 1$. The first tool which can improve our predictions is the two-step-RG. In this limit, $g = K_0 << 1$, the initial flow will pin $\theta_0 = 0$ which to first order means that $\theta_0 = 0$ can be inserted and the electric

field term of the legs neglected. Doing this leads to the same Hamiltonian as found in the limit of $g \to 0$ which was investigated in chapter 5. This analysis predicted a gapless phase, such that the two-step-RG predicts it to be extended for a finite g. The next tool is the quasi-second order analysis.

In a similar fashion as previously one should look at the normalized partition function shown in Eq. (5.3.11). Due to the initial flow one can write

$$S_0' = \int \mathrm{d}^2x \left[\sum_{s=0,\uparrow,\downarrow} \frac{1}{2\pi K_s} \left(\frac{(\partial_\tau \theta_s)^2}{v} + v(\partial_x \theta_s)^2 \right) \underbrace{-m_{\theta,0}' \cos{(N\theta_0)}}_{S_{\theta,0}'} \right] \tag{6.1.2}$$

$$S_1' = -\int \mathrm{d}^2x \left(2m_\phi' \cos{(\frac{N}{\sqrt{2}}\phi_\rho)} \cos{(\frac{N}{\sqrt{2}}\phi_\sigma)} + 2m_\theta' \cos{(\frac{N}{\sqrt{2}}\theta_\rho)} \cos{(\frac{N}{\sqrt{2}}\theta_\sigma)} + m_{\phi,0}' \cos{(N\phi_0)} \right.$$

$$\left. +2\lambda' \cos{(\sqrt{2}\theta_\sigma - \theta_0)} + 4g' \cos{(\frac{\phi_\rho}{\sqrt{2}})} \cos{(\frac{\phi_\sigma}{\sqrt{2}} + \phi_0)} \right) = S_\phi + S_\theta + S_{\phi,0} + S_\lambda + S_g \tag{6.1.3}$$

$$S_\lambda' \equiv -\int \mathrm{d}^2x \left(2\lambda' \cos{(\sqrt{2}\theta_\sigma - \theta_0)} \right) , \quad S_g' \equiv -\int \mathrm{d}^2x \left(4g' \cos{(\frac{\phi_\rho}{\sqrt{2}})} \cos{(\frac{\phi_\sigma}{\sqrt{2}} + \phi_0)} \right)$$

$$S_{\phi,0}' \equiv -\int \mathrm{d}^2x \left(m_{\phi,0}' \cos{(N\phi_0)} \right) \tag{6.1.4}$$

To all order one finds $S_{\phi,0}'$ being killed due to θ_0 being pinned. For S_λ' one should to first order simply insert $\theta_0 = 0$, and the higher orders are not taken into account, since they promote the same behavior and are less relevant. Due to the exponential decay S_g is killed to first order and the second order correction is needed

$$\frac{1}{2} \left\langle S_g^2 \right\rangle_0 = 8(g')^2 \int \mathrm{d}^2x_1 \mathrm{d}^2x_2 \left\langle \cos{(\frac{\phi_\rho}{\sqrt{2}}(x_1))} \cos{(\frac{\phi_\sigma}{\sqrt{2}}(x_1) + \phi_0(x_1))} \times \right.$$

$$\left. \cos{(\frac{\phi_\rho}{\sqrt{2}}(x_2))} \cos{(\frac{\phi_\sigma}{\sqrt{2}}(x_2) + \phi_0(x_2))} \right\rangle_0 =$$

$$8(g')^2 \int \mathrm{d}^2x_1 \mathrm{d}^2x_2 \left\langle \cos{(\frac{\phi_\sigma}{\sqrt{2}}(x_1) + \phi_0(x_1))} \cos{(\frac{\phi_\sigma}{\sqrt{2}}(x_2) + \phi_0(x_2))} \right\rangle_0 \times$$

$$\left\langle \cos{(\frac{\phi_\rho}{\sqrt{2}}(x_1))} \cos{(\frac{\phi_\rho}{\sqrt{2}}(x_2))} \right\rangle_0 =$$

$$8(g')^2 \int \mathrm{d}^2x_1 \mathrm{d}^2x_2 \frac{1}{4} \sum_{\mu,\nu=\pm 1} \left\langle e^{\mu_1 i(\frac{\phi_\sigma}{\sqrt{2}}(x_1) + \phi_0(x_1))} e^{\nu_1 i(\frac{\phi_\sigma}{\sqrt{2}}(x_2) + \phi_0(x_2))} \right\rangle_0 \times$$

$$\left\langle \cos{(\frac{\phi_\rho}{\sqrt{2}}(x_1))} \cos{(\frac{\phi_\rho}{\sqrt{2}}(x_2))} \right\rangle_0 =$$

Using the previous approximation of $\left\langle e^{i\alpha\phi_\sigma(x_1)} e^{-i\beta\phi_\sigma(x_2)} \right\rangle_0 \approx 2D\delta(x_1 - x_2)\delta(\beta - \alpha)$ one finds

$$D(g')^2 \int \mathrm{d}^2x \left\langle \cos^2{(\frac{\phi_\rho}{\sqrt{2}})} \right\rangle_0 =$$

$$\frac{D(g')^2}{2} \int \mathrm{d}^2x \left\langle \cos{(\sqrt{2}\phi_\rho)} \right\rangle_0 + \mathrm{Const.} =$$

$$G' \int \mathrm{d}^2x \left\langle \cos{(\sqrt{2}\phi_\rho)} \right\rangle_0 + \mathrm{Const.} , \quad G' \equiv \frac{D(g')^2}{2} \tag{6.1.5}$$

By neglecting the constant and reexponentiating one finds the effective Hamiltonian becoming

$$\underline{H}'_{eff} = \int \frac{dx}{a} \left[\sum_{s=\sigma,\rho} a^2 \left(\frac{1}{K_s}(\partial_x \theta_s)^2 + K_s(\partial_x \phi_s)^2 \right) \right.$$

$$-2M'_\theta \cos\left(\frac{N}{\sqrt{2}}\theta_\rho\right)\cos\left(\frac{N}{\sqrt{2}}\theta_\sigma\right) - 2M'_\phi \cos\left(\frac{N}{\sqrt{2}}\phi_\rho\right)\cos\left(\frac{N}{\sqrt{2}}\phi_\sigma\right) - 2\lambda'\cos\left(\sqrt{2}\theta_\sigma\right)$$

$$\left. +G'\cos\left(\sqrt{2}\phi_\rho\right) \right] \tag{6.1.6}$$

where the primed variables describe the renormalized constants. In Appendix H this second order term appearing is further investigated in relation the system supporting either a deconfined of confined phase.

From the effective Hamiltonian in Eq. (6.1.6) it is now possible to make a scaling analysis. In Tab. 6.4 one finds the scaling dimensions of the different terms, where one should keep in mind that this quasi-second order analysis considers no flow of the Luttinger parameters. The scaling analysis

Δ	Relevant for
$D_\theta = \frac{N}{4}(K_\sigma + K_\rho)$	$K < \frac{4}{N}$
$D_\phi = \frac{N}{4}(1/K_\sigma + 1/K_\rho)$	$K > \frac{N}{4}$
$D_\sigma = \frac{K_\sigma}{N}$	$K < 2N$
$D_g = \frac{1}{NK_\rho}$	$K > \frac{1}{2N}$

Table 6.4| Scaling dimensions. In this table one can read how the different terms in Eq. (6.1.6) scales and for which values they become relevant.

is schematically represented in Fig. 6.5. Performing a two-step-RG analysis on this Hamiltonian will yield the same result as the quasi-second order analysis, and in doing so one finds the predicted transitions shown with dashed lines in Fig. 6.5. For $N = 2$ one finds the transitions of the two sectors to overlap at $K = 1$, such that to the right one finds all ϕ-fields pinned and to the left the θ-fields. For $N > 2$ they do not overlap, and the phase transitions predicted by the two-step-RG takes place for the spin sector at $K = N/2$ and the one for the charge sector at $K = 2/N$. This intermediate dipole phase with ϕ_ρ and θ_σ pinned was also predicted with the quasi-second order analysis for $g \to 0$, and here one sees that this phase grows for a finite g and errases the gapless phase. The quasi-second order RG analysis therefore predicts the gapless phase not be an extended phase but only to be for $g \to 0$. As previously stated this analysis is though not consistent in the orders of S_1 considered and cannot be trusted. Therefore we now tend to the true second order approach.

6.2 Second order RG in momentum space

As previously explained, the second order RG analysis performed in real space does not incorporate the higher order terms, which the quasi-second order analysis showed to be highly relevant. This therefore leads us to consider the momentum space approach instead. The approach differs by keeping track of the fast and slow oscillating modes, and instead of looking at correlation functions this approach looks at the effective action of the renormalized system. The approach taken in finding the first order scaling dimension shown in Eq. (5.2.24-5.2.33) is the one performed, but to second order.

The calculations of all the RG flow equations will not be performed in this thesis, but in the following section the contributions from the electric field term of the legs is calculated, and it is shown how this term yields higher order terms which need to be considered.
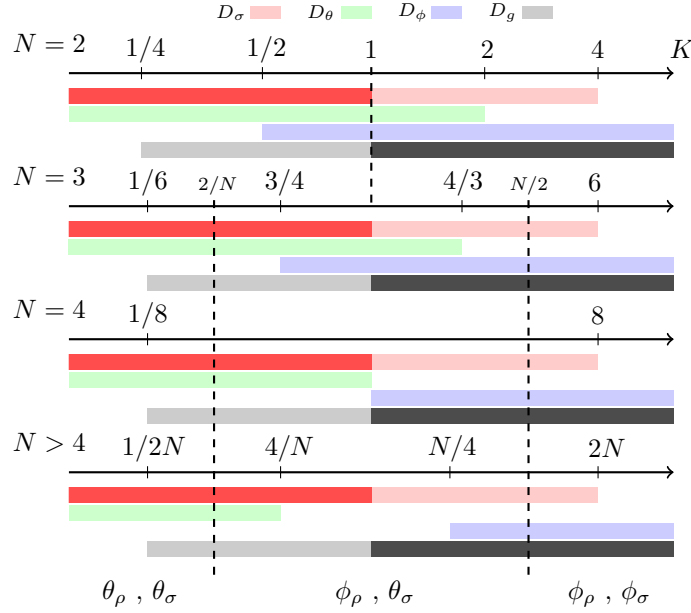
Figure 6.5 | Graphically representation showing where the terms are relevant. This figure illustrates for different N where the terms in Eq. (6.1.6) are relevant as a function of K. The different terms will be relevant for the specific value of K if their color code shows below and the winning terms will be represented by a brighter color. The dashed line for $K = 1$ represents where $D_\sigma = D_g$, and where the phase transition is predicted for $N = 2$. The one at $K = N/2$ represent where the two-step-RG predicts phase transitions to occur in the ρ-sector, and the one at $K = 2/N$ represents where a phase transition is expected in the σ-sector. Below the regions one sees which fields are pinned in addition to θ_0 for $N > 2$.

6.3 The electric field term of the legs

There are two main differences between the procedure performed in momentum and real space. By looking at the effective Hamiltonian instead of the correlation function one finds higher order terms naturally appearing as in [53]. A rather instructive example of this, is found by performing the RG procedure for the two-dimensional Ising model [62]. By doing so one finds Next nearest hopping terms. This procedure will in the same manner have higher order terms appearing in the renormalized action. An example of one of these terms, was the term considered in the quasi-second order analysis in Eq. (6.1.5). This term will also appear in the effective action when considering second order terms, and eventually these will need to be taken into account in the RG-flow equations. In the following part the electric field term of the legs is considered and it is shown how the higher order terms appears, and how this term contributes to the flow equations.

One should start by considering the effective action to second order described by Eq. (5.2.27), where the second order correction becomes

$$S_{eff} = ... - \frac{1}{2}\left(\langle S_1^2 \rangle_> - (\langle S_1 \rangle_>)^2\right) \tag{6.3.1}$$

For the full model one should consider $S_1 = S_\lambda + S_g + S_\phi + S_\theta + S_{\phi,0} + S_{\theta,0}$, where the definitions are given in Eq. (J.1) and (J.2). The first order analysis for the rung tunneling term, Eq. (5.2.24-5.2.33), showed how the first order corrections simply yielded

$$\lambda' = \lambda + d\lambda = \lambda + (2 - D_\lambda)dl \tag{6.3.2}$$

Performing the same analysis for any term to first order will also yield

$$\alpha' = \alpha + d\alpha = \alpha + (2 - D_\alpha)dl \tag{6.3.3}$$

where α will be the coupling constant of the term. This means that

$$\langle S_g \rangle_> = \int_a^\infty d^2x \, (1 + (2 - D_g)dl) \, 4\frac{g}{a} \cos\left(\frac{\phi_\rho}{\sqrt{2}}\right) \cos\left(\frac{\phi_\sigma}{\sqrt{2}} + \phi_0\right) \tag{6.3.4}$$

which leads to

$$(\langle S_g \rangle_>)^2 = \int_a^\infty d^2x_1 d^2x_2 \, (1 + 2(2 - D_g)dl) \, 16\left(\frac{g}{a}\right)^2 \cos\left(\frac{\phi_\rho(x_1)}{\sqrt{2}}\right) \cos\left(\frac{\phi_\sigma(x_1)}{\sqrt{2}} + \phi_0(x_1)\right)$$
$$\cos\left(\frac{\phi_\rho(x_2)}{\sqrt{2}}\right) \cos\left(\frac{\phi_\sigma(x_2)}{\sqrt{2}} + \phi_0(x_2)\right) \tag{6.3.5}$$

To understand how $\cos(\sqrt{2}\phi_\rho)$ appears one only needs to consider the S_g-part of S_1, meaning that the mixing of the different terms are not considered in this analysis, but also they will yield new higher order terms. The following is therefore considered

$$\frac{1}{2}\left(\langle S_1^2 \rangle_> - (\langle S_1 \rangle_>)^2\right) = \ldots + \frac{1}{2}\left(\langle S_g^2 \rangle_> - (\langle S_g \rangle_>)^2\right) \tag{6.3.6}$$

The second term is shown above and the first term, $\langle S_g^2 \rangle_>$, is a bit more tricky to calculate. By expanding it one finds

$$\frac{(4g)^2}{(a4)^2} \int_{ab}^L d^2x_1 d^2x_2 \sum_{\nu_1,\nu_2,\mu_1,\mu_2=\pm 1} \left\langle e^{\mu_1 i \frac{1}{\sqrt{2}}(\phi_\rho^<(x_1)+\phi_\rho^>(x_1))} e^{\mu_2 i\left(\frac{1}{\sqrt{2}}(\phi_\sigma^<(x_1)+\phi_\sigma^>(x_1))+(\phi_0^<(x_1)+\phi_0^>(x_1))\right)} \right.$$
$$\left. e^{\nu_1 i \frac{1}{\sqrt{2}}(\phi_\rho^<(x_2)+\phi_\rho^>(x_2))} e^{\nu_2 i\left(\frac{1}{\sqrt{2}}(\phi_\sigma^<(x_2)+\phi_\sigma^>(x_2))+(\phi_0^<(x_2)+\phi_0^>(x_2))\right)} \right\rangle_> =$$
$$\frac{g^2}{a^2} \int_{ab}^L d^2x_1 d^2x_2 \sum_{\nu_1,\nu_2,\mu_1,\mu_2=\pm 1} e^{i\frac{1}{\sqrt{2}}(\mu_1\phi_\rho^<(x_1)+\nu_1\phi_\rho^<(x_2))} e^{i\left(\frac{1}{\sqrt{2}}(\mu_2\phi_\sigma^<(x_1)+\nu_2\phi_\sigma^<(x_2))+(\mu_2\phi_0^<(x_1)+\nu_2\phi_0^<(x_2))\right)}$$
$$\left\langle e^{i\frac{1}{\sqrt{2}}(\mu_1\phi_\rho^>(x_1)+\nu_1\phi_\rho^>(x_2))} e^{i\left(\frac{1}{\sqrt{2}}(\mu_2\phi_\sigma^>(x_1)+\nu_2\phi_\sigma^>(x_2))+(\mu_2\phi_0^>(x_1)+\nu_2\phi_0^>(x_2))\right)} \right\rangle_> \tag{6.3.7}$$

Because the expectation value is taken with respect to the fast oscillating quadratic part, one does not need to worry about the mixing of the sectors. If only focusing on the fast oscillating modes this leaves

$$e^{\frac{-1}{4}\left(\langle \phi_\rho^>(x_1)^2 \rangle_> + \langle \phi_\rho^>(x_2)^2 \rangle_> + 2\mu_1\nu_1\langle \phi_\rho^>(x_1)\phi_\rho^>(x_2) \rangle_>\right)} e^{\frac{-1}{4}\left(\langle \phi_\sigma^>(x_1)^2 \rangle_> + \langle \phi_\sigma^>(x_2)^2 \rangle_> + 2\mu_2\nu_2\langle \phi_\sigma^>(x_1)\phi_\sigma^>(x_2) \rangle_>\right)}$$
$$e^{\frac{-1}{2}\left(\langle \phi_0^>(x_1)^2 \rangle_> + \langle \phi_0^>(x_2)^2 \rangle_> + 2\mu_2\nu_2\langle \phi_0^>(x_1)\phi_0^>(x_2) \rangle_>\right)} \tag{6.3.8}$$

To handle these correlation functions the result

$$\left\langle \phi_s^>(x_1)\phi_s^>(x_2)\right\rangle_> \approx \frac{C(x_1 - x_2)}{NK_s} \ln\left(\frac{\Lambda_{max}}{\Lambda'_{max}}\right) \tag{6.3.9}$$

from [53] is used, where $\Lambda_{max} = 2\pi/a$ and $\Lambda'_{max} = 2\pi/ab$. The way one should understand the above result is, that due to only considering fast oscillating modes, the individual fields in real space will be extremely localized, such that the fields only will be correlated in the vicinity of $|x_1 - x_2| = 0$.

In the process of bosonizing the system some averaging was done, in order to make the theory continuous. This means, that one should not find any change in the space components of fields on the order of the lattice spacing. Due to this, one should instead of thinking of the two fields being represented by a delta function in real space, imagine the two fields to be localized around $x \pm a/2$. Now each field is associated with a velocity, v. This velocity describes the propagation velocity of a perturbation of the field. In the time component one will therefore have these fields to be localized within a/v, meaning that when they overlap in space it will be on this time scale the two fields will move away from one another. As explained in [53] this means that one can make the approximation $C(\boldsymbol{x}_1 - \boldsymbol{x}_2) \approx \delta(\boldsymbol{x}_1 - \boldsymbol{x}_2)a^2/v = \delta(\boldsymbol{x}_1 - \boldsymbol{x}_2)aN/4\pi$, where the velocity found in Eq. (5.2.6) is used[1]. Using this together with Eq. (5.2.25) one can rewrite the fast oscillating part as

$$
\left(\frac{\Lambda'_{max}}{\Lambda_{max}}\right)^{\frac{1}{2N}\left(\frac{1}{K_\sigma} + \frac{1}{K_\rho} + 2\frac{1}{K_0}\right)} \left(\frac{\Lambda'_{max}}{\Lambda_{max}}\right)^{\frac{1}{2N}\left(\frac{\mu_1\nu_1}{K_\sigma} + \frac{\mu_2\nu_2}{K_\rho} + 2\frac{\mu_2\nu_2}{K_0}\right)C(x_1 - x_2)}
\tag{6.3.10}
$$

where it is noticed that $\frac{1}{2N}\left(\frac{1}{K_\sigma} + \frac{1}{K_\rho} + 2\frac{1}{K_0}\right) = 2D_g$. Using this and making the substitution $\Lambda'_{max}/\Lambda_{max} = 1/b = 1 - dl$ along with rescaling x such that $x \in [a, L]$ one finds

$$
\left\langle S_g^2 \right\rangle_> = \frac{g^2}{a^2}\left[1 - 2D_g dl\right]\left[1 + 2dl\right]^2
$$

$$
\int_a^L \mathrm{d}^2x_1\mathrm{d}^2x_2 \sum_{\mu_1,\mu_2,\nu_1,\mu_2=\pm 1} \left(1 - \frac{1}{2N}\left(\frac{\mu_1\nu_1}{K_\sigma} + \frac{\mu_2\nu_2}{K_\rho} + 2\frac{\mu_2\nu_2}{K_0}\right)C(x_1 - x_2)dl\right)
$$

$$
e^{i\frac{1}{\sqrt{2}}(\mu_1\phi_\rho^<(x_1) + \nu_1\phi_\rho^<(x_2))}e^{i\left(\frac{1}{\sqrt{2}}(\mu_2\phi_\sigma^<(x_1) + \nu_2\phi_\sigma^<(x_2)) + (\mu_2\phi_0^<(x_1) + \nu_2\phi_0^<(x_2))\right)}
\tag{6.3.11}
$$

Where the first square bracket comes from the above substitution and the second is from the rescaling of x_1 and x_2. By only keeping the lowest order of dl and using the above described approximation for $C(x_1 - x_2)$ one finds

$$
\left\langle S_g^2 \right\rangle_> = \frac{g^2}{a^2}\left[1 + (4 - 2D_g)\,dl\right]\left(\int_a^L \mathrm{d}^2x_1\mathrm{d}^2x_2 \sum_{\mu_1,\mu_2,\nu_1,\mu_2=\pm 1} e^{i\frac{1}{\sqrt{2}}(\mu_1\phi_\rho^<(x_1) + \nu_1\phi_\rho^<(x_2))}\right.
$$

$$
e^{\mu_2 i\left(\frac{1}{\sqrt{2}}(\phi_\sigma^<(x_1) + \phi_\sigma^<(x_2)) + (\phi_0^<(x_1) + \phi_0^<(x_2))\right)} - \sum_{\mu_1,\mu_2,\nu_1,\mu_2=\pm 1} \frac{1}{2N}\left(\frac{\mu_1\nu_1}{K_\sigma} + \frac{\mu_2\nu_2}{K_\rho} + 2\frac{\mu_2\nu_2}{K_0}\right)dl
$$

$$
\left.\int_a^L \mathrm{d}^2x_1\mathrm{d}^2x_2 e^{i\frac{1}{\sqrt{2}}(\mu_1\phi_\rho^<(x_1) + \nu_1\phi_\rho^<(x_2))}e^{i\left(\frac{1}{\sqrt{2}}(\mu_2\phi_\sigma^<(x_1) + \nu_2\phi_\sigma^<(x_2)) + (\mu_2\phi_0^<(x_1) + \nu_2\phi_0^<(x_2))\right)}C(x_1 - x_2)\right)
\tag{6.3.12}
$$

Having done the rescaling the superscript can now be neglected. From looking at Eq. (6.3.5) one sees that this term can be written as

$$
\left\langle S_g^2 \right\rangle_> = \left\langle S_g \right\rangle_>^2 - \frac{g^2}{a^2}dl \sum_{\mu_1,\mu_2,\nu_1,\mu_2=\pm 1} \frac{1}{2N}\left(\frac{\mu_1\nu_1}{K_\sigma} + \frac{\mu_2\nu_2}{K_\rho} + 2\frac{\mu_2\nu_2}{K_0}\right)
$$

$$
\int_a^L \mathrm{d}^2x_1\mathrm{d}^2x_2 e^{i\frac{1}{\sqrt{2}}(\mu_1\phi_\rho^<(x_1) + \nu_1\phi_\rho^<(x_2))}e^{i\left(\frac{1}{\sqrt{2}}(\mu_2\phi_\sigma^<(x_1) + \nu_2\phi_\sigma^<(x_2)) + (\mu_2\phi_0^<(x_1) + \nu_2\phi_0^<(x_2))\right)}C(x_1 - x_2)
\tag{6.3.13}
$$

---

[1]One could have done the analysis leading to Eq. (5.2.6) for the fields associated with the gauge bosons as well, and it would also $v = a4\pi/N$ yield the stated result.

from where the second order contribution becomes

$$-\frac{1}{2}\left(\langle S_g^2\rangle_> - (\langle S_g\rangle_>)^2\right) = \frac{g^2}{a^2}dl \sum_{\mu_1,\mu_2,\nu_1,\mu_2=\pm1} \frac{1}{2N}\left(\frac{\mu_1\nu_1}{K_\sigma} + \frac{\mu_2\nu_2}{K_\rho} + 2\frac{\mu_2\nu_2}{K_0}\right)$$

$$\int_a^L \mathrm{d}^2x_1\mathrm{d}^2x_2 e^{i\frac{1}{\sqrt{2}}(\mu_1\phi_\rho^<(x_1)+\nu_1\phi_\rho^<(x_2))}e^{i\left(\frac{1}{\sqrt{2}}(\mu_2\phi_\sigma^<(x_1)+\nu_2\phi_\sigma^<(x_2))+(\mu_2\phi_0^<(x_1)+\nu_2\phi_0^<(x_2))\right)}C(x_1-x_2) \tag{6.3.14}$$

If taking the case of $\mu_2 = -\nu_2$ and $\mu_1 = \nu_1$ one can insert the previous approximation for $C(x_1-x_2)$ and get a finite result. Doing so leads to the following term appearing in the effective action to second order

$$S_{eff} = ... + \frac{g^2}{vN}\left(\frac{1}{K_\sigma} - \frac{1}{K_\rho} - 2\frac{1}{K_0}\right)dl\int\mathrm{d}^2x\cos\left(\sqrt{2}\phi_\rho\right) = ... + C'\int\mathrm{d}^2x\cos\left(\sqrt{2}\phi_\rho\right) \tag{6.3.15}$$

By using the momentum space approach to second order RG one sees this term to naturally appear, which is not the case for the real space approach.

In order to now incorporate this term into the flow equations, one needs to consider that after having done the RG procedure C' becomes finite. Such that in performing the RG procedure again afterwards this term will also yield a first order contribution to the flow equations. This then leads to

$$\frac{\mathrm{d}C'}{dl} = (2-D_G)C' + \frac{Ng^2}{4\pi aN}\left(\frac{1}{K_\sigma} - \frac{1}{K_\rho} - 2\frac{1}{K_0}\right), \quad D_G = \frac{1}{K_\rho N}. \tag{6.3.16}$$

where the initial conditions must be $C'(l=0) = 0$, since the term does not show in the initial action. Having this term appearing to first order also means that it will contribute to the flow equations of the Luttinger parameters. Had one instead considered $\mu_1 = -\nu_1$ and $\mu_2 = \nu_2$ one would find another higher order term of the kind

$$S_{eff} = ... + E'\int\mathrm{d}^2x\cos\left(\sqrt{2}\phi_\sigma + 2\phi_0\right) \tag{6.3.17}$$

and so one can go on with the other terms in S_1. Not all these terms are though as important as others. If considering this E'-term one finds it to be competing with the same terms as the electric field term of the legs. If looking at Eq. (6.0.9) and Fig. 6.3 one sees that the electric field term of the legs, the brown term, will be competing with the blue and green term. The same will hold for the E'-term, so by it being a second order term it is only expected to move the phase boundaries, but not alter the structure of the phase diagram. Instead the C'-term will commute with the BGI term of the θ_0 field, the blue term, and will therefore be able to alter the phase diagram by pinning the ϕ_ρ-field in regions where it to first order would not be pinned.

If instead considering the case of $\nu_1 = -\nu_2$ and $\mu_1 = -\nu_2$ one has to approach the calculations differently since simply taking $C(r) \propto \delta(r)$ will not yield any contribution. This is seen by looking at Eq. (6.3.14), where by inserting $\nu_1 = -\nu_2$ and $\mu_1 = -\nu_2$ one finds

$$-\frac{g^2}{a^2}dl\frac{1}{2N}\left(\frac{1}{K_\sigma} + \frac{1}{K_\rho} + 2\frac{1}{K_0}\right)\int_a^L\mathrm{d}^2x_1\mathrm{d}^2x_2\cos\left(\frac{1}{\sqrt{2}}(\phi_\rho(x_1)-\phi_\rho(x_2))\right)$$

$$\cos\left(\frac{1}{\sqrt{2}}(\phi_\sigma(x_1)-\phi_\sigma(x_2)) + (\phi_0(x_1)-\phi_0(x_2))\right)C(x_1-x_2) \tag{6.3.18}$$

instead of considering the lowest order and insert $x_1 = x_2$ one can expand $x_2 \approx x_1$ to first order. This yields

$$-\frac{g^2}{a^2}dl\frac{1}{2N}\left(\frac{1}{K_\sigma} + \frac{1}{K_\rho} + 2\frac{1}{K_0}\right)\int_a^L\mathrm{d}^2x_1\mathrm{d}^2x_2\cos\left(\frac{1}{\sqrt{2}}(\nabla_{x_1}\phi_\rho(x_1)(x_2-x_1))\right)$$

$$\cos\left(\frac{1}{\sqrt{2}}(\nabla_{x_1}\phi_\sigma(x_1)(x_2-x_1)) + (\nabla_{x_1}\phi_0(x_1)(x_2-x_1))\right)C(x_1-x_2) \tag{6.3.19}$$

Since $C(x_1 - x_2)$ is a function of the relative coordinates it makes sense to change to the center of mass and relative coordinates

$$x_r = x_1 - x_2 , \quad x_R = \frac{x_1 + x_2}{2} \tag{6.3.20}$$

by changing to these coordinates along with expanding around $x_r \approx 0$ leads to

$$-\frac{g^2}{a^2} dl \frac{1}{2N} \left(\frac{1}{K_\sigma} + \frac{1}{K_\rho} + 2\frac{1}{K_0} \right) \int_0^L d^2 x_r \int_a^L d^2 x_R \cos \left(\frac{1}{\sqrt{2}} (\nabla_{x_R} \phi_\rho(x_R)(x_r)) \right)$$

$$\cos \left(\frac{1}{\sqrt{2}} (\nabla_{x_R} \phi_\sigma(x_R)(x_r)) + (\nabla_{x_R} \phi_0(x_R)(x_r)) \right) C(x_r) \approx$$

$$-\frac{g^2}{a^2} dl \frac{1}{2N} \left(\frac{1}{K_\sigma} + \frac{1}{K_\rho} + 2\frac{1}{K_0} \right) \frac{1}{2} \int_0^L d^2 x_r \int_a^L d^2 x_R \left[\frac{1}{2} (\nabla_{x_R} \phi_\rho(x_R))^2 + \right.$$

$$\left. \left(\frac{1}{\sqrt{2}} \nabla_{x_R} \phi_\sigma(x_R) + \nabla_{x_R} \phi_0(x_R) \right)^2 \right] (x_r)^2 C(x_r) + \text{Const.} \tag{6.3.21}$$

where the upper limit for x_R stays L because one should think of $L \to \infty$. Next one should consider that $C(r)$ will be localized differently in time and space. For the time component, t_r, one finds $C(r) \approx 1$ for $t_r \in [-a/2v, a/2v]$, while for the space component, x_r, one has it being ≈ 1 for $x_r \in [-a/2, a/2]$. To get rid of this difference one can scale the time component as $t'_r = vt_r$. By doing so one finds $C(r) \approx 1$ for $|r| \leq a$ and zero everywhere else. If going to polar coordinates and trowing away the constant term the expression states

$$-\frac{g^2}{a^2} dl \frac{1}{2N} \left(\frac{1}{K_\sigma} + \frac{1}{K_\rho} + 2\frac{1}{K_0} \right) \frac{1}{2} \int_a^L d^2 x_R \left[\frac{1}{2} (\nabla_{x_R} \phi_\rho(x_R))^2 + \right.$$

$$\left. \left(\frac{1}{\sqrt{2}} \nabla_{x_R} \phi_\sigma(x_R) + \nabla_{x_R} \phi_0(x_R) \right)^2 \right] \frac{1}{v} \int_0^L d^2 x'_r (x_r)^2 C(x_r) =$$

$$-\frac{g^2}{a^2} dl \frac{1}{2N} \left(\frac{1}{K_\sigma} + \frac{1}{K_\rho} + 2\frac{1}{K_0} \right) \frac{1}{2} \int_a^L d^2 x_R \left[\frac{1}{2} (\nabla_{x_R} \phi_\rho(x_R))^2 + \right.$$

$$\left. \left(\frac{1}{\sqrt{2}} \nabla_{x_R} \phi_\sigma(x_R) + \nabla_{x_R} \phi_0(x_R) \right)^2 \right] \frac{2\pi}{v} \int_0^a dx_r (x_r)^3 =$$

$$-\frac{g^2}{a^2} dl \frac{1}{2N} \left(\frac{1}{K_\sigma} + \frac{1}{K_\rho} + 2\frac{1}{K_0} \right) \frac{1}{2} \int_a^L d^2 x_R \left[\frac{1}{2} (\nabla_{x_R} \phi_\rho(x_R))^2 + \right.$$

$$\left. \left(\frac{1}{\sqrt{2}} \nabla_{x_R} \phi_\sigma(x_R) + \nabla_{x_R} \phi_0(x_R) \right)^2 \right] \frac{2\pi a^4}{4v} \tag{6.3.22}$$

If using the relations

$$\partial_\tau \theta_s = iv_s K_s \partial_x \phi_s , \quad \partial_\tau \phi_s = i\frac{v_s}{K_s} \partial_x \theta s \tag{6.3.23}$$

and the definition of the nabla operator in space-time one finds

$$
S_{eff} = ... - \frac{\pi g^2 a^2}{4Nv} \left(\frac{1}{K_\sigma} + \frac{1}{K_\rho} + 2\frac{1}{K_0} \right) \int \mathrm{d}^2 x_R \left[\frac{1}{2} \left(\left(\frac{1}{vK_\rho} \partial_\tau \theta_\rho \right)^2 + \left(\frac{1}{K_\rho} \partial_x \theta_\rho \right)^2 \right) \right.
$$

$$
+ \left(\frac{1}{\sqrt{2}vK_\sigma} \partial_\tau \theta_\sigma + \frac{1}{vK_0} \partial_\tau \theta_0 \right)^2 + \left(\frac{1}{\sqrt{2}K_\sigma} \partial_x \theta_\sigma + \frac{1}{K_0} \partial_x \theta_0 \right)^2 \right] dl =
$$

$$
... - \frac{\pi g^2 a^2}{4Nv^2} \left(\frac{1}{K_\sigma} + \frac{1}{K_\rho} + 2\frac{1}{K_0} \right) \int \mathrm{d}^2 x_R \left[\frac{1}{2K_\rho} \left(\frac{1}{vK_\rho} (\partial_\tau \theta_\rho)^2 + \frac{v}{K_\rho} (\partial_x \theta_\rho)^2 \right) \right.
$$

$$
\left. + \frac{1}{2K_\sigma} \left(\frac{1}{vK_\sigma} (\partial_\tau \theta_\sigma)^2 + \frac{v}{K_\sigma} (\partial_x \theta_\sigma)^2 \right) + \frac{1}{K_0} \left(\frac{1}{vK_0} (\partial_\tau \theta_0)^2 + \frac{v}{K_0} (\partial_x \theta_0)^2 \right) \right.
$$

$$
\left. + \text{Mixing terms} \right] dl \qquad (6.3.24)
$$

These mixing terms will mix the quadratic part of the spin and gauge boson sector, meaning that at each time integrating out the fast oscillating modes, one would in principle need to diagonolize the quadratic part before moving on. This should be done because all expectation values are taken with respect to the quadratic part, and if it mixes the different sectors then one will $\langle \theta_\sigma \theta_0 \rangle_0 \neq 0$. These are terms are therefore hard to handle and will be neglected.

If looking at the quadratic part of the Hamiltonian in Eq. (J.1) one finds the Luttinger parameters to be renormalized according to

$$
\frac{1}{K_\sigma'} = \frac{1}{K_\sigma} + \left(... - \frac{\pi^2 g^2 a^2}{4Nv^2 K_\sigma^2} \left(\frac{1}{K_\sigma} + \frac{1}{K_\rho} + 2\frac{1}{K_0} \right) \right) dl \qquad (6.3.25)
$$

$$
\frac{1}{K_\rho'} = \frac{1}{K_\rho} + \left(... - \frac{\pi^2 g^2 a^2}{4Nv^2 K_\rho^2} \left(\frac{1}{K_\sigma} + \frac{1}{K_\rho} + 2\frac{1}{K_0} \right) \right) dl \qquad (6.3.26)
$$

$$
\frac{1}{K_0'} = \frac{1}{K_0} + \left(... - \frac{\pi^2 g^2 a^2}{2Nv^2 K_0^2} \left(\frac{1}{K_\sigma} + \frac{1}{K_\rho} + 2\frac{1}{K_0} \right) \right) dl \qquad (6.3.27)
$$

The contributions to the flow equations of the Luttinger parameters therefore become

$$
\frac{dK_\sigma}{dl} = ... + \frac{\pi^2 g^2 a^2}{4Nv^2} \left(\frac{1}{K_\sigma} + \frac{1}{K_\rho} + 2\frac{1}{K_0} \right) \qquad (6.3.28)
$$

$$
\frac{dK_\rho}{dl} = ... + \frac{\pi^2 g^2 a^2}{4Nv^2} \left(\frac{1}{K_\sigma} + \frac{1}{K_\rho} + 2\frac{1}{K_0} \right) \qquad (6.3.29)
$$

$$
\frac{dK_0}{dl} = ... + \frac{\pi^2 g^2 a^2}{2Nv^2} \left(\frac{1}{K_\sigma} + \frac{1}{K_\rho} + 2\frac{1}{K_0} \right) \qquad (6.3.30)
$$

This shows how the second order calculations are performed in momentum space, and by considering the following higher order terms

$$
S_{eff} = S_0 - T \int \mathrm{d}^2 r \cos \left(\sqrt{2} \theta_\sigma - \theta_0 \right) - G \int \mathrm{d}^2 x \left[\cos (\varphi_\uparrow + \varphi_0) + \cos (\varphi_\downarrow - \varphi_0) \right]
$$

$$
- \sum_{s=,\downarrow} \int \mathrm{d}^2 x \left[P \cos N\theta_s + Q \cos N\varphi_s \right] - \int \mathrm{d}^2 r \left[P_0 \cos N\theta_0 + Q_0 \cos N\varphi_0 \right]
$$

$$
+ \sum_{q=\rho,\sigma} \int \mathrm{d}^2 x C_q \cos \left(\sqrt{2}N\varphi_q \right) + \int \mathrm{d}^2 x \left[C_\rho' \cos \sqrt{2}\varphi_\rho + C_\sigma' \cos \left(\sqrt{2}\varphi_\sigma + 2\varphi_0 \right) \right], \qquad (6.3.31)
$$

Michele Burrello found the RG flow equations shown in Appendix I.

6.4 Solving the flow equations numerically

As for the case of $g \to 0$ one needs all parameters estimated along with some upper and lower limit. The parameters $M_{\theta,0}$ and $M_{\phi,0}$ is firstly estimated in the same way as M_θ and M_ϕ, shown in Eq. (5.7.16). This leads to

$$M_{\theta,0} = M_\theta = \frac{N^2}{32g}(1 - \cos(2\pi/N))^2$$

$$M_{\phi,0} = M_\phi = \frac{N^2 g}{32}(1 - \cos(2\pi/N))^2 \tag{6.4.1}$$

Similar to what was done in chapter 5 the upper and lower limit are set by $LC = 0.2$ and the maximum value of $UC = \{3\lambda, 5, 2/\lambda, 3g, 2/g\}$. With the equations stated in Appendix I and the program provided by *Apollonas S. Matsoukas-Roubeas* and *Michele Burrello* the second order analysis predicts the phase diagram shown in Fig. 6.6. Here the **X** phase corresponds to the phase predicted by the quasi-second order analysis, denoted the dipole phase, where θ_0, ϕ_ρ and θ_σ is pinned. Comparing this to the quasi-second order analysis depicted in Fig. 6.5 for $g \ll 1$, one sees that the true second order analysis does indeed predict an extended gapless phase. The quasi-second order analysis though indicated the importance of the second order term $\cos(\sqrt{2}N\phi_\rho)$, which pins ϕ_ρ in the **X** phase, and also how this term shrinks the gapless phase. Next one sees that the phase **C** is completely removed and instead the phase **I** expands into this region.
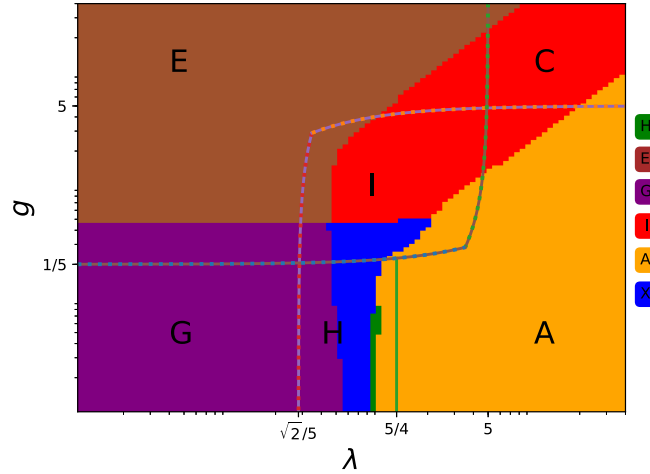
Figure 6.6 | Second order predictions. In this figure one finds the predicted phase diagram using the RG flow equations stated in Eq. (I.13). On top of this, the first order prediction is plotted. This is indicated by the different lines, and the letters inside the regions corresponds the predicted phase by the first order analysis. The colors in the plot show the predicted phase by the second order analysis, and the phase corresponding to the given color is shown to the right. Here one should notice that in comparison with Fig. 6.4 the x-axis shows λ and not its inverse.

In order to distinguish the different predicted phases one should again tend to the observables stated in section 5.4. The behavior in the different regions is given in Table 6.3 except for the behavior in region **X**, which is found in Tab. 6.5.

Phase	Exponential decaying	Constant ~ 1	Algebraic decay
X	$\langle G_\sigma \rangle, \langle M_\rho \rangle$	$\langle M_\sigma \rangle, \langle G_\rho \rangle, \langle W \rangle, \langle R \rangle$	

Table 6.5| Observables in region X. This table shows the behavior of the different observables in region **X**. The phase corresponds to the phase **X** predicted by the quasi-second order analysis for $g \to 0$ in Chapter 5.

6.4.1 Comparing with DMRG results

In this section, the RG predictions will be compared with numerical results provided by *Chia-Min Chung*, which where obtained using density matrix renormalization group (DMRG) techniques. Explaining this technique is beyond the scope of this thesis, and the results will not be discussed but simply stated and compared to the RG predictions.

The first quantity used to distinguish the different phases of the system is the fidelity and the fidelity susceptibility (FS)[2]. These quantities measure the overlap between the ground sate for given set of parameters and the ground state, when these parameters are changed by a small amount. The fidelity will simply measure the overlap while FS measures this relative to how much the parameters change. If close to some phase boundary one both quantities to change rapidly compared to deep inside a phase. In Fig. 6.7 one sees a plot the fidelity for $N = 3$ and $g = 0.001$. This shows a clear signature of a phase transition around $\lambda = 0.75$, where the ground state wave function change rapidly compared to elsewhere. Using the FS *Chia-Min Chung* where able to separate different regions resulting in the
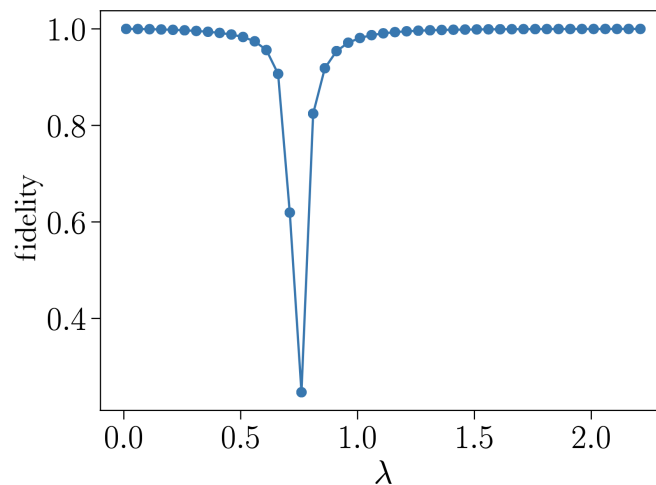
Figure 6.7 | Fidelity. For $N = 3$ and $g = 0.001$ one sees a plot showing the fidelity, which clearly shows signature of a phase transition around $\lambda = 0.75$ where the ground state wave function change rapidly. The figure is provided by *Chia-Min Chung*.

phase diagram shown in Fig. 6.8. In the figure, the blue data points shows different minima of the FS. Here I have to stress, that the color coding is made such to simulate the phase diagram predicted by the RG procedure. To compare, one finds in Fig. 6.9 the phase diagram predicted by RG in the same region. In comparing these two phase diagrams one finds many similarities, but the RG predictions is seen to consistently predict the boundaries to be larger valuers of λ than the DMRG analysis predicts.

Having the FS showing a maximum is though not enough for it to predict a true phase transition. If it is to be a true phase transition, then the FS should diverge with the system size going to infinity.

---

[2]The fidelity is a good quantity to look at when searching for second order phase transitions, while for the BKT type FS becomes a better quantity.
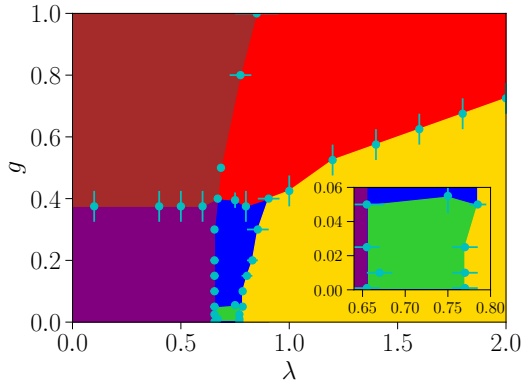
Figure 6.8 | DMRG phase diagram. From the blue points, which indicates a minimum in the fidelity susceptibility, the different phases have been separated. Here the color coding is such to simulate the phase diagram predicted by the RG procedure. This for example means, that the purple region is not predicted by this analysis, to be the same a the phase G. This figure is provided by *Chia-Min Chung*.
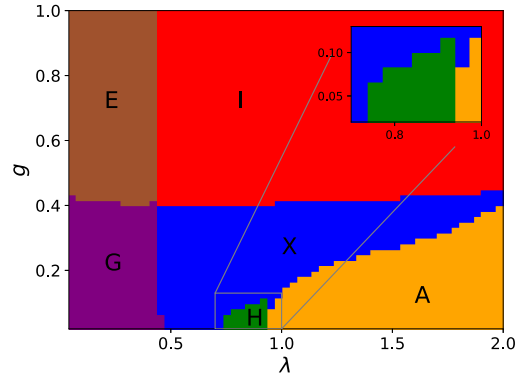
Figure 6.9 | RG phase diagram. This figure shows the phase diagram predicted by the second order RG analysis, with the used flow equations stated in Eq. (I.13).

In Fig. 6.10 and 6.11 one finds two FS scans, where g is kept constant and λ is varied. Here one
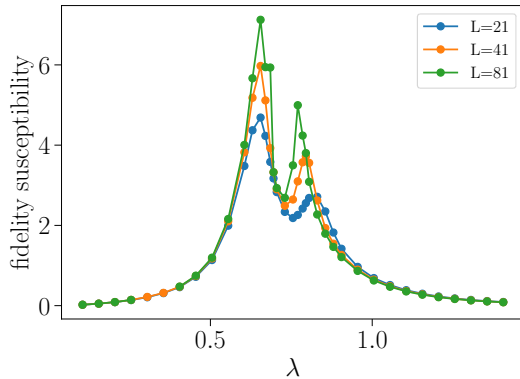
Figure 6.10 | Scan for $g = 0.001$ This figure shows a scan of the fidelity susceptibility as a function of λ for $g = 0.001$, where the different colored graphs corresponds to different system length L. Here one sees that as increasing L the peak sharpens, which indicates this to be a true phase transitions. This figure is provided by *Chia-Min Chung*.
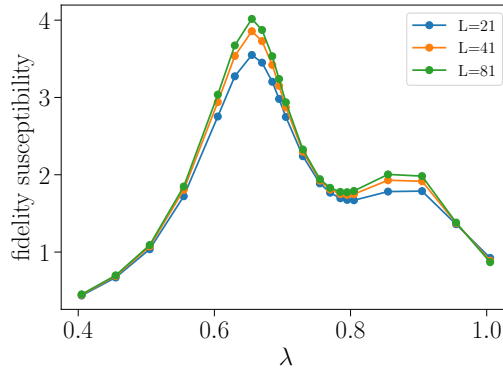
Figure 6.11 | Scan for $g = 0.3$ This figure shows a scan of the fidelity susceptibility as a function of λ for $g = 0.001$, where the different colored graphs corresponds to different system length L. Here one sees that as increasing L the peak does not sharpen, which indicates this to be a cross and not a true phase transitions. This figure is provided by *Chia-Min Chung*.

sees, that for $g = 0.3$ the maximum found in the FS does not seem to diverge with increasing system size. This indicates it to be a crossover and not a phase transition. Instead for $g = 0.001$ the peak

sharpens as the system size is increased, thereby indicating a true phase transition. By performing this analysis *Chia-Min Chung* only found indications of a true phase transition between the predicted gapless region, shown in green in Fig. 6.8, and its surroundings. All other minima showed indications of being a cross over.

In the predicted gapless region *Chia-Min Chung* found M_ρ to show power law behavior while M_σ showed a constant behavior in the bulk. In the green phase the DMRG results therefore predicts the spin sector to be pinned and the charge sector to be unpinned and gapless, which is consistent with the predictions of the H phase. The results are shown in Appendix K. To conclude, the DMRG analysis predicts the system to be in the same gapped phase everywhere except in the green region, which shows gapless behavior in the charge sector.

Chapter 7

Conclusion and Outlook

Throughout this thesis I have investigated $\mathbb{Z}_N$ lattice gauge theories using the Kogut-Susskind Hamiltonian in a ladder geometry. First the $\mathbb{Z}_N$ pure lattice gauge theory was investigated, where only one gapped phase was predicted. In order get a clearer picture of the model, a mapping based on a bond-algebraic duality was presented. Utilizing this, the model was mapped into the 1D quantum N-clock model in both a transverse and longitudinal field. The phase was then investigated by inserting two static charges into the system. This showed the gapped phase to be a deconfined phase.

Next Higgs matter was introduced into the model. Using a perturbative approach this theory was investigated in the limit of $g \to 0$. In the axial gauge this limit was showed to be described by the quantum N-clock model in only a transverse field, and therefore at least one phase transition was expected. Different approaches were then used to find indications of a phase transition, but they all ultimately failed. To remedy this failure the more advanced technique of bosonization was introduced.

In the limit of $g \to 0$ the system containing Higgs matter was then investigated using bosonization techniques. This was done by describing the operators in terms of bosonic fields, from where a 1D continuous description was extracted. Using renormalization group techniques this bosonized description was investigated. To first order this analysis predicted a gapped-gapped phase transition for $N = 2$ while for $N > 2$ an intermediate gapless region showed. From the mapping presented in [47], we knew this to be wrong for $N = 4$ where it was showed that only a gapped-gapped transition should take place. We then build on top of the first order predictions by first performing the two-step-RG procedure. This predicted a gapped-gapped transition for $N < 4$ and still an intermediate gapless phase for $N \geq 4$. Our last attempt before proceeding to the true second order approach was this quasi-second analysis, where a higher order term was considered. This analysis in accordance with[47] predicted only a gapless phase for $N > 4$ and the phase diagrams for $N = 2, 3, 4$ to coincide.

The next step taken was to investigate the system using the true second order RG analysis. This analysis was done by following the real space approach presented in [52, 54]. From it, the RG flow equations were derived and then solved numerically using the program provided by *Apollonas S. Matsoukas-Roubeas* and *Michele Burrello*. The numerical solution predicted the gapless phase to be present for $\lambda \in [0.4, 1]$. Utilizing the second order RG approach in real space showed the limitation of not incorporating higher order terms. This approach was therefore left behind in favor of the second order RG analysis performed in momentum space.

In the last chapter the full model was approached. At first the first order RG predictions were stated. These showed the occurrence of six different phases which characteristics were described. Next the model was approached by deploying the full second order approach in momentum space. This approach was described and the calculations for the electric field term of the legs were performed. In doing so, one saw the occurrence of higher order terms, which then were to be incorporated as a first order term, with the initial condition of the coupling constant being zero when the flow was initiated. The complete set of flow equations were derived by *Michele Burrello* where important higher order terms were incorporated. These flow equations were solved numerically and the predicted

phase diagram was presented and compared to the first order predictions. The second order analysis predicted five gapped phases and one gapless. These predictions were then compared to numerical predictions made by *Chia-Min Chung* using density matrix renormalization group techniques. The RG and DMRG predictions matched rather well, with the exception of the DMRG analysis predicting all the five gapped phases to be the same phase. The DMRG analysis did though still predict the gapless phase, and it predicted it to be in the same neighborhood of the phase diagram as the RG analysis.

To conclude, in applying the bosonization technique it showed possible to incorporate the complicated plaquette interactions and make predictions which partially agreed with those obtained using DMRG techniques. The technique is though still in the process of being developed, and as this analysis showed, it has hard time distinguishing between crossovers and true phase transitions. With this approach it was though possible to establish the main features of the phase diagram, which clearly shows its strength, and one can think of many systems where this technique can be applied to. To name a few, one could consider the same ladder geometry but with different kinds of matter. One could also try to approach the same theory, but instead consider a two dimensional system, which would be a big step in the direction of investigating more realistic systems.

Bibliography

[1] The CMS Collaboration. "A New Boson with a Mass of 125 GeV Observed with the CMS Experiment at the Large Hadron Collider". In: *Science* 338 (Dec. 2012). DOI: 10.1126/science.1230816.

[2] David J. Gross and Frank Wilczek. "Ultraviolet Behavior of Non-Abelian Gauge Theories". In: *Phys. Rev. Lett.* 30 (June 1973). DOI: 10.1103/PhysRevLett.30.1343.

[3] N. Brambilla *et al.* "QCD and strongly coupled gauge theories: challenges and perspectives". In: *Eur. Phys. J.* (May 2014). DOI: 10.1140/epjc/s10052-014-2981-5v.

[4] J. Greensite. "The confinement problem in lattice gauge theory". In: *Progress in Particle and Nuclear Physics* (Feb. 2003). DOI: 10.1016/S0146-6410(03)90012-3.

[5] Kenneth G. Wilson. "Confinement of quarks*". In: *Phys. Rev. D* 10 (Oct. 1974). DOI: 10.1103/PhysRevD.10.2445.

[6] John B. Kogut. "An introduction to lattice gauge theory and spin systems". In: *Rev. Mod. Phys.* 51 (Oct. 1979). DOI: 10.1103/RevModPhys.51.659.

[7] John B. Kogut. "The lattice gauge theory approach to quantum chromodynamics". In: *Rev. Mod. Phys.* 55 (July 1983). DOI: 10.1103/RevModPhys.55.775.

[8] Sinya Aoki *et al.* "Review of lattice results concerning low energy particle physics". In: *arXiv:1310.8555 [hep-lat]* (2013).

[9] Matthias Troyer and Uwe-Jens Wiese. "Computational Complexity and Fundamental Limitations to Fermionic Quantum Monte Carlo Simulations". In: *Phys. Rev. Lett.* 94 (May 2005). DOI: 10.1103/PhysRevLett.94.170201.

[10] Erez Zohar, J. Ignacio Cirac, Benni Reznik. "Quantum simulations of lattice gauge theories using ultracold atoms in optical lattices". In: *Rep. Prog. Phys.* 79 (Jan. 2016). DOI: 10.1088/0034-4885/79/1/014401.

[11] M. Dalmonte and S. Montangero. "Lattice gauge theory simulations in the quantum information era". In: *Cont. Phys.* 57 (Mar. 2016). DOI: 10.1080/00107514.2016.1151199.

[12] Erez Zohar. "Quantum simulation of fundamental physics". In: *Nature* 534 (June 2016). DOI: 10.1038/534480a.

[13] H.-N. Dai *et al.* "Four-body ring-exchange interactions and anyonic statistics within a minimal toric-code Hamiltonian". In: *Nat. Phys.* (Aug. 2017). DOI: 10.1038/nphys4243.

[14] C. Schweizer *et al.* "Floquet approach to $\mathbb{Z}_2$ lattice gauge theories with ultracold atoms in optical lattices". In: *Nat. Phys.* (Sept. 2019). DOI: 10.1038/s41567-019-0649-7.

[15] F.Gör *et al.* "Realization of density-dependent Peierls phases to engineer quantized gauge fields coupled to ultracold matter". In: *Nat. Phys* (Aug. 2019). DOI: 10.1038/s41567-019-0615-4.

[16] Alexander Mil *et al.* "Realization of density-dependent Peierls phases to engineer quantized gauge fields coupled to ultracold matter". In: *arXiv:1909.07641v1* (Sept. 2019).

[17] B. Yang *et al.* "Observation of gauge invariance in a 71-site quantum simulator". In: *arXiv:2003.08945* (Mar. 2020).

[18] Daniel Robaina,1 Mari Carmen Ban uls,1, 2 and J. Ignacio Cirac. "Simulating 2+1d Z3 lattice gauge theory with iPEPS". In: *arXiv:2007.11630* (July 2020).

[19] John Kogut and Leonard Susskind. "Hamiltonian formulation of Wilson's lattice gauge theories". In: *Phys. Rev. D* 11 (Jan. 1975). DOI: 10.1103/PhysRevD.11.395.

[20] T.Banks, R.Myerson, J.Kogut. "Phase transitions in Abelian lattice gauge theories". In: *Nucl. Phys. B* 3 (Oct. 1977). DOI: 10.1016/0550-3213(77)90129-8.

[21] Erez Zohar and Michele Burrello. "Formulation of lattice gauge theories for quantum simulations". In: *Phys. Rev. D* 91 (Mar. 2015). DOI: 10.1016/0550-3213(77)90129-8.

[22] Erez Zohara, Thorsten B. Wahl, Michele Burrello and J. Ignacio Ciraca. "Projected Entangled Pair States with non-Abelian gauge symmetries: An SU(2) study". In: *Ann. Phys.* 374 (Nov. 2016). DOI: 10.1016/j.aop.2016.08.008.

[23] Kai Zapp and Román Orús. "Tensor network simulation of QED on infinite lattices: Learning from (1+1)d, and prospects for (2+1)d". In: *Phys. Rev. D* 95 (Apr. 2017). DOI: 10.1103/PhysRevD.95.114508.

[24] Eduardo Fradkin , Stephen H. Shenker. "Phase diagrams of lattice gauge theories with Higgs fields". In: *Physical Review D* 19.12 (June 1979). DOI: 10.1103/PhysRevD.19.3682.

[25] Erez Zohar, J. Ignacio Cirac, and Benni Reznik. "Quantum simulations of gauge theories with ultracold atoms: Local gauge invariance from angular-momentum conservation". In: *Phys. Rev. A* 88 (Aug. 2013). DOI: 10.1103/PhysRevA.88.023617.

[26] Simone Notarnicola *et al.* "Discrete Abelian gauge theories for quantum simulations of QED". In: *Journal of Physics A: Mathematical and Theoretical* 48 (July 2015). DOI: 10.1088/1751-8113/48/30/30ft01.

[27] Stefan Kühn, J. Ignacio Cirac, and Mari-Carmen Bañuls. "Quantum simulation of the Schwinger model: A study of feasibility". In: *Phys. Rev. A* 90 (July 2014). DOI: 10.1103/PhysRevA.90.042305.

[28] B. van Heck M. Burrello and E. Cobanera. "Topological phases in two-dimensional arrays of parafermionic zero modes". In: *Phys. Rev. B* (May 2013). DOI: 10.1103/PhysRevB.87.195422.

[29] Sebastian Greschner Lorenzo Cardarelli and Luis Santos. "Deconfining Disordered Phase in Two-Dimensional Quantum Link Models". In: *Phys. Rev. Lett.* (Mar. 2020). DOI: 10.1103/PhysRevLett.124.123601.

[30] A. Celi *et al.* "Emerging 2D Gauge theories in Rydberg configurable arrays". In: *arXiv:1907.03311v3 [quant-ph]* (July 2019).

[31] J. M. Drouffe, J. Jurkiewicz, and A. Krzywicki. "Lattice gauge theory with Higgs matter field in the adjoint representation". In: *Phys. Rev. D* 29 (June 1984). DOI: 10.1103/PhysRevD.29.2982.

[32] G. Ortiz, E. Cobanera and Z. Nussinov. "Dualities and the phase diagram of the p-clock model". In: *Nuclear Physics B* 854 (Sept. 2011). DOI: 10.1016/j.nuclphysb.2011.09.012.

[33] Vladimir B Matveev. "Intertwining relations between the Fourier transform and discrete Fourier transform, the related functional identities and beyond". In: *Inverse Problems* 17 (2001).

[34] Eduardo Fradkin. *Field Theories of Condensed Matter Field Theory.* 2nd ed. Cambridge University Press, 2013.

[35] Eduardo Fradkin, Leonard Susskind. "Order and disorder in gauge systems and magnets". In: *Phys. Rev. D* 17 (May 1978). DOI: https://doi.org/10.1103/PhysRevD.17.2637.

[36] Ben Gripaios. *Gauge Field Theory.* Notes for the course Gauge Field Theory. Cavendish Laboratory, JJ Thomson Avenue, Cambridge, CB3 0HE, United Kingdom., Jan. 2016. URL: http://www.precision.hep.phy.cam.ac.uk/wp-content/people/mitov/lectures/GaugeFieldTheory-2020/gft_complete_lecture_notes.pdf.

[37] Erez Zohar, J. Ignacio Cirac, and Benni Reznik. "Quantum simulations of gauge theories with ultracold atoms: local gauge invariance from angular momentum conserva-

tion". In: *Phys. Rev. A* 88 (Aug. 2013). DOI: 10.1103/PhysRevA.88.023617.

[38] Eduardo Fradkin, Leonard Susskind. "Fault-tolerant quantum computation by anyons". In: *Annals of Physics* 303 (Jan. 2003). DOI: https : / / doi . org / 10 . 1016 / S0003-4916(02)00018-0.

[39] Emilio Cobanera , Gerardo Ortiz, and Zohar Nussinov. "The Bond-Algebraic Approach to Dualities". In: *arXiv:1103.2776 [cond-mat.stat-mech]* (June 2011). DOI: 10.1080/00018732.2011.619814.

[40] Emilio Cobanera, Gerardo Ortiz, and Zohar Nussinov. "Holographic symmetries and generalized order parameters for topological matter". In: *Phys. Rev. B* 87 (Jan. 2013). DOI: 10.1103/PhysRevB.87.041105.

[41] R. Coldea *et al.* "Quantum Criticality in an Ising Chain: Experimental Evidence for Emergent E_8 Symmetry". In: *Science* 327 (Jan. 2010). DOI: 10 . 1126 / science . 1180085.

[42] M. C. Ban uls, J. I. Cirac and M. B. Hastings. "Strong and Weak Thermalization of Infinite Nonintegrable Quantum Systems". In: *Phys. Rev. Lett.* 1076 (Feb. 2011). DOI: 10.1103/PhysRevLett.106.050405.

[43] Benjamin Blaß and Heiko Rieger s. "Test of quantum thermalization in the two-dimensional transverse-field Ising model". In: *Scientific RepoRts* 6 (Dec. 2016). DOI: 10.1038/srep38185.

[44] Paul Fendley. "Parafermionic edge zero modes in Z(n)-invariant spin chains". In: arXiv.arXiv (Oct. 2012). DOI: arXiv.

[45] J.B. Kogut, R.B. Pearson, J. Shigemitsu, D.K. Sinclair. "Z_N and N-state Potts lattice gauge theories: Phase diagrams, first-order transitions, β functions, and $1/N$ expansions". In: *Phys. Rev. D* 22 (Nov. 1980). DOI: 10.1103/PhysRevD.22.2447.

[46] G. Sun, T. Vekua, E. Cobanera, and G. Ortiz. "Phase transitions in the $\mathbb{Z}_p$ and U(1) clock models". In: *Phys. Rev. B* 100 (July 2019). DOI: 10.1103/PhysRevB.100.094428.

[47] G. Ortiz, E. Cobanera and Z. Nussinov. "Dualities and the phase diagram of the p-clock model". In: *Nucl. Phys. B* 854 (Jan. 2012). DOI: 10.1016/j.nuclphysb.2011.09.012.

[48] P. Lecheminant, Alexander O. Gogolin, and Alesander A. Nersesyan. "Criticality in self-dual sine-Gordon models". In: *Nucl.Phys.B* 18 (Mar. 2002). DOI: 10 . 1016 / S0550-3213(02)00474-1.

[49] P. Lecheminant, A. O. Gogolin, A. A. Nersesyan. "Criticality in self-dual sine-Gordon models". In: *arXiv:cond-mat/0203294* (June 2002). DOI: 10 . 1016 / S0550 - 3213(02) 00474-1.

[50] Ashley Milsted, Emilio Cobanera, Michele Burrello, and Gerardo Ortiz. "Commensurate and incommensurate states of topological quantum matter". In: *Phys. Rev. B* 90 (Nov. 2014). DOI: 10.1103/PhysRevB.90.195101.

[51] David J. Griffiths. "Introduction to Quantum mechanics". In: Pearson, 2014. Chap. 7.

[52] Thierry Giamarchi. *Quantum Physics in One Dimension.*

[53] Michele Burrello. *Introduction to one-dimensional models.* Notes for the course CMT3. Niels Bohr International Academy and Center for Quantum Devices, University of Copenhagen, Juliane Maries Vej 30, 2100 Copenhagen, Denmark, Mar. 2019.

[54] Eugene H. Kim, J. Sólyom. "Opening of the Haldane gap in anisotropic two- and four-leg spin ladders". In: *PHYSICAL REVIEW B* 60 (Dec. 1999). DOI: https://doi.org/10.1103/PhysRevB.60.15230.

[55] Umberto Borla, Ruben Verresen, Fabian Grusdt, and Sergej Moroz. "Confined Phases of One-Dimensional Spinless Fermions Coupled to $\mathbb{Z}_2$ Gauge Theory". In: *Phys. Rev. Lett.* 124 (Mar. 2020). DOI: 10 . 1103 / PhysRevLett.124.120503.

[56] Steven Howes, Leo P. Kadanoff, Marcel Den Nijs. "Phase diagram of hard-core bosons on clean and disordered 2-leg ladders Mott insulator – Luttinger liquid – Bose glass". In: *PHYSICAL REVIEW B* 84 (Aug. 2011). DOI: https : / / doi . org / 10 . 1103 / PhysRevB.84.054517.

[57] John L. Cardy. "Antiferromagnetic clock models in two dimensions". In: *Physical Review B* (Nov. 1981). DOI: `https://doi.org/10.1103/PhysRevB.24.5128`.

[58] P B Wiegmann. "One-dimensional Fermi system and plane xy model". In: *Phys. C: Solid State Phys.* 11 (Nov. 1978).

[59] Anson Cheung. *Phase Transitions and Collective Phenomena*. Notes for the course Phase Transitions. Cavendish Laboratory, JJ Thomson Avenue, Cambridge, CB3 0HE, United Kingdom., Jan. 2011. URL: `https://www.tcm.phy.cam.ac.uk/~achc2/phase/notes.pdf`.

[60] G. Mussardo. *Statistical Field Theory: An Introduction to Exactly Solved Models in Statistical Physics*. 2020.

[61] Mehran Kardar. "Statistical Physics of Fields". In: Cambridge University Press, 2012. ISBN: 9780511815881.

[62] Tom Kennedy. *Gauge Field Theory*. Course notes for Introduction to Mathematical Physics. Department of Mathematics, The University of Arizona 617 N. Santa Rita Ave., Tucson, AZ 85721-0089 USA, 2018. URL: `https://www.math.arizona.edu/~tgk/541/chap3.pdf`.

[63] Steven Howes, Leo P. Kadanoff, Marcel Den Nijs. "Short Distance Expansions of Correlation Functions in the Sine-Gordon Theory". In: *Nucl. Phys. B* 479 (Nov. 1996). DOI: `https://doi.org/10.1016/0550-3213(96)00279-9`.

Appendices

Appendix A

SR boundaries with Higgs matter

By having introduced matter fields at the vertices one needs to specify what SR boundaries referrers to, since the legs could either terminate with a link or a vertex as depicted in Fig. A.1 and A.2. The main difference in terminating with a vertex is that they leave two extra gauge constrains given by

$$\mathbf{G}_{L,s} = \tau_{L-1,s}\eta_{L,s} , \quad s = \uparrow, \downarrow \tag{A.1}$$

These two constrains can be used to eliminate the d.o.f found at the ending vertices by using the unitary gauge [24, 34]. The Unitary gauge gauges out the Higgs bosons by demanding

$$\zeta \ket{\psi_{uni}} = \ket{\psi_{uni}}. \tag{A.2}$$

Looking at the Hamiltonian in Eq. (4.1.12) one would by omitting all terms containing $\sigma_{L,0}$ find the Hamiltonian for the system with the right boundary terminated as shown in Fig. A.2, so terminating with Higgs matter. With this Hamiltonian one would by choosing the unitary gauge for just the last vertices, hence $\zeta_{L,s}\ket{\psi_{uni}} = \ket{\psi_{uni}}$, end up with

$$\zeta_{L-1,\uparrow}^{\dagger}\sigma_{L-1}\zeta_{L,\downarrow} + \text{H.c} \rightarrow \zeta_{L-1,\uparrow}^{\dagger}\sigma_{L-1} + \text{H.c} \tag{A.3}$$

$$\eta_{L,s} + \eta_{L,s}^{\dagger} \rightarrow \tau_{L-1,s} + \tau_{L-1,s}^{\dagger} \tag{A.4}$$

Where the last term already appears in the Hamiltonian, and one should therefore not show it much attention. The term in Eq. (A.3) is though a quiet interesting term, and it is so because it breaks the global $\mathbb{Z}_N$ symmetry generated by

$$\mathcal{S}_C \equiv \prod_{i=0}^{L} \eta_{i,\uparrow}\eta_{i,\downarrow} \tag{A.5}$$

Actually this symmetry is not broken for the whole system, but if only considering the new system with the Higgs matter at boundary frozen out, hence only letting the product run until $L - 1$, then
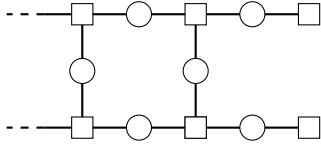
Figure A.1 | Boundary conditions. This figure shows how the boundary of the strip containing site L is constructed.
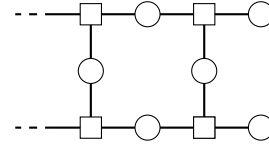
Figure A.2 | Boundary conditions. This figure shows how the boundary of the strip containing site L is constructed.

this symmetry will look broken. From Eq. (4.1.5) one sees that this corresponds to $\mathcal{S}_C \sim e^{i\frac{2\pi}{N}\sum_{\bar{r}}\rho_{\bar{r}}}$, and thereby represents charge conservation. The Hilbert space where one performs the calculations in, after this gauge fixing, will therefore look as though charge is not conserved, even though it is.

If now considering the boundary to be terminated with links as depicted in Fig A.1, one finds the term in Eq. (A.3) to be gauge invariant and can therefore be incorporated into the Hamiltonian[1]. This system will therefore not show charge conservation, but by using $\zeta_{L,s}|\psi_{uni}\rangle = |\psi_{uni}\rangle$ one uses a subspace of the physical Hilbert space where charge conservation looks broken, and the two boundaries is therefore equivalent[2].

---

[1]One finds this by calculation $[G_{L-1,s}, \zeta^{\dagger}_{L-1,s'}\sigma_{L-1,0}] = 0$.

[2]The only difference of the Hamiltonian is that $\tau_{L-1,s} + \tau^{\dagger}_{L-1,s}$ will appear twice with boundaries ending with Higgs matter.

Appendix B

For $g \to 0$ limit

This appendix presents a perturbative calculation of the energy correction found in the $g \ll 1$ when two static charges with opposite charges are present. Compared to the calculation performed in the main text, these are performed in no specific gauge. This leaves space for a lot tedious calculations since physical configurations are represented by multiple states, but one also gain an insight into the actual physical configurations and how the perturbation changes these configurations.

In this limit the Hamiltonian is described by Eq. (3.3.8) and one can construct the ground state either in in τ- or the σ-basis. We begin with the σ-basis. The first step is to create a projection operator which projects each physical state onto it self while projecting all non-physical states onto the null space. The physical Hilbert space is modified due to the introduced charges, such that all physical states satisfies Eq. (3.3.4). Taking this into account on finds the following operator ensuring all of this

$$\Pi_{\bar{x},\bar{y}} \equiv \prod_{\bar{r} \neq \{\bar{x},\bar{y}\}} \sum_{l=1}^{N} \frac{(\boldsymbol{G}_{\bar{r}})^l}{\sqrt{N}} \cdot \sum_{l=1}^{N} \frac{(\omega \boldsymbol{G}_{\bar{x}})^l}{\sqrt{N}} \cdot \sum_{l=1}^{N} \frac{(\bar{\omega} \boldsymbol{G}_{\bar{y}})^l}{\sqrt{N}} \tag{B.1}$$

Where one sees that

$$\boldsymbol{G}_{\bar{x}} \Pi_{\bar{x},\bar{y}} = \bar{\omega} \Pi_{\bar{x},\bar{y}}$$
$$\boldsymbol{G}_{\bar{y}} \Pi_{\bar{x},\bar{y}} = \omega \Pi_{\bar{x},\bar{y}}. \tag{B.2}$$

When looking at the Hamiltonian in Eq. (3.3.8) one sees that due to our smooth-rough boundary condition, the terms $\sigma_{L,\uparrow}$ and $\sigma_{L,\downarrow}$ does not show in the Hamiltonian. This means that the ground state for $g \to 0$ is degenerate since $[H, \tau_{L,\uparrow}] = [H, \tau_{L,\downarrow}] = 0$. The Hamiltonian also commutes with $\boldsymbol{F} \equiv \prod_{\bar{r}} \tau_{\bar{r}}$, so "turning" all the states simultaneously will not change the energy either. The last degeneracy is obtained by flipping all the spins of the rung $\boldsymbol{F}_r \equiv \prod_i \tau_{i,0}$ where $[\boldsymbol{F}_r, H] = 0$. All these symmetries are though equivalent in the physical Hilbert space

$$\prod_{i=1}^{L} (\boldsymbol{G}_{i,\uparrow})^i (\boldsymbol{G}_{i,\downarrow})^i \boldsymbol{F} = \boldsymbol{F}_r$$

$$\tau_{L,\uparrow} = \boldsymbol{F}_r^\dagger$$
$$\tau_{L,\downarrow} = \boldsymbol{F}_r \tag{B.3}$$

Where the last two equations are obtained by multiplying all of the upper or lower gauge generators onto $\tau_{L,\uparrow}$ and $\tau_{L,\downarrow}$ respectively. The conclusion is that the ground state is N-times degenerate and one can choose either one of these generators to generate the symmetry. An important realization is that $\boldsymbol{F}_r$ cannot be constructed from the gauge generators, $\boldsymbol{G}$, meaning that this is not some redundancy of the system.

The minimum energy of the Hamiltonian will be $E_{min} = -2(N-1)/g$, so if one can construct a state with this energy which also fulfills Eq. (3.3.4), it must be the ground state. The N-degenerate states fulfilling this, can be expressed as

$$\{||k\rangle\rangle_\sigma \equiv \Pi_{\bar{x},\bar{y}}(\boldsymbol{F}_r)^k |0,0,...,0\rangle_\sigma = \Pi_{\bar{x},\bar{y}}(\boldsymbol{F}_r)^k ||0\rangle\rangle_\sigma \ , \quad k = 0,1,...,N-1\} \tag{B.4}$$

Where these states fulfill

$$\boldsymbol{G}_{\bar{x}} ||k\rangle\rangle_\sigma = \bar{\omega} ||k\rangle\rangle_\sigma \ , \ \boldsymbol{G}_{\bar{y}} ||k\rangle\rangle_\sigma = \omega ||k\rangle\rangle_\sigma \tag{B.5}$$

$$H ||k\rangle\rangle_\sigma = -2\frac{L-1}{g} ||k\rangle\rangle_\sigma . \tag{B.6}$$

and therefore represent the degenerate ground states of the system in the σ-basis. A thing to notice, is that in this limit one finds $\Delta E(R) = 0$, meaning that introducing the charges will not cost any energy.

One can also choose to express the ground state in the τ-basis. This ground state needs to fulfill the same requirements along with being N-times degenerate. In doing so, it becomes convenient to construct the operator Π_p, which takes any state in the τ-basis, and make it into a superposition of all possible excitations of all plaquettes.

$$\Pi_p \equiv \prod_{i=1}^{L-1} \sum_{j=0}^{N-1} \frac{(\boldsymbol{B}_i)^j}{\sqrt{N}} \ , \quad \boldsymbol{B}_i \equiv \sigma_{i,0}^\dagger \sigma_{i,\uparrow}^\dagger \sigma_{i+1,0} \sigma_{i,\downarrow}. \tag{B.7}$$

This operator holds two important features. Firstly one sees that $(\boldsymbol{B}_i)^l \Pi_p = \Pi_p$; secondly, since this operator consist of $\boldsymbol{B}_i$, which are operators contained in the Hamiltonian, one has that $[\boldsymbol{G}_{\bar{r}}, \Pi_p] = 0$. In constructing the ground state with the two charges, we want Eq. (3.3.4) to be satisfied. A state satisfying this is

$$\Pi_p ||0; \gamma(\bar{x},\bar{y})\rangle\rangle_\tau = \Pi_p \bigotimes_{i \notin \gamma} |0\rangle_{\tau,i} \bigotimes_{j \in \gamma} |1\rangle_{\tau,j} . \tag{B.8}$$

This state satisfy the necessary conditions and have energy $-2(N-1)/g$. What is missing is the degeneracy. This degeneracy comes from gauge invariant operators

$$\boldsymbol{W}_i \equiv \sigma_{i,0}^\dagger \prod_{j=i}^{L} \sigma_{j,\uparrow}^\dagger \sigma_{j,\downarrow}. \tag{B.9}$$

which cannot be constructed from any combination of the $\boldsymbol{B}_i$ operators. A feature of this operator is that $\boldsymbol{B}_i \boldsymbol{W}_i = \boldsymbol{W}_{i+1}$. Having $\Pi_p = \Pi_p \boldsymbol{B}_i$ means that the symmetry generated by all the different $\boldsymbol{W}_i$ actually corresponds to the same symmetry. Therefore one can choose to express the symmetry using solely the last unfinished plaquette operator, $\boldsymbol{W}_L = \sigma_{L,0}^\dagger \sigma_{L,\uparrow}^\dagger \sigma_{L,\downarrow}$. One can now write the degenerate ground state as

$$||m\rangle\rangle_\tau \equiv \Pi_p (\boldsymbol{W}_L)^m ||0; \gamma(\bar{x},\bar{y})\rangle\rangle_\tau . \tag{B.10}$$

In this basis, one can also see that had the boundary been smooth-smooth there would not have been any degeneracy. This comes from $\boldsymbol{W}_i$ no longer being gauge invariant, which means that $\boldsymbol{G}_i ||m\rangle\rangle_\tau \neq ||m\rangle\rangle_\tau$ for any m, and this results in $||m \neq 0\rangle\rangle_\tau$ not being a physical state any more.

Writing the ground state in the τ-basis diagonalize the perturbing Hamiltonian, such that one does not find any mixing of the degenerate ground state. To get an idea of what happens to first order, one can look at

$$\sum_{l=0}^{N-1} \frac{(\boldsymbol{B}_i^\dagger)^l}{\sqrt{N}} \tau_i \sum_{j=0}^{N-1} \frac{(\boldsymbol{B}_i)^j}{\sqrt{N}} = \frac{1}{N} \sum_{l=0}^{N-1} (\boldsymbol{B}_i^\dagger)^l \sum_{j=0}^{N-1} (\boldsymbol{B}_i \bar{\omega})^j \tau_i$$

$$= \frac{1}{N} \sum_{l=0}^{N-1} (\bar{\omega})^l \sum_{j=0}^{N-1} (\boldsymbol{B}_i \bar{\omega})^j \tau_i = 0. \tag{B.11}$$

Which leads to

$$(\Pi_p)^{\dagger}\tau_{\bar{r}}\Pi_p = 0 \text{ for } \bar{r} \neq (N,\uparrow) \text{ or } (N,\downarrow). \tag{B.12}$$

This means that to first order, one can only get a non-zero contribution from $\tau_{L,\uparrow}^{(\tau)}$ or $\tau_{L,\downarrow}^{(\tau)}$, such that this perturbation would split the degeneracy and leave a unique ground state.

To better understand what this ground state looks like, it makes sense to look at what $(\boldsymbol{B}_i)^l$ transforms a state in the τ-basis into. If $(\boldsymbol{B}_i)^l$ acts on the i'th plaquette where all the links are in the $|0\rangle_\tau$ state, one finds the state depicted in Fig. B.1.
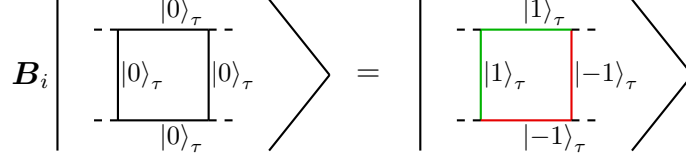
Figure B.1 | Schematic representation of the action of $\boldsymbol{B}_i$. This figure shows how the state changes when $\boldsymbol{B}_i$ acts on a plaquette.

If instead the $\boldsymbol{B}_i$ acts on a plaquette which is a part of the path between the two charges γ. Then the operator will deform the path as seen depicted in Fig. B.2.
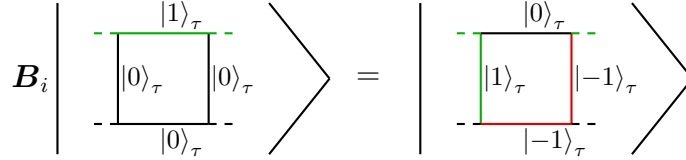
Figure B.2 | Schematic representation of the action of $\boldsymbol{B}_i$. This figure shows how the state changes when $\boldsymbol{B}_i$ acts on a plaquette which intersects the path γ.

Looking at the definition of $||m\rangle\rangle_\tau$ one finds that the operator Π_p will create all possible excitations of all the different plaquettes. This therefore means that the ground state represents a superposition of all possible closed loops excitations[1] and an open string of all possible lengths between $\bar{x}$ and $\bar{y}$, which is similar to what is found in [34]. This means that one can separate the two charges with out adding any additional energy to the system. So in this limit there is no interaction energy between the two charges, and the state is deconfining.

In the thermodynamic limit the bulk properties of the matter will only be marginal influenced by how the boundaries are constructed. So to make the calculations easier, I will insert the unfinished plaquette term

$$-\frac{1}{g}\left(\sigma_{L,0}^{\dagger}\sigma_{L+1,\uparrow}^{\dagger}\sigma_{L,\downarrow} + \text{H.c.}\right) \tag{B.13}$$

into the Hamiltonina. This is possbile due to it being gauge invariant. Inserting this term leads to $[\tau_{L,\uparrow/\downarrow}, H] \neq 0$, such that no degeneracy is present any longer. The new non-degenerate ground states is represented by

$$||GS\rangle\rangle_\sigma \equiv \Pi_{\bar{x},\bar{y}} ||0\rangle\rangle_\sigma \tag{B.14}$$

$$||GS\rangle\rangle_\tau \equiv \Pi_p ||0; \gamma(\bar{x},\bar{y})\rangle\rangle_\tau . \tag{B.15}$$

---

[1]With a "closed loop excitation" is meant an excitation of the kind $\prod_{i=l}^{m} \boldsymbol{B}_i$.

We are now ready to perform the perturbative calculations. From Eq. (B.11) one finds that the first order to be zero. The second order is though non-zero, and one finds two kinds of contributing terms. Looking at the definition of the second order correction

$$E^2 \equiv \sum_{k \neq GS} \frac{|\langle k| H^1 |GS\rangle|^2}{E_{GS}^0 - E_k^0} \tag{B.16}$$

The only $|k\rangle$ states which gives a none zero contribution are states of the kind $|k\rangle = \tau_{i,s}^{(\dagger)} |GS\rangle_\tau{}^2$. Lets take the case for $s = \{\uparrow, \downarrow\}$. For these states we say that a flux quanta has been introduced at site i, because if one acts on the state with $\boldsymbol{B}_i$ the eigenvalues will be ω or $\bar{\omega}$. When acting on $|k\rangle$ with H^1 it will yield a superposition of many states where only two states wont be orthogonal to $|GS\rangle_\tau$. These states are states where the flux quanta introduces in $|k\rangle$ leaves the system, and there is two possible ways. It will either exit at the same link as where it was introduced, or it will exit a the link opposite to it. To further explain this, one can see the operators $\tau_{i,\uparrow}$ and $\tau_{i,\downarrow}$ as operators moving a flux quanta downwards, while $\tau_{i,\uparrow}^\dagger$ and $\tau_{i,\downarrow}^\dagger$ moves it upwards. This is illustrated in Fig. B.3. Back to Eq. (B.18),
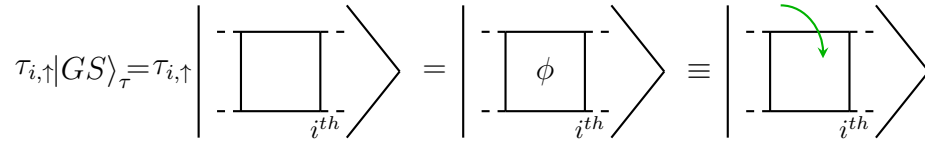
Figure B.3 | Schematic representation of the action of $\tau_{i,\uparrow}$ on $|GS\rangle_\tau$. This figure illustrates how $\tau_{i,\uparrow}$ adds a flux quanta to the i'th plaquette. The ground state is actually in a superposition of all possible excitement of the different plaquettes containing no flux quanta. Therefore one should see the state, after the first equal sign, as a superposition of all possible excitements. The state after the second equal sign is then a superposition of all possible excitement of the different plaquettes where the i'th plaquette contains a flux qunata, ϕ.

one can now take the case of $|k\rangle = \tau_{i,\uparrow} |GS\rangle_\tau$. When $H |k\rangle$ is put together with $\langle GS|_\tau$ the two non-zero terms will be the terms $\tau_{i,\uparrow}\tau_{i,\downarrow} |GS\rangle_\tau$ and $\tau_{i,\uparrow}\tau_{i,\uparrow}^\dagger |GS\rangle_\tau$, which are illustrated in Fig. B.4.
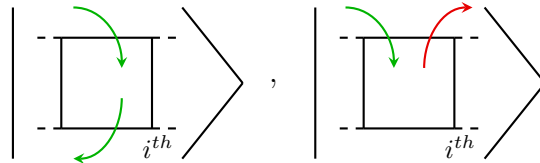
Figure B.4 | Schematic representation of the two non-zero contributions. As explained in Fig. B.3 these states represents superpositions. The green arrow illustrates a τ-operator while the red arrow illustrates a $\tau^\dagger$-operator. The contributing state to the left is denoted a non-trivial contribution, while the state on the right, where the flux enters and exits a the same link, is denoted trivial.

That the non-trivial term actually contributes, can also be seen from

$$\tau_{i,\uparrow}\tau_{i,\downarrow} |GS\rangle = \prod_{j=1}^{i} \boldsymbol{G}_{i,\uparrow}^\dagger \boldsymbol{G}_{i,\downarrow}^\dagger |GS\rangle = \begin{cases} \bar{\omega} |GS\rangle & \text{if } (i,\uparrow) \in \gamma(\bar{x}, \bar{y}) \\ |GS\rangle & \text{if } (i,\uparrow) \notin \gamma(\bar{x}, \bar{y}) \end{cases} \tag{B.17}$$

With $\gamma(\bar{x}, \bar{y})$ being the shortest path connecting the two charges, which in our case are both placed on the top leg, leg 1.

---

[2]One reason why $|k\rangle$ is a different then $|GS\rangle_\tau$ is that the two states will yield different results, if measuring the flux since B_i does not commute with $\tau_{i,s}$.

If instead $|k\rangle = \tau_{i,0}^{(\dagger)} |GS\rangle_\tau$, one realizes that this can only yield trivial contributions to this order. This is because $\tau_{i,0}^{(\dagger)}$ introduces a flux of ω in i'th plaquette and $\bar\omega$ in the (i-1)'th plaquette. So when H^1 acts on $|k\rangle$ it would need to remove two fluxes and it can only remove one. In the end, when calculating the correction, one needs to be careful about how some states are the same or proportional. How some state are alike can be seen from $\tau_{i,\uparrow}\tau_{i,\downarrow} = \prod_{j\leq i} \boldsymbol{G}j,\uparrow^\dagger \boldsymbol{G}j,\downarrow^\dagger$. From this one finds for a generic charge q

$$E^{(2)} = -g\frac{9L + 34 - 4R\left(1 - \cos\left(q\frac{2\pi}{N}\right)\right)}{2(1 - \cos\left(2\pi/N\right))} \tag{B.18}$$

where the constant of 34 comes from the non-trivial terms present at the boundaries. To this order one sees that it will cost energy to separate the two charges and the string tension will depend on the specific charge of the static charges. For $q = 1$ one finds $\Delta E = 2gR$, making the deconfining phase at $g \to 0$ unstable under this perturbation.

The third order contribution can contain terms of the kind $|k\rangle = \tau_{i,0}^{(\dagger)} |GS\rangle_\tau$ giving non-trivial contributions. Actually only non-trivial contributions will contribute to this order. One can see two of such contributions in Fig. B.5, which illustrates the journey of how a flux quanta enters and exits.
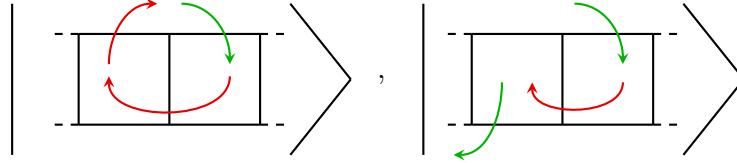
Figure B.5 | Schematic representation of the journey of the flux quanta. These figures represent two possible ways the state $|k\rangle = \tau_{i,0}^{(\dagger)} |GS\rangle_\tau$ can yield non-trivial contributions to third order in perturbation theory.

Appendix C

Dual transformation

This appendix presents a dual mapping, which maps the magnetic field into the electric field. The Hamiltonian considered is the one shown in Eq. (E.1), so the ladder geometry with both Higgs matter and gauge bosons presented in the unitary gauge.

As for the pure gauge theory we can look for a dual mapping, which turns the plaquette term, or the magnetic term, into the electric term. To define this mapping we therefore demand

$$\sigma_{i,0}^{\dagger}\sigma_{i,\uparrow}^{\dagger}\sigma_{i+1,0}\sigma_{i,\downarrow} \quad \longleftrightarrow \quad \tilde{\tau}_{\tilde{i},0} \tag{C.1}$$

where $\tilde{i}$ describes the position between i and $i+1$. Since a dual transformation has to conserve the commutation relations, we find that the dual transformation of $\tau_{i,0}$ must commute in the same way with $\tilde{\tau}_{\tilde{i},0}$ and $\tilde{\tau}_{\tilde{i}-1,0}$ as $\tau_{i,0}$ does with the i'th and (i-1)'th plaquette terms. This is upheld if

$$\tau_{i,0} \quad \longleftrightarrow \quad \tilde{\sigma}_{\tilde{i}-1,0}\tilde{\sigma}_{\tilde{i},0}^{\dagger} \quad , \quad i \neq 0 \tag{C.2}$$

Looking at $\tau_{i,\uparrow}$ and $\tau_{i,\downarrow}$, we also want them to obey the same commutation relations with the i'th plaquette terms. This could be secured by the dual transformation being $\tilde{\sigma}_{\tilde{i},0}$ and $\tilde{\sigma}_{\tilde{i},0}^{\dagger}$ respectively. This mapping would though not be a one-to-one mapping and it would not preserve the d.o.f. This is avoided by the mapping

$$\tau_{i,\uparrow} \quad \longleftrightarrow \quad \tilde{\sigma}_{\tilde{i},0}^{\dagger}\tilde{\sigma}_{\tilde{i},\uparrow}$$
$$\tau_{i,\downarrow} \quad \longleftrightarrow \quad \tilde{\sigma}_{\tilde{i},0}\tilde{\sigma}_{\tilde{i},\downarrow}^{\dagger} \tag{C.3}$$

which leads to

$$\tau_{i,\uparrow}^{\dagger}\tau_{i-1,\uparrow}\tau_{i,0} \quad \longleftrightarrow \quad \tilde{\sigma}_{\tilde{i},0}\tilde{\sigma}_{\tilde{i},\uparrow}^{\dagger}\tilde{\sigma}_{\tilde{i}-1,0}^{\dagger}\tilde{\sigma}_{\tilde{i}-1,\uparrow}\tilde{\sigma}_{\tilde{i}-1,0}\tilde{\sigma}_{\tilde{i},0}^{\dagger} = \tilde{\sigma}_{\tilde{i},\uparrow}^{\dagger}\tilde{\sigma}_{\tilde{i}-1,\uparrow}$$
$$\tau_{i,\downarrow}^{\dagger}\tau_{i-1,\downarrow}\tau_{i,0}^{\dagger} \quad \longleftrightarrow \quad \tilde{\sigma}_{\tilde{i},0}^{\dagger}\tilde{\sigma}_{\tilde{i},\downarrow}^{\dagger}\tilde{\sigma}_{\tilde{i}-1,0}\tilde{\sigma}_{\tilde{i}-1,\downarrow}\tilde{\sigma}_{\tilde{i}-1,0}^{\dagger}\tilde{\sigma}_{\tilde{i},0} = \tilde{\sigma}_{\tilde{i},\downarrow}\tilde{\sigma}_{\tilde{i}-1,\downarrow}^{\dagger} \tag{C.4}$$

Turning to the single $\sigma_{i,s}$, we again look at the rung and the legs separately. Starting with the legs and taking the case of $s = \uparrow$. The dual operators should have a non-zero commutation relation with the dual operators of $\tau_{i,\uparrow}$, $\tau_{i,\uparrow}^{\dagger}\tau_{i-1,\uparrow}\tau_{i,0}$ and $\tau_{i+1,\uparrow}^{\dagger}\tau_{i,\uparrow}\tau_{i+1,0}$. One finds the following mapping to obey the same commutation relations

$$\sigma_{i,\uparrow} \quad \longleftrightarrow \quad \tilde{\tau}_{\tilde{i},\uparrow}$$
$$\sigma_{i,\downarrow} \quad \longleftrightarrow \quad \tilde{\tau}_{\tilde{i},\downarrow}^{\dagger} \tag{C.5}$$

Before approaching $\sigma_{i,0}$, we need to worry about the boundary terms. For the τ operators acting on the boundary, $\tau_{0,0}$ and $\tau_{L+1,0}$, we find that the only commutation relations needed to be conserved

are with the first plaquette term along with the corresponding σ-operator. This leads to

$$\tau_{1,0} \longleftrightarrow \tilde{\sigma}_{1,0}^{\dagger} \tag{C.6}$$

$$\tau_{L,0} \longleftrightarrow \tilde{\sigma}_{L,0} \tag{C.7}$$

Actually Eq. (C.7) does not need $\tilde{\sigma}_{L+1,0}^{\dagger}$ to fulfill the commutation relations described above, but it will make sure, that later it will obey the same commutation relations with the dual of $\sigma_{L+1,0}$. With these mappings, the last line of Eq. (E.1) can now be mapped.

$$\tau_{1,\uparrow}^{\dagger}\tau_{1,0} \longleftrightarrow \tilde{\sigma}_{1,\uparrow}^{\dagger}$$

$$\tau_{L,\uparrow}\tau_{L+1,0} \longleftrightarrow \tilde{\sigma}_{L,\uparrow}\tilde{\sigma}_{L+1,0}^{\dagger}$$

$$\tau_{1,\downarrow}^{\dagger}\tau_{1,0}^{\dagger} \longleftrightarrow \tilde{\sigma}_{1,\downarrow}$$

$$\tau_{L,\downarrow}\tau_{L+1,0}^{\dagger} \longleftrightarrow \tilde{\sigma}_{L,\downarrow}^{\dagger}\tilde{\sigma}_{L+1,0} \tag{C.8}$$

Having done all these mappings, we are now in a position to express the mapping of the σ-operators on the rung. To find this mapping, one could look at Eq. (C.1). From looking at the mapping of Eq. (C.5), one finds the following mapping

$$\sigma_{i,0}^{\dagger}\sigma_{i+1,0} \longleftrightarrow \tilde{\tau}_{\tilde{i},0}\tilde{\tau}_{\tilde{i},\uparrow}\tilde{\tau}_{\tilde{i},\downarrow}^{\dagger} \tag{C.9}$$

Using this mapping as a recursion relation one finds

$$\sigma_{i,0} \longleftrightarrow \tilde{\tau}_{L+1,0}\prod_{j\geq i}^{L}\tilde{\tau}_{j,0}^{\dagger}\tilde{\tau}_{j,\uparrow}^{\dagger}\tilde{\tau}_{j,\downarrow} \quad , \quad \sigma_{L+1,0} \longleftrightarrow \tilde{\tau}_{L+1,0} \tag{C.10}$$

The dual mapping is now complete, and omitting the tilde we are left with the following Hamiltonian.

$$\tilde{\tilde{H}} = -g\left(\sum_{i=1}^{L}\sum_{j=1}^{2}(\sigma_{i,0}^{\dagger}\sigma_{i,s} + \text{h.c.}) + \sum_{i=1}^{L}(\sigma_{i,0}\sigma_{i+1,0}^{\dagger} + \text{h.c.})\right)$$

$$-(g(\sigma_{1,0} + \sigma_{1,0}^{\dagger}) - \frac{1}{\lambda}\sum_{j=1}^{2}(\sigma_{1,j} + \sigma_{1,j}^{\dagger}) - \sum_{i=1}^{L}\left(\frac{1}{g}(\tau_{i,0} + \tau_{i,0}^{\dagger}) + \lambda\sum_{j=1}^{2}(\tau_{i,s} + \tau_{i,s}^{\dagger})\right)$$

$$-\lambda\sum_{i}(\tau_{L+1,0}\prod_{j\geq i}^{L}\tau_{j,0}^{\dagger}\tau_{j,\uparrow}^{\dagger}\tau_{j,\downarrow} + \text{h.c.}) - \frac{1}{\lambda}\left(\sum_{j=1}^{2}\sum_{i=2}^{L-1}(\sigma_{i,s}\sigma_{i+1,j}^{\dagger} + \text{h.c.}) + (\sigma_{L,j}\sigma_{L+1,0}^{\dagger} + \text{h.c.})\right) \tag{C.11}$$

Except for the highly non-local term coming from Eq. (C.10), this Hamiltonian looks much similar to that of three legged N-clock model in a transverse field, and is depicted in Fig. C.1.
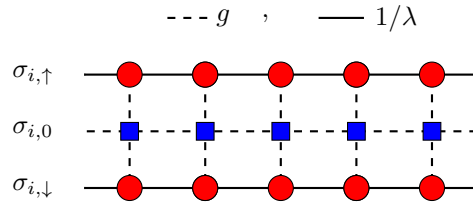
Figure C.1 | Schematic representation three legged system. This figure shows the system described by the Hamiltonian in Eq. (C.11), where the non-local term along with the boundary terms have been neglected. The dashed line represent a ferromagnetic coupling with strength g, while the full line represents a ferromagnetic coupling with strength $1/\lambda$. The legs on the side are experiencing a transverse field of the strength λ, while the center legs is experiencing a transverse field of strength $1/g$.

Appendix D

Showing the deconfined phase for the PLGT in 2D

By using the graphic representation of the different terms in perturbation theory presented in Appendix B, it is shown how the PLGT theory in 2D will support a deconfining phase in the limit of $g \ll 1$ as found in [24, 34].

In Appendix B one found the non-trivial term for $g \ll 1$, when a flux quanta jumped into the system only to leave it again. Having a 2D system yields other kinds of non-trivial terms then for the ladder geometry. For a 2D system a flux quanta cannot simply jump into the system and out again. Instead one can have non-trivial contributions where the flux quanta jumps around in some closed loop as depicted in Fig D.1. If defining the self energy of the charges to be $E_0(g)$, such that if the charges
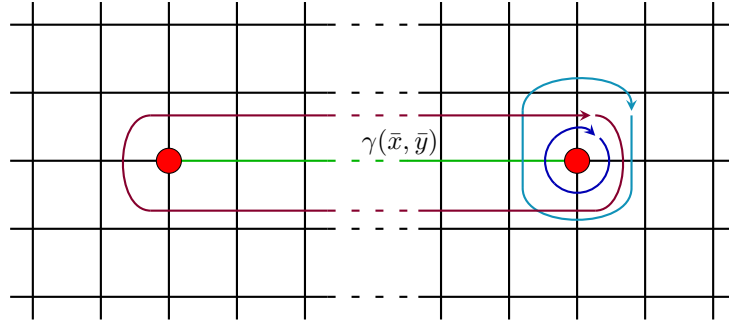
Figure D.1 | Perturbative terms. This figure illustrates different corrections to the energy. The dark blue circle illustrates a forth order non-trivial contribution. Here one finds a magnetic flux quanta jumping around the a charge. The light blue path illustrates a sixth order non-trivial contribution. The purple path illustrates a $2(R + 2)$'th order trivial contribution, which is a contribution which would no differ had the charges not been present.

are placed infinitely fare apart, one would find $\Delta E(R \to \infty) = 2E_0(g)$, where $\Delta E(R)$ is the difference between a system with no charges and one with a pair separated at a distance R. In perturbation theory, this self energy would arise from the non-trivial terms, where the path of the flux quanta encloses one of the charges[1]. If R is chosen to be finite, then at the $2(R + 2)$'th order in perturbation theory a flux quanta can travel around both the charges. This term will yield a contribution similar to having a flux quanta enclosing none of the charges. So choosing R to be finite yields a correction

---

[1] The non-trivial terms where two or more flux quantas encloses both charges are also a part of the self energy.

to ΔE, which can be expressed as

$$\Delta E(g) = 2E_0(g) + A(g)e^{-R/\xi(g)} \tag{D.1}$$

which is the same result as found in [34]. This shows how a true 2D system accommodates a deconfining phase for $g << 1$.

Appendix E

Degeneracy analysis with RR boundaries for $g \to 0$

In this appendix the degeneracy of the ground state manifold is investigated in the limit of $g \to 0$. This is done by choosing rough-rough boundaries, such that system in the unitary gauge is described by

$$\bar{H} = -\frac{1}{g} \sum_{i=0}^{L-1} (\sigma_{i,0}^\dagger \sigma_{i,\uparrow}^\dagger \sigma_{i+1,0} \sigma_{i,\downarrow} + \text{H.c.})$$

$$-\lambda \sum_{i,s=0,\uparrow,\downarrow} (\sigma_{i,s} + \sigma_{i,s}^\dagger) - \frac{1}{\lambda} \sum_{i=0}^{L+1} (\tau_{i,\uparrow}^\dagger \tau_{i-1,\uparrow} \tau_{i,0} + \tau_{i,\downarrow}^\dagger \tau_{i-1,\downarrow} \tau_{i,0}^\dagger + \text{H.c.}) \tag{E.1}$$

If taking the limit of $\lambda \to 0$ the Hamiltonian contains four symmetries generated by

$$\boldsymbol{S}_1 \equiv \prod_{i=-1}^{L} \sigma_{i,\uparrow}$$

$$\boldsymbol{S}_2 \equiv \tau_{i,\uparrow} \tau_{i,\downarrow} \quad \forall\ i$$

$$\boldsymbol{S}_3 \equiv \sigma_{0,\uparrow}^\dagger \sigma_{1,0} \sigma_{0,\downarrow}$$

$$\boldsymbol{S}_4 \equiv \sigma_{L,\uparrow}^\dagger \sigma_{L,0}^\dagger \sigma_{L,\downarrow} \tag{E.2}$$

All these symmetries commutes with the Hamiltonian and leave the ground state manifold N^3 times degenerate. To get rid of some of the degeneracy, we include the two incomplete plaquette terms in the Hamiltonian, similar boundary terms has been added in [32]. These terms are equivalent to $\boldsymbol{S}_3$ and $\boldsymbol{S}_4$, and the system is therefore left with a N times degeneracy. Choosing to express the ground state in the basis of $\boldsymbol{S}_1$ it becomes

$$||k\rangle\rangle_\tau \equiv \Pi_p (S_1)^k |0, 0, ..., 0\rangle_\tau = \Pi_p (S_1)^k ||0\rangle\rangle_\tau, \tag{E.3}$$

where Π_p is defined in Eq. (4.4.5). A valid thing to wonder is why $\boldsymbol{S}_1$ contains the σ-operators on the upper leg and not the lower. This was in fact an arbitrary choice, because the two symmetries are actually the same. If multiplying the $\boldsymbol{S}_1$ by all the plaquette terms including the unfinished one finds

$$\prod_p \boldsymbol{B}_p \boldsymbol{S}_1 = \prod_{i=0}^{L} \sigma_{i,\downarrow}. \tag{E.4}$$

Such that

$$||k\rangle\rangle_\tau = \Pi_p (\boldsymbol{S}_1)^k ||0\rangle\rangle_\tau = \Pi_p (\boldsymbol{B}_p)^k (\boldsymbol{S}_1)^k ||0\rangle\rangle_\tau = \Pi_p (\prod_{i=0}^{L} \sigma_{i,\downarrow})^k ||0\rangle\rangle_\tau . \tag{E.5}$$

If one where to turn on a small but finite g, so going along the bottom line of Fig. 4.2, one will find this degeneracy to immediately split, since $\tau_{i,\uparrow}$ does not commute with $\boldsymbol{S}_1$. If instead having $g \to 0$ and taking λ to be small but finite, so creating a perturbation of the kind $(\sigma_{i,s} + \sigma_{i,s}^\dagger)$, then the degeneracy will not split since the perturbation commutes with $\boldsymbol{S}_1$. This degeneracy will not split until the Lth order, where the perturbation will coupled the different $||k \pm 1 \mod N\rangle\rangle_\tau$ ground states. This means that the energy splitting is exponentially small and goes like $(\lambda)^L = e^{-L/\xi}$, which in the thermodynamic limit is zero. This indicates that the ground state manifold will stay degenerate until $\lambda \sim 1$, hinting that one does find a phase transition along this line. This degeneracy will though not be present for the other possible ways of constructing the boundaries, and this analysis is therefore too reliable on the boundary conditions to be trusted.

Appendix F

Static charges for $g \to 0$

This appendix will show how one obtains the result of $\Delta E = 0$ in the limit of $g \to 0$ in both the axial and unitary gauge.

Starting with the axial gauge. In this gauge the Hamiltonian takes the form presented in Eq. (4.3.1). If inserting the charges the Hamiltonian will not change, since the the electrical field terms of the legs, which would have carried the phases from the static charges, are eliminated by having $g \to 0$. This ultimately means that the ground state energy does not change by the charges being present, and one has $\Delta E = 0$ for all values of λ in this limit.

In the unitary gauge the Hamiltonian with the charges will state

$$\bar{H} = -\frac{1}{g} \sum_{i=0}^{L} (\sigma_{i,0}^\dagger \sigma_{i,\uparrow}^\dagger \sigma_{i+1,0} \sigma_{i,\downarrow} + \text{H.c.})$$

$$-\lambda \sum_{i,s} (\sigma_{i,s} + \sigma_{i,s}^\dagger) - \frac{1}{\lambda} \left(\sum_{i \neq \{x,y\}}^{L} (\tau_{i,\uparrow}^\dagger \tau_{i-1,\uparrow} \tau_{i,0} + \text{H.c.}) + \sum_{i=1}^{L} (\tau_{i,\downarrow}^\dagger \tau_{i-1,\downarrow} \tau_{i,0}^\dagger + \text{H.c.}) \right)$$

$$-\frac{1}{\lambda} (\omega^* \tau_{x,\uparrow} \tau_{x-1,\uparrow}^\dagger \tau_{x,0}^\dagger + \omega \tau_{y,\uparrow} \tau_{y-1,\uparrow}^\dagger \tau_{y,0}^\dagger + \text{H.c.})$$

$$-\frac{1}{\lambda} (\tau_{1,\uparrow}^\dagger \tau_{1,0} + \tau_{L,\uparrow} \tau_{L+1,0} + \tau_{1,\downarrow}^\dagger \tau_{1,0}^\dagger + \tau_{L,\downarrow} \tau_{L+1,0}^\dagger + \text{H.c.}) \tag{F.1}$$

But by using the unitary transformation given by

$$\mathcal{U} \equiv \bar{M}_{\Gamma(\bar{x},\bar{y})} \tag{F.2}$$

where $\bar{M}_{\Gamma(\bar{x},\bar{y})}$ is defined in Eq. (4.4.2), one can map the Hamiltonian into

$$H \to H' = \mathcal{U}^\dagger H \, \mathcal{U} =$$

$$-g \sum_{i,s=0,\uparrow,\downarrow} (\tau_{i,s} + \tau_{i,s}^\dagger) - \frac{1}{g} \sum_{i=0}^{L-1} (\sigma_{i,0}^\dagger \sigma_{i,\uparrow}^\dagger \sigma_{i+1,0} \sigma_{i,\downarrow} + \text{H.c.})$$

$$-\lambda \sum_{i,s=0,\uparrow,\downarrow} (\sigma_{i,s} + \sigma_{i,s}^\dagger) - \frac{1}{\lambda} \sum_{i=0}^{L} (\tau_{i,\uparrow}^\dagger \tau_{i-1,\uparrow} \tau_{i,0} + \tau_{i,\downarrow}^\dagger \tau_{i-1,\downarrow} \tau_{i,0}^\dagger + \text{H.c.})$$

$$-\frac{1}{\lambda} (\tau_{1,\uparrow}^\dagger \tau_{1,0} + \tau_{L,\uparrow} \tau_{L+1,0} + \tau_{1,\downarrow}^\dagger \tau_{1,0}^\dagger + \tau_{L,\downarrow} \tau_{L+1,0}^\dagger + \text{H.c.}) \tag{F.3}$$

which is the Hamiltonian for the system with no charges present. This means that the spectrum of the system with and without the charges are equivalent, and the ground state energies must therefore be the same, hence $\Delta E = 0$.

Appendix G

Bosonization of the PLGT

One could also try to apply the bosonization procedure to the Pure lattice gauge theory. Let us start of by doing this for the PLGT with smooth-rough boundary conditions and with out the unfinished plaquette term. In the axial gauge the Hamiltonian states

$$\underline{H} = -\frac{1}{g} \sum_{i=0}^{L-1} (\sigma_{i+1}^\dagger \sigma_i + \text{H.c.}) - g \sum_{i=0}^{L} (\tau_i + \tau_i^\dagger) - 2g \sum_{i=0}^{L} (\prod_{j \leq i} \tau_j + \prod_{j \leq i} \tau_j^\dagger). \tag{G.1}$$

which leads to

$$H = \int \frac{dx}{a} \left[a^2 \left(\frac{1}{K_g} (\partial_x \theta_g)^2 + K_g (\partial_x \phi_g)^2 \right) - M_{\theta,g} \cos (N\theta_g) - M_{\phi,g} \cos (N\phi_g) \right.$$
$$\left. -4g \cos (\phi_g) \right], \quad K_g \equiv g \tag{G.2}$$

Where the terms has the scaling dimensions shown in Tab. G.1.

Δ	Relevant for
$D_{\theta,g} = \frac{NK_g}{2}$	$K_g < \frac{4}{N}$
$D_{\phi,g} = \frac{N}{2K_g}$	$K > \frac{N}{4}$
$D_l = \frac{1}{2NK_g}$	$K_g > \frac{1}{4N}$

Table G.1| Scaling dimensions. In this table one can read how the different terms in Eq. (G.2) scale under an a first order RG procedure. D_l describes the scaling dimension of the last term in Eq. (G.2).

From the analysis of the descritized Hamiltonian we know that the system should be in a deconfining phase at the special point $g = 0$, but this phase is unstable and for a finite g the system will be in a deconfining phase. One would therefore suspect that turning on a finite g would cement itself by immediately making a term relevant that would kill this confined phase. Looking at Tab. G.1 one sees that by turning on a small g, the phase in the language of bosonization, does not change. Still one finds θ_g to be pinned it being N-times degenerate. What the bosonization does not seem to capture is that by turning on a finite g the degeneracy of the ground state will split, leaving no degeneracy left. Further more the bosonized description does not seem to capture that the deconfining phase is destroyed by turning on a finite g, since the renormalized Hamiltonian becomes

$$\underline{H}_{Re} = -\frac{1}{g} \sum_{i=0}^{L-1} \left(\sigma_i \sigma_{i+1}^\dagger + \text{H.c.} \right) \tag{G.3}$$

which will yield $\Delta E = 0$. This can be seen by going back to the gauge invariant description and inserting the two static charges. This leads to the ground state taking the two forms

$$\Pi_{x,y} \, ||n\rangle\rangle_\sigma \; , \quad n = 0, 1, 2, ...N - 1 \tag{G.4}$$

$$\Pi_p \, ||n; \gamma(x,y)\rangle\rangle_\tau \; , \quad n = 0, 1, 2, ...N - 1 \tag{G.5}$$

which both yields $\Delta E = 0$.

A way to deal with this problem is to incorporate the Higgs matter into the Hamiltonian and take the limit of $\lambda \to 0$. Still considering $g << 1$ the system will find itself in region $\boldsymbol{G}$ of the phase diagram shown in Fig. 6.6. In this region one finds $\cos{(N\theta_g)}$ and $\cos{(\phi_\rho \frac{N}{\sqrt{2}})} \cos{(\phi_\sigma \frac{N}{\sqrt{2}})}$ to be relevant. This will to first order constitute a deconfining phase, but to second order there will appear a term of the kind

$$\propto g^2 \cos{(\sqrt{2}\phi_\rho)} \tag{G.6}$$

which will destroy the deconfining phase, since it will lead discretized term looking like

$$\propto -g^2 \sum_{i=1}^{L} \left(\prod_{j>i} \eta_{j,\uparrow} \eta_{j,\downarrow} + \text{H.c.} \right) \tag{G.7}$$

if one inserts charges then this term takes the form

$$\propto -g^2 \left[\sum_{i \notin (\bar{x}, \bar{y})} \left(\prod_{j>i} \eta_{j,\uparrow} \eta_{j,\downarrow} + \text{H.c.} \right) + \sum_{i \in (\bar{x}, \bar{y})} \left(\omega \prod_{j>i} \eta_{j,\uparrow} \eta_{j,\downarrow} + \text{H.c.} \right) \right] \tag{G.8}$$

since the all the Higgs matter sites due to $\lambda \to 0$ are locked in $|0\rangle_\tau$, this will leave a string tension which depends linearly on R.

So by incorporating the Higgs matter one finds that this phase will actually to be confining, but the ground state is still degenerate which should not be for a finite g.

Another angle one can attack the problem by is going to the dual representation. If again not including the unfinished plaquette term one finds

$$\underline{\tilde{\text{H}}} = -\frac{1}{g} \sum_{i=0}^{L-1} (\tau_i + \tau_i^\dagger) - g \sum_{i=0}^{L-1} (\sigma_i \sigma_{i+1}^\dagger + \text{H.c.}) - 2g \sum_{i=0}^{L} (\sigma_i + \sigma_i^\dagger) - g(\sigma_1 + \sigma_1^\dagger) \tag{G.9}$$

where one can neglected the last boundary term since it will not influence the bulk properties in the thermodynamical limit. Here one sees that the degeneracy of the non-dual Hamiltonian in the limit of $g \to 0$ is not described by a global symmetry but instead it has been projected onto the boundary. The symmetry is now represented by $[\sigma_L, \underline{\tilde{\text{H}}}] = 0$. The bosonized description is

$$\underline{\tilde{\text{H}}} = \int \frac{dx}{a} \left(a^2 (\frac{1}{\tilde{K}_g} (\partial_x \tilde{\theta}_g)^2 + \tilde{K}_g (\partial_x \tilde{\phi}_g)^2) - M_{\theta,g} \cos{(N\tilde{\theta}_g)} - M_{\phi,g} \cos{(N\tilde{\phi}_g)} \right.$$

$$\left. -4g \cos{(\tilde{\theta}_g)} \right) , \quad \tilde{K}_g \equiv \frac{1}{g} \tag{G.10}$$

where the scaling dimensions are shown in Tab. G.2. Again the problem arises, but here it is to some degree more clearly to see the problem. If taking $g = 0$ one should still have the ground state being N-times degenerate with the ground state being

$$\bigotimes_{i=0}^{L-1} |0\rangle_i^\tau \otimes |n\rangle_L^\tau \; , \quad n = 0, 1, 2, ..., N - 1 \tag{G.11}$$

Δ	Relevant for
$D_\theta = \frac{N\tilde{K}_g}{2}$	$\tilde{K}_g < \frac{4}{N}$
$D_\phi = \frac{N}{2\tilde{K}_g}$	$\tilde{K}_g > \frac{N}{4}$
$D_l = \frac{\tilde{K}_g}{2N}$	$\tilde{K}_g < 4N$

Table G.2| Scaling dimensions. In this table one can read how the different terms in Eq. (G.10) scales under an a first order RG procedure. D_l describes the scaling dimension of the last term in Eq. (G.10).

This feature along with the degeneracy being split when turning on a finite g is again not captured. In this description the root of the problem is though more exposed, because how can we ask of the continuous description to capture a boundary symmetry? The remedy to this degeneracy problem can be found in incorporating the unfinished plaquette term

$$-\frac{1}{g}\left(\sigma_{L,0}^\dagger \sigma_{L,\uparrow}^\dagger \sigma_{L,\downarrow} + \text{H.C.}\right) \tag{G.12}$$

Which in the axial gauge becomes the single $\sigma_{L,0}$ term of the rung. This will break the degeneracy, and for the dual description this extra term leads to

$$-\frac{1}{g}\sum_{i=0}^{L-1}(\tau_i + \tau_i^\dagger) \rightarrow -\frac{1}{g}\sum_{i=0}^{L}(\tau_i + \tau_i^\dagger) \tag{G.13}$$

such that no boundary symmetry is present, and the continuous Hamiltonian in Eq. (G.10) will more correctly describe the discretized system, by giving the correct ground states in the two extremes of g. In the non-dual continuous description shown in Eq. (G.2), one will instead find a "$-1/g\cos(\theta_g(L))$"-term appearing, which will as well kill the degeneracy.

Going back to the dual description, one sees that there should occur a phase transition at $D_l = D_\phi$, where the system changes between wanting to pin the θ and the ϕ field. For $N = 2$, which corresponds to the Ising model with both a longitudinal and transverse field, we know that no phase transition should occur. Looking in Tab. G.2 one though sees that D_l will always be more relevant than D_θ. This kills the degeneracy and makes the ground state $||0\rangle\rangle_\sigma$ for $\tilde{K}_g < N$. For $\tilde{K}_g > N$ one instead finds the ground state to be $||0\rangle\rangle_\tau$. Since these operators could as well describe spins, one could imagine applying a magnetic field and adiabatically rotate the longitudinal field into the transverse field and vice versa. These two phases should therefore be adiabatically connected, and no phase transitions is expected.

To conclude, if the bosonized description is to be able to correctly capture the physics of the system, one needs to do two things. Firstly one needs to incorporate the Higgs matter into the Hamiltonian and then take the limit of $\lambda \to 0$ which increases the mass of the Higgs matter to infinity. This will yield a string tension that is linear in R when turning on a finite g. Next one needs to incorporate the unfinished plaquette term to kill the degeneracy since the bosonized description cannot capture how the $\cos(\phi_g)$-term couples the degenerate ground states and ultimately kills the degeneracy.

Appendix H

Making sense of the ϕ symmetry

The symmetries of the different fields can have different physical meaning. Having the Hamiltonian being invariant when taking $\theta_{1,\downarrow} \to \theta_{1,\downarrow} + 2\pi/N$ leads to a degenerate grounds state. The symmetry of the ϕ fields is obscured by it being the dual field of θ and not the conjugated field. For example will having $\phi_{1,\downarrow} \to \phi_{1,\downarrow} + 2\pi/N$ does not lead to any degeneracy, but the symmetry can still have a physical meaning, and this is what is being investigated in this appendix.

Let us start by investigating the deconfining phase in the bosonized description. The two static charges are inserted at $(0,\uparrow)$ and $(L,\uparrow)$ with the opposite charge. The two gauge generators at those positions will act differently on the physical states than the other generators.

$$\boldsymbol{G}_{0,\uparrow} \ket{\psi_{phys}} = \omega^* \ket{\psi_{phys}} \quad , \quad \boldsymbol{G}_{L,\uparrow} \ket{\psi_{phys}} = \omega \ket{\psi_{phys}}$$
$$\boldsymbol{G}_{r,\uparrow} \ket{\psi_{phys}} = \ket{\psi_{phys}} \quad , \text{ for } r \neq 0, L$$
$$\boldsymbol{G}_{r,\downarrow} \ket{\psi_{phys}} = \ket{\psi_{phys}} \quad , \, \forall \, r \tag{H.1}$$

With this constrain, the Hamilton in the axial gauge with SR boundaries become

$$\underline{\mathrm{H}} = -\frac{1}{g} \sum_{i=0}^{L-1} (\sigma_i^\dagger \sigma_{i+1} + \text{h.c.}) - g \left(\sum_{i=0}^{L} \left(\omega \prod_{j \leq i}^{L} \tau_j^\dagger \eta_{j,\uparrow}^\dagger + \right. \right.$$
$$\left. \prod_{j \leq i}^{L+1} \tau_j \eta_{j,\downarrow}^\dagger + \text{h.c.} \right) + \sum_{i=0}^{L} (\tau_i + \tau_i^\dagger) \right) - \frac{1}{\lambda} \sum_{i=1}^{L} \sum_{s=\uparrow,\downarrow} (\eta_{i,s} + \eta_{i,s}^\dagger) -$$
$$\lambda \left(\sum_{i=0}^{L-1} \sum_{s=\uparrow,\downarrow} \left(\zeta_{i,s}^\dagger \zeta_{i+1,s} + \text{H.c} \right) + \sum_{i=0}^{L} (\zeta_{i,\uparrow}^\dagger \sigma_i \zeta_{i,\downarrow} + h.c) \right) \tag{H.2}$$

Following the bosonization procedure one finds

$$\underline{\mathrm{H}} = \int \frac{dx}{a} \left[\sum_{s=\uparrow,\downarrow,0} \left(a^2 \left(\frac{1}{K_s} (\partial_x \theta_s)^2 + K_s (\partial_x \phi_s)^2 \right) - M_{\theta,s} \cos(N\theta_s) - M_{\phi,s} \cos(N\phi_s) \right) - \right.$$
$$\left. -2\lambda \cos(\theta_\uparrow - \theta_\downarrow - \theta_0) - 2g \left(\cos(\phi_\uparrow + \phi_0 + \frac{2\pi}{N}) + \cos(\phi_\downarrow - \phi_0) \right) \right] \tag{H.3}$$

Comparing this Hamiltonian to the one of Eq. (6.0.8), one sees that inserting two static charges like this will correspond to $\phi_\uparrow \to \phi_\uparrow + 2\pi/N$. What one can gain from this comparison is that if the Hamiltonian is invariant under $\phi_s \to \phi_s + 2\pi/N$ then the dynamics of the system will be as if no charges where present. Before moving on, lets see how inserting these charges will translate the ϕ_ρ

104

and ϕ_σ fields. In the case described by Eq. (H.1), the Hamiltonian in terms of these fields become

$$
\begin{aligned}
\underline{H} = \int \frac{dx}{a} \Bigg[&\sum_{s=\sigma,\rho,g} a^2 \left(\frac{1}{K_s} (\partial_x \theta_s)^2 + K_s (\partial_x \phi_s)^2 \right) - M_{\theta,g} \cos{(N\theta_g)} - M_{\phi,g} \cos{(N\phi_g)} - \\
&2M_\theta \cos{(\frac{N}{\sqrt{2}} \theta_\rho)} \cos{(\frac{N}{\sqrt{2}} \theta_\sigma)} - 2M_\phi \cos{(\frac{N}{\sqrt{2}} \phi_\rho)} \cos{(\frac{N}{\sqrt{2}} \phi_\sigma)} - 2\lambda \cos{(\sqrt{2}\theta_\sigma - \theta_g)} \\
&\qquad\qquad\qquad\qquad -4g \cos{(\frac{\phi_\rho}{\sqrt{2}} + \frac{\pi}{N})} \cos{(\frac{\phi_\sigma}{\sqrt{2}} + \phi_g + \frac{\pi}{N})} \Bigg]
\end{aligned} \tag{H.4}
$$

such that one would need to translate both fields simultaneously, in order for the extra phase to cancel. This could be done by

$$
\phi_\rho \to \phi_\rho - \frac{\sqrt{2}\pi}{N}
$$
$$
\phi_\sigma \to \phi_\sigma - \frac{\sqrt{2}\pi}{N} \tag{H.5}
$$

To determine the characteristics of the deconfining phase, lets investigate the point where $g = 0$ and $\lambda \ll 1$ see what happens when turning on a small g.

For $g = 0$ one finds $\phi_{\rho,\sigma}$ and θ_g to be pinned along with system being invariant under the translation shown in Eq. (H.5). This means that in this limit inserting two charges will not change the Hamiltonian of the system and dynamics along with the energy will therefore be the same. This is in agreement with result from perturbation theory, which also showed this to be a deconfining phase.

If now turning on a small g, which in the limit of $\lambda \to 0$ will lead to the system being in a confined phase, the system will still pin the same fields. If only considering the first order terms the system will still contain the translational symmetry described by Eq. (H.5), but the second order terms will not. Having a finite g will lead to a second order term looking like

$$
H = \int \mathrm{d}x... + G' \cos{(\sqrt{2}\phi_\rho)} \tag{H.6}
$$

as shown in Eq. (6.1.6) where $G' \propto (g')^2$ and g' describing the renormalized parameter. This comes from the electric field of the legs. This second order term will break the translation symmetry which will lead to expecting the energy of the system being different when inserting two static charges. This means that in region $\boldsymbol{G}$, the system is expected to be deconfined for $g = 0$ while for finite g it is expected to be in a confined phase.

Let us further investigate the case of region $\boldsymbol{G}$ by translating the renormalized bosonized Hamiltonian back to the discretized Hamiltonian, in order to establish the confined behavior for $g > 0$. If we in this region initiate the initial RG flow, we will as previously explained find $\phi_{\rho,\sigma}$ and θ_g pinned. Having θ_g pinned will lead to electric term of the legs being killed to first order, but there will be a second order contribution as shown in Eq. (H.6). This term breaks the translational symmetry of the ϕ-fields and leads to the following term in the discretized Hamiltonian

$$
\underline{H}' = -\frac{1}{K_g'} \sum_i \left(\sigma_i \sigma_{i+1}^\dagger + \text{H.c.} \right) - \sum_{i=0}^{L} \sum_{s=\uparrow,\downarrow} K_s' \left(\eta_i + \eta_i^\dagger \right) - G' \sum_{i=0}^{L} \left(\prod_{j \le i} \eta_{j,\downarrow} \eta_{j,\uparrow} + \text{H.c} \right) \tag{H.7}
$$

Where G' will be a small parameter since under the initial flow the electric field term of the legs is irrelevant. Now by realizing that the last terms is a second order term coming from the electric field term of the legs, one will end up with the following Hamiltonian by inserting the two static charges at

$\bar{x}$ and $\bar{y}$

$$\underline{\mathrm{H}} = -\frac{1}{K_g'} \sum_i \left(\sigma_i \sigma_{i+1}^\dagger + \mathrm{H.c.} \right) - \sum_{i=0}^{L} \sum_{s=\uparrow,\downarrow} K_s' \left(\eta_i + \eta_i^\dagger \right) - G' \sum_{i \notin \gamma(\bar{x},\bar{y})} \left(\prod_{j \leq i} \eta_{j,\downarrow} \eta_{j,\uparrow} + \mathrm{H.c} \right)$$

$$- G' \sum_{i \in \gamma(\bar{x},\bar{y})} \left(\omega \prod_{j \leq i} \eta_{j,\downarrow} \eta_{j,\uparrow} + \mathrm{H.c} \right) \qquad \text{(H.8)}$$

Where γ describes the direct path between the two static charges in the top leg. Having the distance between the two charges to be of length R, there will in the last summation be R terms.

Since G' is a small parameter, one can see this as a perturbation. Since the gauge bosons decouples from the Higgs matter these can be neglected. For the Higgs matter the ground state to the zeroth order becomes $||0\rangle\rangle_\tau$. Taking the perturbation into account, one finds that to first order there will be a correction to the energy due to the static charges. This correction will be linear in R. If one defines ΔE as the difference in energy between having the two static charges and not, then one finds

$$\Delta E = 2G' \left(1 - \cos\left(\frac{2\pi}{N} \right) \right) R \qquad \text{(H.9)}$$

Since $G' \propto (g')^2$ one finds that when turning on a finite g this second order term will make the region $\boldsymbol{G}$ a confined phase instead of the deconfined phase at $g = 0$. With this symmetry argument one can therefore talk about the line for $g = 0$ being a special line, where the translational symmetry of the ϕ-fields is present and the system is therefore in a deconfined phase.

Appendix I

Second order RG flow equations

Here the second order RG flow equations found by *Michele Burrello* for Eq. (6.3.31) are stated.

$$\frac{\mathrm{d}P}{\mathrm{d}l} = \left[2 - \frac{N}{4}\left(K_\rho + K_\sigma\right)\right]P \tag{I.1}$$

$$\frac{\mathrm{d}Q}{\mathrm{d}l} = \left[2 - \frac{N}{4}\left(\frac{1}{K_\rho} + \frac{1}{K_\sigma}\right)\right]Q \tag{I.2}$$

$$\frac{\mathrm{d}P_0}{\mathrm{d}l} = \left[2 - \frac{NK_0}{2}\right]P_0 \tag{I.3}$$

$$\frac{\mathrm{d}Q_0}{\mathrm{d}l} = \left[2 - \frac{N}{2K_0}\right]Q_0 \tag{I.4}$$

$$\frac{\mathrm{d}T}{\mathrm{d}l} = \left(2 - \frac{K_\sigma}{N} - \frac{K_0}{2N}\right)T \tag{I.5}$$

$$\frac{\mathrm{d}G}{\mathrm{d}l} = \left(2 - D_g\right)G - \frac{C'_\rho Ga^2}{4NK_\rho v} - \frac{C'_\sigma Ga^2}{4Nv}\left(\frac{1}{K_\sigma} + \frac{2}{K_0}\right) \tag{I.6}$$

$$\frac{\mathrm{d}C_\rho}{\mathrm{d}l} = \left(2 - 2\frac{N}{K_\rho}\right)C_\rho + \frac{Q^2a^2}{v}\left(\frac{N}{4K_\rho} - \frac{N}{4K_\sigma}\right) \tag{I.7}$$

$$\frac{\mathrm{d}C_\sigma}{\mathrm{d}l} = \left(2 - 2\frac{N}{K_\sigma}\right)C_\sigma - \frac{Q^2a^2}{v}\left(\frac{N}{4K_\rho} - \frac{N}{4K_\sigma}\right) \tag{I.8}$$

$$\frac{\mathrm{d}C'_\rho}{\mathrm{d}l} = \left(2 - \frac{1}{K_\rho N}\right)C'_\rho + \frac{G^2a^2}{4Nv}\left[\frac{1}{K_\rho} - \frac{1}{K_\sigma} - \frac{2}{K_0}\right] \tag{I.9}$$

$$\frac{\mathrm{d}C'_\sigma}{\mathrm{d}l} = \left(2 - \frac{1}{K_\sigma N} - \frac{2}{NK_0}\right)C'_\sigma - \frac{G^2a^2}{4Nv}\left[\frac{1}{K_\rho} - \frac{1}{K_\sigma} - \frac{2}{K_0}\right] - \tag{I.10}$$

$$\frac{\mathrm{d}K_\rho}{\mathrm{d}l} = -\frac{\pi N^2 P^2 a^4 K_\rho^2 \left(K_\sigma + K_\rho\right)}{4v^2} + \frac{\pi N^2 Q^2 a^4}{4v^2}\left(\frac{1}{K_\sigma} + \frac{1}{K_\rho}\right)$$

$$+ \frac{8\pi N^2 C_\rho^2 a^4}{4v^2 K_\rho} + \frac{2\pi C'^2_\rho a^4}{N^2 v^2 K_\rho} + \frac{\pi G^2 a^4}{4N^2 v^2}\left[\frac{1}{K_\rho} + \frac{1}{K_\sigma} + \frac{2}{K_0}\right] \tag{I.11}$$

$$\frac{\mathrm{d}K_\sigma}{\mathrm{d}l} = -\frac{\pi N^2 P^2 a^4 K_\sigma^2 \left(K_\sigma + K_\rho\right)}{4v^2} + \frac{\pi N^2 Q^2 a^4}{4v^2}\left(\frac{1}{K_\sigma} + \frac{1}{K_\rho}\right) + \frac{2\pi N^2 C_\sigma^2 a^4}{v^2 K_\sigma}$$

$$-\frac{2\pi T^2 a^4 K_\sigma^2}{N^2 v^2}\left(K_\sigma + \frac{K_0}{2}\right) + \frac{2\pi C'^2_\sigma a^4}{N^2 v^2}\left(\frac{1}{K_\sigma} + \frac{1}{K_0}\right) + \frac{\pi G^2 a^4}{4N^2 v^2}\left[\frac{1}{K_\rho} + \frac{1}{K_\sigma} + \frac{2}{K_0}\right] \tag{I.12}$$

$$\frac{\mathrm{d}K_0}{\mathrm{d}l} = \frac{\pi N^2 Q_0^2 a^4}{v^2 K_0} - \frac{\pi N^2 P_0^2 a^4 K_0^3}{v^2}$$

$$-\frac{\pi T^2 a^4 K_0^2}{N^2 v^2}\left(K_\sigma + \frac{K_0}{2}\right) + \frac{2\pi C'^2_\sigma a^4}{N^2 v^2}\left(\frac{1}{K_\sigma} + \frac{2}{K_0}\right) + \frac{\pi G^2 a^4}{2N^2 v^2}\left[\frac{1}{K_\rho} + \frac{1}{K_\sigma} + \frac{2}{K_0}\right] \tag{I.13}$$

Appendix J

Second order RG for $g = 0$ in real space

In this appendix one finds second second order RG calculations performed using the real space approach. In the main text this was done primarily by following [52], in this section [54] will instead be follow. These calculations will also be explicit shown for the ϕ BGI term. Again we have

$$S_0 = \int \mathrm{d}^2x \left[\frac{K_\sigma}{2\pi} \left(\frac{(\partial_\tau \theta_\sigma)^2}{v} + v(\partial_x \theta_\sigma)^2 \right) + \frac{K_\rho}{2\pi} \left(\frac{(\partial_t \theta_\rho)^2}{v} + v(\partial_x \theta_\rho)^2 \right) \right] \tag{J.1}$$

$$S_1 = \int \mathrm{d}^2x \left[2m_\theta \cos\left(\frac{N}{\sqrt{2}}\theta_\rho\right) \cos\left(\frac{N}{\sqrt{2}}\theta_\sigma\right) \right.$$
$$\left. + 2m_\phi \cos\left(\frac{N}{\sqrt{2}}\phi_\rho\right) \cos\left(\frac{N}{\sqrt{2}}\phi_\sigma\right) + \frac{2\lambda}{a} \cos\left(\sqrt{2}\theta_\sigma\right) \right] \tag{J.2}$$

Where as shown previously the first order terms all yields zero, so we go directly to the second order contribution

$$\frac{1}{2} \left\langle \prod_{s=\sigma,\rho} e^{-i\phi_s(x_1)} e^{i\phi_s(x_2)} S_1^2 \right\rangle_0 =$$

$$\frac{1}{2}(2m_\phi)^2 \frac{1}{2^4} 4 \int \mathrm{d}^2x_3 \mathrm{d}^2x_4 \prod_{s=\sigma,\rho} \left(\left\langle e^{-i\phi_s(x_1)} e^{i\phi_s(x_2)} e^{-i\frac{N}{\sqrt{2}}\phi_s(x_3)} e^{i\frac{N}{\sqrt{2}}\phi_s(x_4)} \right\rangle_0 + \right.$$
$$\left. \left\langle e^{-i\phi_s(x_1)} e^{i\phi_s(x_2)} e^{i\frac{N}{\sqrt{2}}\phi_s(x_3)} e^{i\frac{N}{\sqrt{2}}\phi_s(x_4)} \right\rangle_0 \right) \tag{J.3}$$

The four in front accounts for the multiplicity coming from having $e^{-i\phi_i(x_3)} e^{-i\phi_i(x_4)}$ contributing the same as $e^{i\phi_i(x_3)} e^{i\phi_i(x_4)}$ and $e^{-i\phi_i(x_3)} e^{i\phi_i(x_4)}$ contributing the same as $e^{i\phi_i(x_3)} e^{-i\phi_i(x_4)}$. This leads to

$$\frac{m_\phi^2}{2} \int \mathrm{d}^2x_3 \mathrm{d}^2x_4 \prod_{s=\sigma,\rho} \left(e^{\frac{-1}{2}\left\langle \left(-\phi_s(x_1)+\phi_s(x_2)-\frac{N}{\sqrt{2}}\phi_s(x_3)+\frac{N}{\sqrt{2}}\phi_s(x_4) \right)^2 \right\rangle_0} + \right.$$
$$\left. e^{\frac{-1}{2}\left\langle \left(-\phi_s(x_1)+\phi_s(x_2)+\frac{N}{\sqrt{2}}\phi_s(x_3)+\frac{N}{\sqrt{2}}\phi_s(x_4) \right)^2 \right\rangle_0} \right) \tag{J.4}$$

Since the second part is not invariant under a translation of the ϕ-fields it will be zero and we are left with

$$\frac{m_\phi^2}{2} \int \mathrm{d}^2x_3 \mathrm{d}^2x_4 \prod_{s=\sigma,\rho} e^{\frac{-1}{2}\left\langle \left(-\phi_s(x_1)+\phi_s(x_2)-\frac{N}{\sqrt{2}}\phi_s(x_3)+\frac{N}{\sqrt{2}}\phi_s(x_4) \right)^2 \right\rangle_0} \tag{J.5}$$

If one again had not taking $L \to \infty$ then the otherwise neglected terms would again yield a contribution which was not translational invariant and proportional to $1/L$. Moving on this leads to

$$\frac{m_\phi^2}{2} \int d^2 x_3 d^2 x_4 \prod_{s=\sigma,\rho} \exp \left(- \left((1 + \frac{N^2}{2}) \langle \phi_s^2 \rangle_0 - \langle \phi_s(x_1) \phi_s(x_2) \rangle_0 + \frac{N}{\sqrt{2}} \langle \phi_s(x_1) \phi_s(x_3) \rangle_0 - \right. \right.$$

$$\left. \left. \frac{N}{\sqrt{2}} \langle \phi_s(x_1) \phi_s(x_4) \rangle_0 - \frac{N}{\sqrt{2}} \langle \phi_s(x_2) \phi_s(x_3) \rangle_0 + \frac{N}{\sqrt{2}} \langle \phi_s(x_2) \phi_s(x_4) \rangle_0 - \frac{N^2}{2} \langle \phi_s(x_3) \phi_s(x_4) \rangle_0 \right) \right) \quad \text{(J.6)}$$

Using the same notation as previously this can be rewritten into

$$\frac{m_\phi^2}{2} \int d^2 x_3 d^2 x_4 \prod_{s=\sigma,\rho} \left(\frac{a}{|\mathbf{z}_{1,2}|} \right)^{\frac{1}{K_s N}} \left(\frac{|\mathbf{z}_{1,3}||\mathbf{z}_{2,4}|}{|\mathbf{z}_{1,4}||\mathbf{z}_{2,3}|} \right)^{\frac{1}{\sqrt{2}K_s}} \left(\frac{a}{|\mathbf{z}_{3,4}|} \right)^{\frac{N}{2K_s}} \quad \text{(J.7)}$$

To handle this integral it is useful to change the coordinates as

$$\mathbf{r} \equiv \mathbf{r}_4 - \mathbf{r}_3 , \quad \mathbf{R} \equiv \frac{1}{2} (\mathbf{r}_4 + \mathbf{r}_3) , \quad \text{where} \quad \mathbf{r}_i \equiv v \tau_i \hat{x} + x_i \hat{y} \quad \text{(J.8)}$$

Inserting this yields

$$\frac{m_\phi^2}{2v^2} \left(\frac{a}{|\mathbf{z}_{1,2}|} \right)^{\frac{1}{K_\rho N} + \frac{1}{K_\sigma N}} \int d^2 \mathbf{R} d^2 \mathbf{r} \left(\frac{|\mathbf{R} - (1/2)\mathbf{r} - \mathbf{r}_1||\mathbf{R} + (1/2)\mathbf{r} - \mathbf{r}_2|}{|\mathbf{R} + (1/2)\mathbf{r} - \mathbf{r}_1||\mathbf{R} - (1/2)\mathbf{r} - \mathbf{r}_2|} \right)^{\frac{1}{\sqrt{2}K_\rho} + \frac{1}{\sqrt{2}K_\sigma}} \left(\frac{a}{|\mathbf{r}|} \right)^{\frac{N}{2K_\rho} + \frac{N}{2K_\sigma}} \quad \text{(J.9)}$$

Now further a head in these calculation we would like to integrate out $|\mathbf{r}| \in [a, ab]$ and the rest of the $\mathbf{r}$ integral will be left untouched. The part we care about is therefore the small $|\mathbf{r}|$ part and therefore integrand is expanded around $|\mathbf{r}| = 0$. This is done by going to polar coordinates for the $\mathbf{r}$ integral, such that one can look at the following

$$\int_0^{2\pi} d\theta \left(\frac{|\mathbf{R} - (1/2)\mathbf{r} - \mathbf{r}_1||\mathbf{R} + (1/2)\mathbf{r} - \mathbf{r}_2|}{|\mathbf{R} + (1/2)\mathbf{r} - \mathbf{r}_1||\mathbf{R} - (1/2)\mathbf{r} - \mathbf{r}_2|} \right)^{\frac{1}{\sqrt{2}K_\rho} + \frac{1}{\sqrt{2}K_\sigma}} \approx$$

$$2\pi + r^2 \frac{\pi}{2} \left(\frac{1}{\sqrt{2}K_\rho} + \frac{1}{\sqrt{2}K_\sigma} \right)^2 \frac{\left(|\mathbf{R} - \mathbf{r}_1|^2 + |\mathbf{R} - \mathbf{r}_2|^2 - 2(\mathbf{R} - \mathbf{r}_1) \cdot (\mathbf{R} - \mathbf{r}_2) \right)}{|\mathbf{R} - \mathbf{r}_1|^2 |\mathbf{R} - \mathbf{r}_2|^2} \quad \text{(J.10)}$$

Where θ here is the angle of the $\mathbf{r}$ integral. The constant term along with the two first terms in the fraction is what is denoted disconnected pieces in [54, 63] and will be eliminated by

$$\frac{1}{2} \left\langle \prod_{s=\sigma,\rho} e^{-i\phi_s(x_1)} e^{i\phi_s(x_2)} \right\rangle_0 \langle S_1^2 \rangle_0 \quad \text{(J.11)}$$

This leads to

$$\int_0^{2\pi} d\theta \left(\frac{|\mathbf{R} - (1/2)\mathbf{r} - \mathbf{r}_1||\mathbf{R} + (1/2)\mathbf{r} - \mathbf{r}_2|}{|\mathbf{R} + (1/2)\mathbf{r} - \mathbf{r}_1||\mathbf{R} - (1/2)\mathbf{r} - \mathbf{r}_2|} \right)^{\frac{1}{\sqrt{2}K_\rho} + \frac{1}{\sqrt{2}K_\sigma}} =$$

$$-r^2 \frac{\pi}{2} \left(\frac{1}{K_\rho} + \frac{1}{K_\sigma} \right)^2 \frac{(\mathbf{R} - \mathbf{r}_1) \cdot (\mathbf{R} - \mathbf{r}_2)}{|\mathbf{R} - \mathbf{r}_1|^2 |\mathbf{R} - \mathbf{r}_2|^2} + \text{disconnected pieces} \quad \text{(J.12)}$$

Utilizing

$$\frac{\mathbf{R} - \mathbf{r}_j}{|\mathbf{R} - \mathbf{r}_j|^2} = \nabla_{\mathbf{R}} \ln \left(\frac{|\mathbf{R} - \mathbf{r}_j|}{a} \right) \quad \text{(J.13)}$$

leaves us with

$$-\pi \left(\frac{m_\phi}{2v}\right)^2 \left(\frac{1}{K_\rho} + \frac{1}{K_\sigma}\right)^2 \left(\frac{a}{|\mathbf{z}_{1,2}|}\right)^{\frac{1}{K_\rho N}} \int d^2\mathbf{R} \nabla_\mathbf{R} \ln\left(\frac{|\mathbf{R} - \mathbf{r}_1|}{a}\right) \cdot \nabla_\mathbf{R} \ln\left(\frac{|\mathbf{R} - \mathbf{r}_2|}{a}\right)$$
$$\int dr \left(\frac{a}{r}\right)^{\frac{N}{2K_\rho} + \frac{N}{2K_\sigma}} r^3 \qquad (J.14)$$

For the $\mathbf{R}$ integral an integration by part is performed where the surface term is neglected.

$$\pi \left(\frac{m_\phi}{2v}\right)^2 \left(\frac{1}{K_\rho} + \frac{1}{K_\rho}\right)^2 \left(\frac{a}{|\mathbf{z}_{1,2}|}\right)^{\frac{1}{K_\rho N}} \int d^2\mathbf{R} \nabla_\mathbf{R}^2 \ln\left(\frac{|\mathbf{R} - \mathbf{r}_1|}{a}\right) \ln\left(\frac{|\mathbf{R} - \mathbf{r}_2|}{a}\right) \int dr \left(\frac{a}{r}\right)^{\frac{N}{2K_\rho} + \frac{N}{2K_\sigma}} r^2$$
$$(J.15)$$

From where the following relation becomes useful

$$\nabla_\mathbf{R}^2 \ln\left(\frac{|\mathbf{R} - \mathbf{r}|}{a}\right) = 2\pi\delta^2(\mathbf{R} - \mathbf{r}) \qquad (J.16)$$

to retrieve

$$\left(\frac{m_\phi}{2v}\right)^2 \left(\frac{1}{K_\rho} + \frac{1}{K_\rho}\right)^2 \pi \left(\frac{a}{|\mathbf{z}_{1,2}|}\right)^{\frac{1}{K_\rho N}} \ln\left(\frac{|\mathbf{r}_1 - \mathbf{r}_2|}{a}\right) \int d^2\mathbf{r} \left(\frac{a}{r}\right)^{\frac{N}{2K_\rho} + \frac{N}{2K_\sigma}} r^3 =$$
$$-\pi \left(\frac{m_\phi}{2v}\right)^2 \left(\frac{1}{K_\rho} + \frac{1}{K_\rho}\right)^2 \left(\frac{a}{|\mathbf{z}_{1,2}|}\right)^{\frac{1}{K_\rho N}} \ln\left(\frac{a}{|\mathbf{z}_{1,2}|}\right) \int dr \left(\frac{a}{r}\right)^{\frac{N}{2K_\rho} + \frac{N}{2K_\sigma}} r^3 \qquad (J.17)$$

In doing this RG procedure of integrating out the d.o.f. of the smallest length scales, we want the expression of the correlation after the procedure to be similar to one before. Doing this means that one can express how the different parameters scale. We will therefore like to express the result as

$$\left\langle \prod_{s=\sigma,\rho} e^{-i\phi_s(x_1)} e^{i\phi_s(x_2)} e^{-S_1} \right\rangle_0 = \left(\frac{a}{|\mathbf{z}_{1,2}|}\right)^{\frac{1}{NK_\rho^{\text{eff}}} + \frac{1}{NK_\sigma^{\text{eff}}}} \qquad (J.18)$$

To ensure this form the expression is put into a form, such that it can be reexponentiate.

$$\left\langle \prod_{s=\sigma,\rho} e^{-i\phi_s(x_1)} e^{i\phi_s(x_2)} e^{-S_1} \right\rangle_0 \approx$$
$$\left(\frac{a}{|\mathbf{z}_{1,2}|}\right)^{\frac{1}{K_\rho N} + \frac{1}{K_\sigma N}} - \left(\frac{m_\phi}{2v}\right)^2 \left(\frac{1}{K_\rho} + \frac{1}{K_\rho}\right)^2 \left(\frac{a}{|\mathbf{z}_{1,2}|}\right)^{\frac{1}{K_\rho N} + \frac{1}{K_\sigma N}} \pi \ln\left(\frac{a}{|\mathbf{z}_{1,2}|}\right) \times$$
$$\int dr \left(\frac{a}{r}\right)^{\frac{N}{2K_\rho} + \frac{N}{2K_\sigma}} r^3 = \left(\frac{a}{|\mathbf{z}_{1,2}|}\right)^{\frac{1}{K_\rho N} + \frac{1}{K_\sigma N}} \left(1 - \ln\left(\frac{a}{|\mathbf{z}_{1,2}|}\right)^A\right) \approx$$
$$\left(\frac{a}{|\mathbf{z}_{1,2}|}\right)^{\frac{1}{K_\rho N} + \frac{1}{K_\sigma N} - A} = \left(\frac{a}{|\mathbf{z}_{1,2}|}\right)^{\frac{1}{NK_\rho^{\text{eff}}} + \frac{1}{NK_\sigma^{\text{eff}}}} \qquad (J.19)$$

Between the two last lines it is assumed that the quantity inside the parentheses is small such that it can be exponentiated. From this we can now see how K_ρ and K_σ behaves under the RG procedure due to the background interaction term. Lets continue by looking at the exponent.

$$\frac{1}{NK_\rho^{\text{eff}}} + \frac{1}{NK_\sigma^{\text{eff}}} = \frac{1}{NK_\rho} + \frac{1}{NK_\sigma} - A =$$
$$\frac{1}{NK_\rho} + \frac{1}{NK_\sigma} - \left(\frac{m_\phi}{2v}\right)^2 \left(\frac{1}{K_\rho} + \frac{1}{K_\rho}\right)^2 \pi \int_a^\infty dr \left(\frac{a}{r}\right)^{\frac{N}{2K_\rho} + \frac{N}{2K_\sigma}} r^3 \qquad (J.20)$$

The next step is to integrate out the d.o.f of the smallest length scales. To do this the parameter $b = 1 + dl$ is introduced where dl is in infinitesimal quantity. Using b, the integral is separated into

$$\left(\frac{m_\phi}{2v}\right)^2 \left(\frac{1}{K_\rho} + \frac{1}{K_\rho}\right)^2 \pi \int_a^\infty \mathrm{d}r \left(\frac{a}{r}\right)^{\frac{N}{2K_\rho} + \frac{N}{2K_\sigma}} r^3 =$$

$$\left(\frac{m_\phi}{2v}\right)^2 \left(\frac{1}{K_\rho} + \frac{1}{K_\rho}\right)^2 4 \int_a^\infty \frac{\mathrm{d}r}{a} \left(\frac{a}{r}\right)^{\frac{N}{2K_\rho} + \frac{N}{2K_\sigma} - 3} =$$

$$\left(\frac{m_\phi}{2v}\right)^2 \left(\frac{1}{K_\rho} + \frac{1}{K_\rho}\right)^2 4 \left(\int_a^{ab} \frac{\mathrm{d}r}{a} \left(\frac{a}{r}\right)^{\frac{N}{2K_\rho} + \frac{N}{2K_\sigma} - 3} \int_{ab}^\infty \frac{\mathrm{d}r}{a} \left(\frac{a}{r}\right)^{\frac{N}{2K_\rho} + \frac{N}{2K_\sigma} - 3}\right) =$$

$$\left(\frac{m_\phi}{2v}\right)^2 \left(\frac{1}{K_\rho} + \frac{1}{K_\rho}\right)^2 4 \left((b - 1) + b^{4 - \left(\frac{N}{2K_\rho} + \frac{N}{2K_\sigma}\right)} \int_a^\infty \frac{\mathrm{d}r'}{a} \left(\frac{a}{r'}\right)^{\frac{N}{2K_\rho} + \frac{N}{2K_\sigma} - 3}\right) \equiv$$

$$\left(\frac{m_\phi}{2v}\right)^2 \left(\frac{1}{K_\rho} + \frac{1}{K_\rho}\right)^2 4 ln(b) + \left(\frac{\tilde{m}_\phi}{2v}\right)^2 \left(\frac{1}{K_\rho} + \frac{1}{K_\rho}\right)^2 4 \int_a^\infty \frac{\mathrm{d}r'}{a} \left(\frac{a}{r'}\right)^{\frac{N}{2K_\rho} + \frac{N}{2K_\sigma} - 3} \tag{J.21}$$

Where the tilde represent the renormalized constants. This leads to the first RG equation for M_ϕ.

$$\tilde{m}_\phi = m_\phi b^{2 - \left(\frac{N}{4K_\rho} + \frac{N}{4K_\sigma}\right)} \tag{J.22}$$

where one has $b^n = 1 + ndl$, such that it can be expressed as

$$\tilde{m}_\phi = m_\phi + \frac{\mathrm{d}m_\phi}{\mathrm{d}l} \cdot \mathrm{d}l \tag{J.23}$$

the RG equation can be read off as

$$\frac{dm_\phi}{dl} = m_\phi \left(2 - \left(\frac{N}{4K_\rho} + \frac{N}{4K_\sigma}\right)\right) \tag{J.24}$$

Which agrees with the first order scaling dimension previously found.

Next we focus on the Luttinger parameters K_ρ and let just remind ourself that this analysis was solely done for one of the terms in S_1, meaning that we will just find one of the contribution to the RG flow equations. As previously explained we want to make the correlation to be of similar form as before. Before integrating out the smallest length scales we had

$$\left\langle \prod_{s = \sigma, \rho} e^{-i\phi_s(x_1)} e^{i\phi_s(x_2)} e^{-S_1} \right\rangle_0 \approx \left(\frac{a}{|\mathbf{z}_{1,2}|}\right)^{\frac{1}{NK_\rho} + \frac{1}{NK_\sigma} - \left(\frac{m_\phi}{2v}\right)^2 \left(\frac{1}{K_\rho} + \frac{1}{K_\rho}\right)^2 \pi \int_a^\infty \mathrm{d}r \left(\frac{a}{r}\right)^{\frac{N}{K_\rho}} r^3} \tag{J.25}$$

After integrating out the D.O.F we will then write it as

$$\left(\frac{a}{|\mathbf{z}_{1,2}|}\right)^{\frac{1}{NK_\rho} + \frac{1}{NK_\sigma} + \left(\frac{\tilde{m}_\phi}{2v}\right)^2 \left(\frac{1}{K_\rho} + \frac{1}{K_\rho}\right)^2 \pi \int_a^\infty \mathrm{d}r \left(\frac{a}{r}\right)^{\frac{N}{2K_\rho} + \frac{N}{2K_\sigma}} r^3} \tag{J.26}$$

From which we can find $\tilde{K}_\rho$ to be

$$\frac{1}{N\tilde{K}_\rho} + \frac{1}{N\tilde{K}_\sigma} = \frac{1}{NK_\rho} + \frac{1}{NK_\sigma} - \left(\frac{m_\phi}{2v}\right)^2 \left(\frac{1}{K_\rho} + \frac{1}{K_\rho}\right)^2 4 dl \tag{J.27}$$

Since the background interaction terms acts in the exact same way on both the charge and spins sector, one finds that the change in the Luttinger parameters due to this term must be equivalent. From this one can therefore deduct

$$\frac{\mathrm{d}}{\mathrm{d}l} \left(\frac{1}{K_s N}\right) = -\frac{1}{2} \left(\frac{m_\phi}{2v}\right)^2 \left(\frac{1}{K_\rho} + \frac{1}{K_\sigma}\right)^2 \pi a^4 \tag{J.28}$$

such that the contribution from this term to the RG equations becomes

$$\frac{dK_s}{dl} = ... + K_s^2 \left(\frac{M_\phi^2 N^3}{2^7 \pi} \right) \left(\frac{1}{K_\rho} + \frac{1}{K_\sigma} \right)^2 \tag{J.29}$$

Where it has been inserted that $v = 4\pi a/N$.

If instead looking at

$$\left\langle \prod_{s=\sigma,\rho} e^{-i\theta_s(x_1)} e^{i\theta_s(x_2)} e^{-S_1} \right\rangle_0 \tag{J.30}$$

One will find the contribution from the M_θ-term. To find this one can simply make the dual mapping of $\theta, \phi \to \phi, \theta$ and $K_s \to K_s^{-1}$. This will leave the same quadratic part and exchange the θ and ϕ fields. This means that the BGI term for the ϕ-fields turns into the one for the θ fields except for the constant in front. This analysis above is therefore corresponds to the analysis performed for the BGI term of the θ-fields if taking $K_s \to K_s^{-1}$. The BGI term of the θ-fields therefore contribute as follows

$$\frac{dK_s}{dl} = ... - \frac{M_\theta^2 N^3}{2^7 \pi} (K_\rho + K_\sigma)^2 \tag{J.31}$$

For the rung tunneling term, one can choose to only look at

$$\left\langle e^{-i\theta_\sigma(x_1)} e^{i\theta_\sigma(x_2)} e^{-S_1} \right\rangle_0 \tag{J.32}$$

since this term only acts within the spin sector. Doing the same calculations as above yields the following contribution

$$\frac{dK_\sigma}{dl} = ... - K_\sigma^2 \frac{\lambda}{2^5 \pi N}$$
$$\frac{d\lambda}{dl} = \lambda(2 - \frac{K_\sigma}{N}) \tag{J.33}$$

For $g = 0$ the real space second order RG calculations therefore leads to flow equations shown below

$$\frac{dK_\sigma}{dl} = \frac{M_\phi^2 N}{16} K_\sigma^2 \left(\frac{1}{K_\rho} + \frac{1}{K_\sigma} \right)^2 - \frac{M_\theta^2 N}{16} (K_\rho + K_\sigma)^2 - K_\sigma^2 \frac{\lambda}{2^5 \pi N}$$
$$\frac{dK_\rho}{dl} = \frac{M_\phi^2 N}{16} K_\rho^2 \left(\frac{1}{K_\rho} + \frac{1}{K_\sigma} \right)^2 - \frac{M_\theta^2 N}{16} (K_\rho + K_\sigma)^2$$
$$\frac{d\lambda}{dl} = \lambda(2 - \frac{K_\sigma}{N})$$
$$\frac{dM_\phi}{dl} = M_\phi \left(2 - \frac{N}{4} \left(\frac{1}{K_\rho} + \frac{1}{K_\sigma} \right) \right)$$
$$\frac{dM_\theta}{dl} = M_\theta \left(2 - \frac{N}{4} (K_\rho + K_\sigma) \right) \tag{J.34}$$

Using these RG equations one finds the gapless phase to approximately appear for $\lambda \in [0.4, 1]$ and some of the RG flow is seen solved in Fig. 5.7.

Appendix K

Numerical evidence of a gapless phase
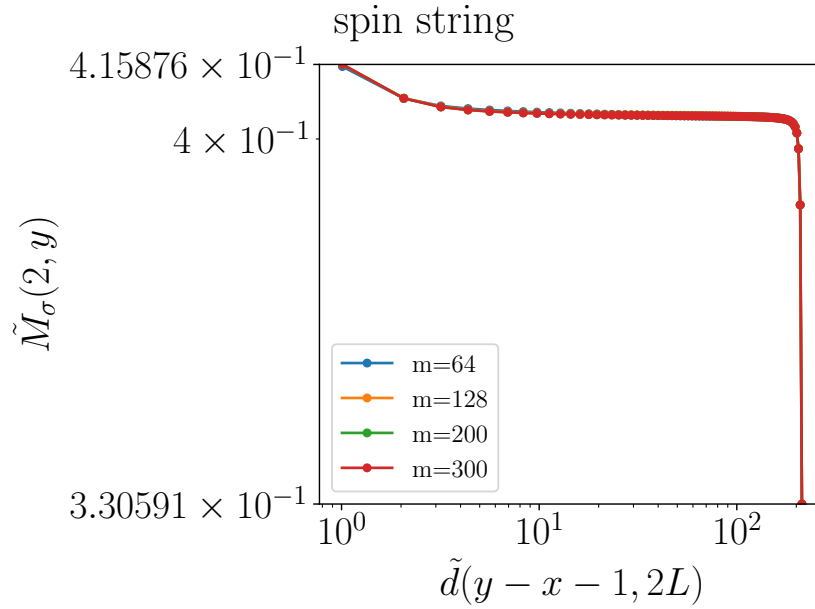
Figure K.1 | $\langle M_\sigma \rangle$. This figure shows the behavior of $\langle M_\sigma(|y - x|) \rangle$ for $g = 0.001$ and $\lambda = 0.75$, so inside the predicted gapless phase. Away from the boundaries this shows constant behavior as predicted in the phase $\boldsymbol{H}$. The quantity m describes the bond dimension of the simulation. The figure is provided by *Chia-Min Chung*.
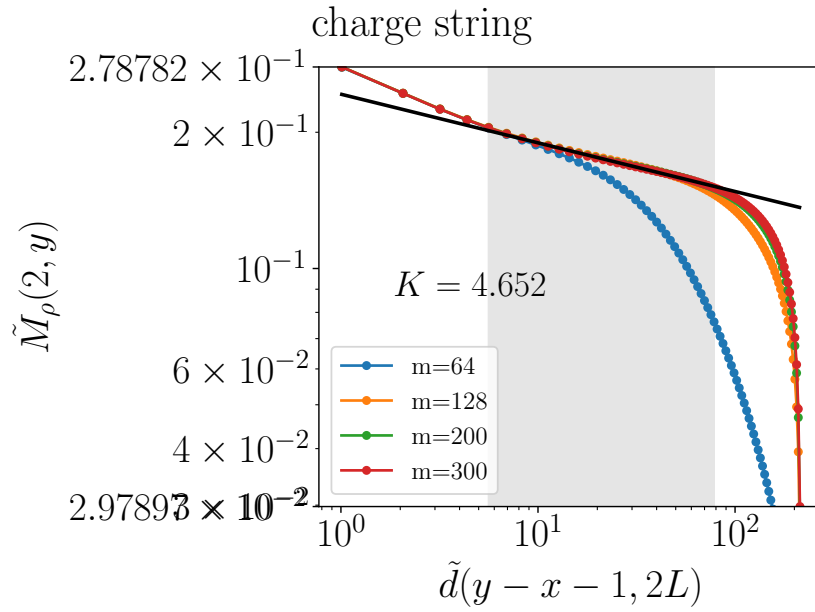
Figure K.2 | $\langle M_{\rho} \rangle$. This figure shows the behavior of $\langle M_{\rho}(|y-x|)\rangle$ for $g = 0.001$ and $\lambda = 0.75$, so inside the predicted gapless phase. Away from the boundaries this shows power law behavior as predicted in the phase $\boldsymbol{H}$. From the power law behavior in the gray region the Luttinger parameter K is estimated to be around 4.7, and the quantity m describes the bond dimension of the simulation. The figure is provided by *Chia-Min Chung*.